On the Renormalization Group Flow of Gravity

PhD Thesis

Pedro F. Machado

Machado, Pedro Farias

On the Renormalization Group Flow of Gravity
PhD thesis
Institute for Theoretical Physics
Utrecht University
ISBN: 978-90-393-6267-9
Printed by Ipskamp Drukkers, The Netherlands

On the Renormalization Group Flow of Gravity

Over de Renormalisatie Groep Stroming van de Zwaartekracht

(met een samenvatting in het Nederlands)

Proefschrift

ter verkrijging van de graad van doctor aan de Universiteit Utrecht op gezag van de rector magnificus, prof.dr. J.C. Stoof, ingevolge het besluit van het college voor promoties in het openbaar te verdedigen op vrijdag 8 januari 2010 des middags te 12.45 uur

door

Pedro Farias Machado

geboren op 3 augustus 1982 te Belo Horizonte, Brazilië

Promotor: Prof.dr. R. Loll

Dit proefschrift werd mogelijk gemaakt met financiele steun van de Nederlandse Organisatie voor Wetenschappelijk Onderzoek (NWO).

To my parents

Contents

1 Introduction

Lutar com palavras
é a luta mais vã
- Carlos Drummond de Andrade
(Brazilian poet, 1902 - 1987). [1]

It is a well appreciated fact that the behavior of physical systems depends upon the length scales at which they are probed. Quarks, for example, are confined to bound states at the hadronic level and yet behave as freely interacting particles at vanishing length scales. As the microscopic interactions between the putative degrees of freedom of a system combine to generate a particular leading dynamics at each length scale, understanding a system's behavior implies understanding how these effective dynamics and, as a result, physical quantities behave across different length regimes. One of the greatest insights of modern theoretical physics [1–3] was the realization that we could encode and study this scale dependence in the measurable, microscopic parameters specifying the system, namely, the coupling constants of the theory. The development of these ideas culminated in Wilson's formulation of the renormalization group in the early 70's [4–6].

The renormalization group framework [7] has proven to be an extremely powerful tool in theoretical physics, and its application has led to important results and crucial insights into a variety of systems, from classical [8] to quantum [9], from solid state [10] to high energy physics [11], from phase transitions in magnets [12] to the behavior of fundamental particles in the atomic nucleus [13]. The techniques within this framework all share a common procedure, which characterizes the approach. For convenience, we will exemplify this procedure for the case of a field theory described by the action $S\big[\phi^A, g_i\big]$, where ϕ^A are the fields in the

[1] "Fighting with words / is the vainest of fights"

theory and g_i the coupling constants. For a given momentum scale k, a renormalization group algorithm allows us to eliminate all field fluctuations with momenta larger than k from the theory, and reencode the contribution of these excluded modes to the theory's dynamics by readjusting, or renormalizing, the couplings g_i. The result is an effective description of the system at the scale k. As we progressively vary k, the resulting group of renormalization transformations induces a flow of the renormalized g_i in the theory's parameter space. This is the theory's renormalization group flow.

By following a theory's renormalization group flow from high energies in the ultraviolet (UV) to low energies in the infrared (IR), we can consistently treat processes which extend across different scales but which are governed by the same underlying microscopic physics. In this sense, understanding the behavior of a system implies understanding its renormalization group flow. In the present work, we will investigate the renormalization group flow of quantum gravity.

Reconciling quantum physics with general relativity is one of the major open challenges facing theoretical physics today. On the one hand, general relativity is an extremely successful theory of gravitational phenomena, significantly well-tested over a wide range of length scales, from the microscopic ($\ell \sim 10^{-2}\,\mathrm{cm}$) to the cosmological ($\ell \sim 10^{28}\,\mathrm{cm}$). Furthermore, for typical interaction energies between subatomic particles ($k \sim 100\,\mathrm{GeV}$), the gravitational force between them is so weak when compared to the other forces present, that the former may be essentially neglected in our quantum description of the system. On the other hand, as we start probing progressively higher energy scales and approach the Planck regime of $k_{\mathrm{Pl}} = 1/\sqrt{G} \sim 10^{19}\mathrm{GeV}$, where G is Newton's constant, quantum corrections to gravitational processes become increasingly non-negligible and the gravitational force becomes comparable with the other subatomic forces. When attempting to accommodate such issues by promoting general relativity to a quantum theory using the well-established methods of perturbative quantization, however, one encounters a significant problem, as gravity is notoriously non-renormalizable at the perturbative level [14].

The root of this problem can be traced to the fact that Newton's constant G, in terms of which we define the perturbative theory, has dimensions of inverse energy squared in natural units. This has two consequences. First, as the strength of the gravitational coupling scales as $\tilde{G} \equiv Gk^2$, physical quantities constructed from this dimensionless parameter may be likewise expected to grow without bound with k. Secondly, to render the theory finite in the presence of non-renormalizable divergences appearing already at one-loop order for matter-coupled gravity [15–18] and two-loop order for pure gravity [19, 20], new counterterms must be introduced at each order in the perturbative expansion, each of which parametrized by new coupling constants which must be determined experimentally. When the interaction energies reach $k = k_{Pl}$, the perturbative series in Gk^2 diverges, as all loop orders contribute equally to the expansion, and an infinite number of couplings has to be fixed.

If one is interested in scales $k \ll k_{\mathrm{Pl}}$, it is possible to avoid these issues. Fol-

lowing an effective field theory approach [21], we may cut off the loop momenta at a given scale, organize the action in an energy expansion in curvature invariants and truncate this expansion to the desired order of accuracy for computations of a given physical process. This allows us to make unambiguous quantum gravity predictions, such as, e.g., computing quantum corrections to the Newtonian potential [22], irrespective of the Planckian behavior of the theory. Still, for physics at the Planck regime, as the number of relevant terms in the expansion becomes infinite, the non-renormalizability of perturbatively quantized general relativity entails a complete loss of predictive power.

Since the partial failure of this perturbative quantization program, a number of approaches have been developed and advanced as candidate theories of quantum gravity (see [23, 24] for reviews). Due to the considerable difficulties these theories face in generating predictions that may be tested experimentally and, to some extent, in even defining observables in a quantum gravitational context [25], the question of their physical validity remains unsettled. From a theoretical perspective, however, these theories offer possible solutions to the problem of the renormalizability of gravity. These solutions predominantly follow two (occasionally complementary) strategies. The first strategy entails modifying the theory at the fundamental level. Examples include redefining the fundamental field degrees of freedom in terms of which quantization is effected, so that the metric and matter fields emerge only as low energy aproximations and renormalizability is restored at the level of the fundamental theory (viz. string theory [26]), or enlarging or reducing the symmetries of the theory at the Planck-regime (viz. supergravity [27, 28] and anisotropic scaling models [29], respectively), which then act to render the theory free from uncontrollable divergences. The second strategy consists in following a non-perturbative approach to quantum gravity, by, e.g., employing a path integral quantization procedure (viz. causal dynamical triangulations [30] or causal set theory [31]) or canonically quantizing space-time on the basis of a loop algebra (viz. loop quantum gravity [32]). This strategy is based on the idea that the problem with perturbatively quantized gravity might lie in the use of perturbative quantization itself, and that non-perturbative effects might render a quantum theory of general relativity well-defined at the Planck scale despite its non-renormalizability at the perturbative level.

A concrete realization of this idea from a renormalization group perspective is Weinberg's asymptotic safety scenario [33, 34]. The asymptotic safety scenario envisages the existence of a non-trivial fixed point of the renormalization group flow of gravity, with a finite number of UV-attractive directions, controlling the behavior of the theory in the UV. As we will see in more detail shortly, the fact that the theory flows towards the fixed point in the UV implies that $\tilde{G}$ will tend to a finite value $\tilde{G} = \tilde{G}^*$ as $k \to \infty$, while the fact that the fixed point has a finite number of UV-attractive directions implies that only a finite number of couplings have to be fixed experimentally to fully determine the behavior of the theory at all scales. The end result is a theory that is both predictive and free from uncontrollable divergences at and beyond the Planck scale.

Notably, the asymptotic safety conjecture can be seen as a statement about the behavior of an effective field theory description of quantum gravity as we follow its renormalization group flow in the high energy limit. Provided an appropriate renormalization group algorithm is available, this conjecture may be to a large extent probed irrespective of the details of the theory at its fundamental level. Over recent years, functional renormalization group methods have been developed [35] with which we can accomplish that, and which for the first time allow us to directly investigate the renormalization group behavior of four-dimensional quantum gravity in a non-perturbative setting [35–41].

Employing these methods, we can start mapping the gravitational renormalization group flow. This thesis contributes a step in this direction.

Effective field theories and the Wilsonian renormalization group

In the present work, we will approach the renormalization group flow of gravity from a Wilsonian perspective on the renormalization group [7] and following the spirit of effective field theories. To this effect, let us start by considering the following action functional for pure gravity,

$$\Gamma_{\text{eff}}(k) = \int d^4x\sqrt{-g}\left[g_0(k) + g_2(k)R + g_4(k)R^2 + g_{4a}(k)R_{\mu\nu}R^{\mu\nu} + \ldots\right] , \quad (1.1)$$

containing all diffeomorphism invariant terms constructed from the metric and its derivatives. Here, the running couplings $g_i(k)$ have canonical mass dimension $d_i = 4-i$, and we may conveniently re-express them in terms of their dimensionless counterparts, $\tilde{g}_i = k^{-d_i}g_i(k)$. In addition, we have defined $g_0 = -\Lambda/8\pi G$ and $g_1 = 1/16\pi G$, where Λ and G are the cosmological and Newton's constant, respectively. The two lowest order terms in the expression above are exactly the terms present in the Einstein-Hilbert action, which encodes classical gravity and serves as the starting point for perturbative quantization. Lastly, we should note that this action may also contain non-local operators.

The functional (1.1) provides an effective description of gravitational physics at the scale k and may be seen as the result of an unspecified coarse-graining procedure whereby all field fluctuations with momenta greater than k have been integrated out. The coupling constants g_i are subject to a renormalization group flow, which is defined in the infinite-dimensional 'theory space' parametrized by the dimensionless couplings $\tilde{g}_i$ and is given by the beta functions

$$\beta_i(\tilde{g}_i) = k\frac{d\tilde{g}_i}{dk} . \quad (1.2)$$

A fixed point $\{\tilde{g}_i^*\}$ of the flow is given by the vanishing of these beta equations, i.e., $\{\beta_i(\{\tilde{g}_i^*\}) = 0\}$.

A renormalization group trajectory in theory space thereby connects a family of coarse grained actions $\Gamma_{\text{eff}}(k)$, each of which describes the physics at different momentum scales. We define the set of trajectories attracted to a fixed point

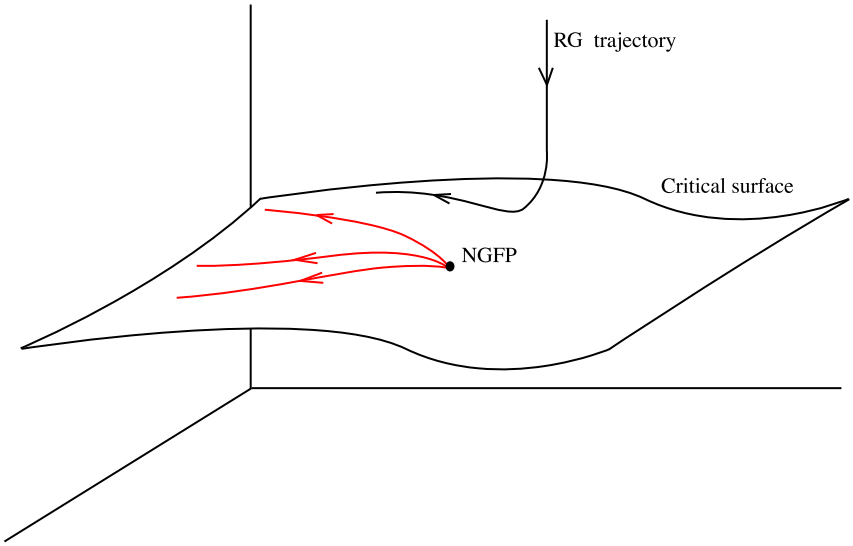

Figure 1.1: The UV critical surface $\mathcal{S}_{\rm UV}$ associated with the NGFP. The renormalized trajectories emanating from the NGFP and spanning this surface are shown in red and the arrows point in the direction of decreasing k. Trajectories not lying on the surface are attracted towards it as k decreases.

as $k \to \infty$ as the UV critical surface $\mathcal{S}_{\rm UV}$ associated with the latter (see Figure 1.1). Around the fixed point, the linearized renormalization group flow $k\partial_k \tilde{g}_i = \mathbf{B}_{ij}(\tilde{g}_j - \tilde{g}_j^*)$ is governed by the stability matrix

$$\mathbf{B}_{ij} = \partial_j \beta_i|_{\{\tilde{g}_i^*\}} \ . \tag{1.3}$$

The attractivity properties of the fixed point are determined by the stability coefficients θ_i, defined as minus the eigenvalues of the stability matrix. Eigendirections associated with stability coefficients with positive real part are UV attractive, or UV-relevant, while eigendirections related to stability coefficients with negative real part are UV repulsive, or UV-irrelevant. The dimensionality of the UV critical surface is given by the number of UV-relevant directions associated with the fixed point and corresponds to the number of independent parameters in the theory - i.e., with the essential couplings that must be determined by experiments. If these couplings are found to lie on the UV critical surface, the theory will possess a well-defined UV limit.

From the definition of the beta function, (1.2), we can see that $\{\tilde{g}_i^* = 0\}$ is a fixed point of the flow. This is the Gaussian fixed point (GFP), corresponding to the free theory and in the neighborhood of which we apply the standard perturbative approach. The stability coefficients associated with this fixed point are given by the canonical dimensions of the (dimensionful) couplings. In the case of (1.1),

restricting ourselves to the subspace spanned by the Einstein-Hilbert terms, the stability coefficients of the GFP are $\theta_1 = 2$ and $\theta_2 = -2$, as given by the canonical dimensions of Λ and G, respectively. Owing to the negative mass dimension of Newton's constant, the only relevant direction is at $G = 0$, amounting to a trivial theory with just the cosmological term, and, as soon as we turn on Newton's constant, the flow is then carried away from the GFP in the UV. Thus, already at the level of the Einstein-Hilbert terms only, the theory will not lie on the critical surface of the GFP, and we can expect its couplings to diverge as we follow the flow to higher energy scales, signaling its perturbative non-renormalizability from the Wilsonian viewpoint.

In the case $\{\tilde{g}_i^* \neq 0\}$, we call the fixed point a non-Gaussian fixed point (NGFP). It is on the existence of this kind of fixed point that the asymptotic safety scenario for gravity hinges.

The Asymptotic Safety scenario

Asymptotic safety may be thought of as a non-perturbative, generalized notion of renormalizability. A theory is said to be asymptotically safe if two conditions are met with respect to its renormalization group flow, namely, that there exists a fixed point to which the renormalization group trajectory of the theory is attracted in the UV, and that the UV critical surface $\mathcal{S}_{\rm UV}$ associated with this fixed point is finite-dimensional. The first condition entails the theory has a sensible UV limit, as all its dimensionless (essential) couplings will tend to finite values as $k \to \infty$. The second condition entails that only finitely many experiments are required to fix all of its independent parameters. Therefore, the theory is predictive and well-behaved in the UV.

In the special situation in which this fixed point is the GFP, the theory is said to be asymptotically free, and the UV critical surface is spanned by the eigendirections associated with the couplings which are renormalizable from the perturbative perspective. This is the case for quantum chromodynamics. We can hence consider asymptotic freedom to be a particular realization of asymptotic safety.

In a more general situation, we can expect this fixed point, if existing, to be a NGFP. An example of a perturbatively non-renormalizable model which is governed by such a fixed point is the two-dimensional Gross-Neveu model with a $-p^{2+\epsilon}$ propagator, which has been rigorously proven to be non-perturbatively renormalizable at its NGFP [42].

The asymptotic safety scenario for gravity is the conjecture that the UV behavior of the theory is controlled by a NGFP with the properties just described. If realized, this scenario would ensure that quantized gravity is predictive and well defined at all energy scales. For convenience, we will drop the qualifier 'gravity' when discussing asymptotic safety in what follows, with the understanding that all our remarks on this conjecture, unless otherwise noted, will concern the gravitational case.

A generic consequence of asymptotic safety is the phenomenon of dimensional reduction in the UV limit [43]. We will present this argument for the case of the graviton propagator, but we note that this effect generalizes to the propagation of arbitrary fields [44]. The beta function for the dimensionless Newton's constant in d-dimensional gravity is given by

$$k\partial_k \tilde{G} = (d - 2 + \eta_G(\tilde{g}_i))\, \tilde{G}\,, \tag{1.4}$$

where η_G is the anomalous dimension of Newton's constant and is a function of all the couplings. The vanishing of this beta function at a NGFP then implies $\eta_G = 2 - d$. The propagator of a field with anomalous dimension η behaves like $p^{-2+\eta}$, and therefore, in the vicinity of the NGFP and for $d = 4$ the graviton propagator will behave like p^{-4}, which depends logarithmically on distance in terms of position space. This logarithmic dependence is characteristic of two-dimensional fields. In the UV limit, spacetime is then effectively two-dimensional. This spontaneous dimensional reduction of gravity was first observed within the framework of Causal Dynamical Triangulations in the context of the spectral dimension [46], but this feature has now been found to be present in a variety of other quantum gravity approaches [47], offering encouraging prospects for the asymptotic safety scenario.

Support for this conjecture has also been found by calculations in $2 + \epsilon$ spacetime dimensions [48, 49], large N expansions [50] (where N is the number of matter fields considered), as well as studies of the symmetry reduced Euclidean path integral [51, 52]. Furthermore, Monte Carlo simulations of quantum gravity at energy scales slightly smaller than the Planck scale have found no disagreements with asymptotic safety yet [53] and may be able to test this scenario in the future by probing scales in which the NGFP becomes dominant. Most of the recent progress on this issue, however, has been made via the application of functional renormalization group methods [54] to four-dimensional gravity [35], by means of which growing evidence for the existence of a candidate NGFP realizing the AS scenario has been established. It is these methods that we will employ in this thesis.

The asymptotic safety conjecture is a first and main issue concerning the renormalization group flow of gravity that we wish to tackle in the present work. A second issue we wish to address concerns the gravitational physics of the deep infrared.

Cosmological RG effects and non-local operators

While quantum gravitational effects are widely expected to dominate at the Planck scale, it has been suggested that these effects might also play an important role at the extremely large, cosmological length scales [55, 56]. In particular, it has been argued that cosmological phenomena such as the current accelerated expansion of the universe might have their origin in infrared modifications to our effective low-energy theory of gravity, as induced by quantum contributions [57].

From a renormalization group perspective, we can heuristically motivate this argument in the following way. We know the universe is quantum at its fundamental level. Hence, whichever gravitational action may capture the dynamics of some observed large scale phenomenon, it will be the result of the integrating out of quantum degrees of freedom down to the appropriate scale. Assuming it were possible to correctly implement this coarse graining procedure, it is conceivable that the resulting effective action might not exactly reduce to the Einstein-Hilbert in the low-energy regime, while still being consistent with the current, very stringent tests of general relativity. In particular, this action might contain terms with inverse powers of derivatives of the metric, i.e., non-local operators, which become relevant in the deep IR, driving the effective dynamics at that scale. A physically motivated example of this is the non-local effective action induced by the quantum trace anomaly of the stress-energy tensor, the 'conformal anomaly', as the result of integrating out the matter degrees of freedom in matter-coupled gravity.

Furthermore, already at the classical level non-local modifications to general relativity have been advanced as an explanation of low energy, cosmological phenomena and an alternative to dark energy [58]. These modifications, which are of $f(R)$ form, where R is the curvature scalar, can be argued to generate physically reasonable dynamics [59] while still satisfying observational constraints [60].

From the point of view of our Wilsonian renormalization group, the effect of such non-local terms in the renormalization group flow of gravity must then be considered, and the presence of these terms might have a significant impact on the IR features of the flow. This is the second issue we wish to investigate in the present work.

The flow equation

The main tool we will use in our study of the gravitational renormalization group flow is the functional renormalization group equation (FRGE) [54],

$$\partial_t \Gamma_k[\Phi, \bar{\Phi}] = \tfrac{1}{2}\mathrm{STr}\left[\left(\frac{\delta^2 \Gamma_k}{\delta \Phi^A \delta \Phi^B} + \mathcal{R}_k\right)^{-1} \partial_t \mathcal{R}_k\right], \tag{1.5}$$

which describes the dependence of the effective average action Γ_k on the renormalization group scale k and implements a continuous version of the Wilsonian renormalization group. Here, Φ and $\bar{\Phi}$ respectively denote the physical fields and their background value, $t = \log(k/k_0)$, and the supertrace STr is a generalized functional trace which includes a minus sign for ghosts and fermions, and a factor two for complex fields.

The effective average action Γ_k defines an effective field theory valid near the scale k and can be thought of as the result of integrating out all quantum fluctuations with momenta $p^2 \geq k^2$. This coarse graining is implemented by means of the cutoff $\mathcal{R}_k$, which provides a k-dependent massive term for fluctuations with

$p^2 < k^2$ so that, at the level of the path integral, the contributions of these low-momenta fluctuations are suppressed and only the high momentum modes are integrated out. As $k \to 0$, the effective average action then reduces to the ordinary effective action Γ, and all the Green's functions of the theory are recovered. Owing to its cutoff structure, the FRGE has the remarkable property of being finite and locally well-defined in momentum space at all energy scales. In particular, while a theory might require a UV regulator at the level of its path integral, at the FRGE level this regularization is not needed.

The FRGE formalism differs from the continuous formulation of Wilson's renormalization group in terms of the Polchinski equation [11] in that here the coarse graining is implemented by means of an IR cutoff and at the level of the effective average action Γ_k, rather than a UV cutoff at the level of a Wilsonian (bare) action S_k. However, these two formalisms are related via a Legendre transform and momentum-dependent field rescalings [61, 62]. At the formal level, they thus represent two realizations of the same exact renormalization group and we can expect the physics they carry to be identical.[2]

The FRGE framework provides a powerful setup for studying the renormalization group flow of field theories [65, 66]. However, as it is defined in the infinite-dimensional theory space of all action functionals compatible with the symmetries of the theory, it cannot be solved exactly and in order to extract physics from it we must resort to approximations. Beyond perturbation theory, a standard non-perturbative approximation scheme is the truncation of the theory space, whereby the flow of the full theory is projected onto a subspace spanned by a finite number of the interaction monomials in the theory. The availability of different approximation schemes is a useful feature of the FRGE method, lending it versatility and allowing for internal consistency checks. At the same time, estimating the reliability of results within a given approximation is then a central issue within this approach. This issue is particularly acute in the cases in which we do not know the fundamental theory underlying the flow or do not have much external data against which FRGE results may be compared, as happens in quantum gravity. In a non-perturbative setting, an important test for the quality of truncation approximations consists in gradually enlarging the truncation subspace and investigating the stability of previous findings under this extension. The latter is the general strategy we shall follow in the present work.

An outline

This thesis is organized as follows. In Chapter 2, we review the FRGE and effective average action formalism in detail and focus on issues arising in its application to gravity. We discuss its relation to the one-loop effective action and to UV regularized actions, and expand on the approximation schemes used within this

[2] At the practical level, this equivalence is generally broken once approximations to the exact flows are introduced. A notable exception is the case of the Local Potential Approximation [63, 64].

approach. Lastly, we discuss the inclusion of matter fields within the gravitational setting and illustrate the different ways in which a cutoff $\mathcal{R}_k$ may be constructed within the theory and the way the beta functions are usually extracted.

In Chapter 3, we begin our investigations by studying the renormalization group flow of matter-coupled gravity in a conformally reduced setting [67], in which quantum fluctuations are restricted to the conformal part of the metric only, and considering truncations of the form of the non-local effective action induced by the conformal anomaly, which occurs as a result of integrating out the matter degrees of freedom. This reduced setup provides a first testing ground in which to investigate the effect of non-local operators on the flow, as well as the issue of the non-perturbative renormalizability of gravity. Within this simplification, we find there are two ways to implement the cutoff, which respectively break or preserve the Weyl invariance, i.e., the invariance of the theory under local scale transformations. In the Weyl-invariance preserving case, which we may trace to background independence in the full diffeomorphism invariant theory, we establish the existence of a NGFP in accordance with the asymptotic safety scenario. In the Weyl-breaking case, we recover under a particular approximation the beta functions which have been previously obtained within this setting via perturbative calculations [68], and which have been argued to provide the theory with a non-zero fixed point driving its IR dynamics. Partially foreshadowing the case of the complete theory, the results in these two disparate settings provide tentative support for the asymptotic safety scenario and suggest that non-local terms might play a non-trivial renormalization group role in the IR.

Motivated by our findings in the conformal sector, we move to full diffeomorphism invariant gravity in Chapter 4, and construct a flow equation in which to study truncations of the $f(R)$ form in d spacetime dimensions, where $f(R)$ is any function of the Ricci scalar R. This setting allows us to generalize the FRGE to a very large class of truncations, of which the Einstein-Hilbert action is an example, and serves as a basis for the analysis in the subsequent chapter. Restricting $f(R)$ to the Einstein-Hilbert case, we briefly review the gravitational renormalization group flow arising from that truncation, in which evidence for a NGFP was first established [36–39]. For $d = 4$ and a particularly convenient realization of the cutoff function, we derive an autonomous partial differential equation governing the renormalization group flow of $f(R)$ gravity and describing the fixed functionals of the flow. Using this partial differential equation, we independently recover the results of [41, 69], which successively reveal the existence of a NGFP with a three-dimensional UV critical surface in truncations including polynomials of the scalar curvature up to order six.

Armed with the generic flow equation above, in Chapter 5 we investigate non-local truncations of $f(R)$ form, that is, truncations which contain inverse powers or non-polynomial functions of the curvature scalar, motivated by models of IR modified gravity. Remarkably, we find that these non-local interactions can be consistently decoupled from the renormalization group flow and hence, if set to zero at a particular scale, will not be generated dynamically by quantum effects.

We investigate in detail the non-perturbative renormalization group flow of non-local extensions of the Einstein-Hilbert truncation including $\int d^d x \sqrt{g} \ln(R)$ and $\int d^d x \sqrt{g} R^{-n}$ interactions, respectively. The fixed point structure of the former truncation exhibits an infrared attractive fixed point which dynamically drives a positive cosmological constant to zero, hinting that renormalization group effects in the IR might be responsible for the observed tiny value of Λ. Analyzing the resulting beta functions, however, we find that truncations of this form are generally insufficient to capture the renormalization group flow of gravity in the UV and cannot be refined by the addition of other terms to the truncation subspace. This finding leads us to use our decoupling result to consistently exclude such interactions from the renormalization group flow. We can therefore constrain the space of putative asymptotically safe gravity theories to effective average actions not containing these non-local terms.

In Chapter 6, importantly, we move beyond the $f(R)$ setting. While all studies of truncated renormalization group flows so far considered have provided consistent support for the non-perturbative renormalizability of gravity, one caveat of those truncations is that, by considering powers of the curvature scalar only, they omit tensorial interactions which could in principle have a major impact on the UV behavior of gravity and the asymptotic safety conjecture, such as the four-derivative propagator for the helicity two states. It is precisely terms of the latter form that feature as non-renormalizable counterterms in the perturbative quantization of general relativity [15, 19, 20]. Driven by these considerations, we go beyond the $f(R)$ setting by studying a four-derivative truncation containing a Weyl-squared term. In addition, we extend this truncation to include a minimally coupled free scalar field, noting that this setup then provides the prototype of a gravitational theory which is perturbatively non-renormalizable at one-loop level [15]. Most notably, in both of these truncations, we establish the existence of a NGFP with three UV-attractive directions.

From these results, a coherent picture of the renormalization group flow of gravity is beginning to emerge. Crucial to this picture is a non-perturbative treatment of the gravitational flow, which may disclose features that are not captured at the level of the perturbative approach. Our studies provide strong evidence for the asymptotic safety scenario. This suggests that the metric field in our low energy theory of gravity may continue to be an appropriate degree of freedom for describing gravitational processes at the Planck scale, and that quantized gravity may remain predictive in the high energy limit without the need to introduce new fields or symmetries to the theory. In Chapter 7, we collect the results and insights gathered in our analysis, discuss the main open issues within our approach and delineate the avenues for future research.

2

The functional renormalization group equation

In this chapter, we present and review the functional renormalization group equation (FRGE) formalism, which is the framework under which our investigations of the non-perturbative renormalization group flow of gravity have been conducted. We will first introduce the formalism for the case of a scalar field theory, noting that all of its relevant features are already present at this level and carry through, mutatis mutandis, to the more involved case of gauge theories. In the second half of the chapter, we move to the case of gravity, constructing a generic flow equation for gravitational theories and discussing some issues that arise specifically in that setting. Lastly, we consider the inclusion of matter fields within the gravitational FRGE and use that to illustrate the technique by which the functional traces in this equation are commonly evaluated and the beta functions extracted.

2.1 The FRGE and its approximations

2.1.1 The FRGE formalism

The two central components in the FRGE formalism [65, 66, 70] are the effective average action Γ_k, a coarse-grained action which defines an effective field theory describing physical processes near the scale k, and the FRGE itself, which controls the k-dependence of the effective average action as we vary this scale.

The effective average action

We may think of the effective average action Γ_k as a scale-dependent version of the ordinary effective action which arises from integrating out all field fluctuations with momenta larger than k. This continuous-space coarse graining procedure is similar in spirit to a discrete Kadanoff-Wilson-type coarse graining [7], but with

the crucial differences that is it effected by means of an IR cutoff and implemented at the level of the effective, rather than bare action.

To illustrate, consider the case of a scalar field theory defined by the otherwise unspecified action $S[\phi]$, describing physics at the scale k_0. In order to coarse grain over the field modes with momenta larger than some $k < k_0$, we modify this action to include the IR cutoff term

$$\Delta S_k[\phi] = \int d^4x\, \phi(x)\mathcal{R}_k\phi(x), \tag{2.1}$$

the kernel of which, $\mathcal{R}_k$, we will call the IR cutoff. The IR cutoff may be built out of any appropriate differential operator $\mathcal{O}$ whose eigenfunctions $\mathcal{O}\chi_i = \lambda_i\chi_i$ can be taken as a suitable basis in which to expand the fields.[1] The particular form of $\mathcal{R}_k(z)$ is arbitrary, apart from the requirement that it monotonically interpolate between $\mathcal{R}_k(z) = 0$ as $z/k^2 \to \infty$ and $\mathcal{R}_k(z) \propto k^2$ as $z/k^2 \to 0$. As a result, fluctuation modes with $\lambda_i < k^2$, or 'low momentum modes', acquire a k-dependent mass term, while modes with $\lambda_i \geq k^2$, or 'high momentum modes', are not affected.

From this modified action, we can define the k-dependent generating functional of connected Green's functions, $W_k[J]$, via

$$e^{-W_k[J]} \equiv \int \mathcal{D}\phi \exp\left(-S[\phi] - \Delta S_k[\phi] + \int d^4x J\phi\right). \tag{2.2}$$

Formally evaluating the path integral, we can see that, by virtue of the cutoff term, all high momentum modes are integrated out, while all low momentum modes, being suppressed by the mass term, remain unaffected. That is to say, field modes with momenta larger than k have been coarse grained over.

Denoting the 'classical fields' by

$$\varphi = \langle\phi\rangle_k = \frac{\delta W_k[J]}{\delta J}, \tag{2.3}$$

and the Legendre transform of $W_k[J]$ with respect to J by

$$\tilde{\Gamma}_k[\varphi] = W_k[J] - \int d^4x J\varphi, \tag{2.4}$$

the effective average action is then defined by

$$\Gamma_k[\varphi] = \tilde{\Gamma}_k[\varphi] - \Delta S_k[\varphi]. \tag{2.5}$$

The effective average action thus interpolates between the standard effective action $\Gamma = \Gamma_{k\to 0}$ as $k \to 0$ and our original action $S[\phi]$ as $k \to k_0$, and, evaluated at

[1] For the purposes of this exposition we have assumed $\mathcal{O}$ to be a second-order operator and employed a notation consistent with a discrete spectrum, but a similar reasoning would apply to operators of higher order or with continuous spectra.

tree level, it accurately describes physical processes occurring at momentum scales of order k, incorporating all quantum effects originating from the high-momentum modes . Note that, in the former limiting case, all quantities like classical fields, Green's functions, S matrices, as standardly defined, are recovered.

The flow equation

As we will explicitly see in the case of gravity later, the k-dependence of Γ_k is exactly governed by the functional renormalization group equation,

$$k\partial_k\Gamma_k[\varphi] = \frac{1}{2}\mathrm{Tr}\left[\frac{k\partial_k\mathcal{R}_k}{\Gamma_k^{(2)}+\mathcal{R}_k}\right], \tag{2.6}$$

where the trace here is taken over the eigenvalues of the operator $\mathcal{O}$, for simplicity, and where we have defined the Hessian, or inverse propagator, $\Gamma_k^{(2)} = \delta^2\Gamma/\delta\varphi\delta\varphi$. In the general case, $\mathcal{O}$ may be any operator in terms of which we can express the inverse propagator, and its eigenbasis need not be the basis in terms of which we evaluate the trace. In addition, it is generally convenient to split the IR cutoff into a matrix part and a scalar function encoding the scale-dependent mass term, $\mathcal{R}_k(\mathcal{O})|_{\phi\phi} = \mathbf{Z}_{\phi\phi}R_k(\mathcal{O})$. We call the latter the cutoff profile, or 'shape', function. The FRGE can be seen as a renormalization group improved one-loop equation encoding the beta functions of our effective theories. Letting

$$\Gamma_k[\varphi] = \sum_{n=0}^{\infty}\sum_i g_n^{(i)}(k)\mathcal{P}_n^{(i)}(\varphi), \tag{2.7}$$

where $g_n^{(i)}$ are the coupling constants and $\mathcal{P}_n^{(i)}$ are all the operators of order n in the field and its derivatives compatible with the symmetries of the theory, the left-hand side of this equation reads

$$k\partial_k\Gamma_k[\varphi] = \sum_{n=0}^{\infty}\sum_i \beta_n^{(i)}(k)\mathcal{P}_n^{(i)}(\varphi), \tag{2.8}$$

where $\beta_n^{(i)}(k) = k\partial_k g_n^{(i)}(k)$ are the beta functions of the (dimensionful) couplings, and we may thus think of the right-hand side of the FRGE as a 'beta functional'. When analyzing the properties of the renormalization group flow, on the other hand, it is convenient to switch to dimensionless couplings $\tilde{g}_n^{(i)} = k^{-d_n}g_n^{(i)}$ and associated beta functions $\beta_n^{(i)} \equiv k\partial_k\tilde{g}_n^{(i)}$, which may be readily constructed from their dimensionful counterparts. Recall that it is at the level of the dimensionless couplings that a fixed point $\tilde{g}^*$ of the renormalization group is defined, i.e., $\beta_n^{(i)}(\tilde{g}^*) = 0\,\forall i, n$.

The FRGE has two remarkable properties. First, due to its IR regulator structure (see Figure 2.1, the contributions to the flow equation are localized

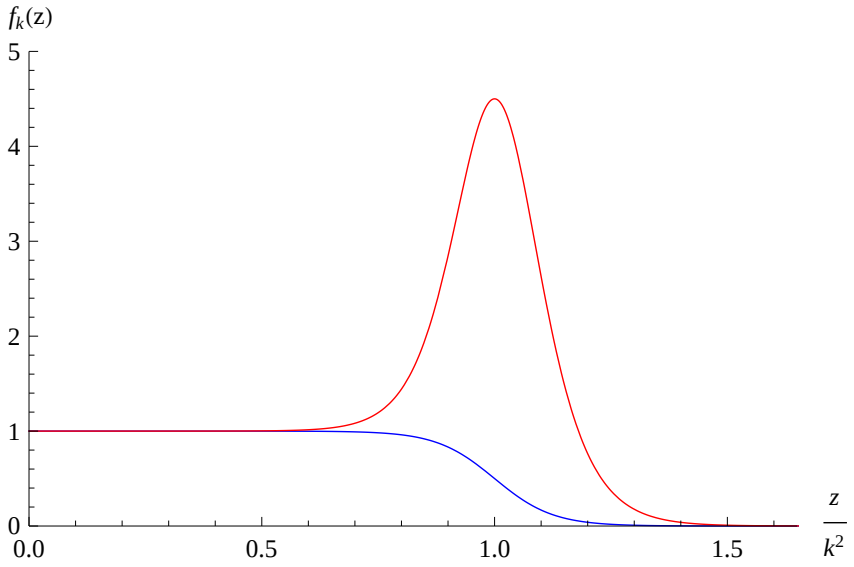

Figure 2.1: A typical non-singular cutoff profile function R_k (blue) and its scale derivative $k\partial_k R_k$ (red).

on modes with momenta near k^2, so that the trace remains divergence-free and locally well-defined in momentum space at all scales. As a consequence, while a theory might require a UV regulator at the level of its path integral, at the level of the FRGE this regularization is not needed. We can understand this point from a more heuristic perspective by noting that evolving $\Gamma_{\hat{k}}$ from an initial scale where it is well-defined to $\Gamma_{\hat{k}+\delta k}$ at a higher scale by means of the FRGE implies integrating over the field modes with momentum range restricted to δk, so the integration always remains convergent.

Secondly, while the FRGE is commonly derived and motivated via the use of a regularized path integral (however surreptitiously introduced, as above), and consequently of a UV bare action, in its usual presentation, its solutions are independent of $S_{\text{bare}}[\phi]$. The bare action will enter only as an initial condition of the flow at the formal level via $S[\phi]$ at $k = k_0$, but knowledge of it is not required to compute the beta functions of the theory and, hence, to follow the renormalization group flow of Γ_k. As the physics of a theory is carried by the renormalized, rather than bare, action, if we have a $\Gamma_{\hat{k}}$ correctly capturing the physics of the system at a particular scale $\hat{k}$, it is legitimate to use the FRGE to evolve this action to other scales to capture the new physics. In particular, owing to the convergence properties of the FRGE, it is legitimate to study Γ_k as $k \to \infty$ and the resulting limit (if existing) need not, and typically will not, coincide with the presumed S_{bare}. The issue of the relation between the effective average

action and the bare action in a path integral formalism has been addressed in a gravitational context in [71], where it was explicitly shown that, if one specifies a measure and a regularization scheme, it is in principle possible to recover a regularized path integral and a bare action from the renormalized trajectories of Γ_k, provided the limit $\Gamma_{k\to\infty}$ is well-defined. This issue was there christened the 'reconstruction problem'.

2.1.2 Renormalization and the UV regularized FRGE

The fact that the FRGE remains always locally well defined in momentum space and that the beta functions therein obtained encode the behavior of our effective field theory Γ_k at all energy scales does not, of course, imply that our theory will remain well defined at all energy scales. As we have discussed, a sufficient condition that a theory possess a well-defined UV limit is that it be attracted to a fixed point of its renormalization group flow as $k \to \infty$, i.e., that $\Gamma_{k\to\infty} = \Gamma^*$, where Γ^* is the fixed point action. Recalling that the set of all renormalization group trajectories in theory space which flow towards the fixed point as $k \to \infty$ define the UV critical surface $\mathcal{S}_{\rm UV}$, we can equivalently state this condition as the requirement that the theory lie on this UV critical surface.

To ensure that the theory be predictive, recall that we need to impose a second condition, namely, that the dimensionality of the UV critical surface be finite. As mentioned, the dimensionality of $\mathcal{S}_{\rm UV}$ is given by the number of relevant essential parameters in the theory. If the number of such parameters is finite, we only need to perform a finite number of experiments at some scale $\hat{k}$ to completely determine our position in theory space. The end result is a theory that in principle allows us to unambiguously compute observable quantities free from divergences at all energy scales - in other words, a theory that is asymptotically safe.

The property of the asymptotic safety of field theories has already been introduced previously. We have repeated it here to highlight two points. First, inasmuch as the asymptotic safety question is a question about the predictiveness of our physical theories, and hence something that is ultimately decided at the level of effective actions, the FRGE is a very good tool for tackling this question. Secondly, finding a complete renormalization group trajectory from $\Gamma_{k\to 0} = \Gamma$ to $\Gamma_{k\to\infty}$ by means of the FRGE is equivalent to solving our theory for all energy scales, without the need to employ any UV regularization.

One might wonder how Γ_k relates to an UV-regularized analogue. This question has been considered in detail in [71], and here we outline the argument therein presented. Introducing a UV cutoff Λ_c in the theory and appropriately regularizing the path integral in (2.2), we can define a UV-regularized effective average action Γ_{k,Λ_c} by essentially following the same steps as in (2.3)-(2.5). This action will satisfy the UV-regularized FRGE

$$k\partial_k \Gamma_{k,\Lambda_c}[\varphi] = \frac{1}{2}\mathrm{Tr}_{\Lambda_c}\left[\frac{k\partial_k \mathcal{R}_k}{\Gamma^{(2)}_{k,\Lambda_c} + \mathcal{R}_k}\right], \tag{2.9}$$

where the trace is restricted to the subspace of $\mathcal{O}$ spanned by eigenfunctions with eigenvalues $\lambda_i \leq \Lambda_c^2$. To remove the regulator from this equation, it is sufficient to assume that a profile function for the cutoff $\mathcal{R}_k$ is chosen such that the numerator in the regularized trace falls sufficiently fast to make the trace well-defined as $\Lambda_c \propto \infty$. The result is just the ordinary, regulator-free FRGE.

In addition, in the case of a generic cutoff profile function, the difference between the FRGE (2.6) and its UV-regulated analogue (2.9) is negligible for all $k \ll \Lambda_c$. This is due to the fact that for any $k \leq \Lambda_c$ the IR cutoff structure ensures that contributions from modes with $\lambda_i > \Lambda_c$ entering (2.6) decay very quickly - i.e., the contributions are still localized around k. As we can in principle make the cutoff Λ_c as large as we want, the two equations will virtually yield the same solutions for any finite k. In addition, for the particular case that the profile function is that of the optimized cutoff, $\mathcal{R}_k(z) = (k^2 - z)\theta(k^2 - z)$ [72], this difference vanishes and the solutions $\{\Gamma_{k,\Lambda}, 0 \leq k \leq \Lambda_c\}$ for the regularized FRGE become simply the restriction of the solutions $\{\Gamma_k, 0 \leq k \leq \infty\}$ of the regulator-free FRGE in the interval $k < \Lambda_c$. As all physically observable quantities are independent of $\mathcal{R}_k$, this argument will hold generally for any observable we may compute. Therefore, removing the UV regulator is a trivial procedure under the FRGE and the regulator-free Γ_k does indeed capture all the relevant physics.

2.1.3 Approximation schemes

In most cases, applications of the FRGE formalism in the study of the renormalization group properties of a theory rely on approximations of the full, exact flow. The reason for that can already be seen from the definition of the effective average action, namely, it is a functional defined in the infinite-dimensional theory space spanned by all the interaction monomials consistent with the symmetries of a theory and parametrized by all the couplings associated to these operators. Even if we started from a $\Gamma_{\hat{k}}$ at a particular scale containing only a finite number of non-zero couplings, there is no way of a priori knowing that other couplings will not be turned on by the flow as we move away from this initial condition. As it is generally impossible to follow the renormalization group flow of this infinite number of couplings, approximation schemes are required within the FRGE approach.

Perturbation theory

One possibility is the use of perturbation theory. In the one-loop approximation of the FRGE, all the couplings appearing on its right-hand side, including any couplings that may appear in the definition of the cutoff $\mathcal{R}_k$, are kept fixed to some k-independent value, so that the effective average action Γ_k appearing under the trace is effectively replaced by a fixed 'bare' action S. In this case, the FRGE describes the running of the one-loop effective action in dependence of the cutoff

k, i.e.,

$$k\partial_k \Gamma_k^{(1)}[\varphi] = \frac{1}{2}\mathrm{Tr}\left[\frac{k\partial_k \mathcal{R}_k}{S_k^{(2)} + \mathcal{R}_k}\right] . \tag{2.10}$$

Recalling that, given a bare action S, the one-loop effective action is given by

$$\Gamma^{(1)} = S + \frac{1}{2}\mathrm{Tr}\ln\left[\frac{\delta^2 S}{\delta\varphi\delta\varphi}\right] , \tag{2.11}$$

and introducing the cutoff term (2.1), we can see that the resulting one-loop effective average action,

$$\Gamma_k^{(1)} = S + \frac{1}{2}\mathrm{Tr}\ln\left[\frac{\delta^2 S}{\delta\varphi\delta\varphi} + \mathcal{R}_k\right] , \tag{2.12}$$

exactly satisfies the one-loop FRGE (2.10). When applied to familiar quantum field theories in this approximation, all well known beta functions are recovered [41, 65, 66]. Going beyond one-loop order, explicit sample computations showing that the FRGE correctly reproduces perturbation theory were considered in [73, 74].

Truncations

If, however, one is interested in the non-perturbative properties of the flow, no information will be gained by employing the perturbative scheme described above that may not be in principle recovered via other perturbation theory techniques. A common non-perturbative approximation scheme is the truncation of the renormalization group flow [61, 62, 65, 70], which is the procedure we will follow in this work. In this scheme, we make an ansatz for Γ_k which only retains a subset of all the interaction monomials in the theory, substitute this ansatz into the exact FRGE and thereby project the full renormalization group flow onto the subspace spanned by the truncation. Evaluating the right-hand side of the flow equation, discarding all the terms which are not in this truncated subspace and equating the coefficients of the remaining operators on both sides of the equation, we can then construct the beta function for the couplings parametrizing our space. In particular, these beta functions will contain genuine non-perturbative information. Depending on the number of couplings included in the ansatz, this procedure leads either to a coupled system of ordinary differential equations (finite number of couplings) or to a partial differential equation (infinite number of couplings) governing the scale-dependence of the truncated Γ_k.

A difficulty with this non-perturbative scheme is that of estimating the reliability of the truncation, since the truncations are not guided by an obvious small expansion parameter. In addition, in most cases the renormalization group flow will not close on the truncation subspace, so we are discarding terms that may potentially affect the running of the couplings we are retaining. Finding good

truncation subspaces thus generally requires some physics insight about the interaction terms which are relevant for describing the problem at hand and usually involves some educated guesswork.

In particular, with regards to the existence of fixed points, it is known that truncated flows can give rise to spurious fixed point solutions. The physical fixed points of the flow are those solutions that persist upon extending the truncated flow to the full theory space. This is well understood in the case of scalar field theory in the local potential approximation [61, 75], where it can be shown how physical solutions are recovered among all the apparent fixed points of the flow.

In more involved theories, however, where such general procedures are absent, the most important way of assessing the reliability of results established in a given truncation is checking their stability under the gradual extension of the truncation subspace. Results are considered to be reliable if all the relevant quantities computed in previous truncations, such as the values of fixed points and the dimensionless quantities in the theory, are not greatly affected by the presence of the new terms in the enlarged truncation and are seen to converge to given values. In this respect, when discussing the evidence for a non-trivial fixed point of gravity in the subsequent chapters, we should stress that the encouraging results are not only that such fixed point solutions have been found in all truncations studied, but also that these solutions share similar properties across those truncations. Hence, they constitute plausible candidates for the physical fixed point of the flow.

A second, indirect way of estimating the quality of the truncation is investigating the cutoff dependence of the results. While the choice of the cutoff profile function and of the differential operator entering the cutoff introduces a scheme dependence on the results, physical quantities computed within the formalism should be independent of these choices. Truncations, on the other hand, generally introduce spurious cutoff dependences, which can thus serve as further estimators of the quality of the approximation. Notably, this can also be used to one's advantage, so as to define an optimization criterion for the cutoff profile [72, 76] with respect to which such dependence is minimized and the truncated flow is rendered most stable.[2]

2.2 The FRGE in gravity

After reviewing the FRGE formalism, we can now start moving towards its application to the renormalization group flow of gravity. Since we will consider explicit forms of the gravitational FRGE and its truncations from the next chapter onwards, we will here focus rather on some general issues arising in the gravitational setting.

[2] For explicit examples of this optimization analysis, see [70, 75, 77, 78].

2.2.1 Diffeomorphism-invariance and flow equations

Following [35], our starting point for the effective average action in gravity is the diffeomorphism invariant action for d-dimensional *Euclidean* quantum gravity, $S[\gamma_{\mu\nu}]$. In contrast with the relatively simple case of scalar field theory from the previous section, a first possible complication arising here is the issue of gauge invariance. In order to assure that the IR cutoff does not interfere with diffeomorphism invariance and that our FRGE respects this symmetry, we employ the background field method, decomposing the metric $\gamma_{\mu\nu}$ into an arbitrary but fixed background field $\bar{g}_\mu\nu$ and a (not necessarily small) fluctuation field $h_{\mu\nu}$ via

$$\gamma_{\mu\nu} = \bar{g}_{\mu\nu} + h_{\mu\nu} \,, \tag{2.13}$$

and, crucially, construct the IR cutoff in terms of the background metric only, i.e., $\mathcal{R}_k(\bar{\mathcal{O}})$, where $\bar{\mathcal{O}}[\bar{g}]$.

Taking the gauge to have been fixed with gauge fixing term

$$S^{\rm gf}[h;\bar{g}] = \frac{1}{2}\int d^4x\sqrt{\bar{g}}\, F_\mu[h;\bar{g}]\, \bar{g}^{\mu\nu} F_\nu[h;\bar{g}] \,, \tag{2.14}$$

for some $F_\mu \sim \mathcal{F}_\mu^{\alpha\beta} h_{\alpha\beta}$, and resulting ghost fields $C_\mu, \bar{C}_\mu$ [3] and denoting the classical counterparts of the latter and of the metric fluctuations by c_μ, $\bar{c}_\mu$ and $\bar{h}_{\mu\nu}$, respectively, the effective average action for gravity is the functional

$$\Gamma_k[\bar{h}, c, \bar{c}; \bar{g}] \,. \tag{2.15}$$

Letting $g_{\mu\nu} \equiv \bar{g}_{\mu\nu} + \bar{h}_{\mu\nu}$ and defining the more convenient

$$\Gamma_k[g, \bar{g}, c, \bar{c}] \equiv \Gamma_k[g - \bar{g}, c, \bar{c}; \bar{g}] \,, \tag{2.16}$$

one can show this functional is invariant under the general coordinate transformations

$$\Gamma_k[\Phi + \mathcal{L}_v\Phi] = \Gamma[\Phi] \,, \quad \Phi \equiv \{g_{\mu\nu}, \bar{g}_{\mu\nu}, c_\mu, \bar{c}_\mu\} \,, \tag{2.17}$$

where $\mathcal{L}_v$ denotes the Lie derivative with respect to the vector field v^μ.

This functional obeys the FRGE

$$\begin{aligned} k\partial_k\Gamma_k[\bar{h}, c, \bar{c}] =& \frac{1}{2}{\rm Tr}\left[\frac{k\partial_k\mathcal{R}_k}{\Gamma_k^{(2)} + \mathcal{R}_k}\right]_{\bar{h}\bar{h}} + \frac{1}{2}{\rm Tr}\left[\frac{k\partial_k\mathcal{R}_{k,c\bar{c}}}{\left(\Gamma_k^{(2)} + \mathcal{R}_k\right)_{c\bar{c}}}\right] \\ & - \frac{1}{2}{\rm Tr}\left[\frac{k\partial_k\mathcal{R}_{k,c\bar{c}}}{\left(\Gamma_k^{(2)} + \mathcal{R}_k\right)_{\bar{c}c}}\right] \,, \end{aligned} \tag{2.18}$$

[3] For simplicity, we are assuming there are only two ghosts present, but the argument naturally generalizes to more of such fields.

where the cutoff has been imposed also on the ghost fluctuations and where we have defined

$$\left[\left(\Gamma_k^{(2)}\right)_{\bar{c}c}\right]_\mu^\nu = \frac{1}{\sqrt{\bar{g}}}\frac{\delta}{\delta c^\mu}\frac{1}{\sqrt{\bar{g}}}\frac{\delta\Gamma_k}{\delta\bar{c}_\nu}\,, \tag{2.19}$$

and

$$\left[\left(\Gamma_k^{(2)}\right)_{\bar{h}\bar{h}}\right]_{\mu\nu}^{\alpha\beta} = \frac{1}{\sqrt{\bar{g}}}\frac{\delta}{\delta g^{\mu\nu}}\frac{1}{\sqrt{\bar{g}}}\frac{\delta\Gamma_k}{\delta g_{\alpha\beta}}\,. \tag{2.20}$$

The ordinary effective action is obtained in the limit

$$\Gamma[g] = \lim_{k\to 0}\Gamma_k[g,g,0,0]\,. \tag{2.21}$$

Note that, unlike the case of perturbatively quantized gravity, the background metric $\bar{g}_{\mu\nu}$ is not a concretely fixed classical spacetime here, but rather an arbitrarily chosen metric that we introduce only at intermediate steps of the quantization. The quantity in which we are ultimately interested is $\bar{\Gamma}_k[g] \equiv \Gamma_k[g,g,0,0]$, which is what we would use to calculate all physical observables and which is a gauge invariant functional of one gauge field only. Following the renormalization group flow of this functional, however, requires us to retain the dependence on both the ghosts and background metric.

Lastly, note that, being constructed from the background field only, the IR cutoff $\mathcal{R}_k$ induces an extra background field dependence on the flow which, at the level of diffeomorphism invariance, leads to a modified Ward identity for Γ_k [35, 79, 81]. This modified Ward identity commutes with the flow and reduces to the standard Ward identity for $k \to 0$, since $\mathcal{R}_k$ vanishes in that limit by construction. Thus, exact solutions to the FRGE will preserve the gauge invariance of the full theory. For approximated solutions, however, this will not necessarily be the case. Deviations from these identities in truncated flows thus in principle serve as good estimators for the reliability of a truncation.

The issue of gauge invariance and background field dependence in the FRGE formalism has been reviewed in detail in [70,81] for the general case of non-Abelian gauge theories and an explicit analysis for Yang-Mills theories in the axial gauge can be found in [128]. A detailed analysis for the case of gravity, however, remains a challenging task.

2.2.2 Truncation ansatz and background field dependence

The last points above motivate the following remark [79]. As we have discussed, when performing calculations within the FRGE framework, we must employ approximation schemes, the most common non-perturbative one of which is the truncation of the theory space. In all but one [80] investigations of the gravitational renormalization group conducted within this framework, the flow has been projected onto a truncated subspace captured by the ansatz [4]

$$\Gamma_k[g,\bar{g},c,\bar{c}] = \bar{\Gamma}_k[g] + \hat{\Gamma}_k[g,\bar{g}] + S_{\rm gf}[g-\bar{g};\bar{g}] + S_{\rm gh}[g-\bar{g},c,\bar{c};\bar{g}]\,. \tag{2.22}$$

[4] The calculations in [80] consider the renormalization group running also in the ghost sector.

In this ansatz, the running of the ghosts has been neglected, $S_{\rm gh}$ being the classical ghost term, and the classical gauge-fixing term $S_{\rm gf}$ has been pulled out from Γ_k. In addition, the term $\bar{\Gamma}_k$ depends on the physical fields only and $\hat{\Gamma}_k$ encodes the deviations from $\bar{\Gamma}_k[g]$ for $g \neq \bar{g}$, vanishing for $g = \bar{g}$, and includes, e.g., the quantum corrections to the gauge-fixing sector. Noting that the classical terms are k-independent by definition, substituting (2.22) into (2.18) yields

$$k\partial_k\bar{\Gamma}_k[g] + k\partial_k\hat{\Gamma}_k[g,\bar{g}] = \frac{1}{2}\mathrm{Tr}\left[\frac{k\partial_k\mathcal{R}_k^{\rm grav}}{\Gamma_k^{(2)}[g,\bar{g}] + \mathcal{R}_k^{\rm grav}}\right] - \mathrm{Tr}\left[\frac{k\partial_k\mathcal{R}_k^{\rm gh}}{-\mathcal{M}[g,\bar{g}] + \mathcal{R}_k^{\rm gh}}\right], \tag{2.23}$$

with $\mathcal{M}$ being the Faddeev-Popov kinetic operator associated with (2.14) and where $\Gamma_k^{(2)}$ is a second functional derivative at fixed $\bar{g}_{\mu\nu}$ with respect to $g_{\mu\nu}$.

Nearly every truncation so far considered in the literature has additionally set $\hat{\Gamma}_k = 0$, in which case the FRGE above reduces to a flow equation for the single metric $g_{\mu\nu}$. The reasoning for the latter simplification is threefold. First, it has been suggested [35] that, at least at the level of the modified Ward identities of the theory, neglecting $\hat{\Gamma}_k$ is a good first approximation. Secondly, it has been argued that this is consistent with treating the theory at a fixed point of the gauge coupling [37, 81], which should be present in the flow. Lastly, and perhaps most importantly, treating bimetric truncations is a technically very challenging task. Also in the present work, the truncations analyzed will be of the form (2.22) with $\hat{\Gamma}_k = 0$. However, we should bear in mind that by neglecting this term we are throwing away all the $\bar{g}$-background dependence of the theory [79].

Over and above the arguments motivating these approximations, there is no a priori way of judging with certainty what the effect of these approximations may turn out to be. The outcome of recent studies that do not employ these simplifications is relatively encouraging. Results in initial investigations of the running of the ghost sector [80] exhibit little quantitative difference with the results previously otherwise obtained and suggest that the running of the ghost sector will largely decouple from the rest of the gravitational renormalization group flow. A study of bimetric $\hat{\Gamma}_k \neq 0$ truncations in a simplified setting [79], on the other hand, indicates that, while going beyond the $\hat{\Gamma}_k = 0$ approximation will not alter the qualitative picture that has been so far obtained, it will lead to quantitative differences with respect to the numerical values of the fixed points and critical coefficients and thus warrants further investigation.

2.3 Matter fields and cutoff schemes

Although we have so far considered flow equations for the case of pure gravity only, it is a relatively straightforward procedure to couple matter to the gravitational flow [82–84]. Wrapping up our introduction to the FRGE formalism in the present chapter, this will serve as a useful setting in which to illustrate how the cutoff is

implemented at the level of the flow equation, as well as the techniques commonly used for the evaluation of the functional traces it contains. The procedure outlined is essentially the same as for the pure gravity flow, but technically less involved. To this effect, let us consider the case of 4d gravity minimally coupled to n_S massless scalars fields ϕ, n_D massless Dirac fields ψ, and n_M massless Maxwell fields A_μ, and given by the ansatz

$$\begin{aligned}\Gamma_k[g,\bar{g},\phi,\psi,A_\mu] &= \Gamma_k^{\rm gr} + \Gamma^{\rm mat} \\ &= \Gamma_k^{\rm gr} + \int d^4x\sqrt{g}\sum\Big[\tfrac{1}{2}\nabla_\mu\phi\nabla^\mu\phi + \bar{\psi}D\psi \\ &\qquad + \big(\tfrac{1}{4}F_{\mu\nu}F^{\mu\nu} + \tfrac{1}{2}(\nabla^\mu A_\mu)^2 - \bar{c}\,\Box c\big)\Big]\,.\end{aligned} \tag{2.24}$$

Here, $\Gamma_k^{\rm gr}$ contains the pure gravity terms, which we will leave unspecified, $D = \gamma^a e_a{}^\mu\nabla_\mu$, is the Dirac operator with $e_a{}^\mu$ being the vierbein of $g_{\mu\nu}$, and we have fixed the Lorenz gauge for the Maxwell fields, leading to the last term above as the action for the ghost fields $\bar{c}, c$.

We wish to compute the contribution of this matter action to the gravitational beta functions up to the curvature-squared terms. The first step is to compute the second variations. Owing to the structure of the FRGE and the background field formalism, we are free to choose whichever background field configuration is most convenient to perform our calculations. The results thus obtained will be genuinely background independent, with the proviso that we might not be able to distinguish all the operators entering our truncation subspace in some backgrounds, rendering them unsuitable for our calculation - e.g., a flat metric background will not be able to distinguish any of the curvature monomials higher than zeroth order in a gravitational truncation, to take an extreme example. In the case of (2.24), we exploit this freedom to set $\psi = \bar{\psi} + \delta\psi$ with $\bar{\psi} = 0$, and similarly for the other matter fields, so that the second variations of the matter part of the ansatz are quadratic in the matter field fluctuations only and contain no cross terms, i.e.,

$$\begin{aligned}\delta^2\Gamma^{\rm mat} = \int d^4x\sqrt{\bar{g}}\sum\Big[&-\tfrac{1}{2}\delta\phi\Box\delta\phi + \delta\bar{\psi}\bar{D}\delta\psi - \tfrac{1}{2}\delta A_\nu\big(\bar{g}^{\mu\nu}\Box - \bar{R}^{\mu\nu}\big)\,\delta A_\mu \\ &+ \delta\bar{c}\Box\delta c\Big]\,,\end{aligned} \tag{2.25}$$

from which we may directly read off the Hessians for the individual fields.

Once the inverse propagators are computed, the cutoff must be implemented. At a general level, for a given field χ whose inverse propagator $\Gamma^{(2)}_{\chi\chi}$ is a function of the differential operator $\mathcal{O}$, the cutoff $\mathcal{R}_k^{\chi\chi}$ must be chosen such that it leads to the replacement

$$\mathcal{O} \to P_k(\mathcal{O}) \equiv \mathcal{O} + \mathcal{R}_k(\mathcal{O})\,. \tag{2.26}$$

Looking at the operator structure of (2.25), we can see we have a slight freedom in how to realize this prescription, depending on what we take to be $\mathcal{O}$. This is

our freedom to implement different cutoff schemes. Following the classification of [41], let us generally write $\mathcal{O} = -\nabla^2 + \mathbf{E}$, where D is a covariant derivative with respect to both the metric and possible gauge connections associated with the degrees of freedom of the field and $\mathbf{E}$ is a linear map acting on the field. Let us further split $\mathbf{E} = \mathbf{Q} + \mathbf{E}_k$, where $\mathbf{E}_k$ depends on the couplings of the theory and $\mathbf{Q}$ is coupling independent. We then call a "type I cutoff" the cutoff constructed from $-\nabla^2$ only, i.e., $\mathcal{R}_k(-\nabla^2)$; "type II cutoff", the cutoff built via $\mathcal{R}_k(-\nabla^2+\mathbf{Q})$, and lastly, "type III cutoff", or spectrally adjusted cutoff, the cutoff built from $\mathcal{R}_k(-\nabla^2 + \mathbf{E})$.

In the case of our matter Hessians, we implement a type II cutoff with the potentials

$$Q_S = 0\,, \quad Q_D = \frac{R}{4}\,, \quad Q_M = Ric\,, \quad Q_{\rm gh} = 0\,, \tag{2.27}$$

where Ric maps vectors onto vectors via $\mathrm{Ric}(B)_\mu = R^\nu_\mu B_\nu$. Letting $\mathcal{O}_I \equiv -\nabla^2 + Q_I$ for the field species I and inverting the modified propagators $\Gamma^{(2)}(\mathcal{O}_I) + \mathcal{R}_k(\mathcal{O}_I)$, we arrive at the FRGE

$$\begin{aligned} k\partial_k\Gamma_k = &\frac{n_S}{2}\mathrm{Tr}\left[\frac{k\partial_k\mathcal{R}_k(\mathcal{O}_S)}{P_k(\mathcal{O}_S)}\right] - \frac{n_D}{2}\mathrm{Tr}\left[\frac{k\partial_k\mathcal{R}_k(\mathcal{O}_D)}{P_k(\mathcal{O}_D)}\right] \\ &+ \frac{n_M}{2}\mathrm{Tr}\left[\frac{k\partial_k\mathcal{R}_k(\mathcal{O}_M)}{P_k(\mathcal{O}_M)}\right] - n_M\mathrm{Tr}\left[\frac{k\partial_k\mathcal{R}_k(\mathcal{O}_M)}{P_k(\mathcal{O}_M)}\right]\,, \end{aligned} \tag{2.28}$$

where we have omitted the pure gravity traces on the right-hand side.

The crucial step is now the evaluation of the traces. At a general level, the truncations we may consider when investigating the renormalization group flow of gravity are limited only by our ability to evaluate the traces. While in some particular situations traces may be performed by explicitly carrying out the spectral sum (e.g. [67, 80, 85]), a common computational technique is the asymptotic expansion of the heat kernel, which we will briefly review.

Let $\mathrm{Tr}W(\mathcal{O})$ be the functional trace we are interested in evaluating for d-dimensional spacetime and, for simplicity, let us assume $\mathcal{O}$ is a minimal operator of order 2 which commutes with all the other quantities inside the trace. Introducing $\tilde{W}(s)$ as the Laplace anti-transform of $W(z)$, we can write

$$\mathrm{Tr}W(\mathcal{O}) = \int_0^\infty ds\,\mathrm{Tr}\,e^{-s\mathcal{O}}\tilde{W}(s)\,. \tag{2.29}$$

Recalling that the trace of the heat kernel of $\mathcal{O}$ has the known asymptotic expansion for $s \to 0$,

$$\begin{aligned} \mathrm{Tr}e^{-s\mathcal{O}} = \frac{1}{(4\pi)^{\frac{d}{2}}}\int d^dx\sqrt{g}\Big[&\mathrm{tr}\mathbf{b}_0(\mathcal{O})s^{-\frac{d}{2}} + \mathrm{tr}\mathbf{b}_2(\mathcal{O})s^{-\frac{d}{2}+1} + \dots \\ &+ \mathrm{tr}\mathbf{b}_d(\mathcal{O}) + \mathrm{tr}\mathbf{b}_{d+2}(\mathcal{O})s + \dots\Big] \end{aligned} \tag{2.30}$$

where the heat kernel coefficients $\mathbf{b}_n$ are linear combinations of curvature tensors and their derivatives of order $2n$ in the derivatives of the metric, and defining

$$Q_n[W] = \int_0^\infty ds\, s^{-n} \tilde{W}(s) \tag{2.31}$$

and $B_n = \int d^d x \sqrt{g} \mathrm{tr} \mathbf{b}_n$, we arrive at

$$\begin{aligned} \mathrm{Tr} W(\mathcal{O}) = \frac{1}{(4\pi)^{\frac{d}{2}}} \Big[& Q_{\frac{d}{2}}(W) B_0(\mathcal{O}) + Q_{\frac{d}{2}-1}(W) B_2(\mathcal{O}) + \dots \\ & + Q_0(W) B_d(\mathcal{O}) + Q_{-1}(W) B_{d+2}(\mathcal{O}) + \dots \Big] . \end{aligned} \tag{2.32}$$

Making use of the Mellin transform, the functional $Q_n[W]$ can be reexpressed in terms of the original function $W(z)$,

$$Q_n[W] = \frac{(-1)^i}{\Gamma(n+i)} \int_0^\infty dz\, z^{n+i-1} \frac{d^i W(z)}{dz^i} , \quad i > -n\,,\ i \in \mathbb{N}\,. \tag{2.33}$$

For $n > 0$ and $n \leq 0 \in \mathbb{Z}$, it is convenient to choose $i = 0$ and $i = -n + 1$, respectively. Then, assuming that $\lim_{z\to\infty} W(z) = 0$ sufficiently fast, (2.33) simplifies to

$$\begin{aligned} Q_n[W] &= \frac{1}{\Gamma(n)} \int_0^\infty dz\, z^{n-1}\, W(z)\,, \quad n > 0\,, \\ Q_{-\tilde{n}}[W] &= (-1)^{\tilde{n}} \left. \frac{d^{\tilde{n}} W(z)}{dz^{\tilde{n}}} \right|_{z=0} , \quad \tilde{n} = -n \in \mathbb{N}\,. \end{aligned} \tag{2.34}$$

This includes the special case $Q_0[W] = W[0]$. For the techniques for calculating the heat kernel coefficients of a differential operator, as well as their expressions for the cases of particular operators we have considered in this work, we refer to Appendix D.

Applying the algorithm just outlined to (2.28), we find

$$\begin{aligned} k\partial_k \Gamma_k = & \frac{1}{2} \frac{1}{(4\pi)^2} \int d^4x \sqrt{g} \Big\{ (n_S - 4n_D + 2n_M) Q_2 \left(\frac{k\partial_k R_k}{P_k} \right) \\ & + \frac{1}{6} \bar{R} (n_S + 2n_D - 4n_M) Q_1 \left(\frac{k\partial_k R_k}{P_k} \right) \\ & + \frac{1}{180} \Big[(3n_S + 18n_D + 36n_M) \bar{C}^2 - (n_S + 11n_D + 62n_M) \bar{E} \\ & + 5n_S \bar{R}^2 + 12(n_S + n_D - 3n_M) \bar{\nabla}^2 \bar{R} \Big] + \mathsf{O}(\bar{\nabla}^6) \Big\} , \end{aligned} \tag{2.35}$$

where $\bar{C}^2$ is the square of Weyl's tensor, $\bar{E}$ is the integrand of Euler's topological invariant in four dimensions and $\mathsf{O}(\bar{\nabla}^6)$ represents curvature invariants of order

six in the derivatives of the metric. Finally, the contribution of the matter fields to the running of the couplings can be read off from the coefficients of the associated operators on the right-hand side.

Before ending this chapter, let us briefly comment on the issue of scheme-dependence. As we have mentioned, the cutoff function will introduce some scheme dependence into Γ_k, in a manner not dissimilar to the scheme dependence of the renormalized effective action in perturbative QFT. However, we do expect some quantities to be scheme independent, as is also the case in perturbation theory. In particular, the beta-functions of the dimensionless couplings should be universal quantities and not depend on our cutoff choice. And indeed, considering (2.35), we can see that the coefficients in front of the four-derivative terms, which will enter the beta-functions of the dimensionless couplings, do not depend on R_k.

Having covered most of the essential groundwork, we can now start exploring the non-perturbative renormalization group flow behavior of gravity in explicit settings.

3

Gravitational truncations in the conformal sector

Based on P. F. Machado and R. Percacci, *Conformally reduced quantum gravity revisited*, Phys. Rev. D 80, 024020 (2009), arXiv:0904.2510 [hep-th].

In this chapter, we apply the functional renormalization group equation to the study of matter-coupled four-dimensional gravity, in the approximation where only the conformal factor is dynamical. We consider truncations of the effective average action containing local terms up to second order in curvature as well as non-local terms responsible for the conformal anomaly of massless matter fields. We describe two ways of defining the renormalization group flow of gravity within this approximation, which respectively break or preserve Weyl invariance, and discuss the existence of fixed points of the resulting flows.

3.1 Conformally reduced gravity

Although the conformal factor is not dynamical in classical general relativity, in quantum gravity its fluctuations could be as important, or even more important, than those of the spin two components of the metric. It may thus be instructive to study a toy version of quantum gravity where only the conformal part of the metric is allowed to fluctuate. We will refer to this theory as conformally reduced quantum gravity.

As we have discussed in Chapter 2, the renormalization group running of the gravitational couplings can be fruitfully investigated by means of the functional renormalization group equation (FRGE) framework. While the main focus of studies within this approach has been on the UV behavior of gravity, with the aim of establishing the existence of a non-trivial fixed point in accordance with the asymptotic safety scenario, this type of analysis can also be applied to IR physics, and there have been works suggesting that the renormalization group running

is responsible for astrophysical [86–89] and cosmological [90, 91] effects. Most calculations within this approach have been carried out by taking into account all the degrees of freedom of the metric, but, recently, this method has been applied also to conformally reduced gravity [67, 85].

In the present chapter, we will use the FRGE to study the renormalization group flow of matter-coupled conformally reduced gravity. From a physical point of view, it is not clear that this severe restriction to the conformal sector still captures the essential features of gravity. On the one hand, this sector has been argued to drive gravitational dynamics in the extreme infrared [68, 92–96] and, in the study of certain conformally reduced truncations within the FRGE approach [67, 85], it was also shown to yield a UV fixed point with the same qualitative features as those obtained in the case of full gravity. On the other hand, by disregarding the effect of the transverse gravitons, sidestepping the issue of gauge fixing and essentially reducing the dynamics of gravity to that of a scalar field, we can expect that due to this simplification important physics is neglected. From a theoretical point of view, however, the conformal reduction serves at least as a good theoretical laboratory in which to test various ideas and, from the FRGE perspective, first investigate the gravitational renormalization group running in the presence of interaction terms which may not be technically treatable at present in the case of full gravity. The non-local truncations we will shortly analyze provides an example of such technically cumbersome terms.

While gravity at the classical level is captured by the Einstein-Hilbert action, and while the latter serves as the starting point for perturbative quantization, at the quantum level other terms may also play a significant role. At very high energies, higher derivative terms become important and must be included in an effective field theory treatment of (quantum) gravitational interactions. At very low energies, on the other hand, non-local terms are expected to become relevant. Among the latter, particularly interesting are those coming from the Riegert action [97], which reproduces the trace anomaly of the stress-energy tensor, or conformal anomaly, induced by the quantum matter fields. It is non-local terms of this form that will be included in the conformally reduced truncations studied in this chapter.

The dynamics of conformally reduced gravity including such terms has been previously studied in a series of papers by Antoniadis, Mazur and Mottola [68, 92–96, 98]. Following the logic of two-dimensional conformal field theories, it was argued in these papers that the theory possesses an infrared (IR) fixed point in its renormalization group flow, which could lead to screening of the cosmological constant and simulate dark energy [57, 99–101].

Establishing a relation between the beta functions computed by Antoniadis and Mottola [68] and the FRGE beta functions is one of the goals of the work presented here. Anticipating our results, we shall see that Antoniadis and Mottola's beta functions can be obtained from the FRGE within certain approximations, but applying a procedure that breaks scale invariance. We will explain and comment on this statement in detail in the following sections.

3.1.1 The dynamics of the conformal factor

We will now describe our approach to the dynamics of the conformal factor, emphasizing possible alternatives. We will use the background field method (viz. Section 2.2.1) and, following the procedure used both by Antoniadis et al. and in [67, 85], we will first fix a fiducial metric $\hat{g}_{\mu\nu}$ and consider only metrics which are conformally related to $\hat{g}_{\mu\nu}$,

$$g_{\mu\nu} = \phi^2 \hat{g}_{\mu\nu} \ . \tag{3.1}$$

The function ϕ is the conformal factor whose dynamics we wish to study. Because it cannot vanish, we can choose it to be positive, and in the following we will find it convenient to write $\phi = e^{\sigma}$. The role of $\hat{g}_{\mu\nu}$ is to identify a conformal equivalence class of metrics and to provide a reference point in this equivalence class. When restricted to the chosen conformal equivalence class, the action, which originally is a functional of $g_{\mu\nu}$, becomes a functional of $\hat{g}_{\mu\nu}$ and ϕ, or equivalently of $\hat{g}_{\mu\nu}$ and σ, which we will denote

$$\hat{S}(\hat{g}_{\mu\nu}, \sigma) = S(e^{2\sigma}\hat{g}_{\mu\nu}) = S(g_{\mu\nu}) \ . \tag{3.2}$$

No approximation is involved in this step. Note that by construction $\hat{S}$ is invariant under the transformation

$$(\hat{g}_{\mu\nu}, \sigma) \mapsto (e^{2\omega}\hat{g}_{\mu\nu}, \sigma - \omega) \ , \tag{3.3}$$

for any function ω. We will refer to this as a Weyl transformation of $\hat{g}_{\mu\nu}$. A priori, there is a slight risk of confusion between these transformations and Weyl transformations of $g_{\mu\nu}$, which are transformations $g_{\mu\nu} \mapsto e^{2\omega} g_{\mu\nu}$ [1]. We will always try to make this difference clear.

We then apply the background field method to the conformal factor only. In principle, there are different ways of doing this. In [67, 85] the conformal factor is expanded as

$$\phi = \bar{\phi} + \delta\phi \ , \tag{3.4}$$

where $\bar{\phi}$ is the background. Alternatively, one could write $\phi = e^{\sigma}$, $\bar{\phi} = e^{\bar{\sigma}}$ and expand

$$\sigma = \bar{\sigma} + \delta\sigma \ . \tag{3.5}$$

Although these two procedures lead to similar results, they are not strictly speaking equivalent within the truncation approximation we will subsequently employ. In this paper we will follow the latter procedure, as it is better adapted to the action of Weyl transformations.

When σ is decomposed as in (3.5), the transformation (3.3) can be attributed either to the fluctuation $\delta\sigma$ or to the background $\bar{\sigma}$. In the first case, we

[1] Note that if the original action is Weyl invariant, in the sense that $S(e^{2\omega}g_{\mu\nu}) = S(g_{\mu\nu})$, then $\hat{S}$ is independent of σ.

speak of "quantum Weyl transformations", in the second, of "background Weyl transformations". It is the latter transformations

$$(\hat{g}_{\mu\nu}, \bar{\sigma}, \delta\sigma) \mapsto (e^{2\omega}\hat{g}_{\mu\nu}, \bar{\sigma} - \omega, \delta\sigma) \tag{3.6}$$

that one can preserve when using the background field method, as we shall discuss in Section 3.2.2. We should also note that this group does not play the role of a gauge group, since it acts nontrivially on $\hat{g}_{\mu\nu}$, while in the conformal reduction we only treat σ as a quantum field.

3.1.2 A non-local conformal truncation

In this section we specify the class of gravitational actions we will study via the FRGE. We emphasize again that these functionals will not be used as bare actions in the definition of a functional integral, but rather as approximate forms for a coarse-grained quantum effective action - i.e., they constitute the terms entering our truncation of the conformally reduced gravitational renormalization group flow. With this proviso in mind, we will simply call these functionals "actions". They will consist of one part which is local in the metric $g_{\mu\nu}$ and another part which can be seen as coming from the quantum loops of matter fields, and which is non-local when written as a functional of $g_{\mu\nu}$. Restricting ourselves to terms with at most four derivatives, the local part is

$$S(g_{\mu\nu}) = \int dx \sqrt{g} \left[g_0 + g_2 R + g_4 R^2 \right] \ , \tag{3.7}$$

where g_i are coupling constants of mass dimension $4-i$. There are other terms one can write with four derivatives, but they are either total derivatives (the Euler term, $\Box R$), or invariant under Weyl transformations of $g_{\mu\nu}$ (the Weyl tensor squared), and therefore independent of σ. Using (3.1) in (3.7) and defining $\hat{\Box} = \hat{\nabla}^2$, we have

$$\begin{aligned} \hat{S}(\hat{g}_{\mu\nu}, \sigma) = \int dx \sqrt{\hat{g}} \Big[& g_0 e^{4\sigma} + g_2 e^{2\sigma} (\hat{R} - 6\hat{\Box}\sigma - 6(\hat{\nabla}\sigma)^2) \\ & + g_4 (\hat{R} - 6\hat{\Box}\sigma - 6(\hat{\nabla}\sigma)^2)^2 \Big] \ . \end{aligned} \tag{3.8}$$

In the following, we will need the linearized form of this expression. Decomposing σ as in (3.5), and expanding to second order in $\delta\sigma$,

$$\begin{aligned} \hat{S}^{(2)} = \int dx \sqrt{\hat{g}}\, \delta\sigma \Big\{ & 8 g_0 e^{4\bar{\sigma}} + 2 e^{2\bar{\sigma}} g_2 \big[\hat{R} - 6\hat{\Box}\bar{\sigma} - 6^2 (\hat{\nabla}\bar{\sigma})^2 - 6\hat{\nabla}^\mu \bar{\sigma} \hat{\nabla}_\mu - 3\hat{\Box} \big] \\ & + g_4 \big[-144 \hat{\Box}\bar{\sigma}\hat{\nabla}^\mu\bar{\sigma}\hat{\nabla}_\mu - 144 \hat{\nabla}^\mu (\hat{\nabla}\bar{\sigma})^2 \hat{\nabla}_\mu + 12 \hat{\nabla}^\mu \hat{R} \hat{\nabla}_\mu \\ & + 144 \hat{R}^{\mu\nu} \hat{\nabla}_\mu \bar{\sigma} \hat{\nabla}_\nu - 72 (\hat{\nabla}\bar{\sigma})^2 \hat{\Box} - 144 \hat{\Box}\bar{\sigma}\hat{\Box} + 12 \hat{R}\hat{\Box} \\ & + 144 (\hat{\nabla}^\mu \hat{\nabla}^\nu \bar{\sigma} - \hat{\nabla}^\mu \bar{\sigma} \hat{\nabla}^\nu \bar{\sigma}) \hat{\nabla}_\mu \hat{\nabla}_\nu + 36 \hat{\Box}^2 \big] \Big\} \delta\sigma \ . \end{aligned} \tag{3.9}$$

In addition, we will also consider the effect of minimally coupled massless matter. Introducing n_S scalar fields ϕ, n_D Dirac fields ψ and n_M Maxwell fields A_μ, the (gauge fixed) matter part of the action reads

$$S_{\rm mat} = \int d^4x\sqrt{g}\sum\Big\{\,\big[\tfrac{1}{4}F_{\mu\nu}F^{\mu\nu} + \tfrac{1}{2}(\nabla^\mu A_\mu)^2 - \bar{c}\,\Box c\big] + \tfrac{1}{2}\nabla_\mu\phi\nabla^\mu\phi + \bar{\psi}D\psi\Big\}\,, \tag{3.10}$$

where the sums extend over all particle species. Here, $D = \gamma^a e_a{}^\mu\nabla_\mu$, is the Dirac operator ($e_a{}^\mu$ is the vierbein of $g_{\mu\nu}$) and the third term above is the action for the ghost fields $\bar{c}, c$, which arise when fixing the Lorenz gauge for the Maxwell fields. Performing the conformal reduction (3.1) and applying the background field method with the matter background fields set to zero, the second variation of the matter and ghost parts of the action is then given by

$$\begin{aligned} S^{(2)}_{\rm mat} = \int d^4x\sqrt{\hat{g}}\sum\Big\{ &-\tfrac{1}{2}\delta A_\nu\Big[\hat{g}^{\mu\nu}(\hat{\Box} + 2\hat{\nabla}^\lambda\bar{\sigma}\hat{\nabla}_\lambda + \hat{\Box}\bar{\sigma} + 2(\hat{\nabla}\bar{\sigma})^2) \\ &- (R^{\mu\nu} - 2\hat{\nabla}^\mu\hat{\nabla}^\nu\bar{\sigma} + 2\hat{\nabla}^\mu\bar{\sigma}\hat{\nabla}^\nu\bar{\sigma})\Big]\delta A_\mu \\ &+ e^{2\bar{\sigma}}\delta\bar{c}\left(\hat{\Box} + 2\hat{\nabla}^\mu\bar{\sigma}\hat{\nabla}_\mu\right)\delta c - \tfrac{1}{2}e^{2\bar{\sigma}}\delta\phi\left(\hat{\Box} + 2\hat{\nabla}^\mu\bar{\sigma}\hat{\nabla}_\mu\right)\delta\phi \\ &+ e^{3\bar{\sigma}}\delta\bar{\psi}\left(\hat{D} + \gamma^a e_a{}^\mu\hat{\Phi}_\mu\right)\delta\psi\Big\}\,, \end{aligned} \tag{3.11}$$

where $\hat{\Phi}_\mu \equiv 2\hat{e}_{a\mu}\hat{e}_b{}^\nu\partial_\nu\sigma\Sigma^{ab}$ and Σ^{ab} is the connection. As we have seen in Section 2.3 for the case of full gravity, these matter fields will contribute to the beta functions of the gravitational couplings g_0, g_2, g_4. This is a purely local effect, which is related to the appearance of UV divergences when the cutoff goes to infinity. On the other hand, the presence of matter fields also gives rise to non-local terms, among which there are those responsible for the conformal anomaly [102],

$$\langle T^\mu{}_\mu\rangle = \frac{2}{\sqrt{g}}g_{\mu\nu}\frac{\delta\Gamma}{\delta g_{\mu\nu}} = b\,C^2 + b'E + \left(b'' + \frac{2}{3}b\right)\Box R\ , \tag{3.12}$$

where $T_{\mu\nu}$ is the stress-energy tensor. Here, $E = R_{\mu\nu\rho\sigma}R^{\mu\nu\rho\sigma} - 4R_{\mu\nu}R^{\mu\nu} + R^2$ is the integrand of the Euler invariant, $C^2 = C_{\mu\nu\rho\sigma}C^{\mu\nu\rho\sigma}$ is the square of the Weyl tensor, and the coefficients b and b' are related to the number and species of matter fields and read

$$\begin{aligned} b &= \frac{1}{120(4\pi)^2}\,(n_S + 6n_D + 12n_M)\,, \\ b' &= -\frac{1}{360(4\pi)^2}\,(n_S + 11n_D + 62n_M)\,. \end{aligned} \tag{3.13}$$

Since the last term in (3.12) can be obtained from the variation of a local counterterm proportional to $\int dx\sqrt{g}R^2$, the coefficient b'' is arbitrary. This term

is already accounted for in the local action (3.7), and for convenience we will assume that g_4 has been redefined in such a way that $b'' + \frac{2}{3}b = -\frac{2}{3}b'$.

The remaining two terms in the conformal anomaly (3.12) cannot be obtained as the variation of a local functional. Following [68], those non-local counterterms responsible for generating this remaining part of the anomaly will also be taken into account. They constitute the Riegert action [97] and are given by

$$W(g_{\mu\nu}) = \frac{1}{8}\int dx\,\sqrt{g}\left(E - \frac{2}{3}\Box R\right)\Delta_4^{-1}\left[2b\,C^2 + b'\left(E - \frac{2}{3}\Box R\right)\right] , \qquad (3.14)$$

where Δ_4 is the conformally covariant fourth-order operator

$$\Delta_4 = \Box^2 + 2R^{\mu\nu}\nabla_\mu\nabla_\nu - \frac{2}{3}R\Box + \frac{1}{3}\nabla^\mu R\nabla_\mu \ . \qquad (3.15)$$

We should note that the non-local operators resulting from this action cannot currently be treated by FRGE methods in the full gravity case. This motivates their study in a conformally reduced setting.

The defining property of this functional is that its variation under an infinitesimal conformal transformation reproduces (3.12). At the expense of introducing an additional auxiliary field, one can also define a local functional having the same property. This so called Wess–Zumino action is (minus) the change of the Riegert action under a finite conformal transformation,

$$\Gamma_{WZ}(g_{\mu\nu},\sigma) = -W(e^{2\sigma}g_{\mu\nu}) + W(g_{\mu\nu}) \ . \qquad (3.16)$$

It is explicitly given by

$$\Gamma_{WZ}(g_{\mu\nu},\sigma) = -\int dx\,\sqrt{g}\left\{b\,C^2\sigma + b'\left[\left(E - \frac{2}{3}\Box R\right)\sigma + 2\sigma\Delta_4\sigma\right]\right\} , \qquad (3.17)$$

and, by construction, it satisfies the "cocycle" condition (also called the Wess-Zumino consistency condition),

$$\Gamma_{WZ}(e^{2\omega}g_{\mu\nu},\sigma-\omega) - \Gamma_{WZ}(g_{\mu\nu},\sigma) + \Gamma_{WZ}(g_{\mu\nu},\omega) = 0 \ . \qquad (3.18)$$

Although σ plays the role of a conformal transformation in (3.16), we can think of it as a new scalar field, transforming under Weyl transformations as in (3.3). Then, by equation (3.18), the Wess–Zumino action has the same transformation as the non-local Riegert action (this property motivates the sign in the definition of Γ_{WZ}).

Let us now treat the functional W in the same way as the local action (3.7). As in (3.2), we first define $\hat{W}(\hat{g}_{\mu\nu},\sigma) \equiv W(e^{2\sigma}\hat{g}_{\mu\nu})$, and from equation (3.16) we then see that

$$\hat{W}(\hat{g}_{\mu\nu},\sigma) = W(g_{\mu\nu}) = W(\hat{g}_{\mu\nu}) - \Gamma_{WZ}(\hat{g}_{\mu\nu},\sigma) \ . \qquad (3.19)$$

Using equations (3.16) and (3.18), one can check that this functional is indeed invariant under the Weyl transformations (3.3). Of course, if one is only interested in the dynamics of the conformal factor for a fixed fiducial metric, the first term on the right-hand side can be ignored, but one should remember that it is essential for Weyl invariance.

Next, we introduce the background field decomposition (3.5) for σ. Defining the background metric $\bar{g}_{\mu\nu} = e^{2\bar{\sigma}}\hat{g}_{\mu\nu}$ and again using (3.18) and (3.16), we can write (3.19) as

$$\hat{W}(\hat{g}_{\mu\nu}, \sigma) = W(\bar{g}_{\mu\nu}) - \Gamma_{WZ}(\bar{g}_{\mu\nu}, \delta\sigma) \ . \tag{3.20}$$

Note that only the second term depends on the quantum field $\delta\sigma$. From (3.17), we thus see that the expansion of W to second order in the fluctuation is

$$\hat{W}^{(2)} = 2b' \int dx \, \sqrt{\hat{g}} \, \delta\sigma \hat{\Delta}_4 \delta\sigma = 2b' \int dx \, \sqrt{\bar{g}} \, \delta\sigma \bar{\Delta}_4 \delta\sigma \ , \tag{3.21}$$

where $\hat{\Delta}_4$ and $\bar{\Delta}_4$ are the operators (3.15) constructed with the metrics $\hat{g}_{\mu\nu}$ and $\bar{g}_{\mu\nu}$ respectively.

3.2 Conformally reduced quantum gravity revisited

3.2.1 The FRGE and the conformal anomaly

In order to extract the beta functions of the theory, we make use of the Functional Renormalization Group Equation (FRGE)

$$\partial_t \Gamma_k = \frac{1}{2} \mathrm{STr} \left[\left(\frac{\delta^2 \Gamma_k}{\delta \mathbf{\Phi} \delta \mathbf{\Phi}} + \mathcal{R}_k \right)^{-1} \partial_t \mathcal{R}_k \right] , \tag{3.22}$$

which, as discussed in Chapter 2, describes the dependence of a coarse-grained effective action $\Gamma_k[\mathbf{\Phi}]$ on a momentum scale k. Recall that, here, $t := \log k/k_0$, $\mathbf{\Phi}$ are all the fields present in the theory, STr is a functional (super)trace and $\mathcal{R}_k$ is an infrared cutoff suppressing the contributions to the trace of eigenmodes with momenta below k. The coarse-grained effective action reduces to the ordinary effective action in the limit $k \to 0$.

In the sequel, we will apply the FRGE to compute the beta functions of conformally reduced gravity, in the spirit of the previous section. This means that (in addition to the matter fields) the only quantum field that we allow to fluctuate is the conformal factor σ (or equivalently ϕ) and the truncated running effective action is assumed to have the form

$$\begin{aligned} \Gamma_k(\hat{g}_{\mu\nu}, \sigma, \psi) &= \hat{S}(\hat{g}_{\mu\nu}, \sigma) + \hat{W}(\hat{g}_{\mu\nu}, \sigma) + \hat{S}_{\mathrm{mat}}(\hat{g}_{\mu\nu}, \sigma, \psi) \\ &\equiv \Gamma_k^{\mathrm{grav}}(\hat{g}_{\mu\nu}, \sigma) + \hat{S}_{\mathrm{mat}}(\hat{g}_{\mu\nu}, \sigma, \psi) \end{aligned} \tag{3.23}$$

where $\hat{S}$, $\hat{S}_{\rm mat}$ and $\hat{W}$ are given by equations (3.8), (3.11), (3.19), and ψ collectively denotes all matter fields. However, not all terms will run. $\hat{S}_{\rm mat}$ does not change because the fields have no self-interactions and $\hat{W}$ does not change because its coefficients b and b' are fixed functions of the number of matter fields. Thus, only the renormalization group flow of the couplings g_0, g_2 and g_4 will be calculated, while $\hat{W}$ and $\hat{S}_{\rm mat}$ will be kept fixed.

Although only ψ and σ fluctuate, the action still depends parametrically upon the fiducial metric $\hat{g}_{\mu\nu}$ and, as long as the Weyl invariance (3.3) is preserved, the running effective action Γ_k can be regarded as a functional of a single metric $g_{\mu\nu}$. When quantizing and regularizing the theory of the conformal factor described by some action $\hat{S}(\hat{g}, \sigma)$, one faces a choice. The cutoff can be either constructed with the fiducial metric $\hat{g}$ or with the background metric $\bar{g}_{\mu\nu}$ [103]. The former choice breaks the invariance (3.3), because it introduces a dependence on $\hat{g}$ which is not accompanied by a corresponding dependence on σ. The latter choice instead respects the invariance. We shall therefore call these two procedures the "Weyl–breaking" and the "Weyl–invariant" procedure respectively (and we emphasize here that we refer to the Weyl transformations of the metric $\hat{g}_{\mu\nu}$, not of the metric $g_{\mu\nu}$).

These considerations apply both to UV and IR cutoffs. A UV cutoff can be regarded as part of the definition of the functional integral. In this context, the "Weyl–breaking" procedure corresponds to using a translation invariant measure, (formally $\int(d\sigma)$) while the "Weyl–invariant" procedure corresponds to using a Weyl–invariant measure (formally $\int(d\phi) = \int(e^{\sigma} d\sigma)$ [2], and similar considerations also apply to the integration measures over the matter fields. Within the FRGE approach, however, since the beta functions encode the dependence of the renormalized, rather than bare, couplings on the coarse graining scale k, these UV issues are immaterial. As we have discussed, even though the FRGE is commonly formally derived from a functional integral requiring a UV regulator in order to be defined, the trace on the right-hand side of (3.22) is automatically UV-convergent due to the properties of the IR cutoff $\mathcal{R}_k$. Therefore, there is no need to specify any UV regulator. In the following sections, when we talk about Weyl–invariant and Weyl–breaking procedures, we refer to the construction of the IR cutoff $\mathcal{R}_k$, which is used to define the coarse graining of the effective action.

Still, to avoid possible misunderstandings, it is useful to comment here on the significance of the anomaly in the context of the FRGE. The conformal anomaly arises when the "classical" bare action is Weyl invariant but the measure is not, and hence neither is the quantum effective action. This is true also for the coarse-grained affective action Γ_k, for any value of the coarse graining (IR cutoff) scale k. In an "anomalous" theory, the running effective action will thus be noninvariant even in the limit $k \to \infty$, if the limit exists. Now, one could take the point of view that the functional integral and the bare action are merely formal constructions devoid of physical content, and that all the physics is contained in the running

[2] See [104, 105] for a discussion of these integration measures.

effective action Γ_k. One would then never see an "anomaly", but rather one would simply have a quantum theory where Weyl invariance is broken at all scales. The "anomaly" would only be seen if one tried to reconstruct the "classical" (bare) action to which the given effective action corresponds, following [71] (for a specific discussion of functional measures in the context of a FRGE–based treatment of two dimensional Liouville theory, see [106]). While undertaking this reconstruction task may be instructive and useful for some purposes, we would not learn anything new about the renormalization group running of the gravitational couplings we consider here by doing this, and therefore we will not concern ourselves with this issue.

This discussion allows us to preemptively answer a question that may arise in this context. The term $\hat{W}$ is usually regarded as (part of) the effective action obtained by integrating out the matter fields, and one may wonder why we keep $\hat{S}_{\rm mat}$ and $\hat{W}$ simultaneously in the action. The reason for this is that we apply the same coarse graining scale to the gravitational degree of freedom σ and to the matter fields ψ. Thus, as we do not first completely integrate out the matter fields, $\hat{S}_{\rm mat}$ must still be present in the action[3]. On the other hand, as the term $\hat{W}$ describes the effect of the conformal anomaly, it is also present for any finite value of the coarse graining scale. In any case, one can easily remove from the beta functions the contributions coming from the terms $\hat{S}_{\rm mat}$ and/or $\hat{W}$ if one so wishes.

From here on, let us assume that the functional measure of the matter fields in the functional integral is not Weyl invariant, so that Γ_k contains the term $\hat{W}$. The invariance, or lack thereof, of the functional measure of σ only affects the numerical value of the coefficients in $\hat{W}$ [68, 106], and we do not need to commit ourselves to a particular choice for our calculations in the next sections. The possibility of recovering Weyl invariance in that limit has been discussed in the two-dimensional Liouville field theory case in [106], where it was shown that renormalization group trajectories of Γ_k terminate at a conformally invariant field theory as $k \to 0$ provided the initial conditions $\Gamma_{k\to\infty}$ satisfy constraints imposed by the Ward identity of the theory. We will not discuss these matters here. Instead, we will focus on the form of the beta functions, which, as we have stressed, are independent of such considerations.

In [67], it has been explained in detail that choosing the IR cutoff in a Weyl–invariant way corresponds to implementing background independence in the quantum theory. In full gravity, the requirement of diffeomorphism invariance implies that the effective average actions resulting from our renormalization procedure should depend on no preferred reference metric, and that our coarse graining should thus be implemented in terms of a physical, 'proper' momentum scale k. This is the procedure that is always followed in the FRGE approach to asymptotic safety. The procedure for achieving this, using the background field

[3] Of course, at a given energy scale k the degrees of freedom with masses $m > k$ will decouple and therefore in practice we need to consider only the degrees of freedom with masses $m < k$. In the IR limit, only massless fields matter.

method, has been outlined in Section 2.2.1. In the conformally reduced case, in which diffeomorphism invariance becomes Weyl–invariance, this translates into the requirement that we impose the cutoff not on the fiducial metric $\hat{g}_{\mu\nu}$, which should play no distinguished physical role, but on the background metric $\bar{g}_{\mu\nu}$, which is inert under the Weyl transformations (3.6). In the next two sections, we will compare the results of using the Weyl–invariant and the Weyl–breaking implementations of the IR cutoff.

3.2.2 The Weyl–invariant procedure

In [67], the beta functions of the conformal reduction of gravity with the Hilbert action were computed using a "background independent" IR cutoff, constructed from the background metric $\bar{g}_{\mu\nu}$. In this section, we follow a similar procedure, but rather than applying the background field method to ϕ, viz. (3.4), we apply it to σ, viz. (3.5), as we find that the behavior of the theory under Weyl transformations is easier to understand in this way. We also extend the results by including the effect of the R^2 term and of the Riegert action, which will be needed when comparing with the beta functions of [68], as well as the effect of the local matter contribution.

The FRGE (3.22) requires the second variation $\delta^2\Gamma_k^{\rm grav}/\delta\sigma\delta\sigma$, which can be immediately read off equations (3.9) and (3.21). Those variations are written in terms of operators constructed with the fiducial metric $\hat{g}_{\mu\nu}$ and the background field $\bar{\sigma}$, but, in order to guarantee that (background) Weyl invariance is preserved, it is convenient to rewrite them in terms of the metric $\bar{g}_{\mu\nu}$. For the Riegert action, this has already been done in (3.21). For the rest, we observe that, since (3.8) is invariant under Weyl transformations and $\delta\sigma$ is invariant under background Weyl transformations (3.6), the operator appearing in square brackets in (3.9) must also be invariant under background Weyl transformations. Indeed, this can be verified by a straightforward if somewhat tedious calculation. We can then apply a transformation (3.6) with parameter $\omega = \bar{\sigma}$ to the second variation, leading to the substitutions $\hat{g}_{\mu\nu} \to \bar{g}_{\mu\nu}$ and $\bar{\sigma} \to 0$ in (3.9), so that

$$\frac{\delta^2\Gamma_k^{\rm grav}}{\delta\sigma\delta\sigma} = \sqrt{\bar{g}}\Big[16g_0 + 4g_2(\bar{R} - 3\bar{\Box}) + g_4(72\bar{\Box}^2 + 24\bar{R}\bar{\Box} + 24\bar{\nabla}^\mu\bar{R}\bar{\nabla}_\mu) + 4b'\bar{\Delta}_4\Big]\,. \tag{3.24}$$

For our purposes, it will be enough to consider the case when $\hat{g}_{\mu\nu}$ is a space of constant curvature, for which

$$\frac{\delta^2\Gamma_k^{\rm grav}}{\delta\sigma\delta\sigma} = \sqrt{\bar{g}}\Big[16g_0 + 4g_2\bar{R} + \big(\big(24g_4 - \tfrac{2}{3}b'\big)\,\bar{R} - 12g_2\big)\,\bar{\Box} + (72g_4 + 4b')\,\bar{\Box}^2\Big]\,. \tag{3.25}$$

A similar reasoning applies to the second variation of the local matter contribution.

As we have seen in Section 2.3, there is a relatively large freedom in defining the IR cutoff $\mathcal{R}_k$. A convenient choice, which we will employ here, is that of an operator whose eigenfunctions are taken as a basis in the functional space that one is integrating over. The cutoff is then imposed on the eigenvalues of this operator [4].

We begin by choosing this operator to be $-\Box$, as done in [67]. As per our cutoff scheme classification in Section 2.3, we will call this a "type I cutoff". Following the prescription (2.26), we then construct the cutoff operator $\mathcal{R}_k$ such that it leads to the replacement of $-\Box$ by $P_k(-\Box) = -\Box + R_k(-\Box)$ in the inverse propagator, where R_k is a suitable profile function suppressing the propagation of field modes below the scale k. In our subsequent calculations, we will choose as this profile function the so-called optimized cutoff [72] $R_k(z) = (k^p - z)\theta(k^p - z)$, where θ is the step function and p is the order of the operator z. This prescription leads to

$$\mathcal{R}_k = \sqrt{\bar{g}}\Big[(72g_4 + 4b')(P_k^2 - \Box^2) - \big(\big(24g_4 - \tfrac{2}{3}b'\big)\,\bar{R} - 12g_2\big)\,R_k\Big]\,, \tag{3.26}$$

and we thus arrive at

$$\begin{aligned}\partial_t\Gamma_k =& \frac{1}{2}\mathrm{Tr}\left\{\frac{\big[6g_2 - \big(12g_4 - \frac{1}{3}b'\big)\,\bar{R} + 4(18g_4 + b')P_k\big]\,\partial_t R_k}{8g_0 + 2g_2 - \big[\big(12g_4 - \frac{1}{3}b'\big)\,\bar{R} - 6g_2\big]\,P_k + (36g_4 + 2b')P_k^2}\right.\\ &\left. + \frac{6\beta_2 R_k + 36\beta_4\left(P_k^2 - \Box^2 - \frac{\bar{R}}{3}R_k\right)}{8g_0 + 2g_2 - \big[\big(12g_4 - \frac{1}{3}b'\big)\,\bar{R} - 6g_2\big]\,P_k + (36g_4 + 2b')P_k^2}\right\}\\ &+ \frac{n_S}{2}\mathrm{Tr}\frac{\partial_t R_k}{P_k} - \frac{n_D}{2}\mathrm{Tr}\frac{\partial_t R_k}{P_k + \frac{\bar{R}}{4}} + \frac{n_M}{2}\mathrm{Tr}\frac{\partial_t R_k}{P_k + \frac{\bar{R}}{4}} - n_M\mathrm{Tr}\frac{\partial_t R_k}{P_k}\,,\end{aligned} \tag{3.27}$$

where we have defined $\beta_i \equiv \partial_t g_i$, and the right-hand side terms containing β_i come from deriving the couplings that are contained in $\mathcal{R}_k$. Note that all dependence on $\hat{R}$ and σ is through the background metric $\bar{g}_{\mu\nu}$, which is inert under the background Weyl transformations (3.6), as mentioned. Since the quantum field is also inert, background Weyl invariance is respected. Consequently, the flow will preserve the form of the action (3.8), and to extract the beta functions of g_2 and g_4 we can isolate the coefficient of any one of the operators that they multiply. We evaluate the functional trace on the right-hand side of the FRGE using the heat kernel expansion of the operator $-\Box$, using the method explained in Section 2.3 and the formulas collected in the Appendices, and then equate the coefficient

[4] To avoid possible misunderstandings, let us stress that the functional trace in (3.22) is obviously independent of any choice of functional basis. What we are saying here is that putting a cutoff on the eigenvalues of different operators leads effectively to different cutoff procedures.

of $\bar{R}^i$ with β_i. This gives

$$\begin{aligned}
\beta_0 =& c_0 k^4 + \frac{(6g_2 + (72g_4 + 4b')k^2 + \beta_2 + 9\beta_4 k^2)k^6}{64\pi^2\left(4g_0 + 3g_2k^2 + (18g_4 + b')k^4\right)} \ , \\
\beta_2 =& c_2 k^2 + \frac{1}{192\pi^2}\big[12\left(2g_0(g_2 + 6g_4k^2) + 9g_4(g_2 + 18g_4k^2)k^4\right)k^4 + 3b'^2k^{10} \\
&+ 2(10g_0 + 3g_2k^2 + 81g_4k^4)b'k^6\big]\left[\left(4g_0 + 3g_2k^2 + (18g_4 + b')k^4\right)^2\right]^{-1} \\
&+ \beta_2 \frac{12g_0 + 3g_2k^2 + (90g_4 + 2b')k^4}{384\pi^2\left(4g_0 + 3g_2k^2 + (18g_4 + b')k^4\right)^2} \\
&+ \beta_4 \frac{(16g_0 - 6g_2k^2 + (180g_4 + b')k^4)k^2}{128\pi^2\left(4g_0 + 3g_2k^2 + (18g_4 + b')k^4\right)^2} \ , \\
\beta_4 =& c_4 + \Big\{3\big[g_0^2(464g_2 - 5952g_4k^2)k^2 - 24g_0(31g_2^2 + 198g_2g_4k^2 + 72g_4^2k^4)k^4 \\
&+ 9(29g_2^3 - 744g_2^2g_4k^2 - 12060g_2g_4^2k^4 + 64368g_4^3k^6)k^6\big] \\
&+ 4\big[472g_0^2 - 198g_0(g_2 - 32g_4k^2)k^2 + 9(14g_2^2 - 465g_2g_4k^2 \\
&+ 3186g_4^2k^4)k^4\big]b'k^4 + \left(344g_0 + 75g_2k^2 + 1512g_4k^4\right)b'^2k^8 \\
&+ 28b'^3k^{12}\Big\}\Big\{34560\pi^2\left(4g_0 + 3g_2k^2 + (18g_4 + b')k^4\right)^3\Big\}^{-1} \\
&+ \beta_2k^2\Big\{464g_0^2 + 24g_0(g_2 - 354g_4k^2)k^2 + 27(3g_2^2 - 44g_2g_4k^2 \\
&+ 1548g_4^2k^4)k^4 + 8(14g_0 + 3(g_2 + 36g_4k^2)k^2)b'k^4 + 9b'^2k^8\Big\} \\
&\Big\{23040\pi^2\left(4g_0 + 3g_2k^2 + (18g_4 + b')k^4\right)^3\Big\}^{-1} \\
&- \beta_4k^4\Big\{496g_0^2 + 72g_0(17g_2 + 22g_4k^2)k^2 + 99g_2^2k^4 + 9828g_2g_4k^6 \\
&- 22356g_4^2k^8 + 2(164g_0 + 93g_2k^2 + 918g_4k^4)b'k^4 + 36b'^2k^8\Big\} \\
&\Big\{3840\pi^2\left(4g_0 + 3g_2k^2 + (18g_4 + b')k^4\right)^3\Big\}^{-1} \ ,
\end{aligned} \tag{3.28}$$

where the constants c_i are the local contribution of matter:

$$\begin{aligned}
c_0 =& \frac{1}{32\pi^2}\left(n_S - 4n_D + 2n_M\right) \ , \\
c_2 =& \frac{1}{96\pi^2}\left(n_S + 2n_D - 4n_M\right) \ , \\
c_4 =& \frac{1}{34560\pi^2}\left(29n_S - 11n_D - 62n_M\right) \ .
\end{aligned} \tag{3.29}$$

The above formulae should be looked upon as a system of linear equations for the beta functions β_i. The beta functions themselves are obtained by solving these equations and are somewhat complicated rational functions of the couplings.

It is instructive to rederive the beta functions using a different cutoff procedure. Instead of using the operator $-\Box$ as defining the basis in function space, we can use the fourth-order operator

$$\bar{\mathcal{O}} \equiv \frac{1}{\sqrt{\bar{g}}(72g_{44}+4b')}\frac{\delta^2\Gamma_k^{\rm grav}}{\delta\sigma\delta\sigma} = \Box^2 + \dots\,, \tag{3.30}$$

where the dots stand for the other terms appearing in (3.25). We then define the cutoff $\mathcal{R}_k = \sqrt{\bar{g}}(72g_{44}+4b')R_k(\bar{\mathcal{O}})$, where R_k is the optimized cutoff profile function given above, such that it leads to the replacement

$$\frac{\delta^2\Gamma_k^{\rm grav}}{\delta\sigma\delta\sigma} \to \sqrt{\bar{g}}(72g_{44}+4b')P_k(\bar{\mathcal{O}}) = \sqrt{\bar{g}}(72g_{44}+4b')(\bar{\mathcal{O}}+R_k(\bar{\mathcal{O}}))\,. \tag{3.31}$$

This is an example of a "type III cutoff". In this case, the FRGE simply reduces to

$$\begin{aligned}\partial_t\Gamma_k = &\frac{1}{2}{\rm Tr}\frac{\partial_t R_k(\bar{\mathcal{O}})}{P_k(\bar{\mathcal{O}})} + \frac{n_S}{2}{\rm Tr}\frac{\partial_t R_k}{P_k} - \frac{n_D}{2}{\rm Tr}\frac{\partial_t R_k}{P_k+\frac{\bar{R}}{4}} + \frac{n_M}{2}{\rm Tr}\frac{\partial_t R_k}{P_k+\frac{\bar{R}}{4}} \\ &- n_M{\rm Tr}\frac{\partial_t R_k}{P_k}\,.\end{aligned} \tag{3.32}$$

where the argument of the functions R_k and P_k in the matter traces is still the operator $-\Box$.

Restricting ourselves to the one-loop approximation, whereby the renormalization group running of the couplings in the right-hand side of the FRGE is neglected (viz. Section 2.1.3), we arrive at the beta functions

$$\begin{aligned}\beta_0 =& c_0k^4 + \frac{1}{32\pi^2}\left[\frac{9g_2^2-8g_0(b'+18g_4)}{(b'+18g_4)^2} - \frac{6g_2k^2}{b'+18g_4} + 4k^4\right]\,,\\ \beta_2 =& c_2k^2 + \frac{1}{32\pi^2}\left[\frac{-2b'g_2-90g_2g_4+30b'g_4k^2+432g_4^2k^2}{(b'+18g_4)^2}\right]\,,\\ \beta_4 =& c_4 + \frac{1}{32\pi^2}\left[\frac{29}{540} - \frac{b'^2+36b'g_4-2592g_4^2}{36(b'+18g_4)^2}\right]\,.\end{aligned} \tag{3.33}$$

We can compare these beta functions with the corresponding type I counterparts in the one-loop approximation by dropping the terms that contain β_2 or β_4 on the right-hand side of (3.28). The differences that one observes are a manifestation of the scheme dependence of the results. We expect only the one-loop part of β_4, in the limit $k^2 \gg g_2$, $k^4 \gg g_0$, to be scheme–independent. To this effect, we should expand the denominators of the type I beta functions in powers of g_0 and g_2 and compare term by term. We then see that the leading term of the expansion of β_4 is equal to

$$\frac{7b'^2+252g_4b'+24138g_4^2}{8640\pi^2\left(b'+18g_4\right)^2} \tag{3.34}$$

with both cutoff types, as expected. Higher order terms of β_4 and all the terms in β_0 and β_2 are scheme–dependent. This does not make them physically unimportant, although extracting physical predictions from them requires more work and more care.

One result from the scheme–dependent terms that should be scheme–independent is the existence of a fixed point. A fixed point is a simultaneous zero for the beta functions of the dimensionless variables $\tilde{g}_i = k^{-d_i} g_i$ (with $d_0 = 4$, $d_2 = 2$ and $d_4 = 0$), which are given by

$$\partial_t \tilde{g}_i = -d_i \tilde{g}_i + k^{-d_i} \beta_i \,. \tag{3.35}$$

It is noteworthy that when the beta functions are written out in terms of the variables $\tilde{g}_i$, the cutoff scale k does not appear explicitly anymore, in accordance with the general expectation that the flow equations are autonomous.

We will now briefly discuss the fixed points of (3.28). To make contact with [67], we begin by considering the case when matter is absent. Further reducing ourselves to the Einstein-Hilbert truncation, where $g_4 = 0$, the above equations admit a non-Gaussian fixed point (NGFP) at $\tilde{g}_0 = 0.00404$ and $\tilde{g}_2 = -0.007296$, which corresponds to

$$\text{NGFP} : \left\{ \tilde{\Lambda} = 0.277 \,, \quad \tilde{G} = 2.727 \right\},$$

in addition to the Gaussian fixed point (GFP) at $\{\tilde{\Lambda} = 0, \tilde{G} = 0\}$. These values are numerically very close to the result of [67]; the residual discrepancy can be attributed to the fact that we take σ as the quantum field whereas [67] uses ϕ, and that imposing a cutoff on fluctuations of σ is different from imposing a cutoff on fluctuations of ϕ. As discussed in Chapter 1, the properties of the renormalization group flow around a fixed point $\{\tilde{g}_i^*\}$ are determined by the stability matrix

$$\mathbf{B}_{ij} = \partial_j \beta_i \big|_{\{\tilde{g}_i^*\}} \,. \tag{3.36}$$

In particular, defining the stability coefficients θ_i as minus the eigenvalues of $\mathbf{B}_{ij}$, the number of UV attractive directions of the flow around a fixed point is given by the number of stability coefficients with positive real part. At the NGFP above, the stability coefficients are a complex conjugate pair $\theta_{0,1} = \theta' \pm \theta''$ whose real and imaginary parts read

$$\theta' = 1.97022, \quad \theta'' = 6.86891, \tag{3.37}$$

indicating this fixed point is UV attractive in both directions of the $(\tilde{\Lambda}, \tilde{G})$ plane. In addition, the non-zero imaginary part implies that the renormalization group trajectories in the vicinity of the fixed point are spirals. As we will see in the next chapter, this is the same qualitative behavior as that found for the Einstein-Hilbert truncation in the case of full gravity [38].

Let us now extend the truncation to include the R^2 term. If we set $\tilde{g}_0 = \tilde{g}_2 = 0$, β_4 reduces to the expression (3.34), and in the absence of matter $b' = 0$ this leads to

$$\beta_4 = \frac{149}{17280\pi^2}. \tag{3.38}$$

It is not conceivable that higher-order terms exactly cancel this term, so this indicates that $1/g_4$ is asymptotically free, and there is no fixed point for $\tilde{g}_0 = \tilde{g}_2 = g_4 = b' = 0$. Solving the equations (3.28) numerically in the matter-free case, we find that these beta functions do not admit any non-trivial fixed point with positive $\tilde{G}$. [5] This is in contrast with the full gravity studies of curvature-squared truncations [40,41,107], in which a UV-attractive NGFP with physically acceptable values of the couplings has been found. In our conformally reduced case, the fixed point may reappear when higher powers of curvature are allowed.

In any case, the fixed point does reappear when one takes matter field contributions into account. In the case of, e.g., one massless Maxwell field and no massless Dirac and scalar fields, we find a fixed point at $\tilde{g}_0 = 0.00135$, $\tilde{g}_2 = -0.00168$, $g_4 = 0.00036$, corresponding to

$$\mathrm{NGFP}_{R^2} : \left\{\tilde{\Lambda} = 0.401,\, \tilde{G} = 11.83\right\},$$

and with stability coefficients $\theta_{0,1} = \theta' \pm \theta''$ and θ_3 given by

$$\theta' = 5.21697, \quad \theta'' = 1.67494, \quad \theta_2 = 1.85428. \tag{3.39}$$

Hence, this NGFP is UV-attractive in all eigendirections and the critical surface $\mathcal{S}_{\mathrm{UV}}$ associated with it is three-dimensional, in qualitative agreement with results in matter-coupled gravity [83,108].

3.2.3 The Weyl-breaking procedure

We now want to calculate the beta functions of conformally reduced gravity when the cutoff is defined by means of the fiducial metric $\hat{g}_{\mu\nu}$, instead of the background $\bar{g}_{\mu\nu}$.

We will first use a type I cutoff. To this effect, we follow the same steps as in the previous section, with the crucial difference that the IR cutoff is imposed on the spectrum of $-\hat{\Box}$, rather than $-\Box$. This introduces a dependence on $\hat{\Box}$ which is not compensated by the presence of $e^{\bar{\sigma}}$ factors, and therefore breaks Weyl invariance. As a consequence, the special form of the action (3.8) will no longer be preserved by the flow. To see this, it is instructive to consider the

[5] This is also the case when one uses the parametrization (3.4).

slightly more general class of actions

$$\begin{aligned}\hat{S}(\hat{g}_{\mu\nu},\sigma) = \int d^4x\,\sqrt{\hat{g}}\Big\{ & g_0 e^{4\sigma} + e^{2\sigma}\left[g_{21}\hat{R} - 6g_{22}\hat{\Box}\sigma - 6g_{23}(\hat{\nabla}\sigma)^2\right] \\ & + g_{41}\hat{R}^2 - 12g_{42}\hat{R}\hat{\Box}\sigma - 12g_{43}\hat{R}(\hat{\nabla}\sigma)^2 + 36g_{44}(\hat{\Box}\sigma)^2 \\ & + 36g_{45}((\hat{\nabla}\sigma)^2)^2 + 72g_{46}\hat{\Box}\sigma(\hat{\nabla}\sigma)^2\Big\}\,,\end{aligned} \tag{3.40}$$

which are invariant under (global) scale transformations. These actions become invariant under (local) Weyl transformations when the couplings g_{2i} $(i = 1, 2, 3)$ and g_{4j} $(j = 1, \ldots, 6)$ are separately equal. If the flow preserved local Weyl–invariance, the beta functions of the g_{2i} and g_{4j} should also be the same. We will shortly show that this is not the case.

For the sake of comparison with the preceding section, we begin by analyzing the situation when the background $\bar{\sigma}$ is constant, which allows us to extract the beta equations for the couplings g_0, g_{21} and g_{41}. In this case,

$$\begin{aligned}\frac{\delta^2\Gamma_k^{\rm grav}}{\delta\sigma\delta\sigma} = \sqrt{\hat{g}}\Big\{ & 16g_0 e^{4\bar{\sigma}} + 4g_{21}e^{2\bar{\sigma}}\hat{R} + (72g_{44} + 4b')\,\hat{\Box}^2 \\ & + \left[(24g_{43} - \frac{2}{3}b')\hat{R} - 12(2g_{22} - g_{23})e^{2\bar{\sigma}}\right]\hat{\Box}\Big\}\,.\end{aligned} \tag{3.41}$$

Choosing the cutoff $\mathcal{R}_k$ such that $-\hat{\Box}$ is replaced by $P_k(-\hat{\Box}) = -\hat{\Box} + R_k(-\hat{\Box})$ in the inverse propagator then leads to

$$\begin{aligned}\mathcal{R}_k = \sqrt{\hat{g}}\Big\{ & -\left[(24g_{43} - \tfrac{2}{3}b')\hat{R} - 12(2g_{22} - g_{23})e^{2\bar{\sigma}}\right]R_k \\ & + (72g_{44} + 4b')\,(P_k^2 - \hat{\Box}^2)\Big\}\,.\end{aligned} \tag{3.42}$$

The cutoff for the matter fields follows the same logic. For example, the inverse propagator of the scalar field is $-e^{2\bar{\sigma}}\hat{\Box}$ and we choose the cutoff $e^{2\bar{\sigma}}R_k(-\hat{\Box})$, such that the modified inverse propagator is $e^{2\bar{\sigma}}P_k(-\hat{\Box})$. Note that, in this way, the exponentials cancel between numerator and denominator in the FRGE, and the

matter contribution is $\bar{\sigma}$–independent. The FRGE thus reads

$$\begin{aligned}\partial_t\Gamma_k = \frac{1}{2}\mathrm{Tr}\Bigg\{ &\Big[6(2g_{22}-g_{23})e^{2\bar{\sigma}} - \big(12g_{43}-\tfrac{1}{3}b'\big)\,\bar{R} + 4(18g_{44}+b')P_k\Big]\partial_t R_k \\ &\Big[8g_0e^{4\bar{\sigma}} + 2g_{21}e^{2\bar{\sigma}}\hat{R} + \Big(6e^{2\bar{\sigma}}(2g_{22}-g_{23}) - \big(12g_{43}-\tfrac{1}{3}b'\big)\hat{R}\Big)P_k \\ &+ (36g_{44}+2b')P_k^2\Big]^{-1} + \Big[6(2\beta_{22}-\beta_{23})e^{2\bar{\sigma}}R_k + 36\beta_{44}(P_k^2-\Box^2) \\ &- 12\beta_{43}\hat{R}R_k\Big]\Big[8g_0e^{4\bar{\sigma}} + 2g_{21}e^{2\bar{\sigma}}\hat{R} + \big(6e^{2\bar{\sigma}}(2g_{22}-g_{23}) \\ &- \big(12g_{43}-\tfrac{1}{3}b'\big)\hat{R}\big)P_k + (36g_{44}+2b')P_k^2\Big]^{-1}\Bigg\} \\ &+ \frac{n_S}{2}\mathrm{Tr}\frac{\partial_t R_k}{P_k} - \frac{n_D}{2}\mathrm{Tr}\frac{\partial_t R_k}{P_k+\frac{\hat{R}}{4}} + \frac{n_M}{2}\mathrm{Tr}\frac{\partial_t R_k}{P_k+\frac{\hat{R}}{4}} - n_M\mathrm{Tr}\frac{\partial_t R_k}{P_k}\,.\end{aligned} \tag{3.43}$$

Evaluating the trace via a heat kernel expansion of $-\Box$ and reading off the coefficients of $e^{4\bar{\sigma}}$, $e^{2\bar{\sigma}}\hat{R}$ and $\hat{R}^2$, we arrive at the beta functions

$$\begin{aligned}\beta_0 =& \frac{9\left[(g_{23}-2g_{22})^2-16g_0g_{44}\right]-8b'g_0}{32\pi^2(18g_{44}+b')^2} + \frac{3(g_{23}-2g_{22})}{32\pi^2(18g_{44}+b')^2}\beta_{22} \\ &+ \frac{3\,(2g_{22}-g_{23})}{64\pi^2(18g_{44}+b')^2}\beta_{23} - \frac{9\left[4b'g_0-9((g_{23}-2g_{22})^2-8g_0g_{44})\right]}{64\pi^2(18g_{44}+b')^3}\beta_{44}\,, \\ \beta_{21} =& \frac{9\left[(g_{23}-2g_{22})(g_{44}+2g_{43})-2g_{21}g_{44}\right]-b'g_{21}}{16\pi^2(18g_{44}+b')^2} \\ &- \frac{3(b'(3g_{21}+2g_{22}-g_{23})+18(3g_{21}g_{44}+2(2g_{22}-g_{23})(2g_{44}+3g_{43})))}{64\pi^2(18g_{44}+b')^3}\beta_{44} \\ &+ \frac{3(2g_{22}-g_{23})}{32\pi^2(18g_{44}+b')^2}\beta_{43} + \frac{b'+27g_{44}+18g_{43}}{192\pi^2(18g_{44}+b')^2}(2\beta_{22}-\beta_{23})\,, \\ \beta_{41} =& c_4 + \frac{7b'^2+252b'g_{44}+162(29g_{44}^2+60g_{44}g_{43}+60g_{43}^2)}{8640\pi^2(18g_{44}+b')^2} \\ &+ \frac{b'^2+9b'(9g_{44}+10g_{43})+81(29g_{44}^2+80g_{44}g_{43}+60g_{43}^2)}{960\pi^2(18g_{44}+b')^3}\beta_{44} \\ &- \frac{b'+27g_{44}+18g_{43}}{96\pi^2(18g_{44}+b')^2}\beta_{43}\,.\end{aligned} \tag{3.44}$$

To compare with the beta functions of the previous section, which were also read off as the coefficients of powers of R, we should identify all the g_{2i}'s and all the g_{4j}'s above. We see that these results are clearly very different from the ones obtained in the Weyl–invariant procedure. In particular, we observe that k never

appears explicitly, and only the beta function of g_{41} gets a direct contribution from the matter, via the coefficient c_4.

In order to evaluate the beta functions of the couplings g_{22}, g_{23}, g_{42}....g_{46}, we must now consider the case when $\bar{\sigma}$ is not constant. The second variation of (3.40) is then

$$\begin{aligned}\frac{\delta^2\Gamma_k^{\rm grav}}{\delta\sigma\delta\sigma} = \sqrt{\hat{g}}\Big[&16g_0e^{4\bar{\sigma}} + 4e^{2\bar{\sigma}}\left(g_{21}\hat{R} - 6g_{22}\hat{\Box}\bar{\sigma} - 6g_{23}(\hat{\nabla}\bar{\sigma})^2\right)\\ &- 24g_{23}e^{2\bar{\sigma}}\hat{\nabla}^\mu\bar{\sigma}\hat{\nabla}_\mu + 24g_{43}\hat{\nabla}^\mu\hat{R}\hat{\nabla}_\mu + 288g_{46}\hat{R}^{\mu\nu}\hat{\nabla}_\mu\bar{\sigma}\hat{\nabla}_\nu\\ &- 288g_{45}\big(\hat{\Box}\bar{\sigma}\hat{\nabla}^\mu\bar{\sigma}\hat{\nabla}_\mu + \hat{\nabla}^\mu(\hat{\nabla}\bar{\sigma})^2\hat{\nabla}_\mu\big) + 12(g_{23}-2g_{22})e^{2\bar{\sigma}}\hat{\Box}\\ &- 144g_{45}\left((\hat{\nabla}\bar{\sigma})^2\hat{\Box} + 2\hat{\nabla}^\mu\bar{\sigma}\hat{\nabla}^\nu\bar{\sigma}\hat{\nabla}_\mu\hat{\nabla}_\nu\right) + 24g_{43}\hat{R}\hat{\Box}\\ &+ 288g_{46}(\hat{\nabla}^\mu\hat{\nabla}^\nu\bar{\sigma}\hat{\nabla}_\mu\hat{\nabla}_\nu - \hat{\Box}\bar{\sigma}\hat{\Box}) + 72g_{44}\hat{\Box}^2 + 4b'\hat{\Delta}_4\Big]\,.\end{aligned} \tag{3.45}$$

Note that this expression is equal to (3.9) with the couplings g_i appropriately split into g_{ij}. Since this is no longer a function of $-\hat{\Box}$ alone, we cannot apply a type I cutoff here, as we have done for the constant $\bar{\sigma}$ case. Rather, we shall use a type III procedure, imposing the cutoff on the eigenvalues of the fourth-order operator

$$\hat{\mathcal{O}} \equiv \frac{1}{\sqrt{\hat{g}}(72g_{44}+4b')}\frac{\delta^2\Gamma_k^{\rm grav}}{\delta\sigma\delta\sigma} = \hat{\Box}^2 + \dots\,, \tag{3.46}$$

where, again, the dots indicate the remaining terms in (3.45). Similarly, given the second variation (3.11), for the local matter contribution we shall impose the cutoff on the eigenvalues of the following operators

$$\begin{aligned}\hat{\mathcal{O}}_S &\equiv \hat{\Box} + 2\hat{\nabla}^\mu\bar{\sigma}\hat{\nabla}_\mu\,,\\ \hat{\mathcal{O}}_D &\equiv \hat{\Box} + 2\hat{\nabla}^\mu\bar{\sigma}\hat{\nabla}_\mu - \frac{1}{4}\left(\hat{R} - 6\hat{\Box}\bar{\sigma} - 6(\hat{\nabla}\bar{\sigma})^2\right)\,,\\ \hat{\mathcal{O}}_{M\mu\nu} &\equiv \left(\hat{\Box} + 2\hat{\nabla}^\lambda\bar{\sigma}\hat{\nabla}_\lambda + \hat{\Box}\bar{\sigma} + 2(\hat{\nabla}\bar{\sigma})^2\right)\hat{g}_{\mu\nu} - R_{\mu\nu} + 2\hat{\nabla}_\mu\hat{\nabla}_\nu\bar{\sigma} - 2\hat{\nabla}_\mu\bar{\sigma}\hat{\nabla}_\nu\bar{\sigma}\,.\end{aligned}$$

Limiting ourselves again to a one-loop approximation, the FRGE reads

$$\begin{aligned}\partial_t\Gamma_k = &\frac{1}{2}{\rm Tr}\frac{\partial_t R_k(\hat{\mathcal{O}})}{P_k(\hat{\mathcal{O}})} + \frac{n_S}{2}{\rm Tr}\frac{\partial_t R_k(\hat{\mathcal{O}}_S)}{P_k(\hat{\mathcal{O}}_S)} - \frac{n_D}{2}{\rm Tr}\frac{\partial_t R_k(\hat{\mathcal{O}}_D)}{P_k(\hat{\mathcal{O}}_D)}\\ &+ \frac{n_M}{2}{\rm Tr}\frac{\partial_t R_k(\hat{\mathcal{O}}_M)}{P_k(\hat{\mathcal{O}}_M)} - n_M{\rm Tr}\frac{\partial_t R_k(\hat{\mathcal{O}}_S)}{P_k(\hat{\mathcal{O}}_S)}\,.\end{aligned} \tag{3.47}$$

The heat kernel coefficients that are necessary for the evaluation of these traces to the desired order are known in the literature [109–112]. We have collected the relevant expressions in Appendix D and refer to Appendix C for further details

on the trace evaluation. We then obtain the following beta functions,

$$\begin{aligned}
\beta_0 =& \frac{1}{32\pi^2}\left(-\frac{8g_0}{18g_{44}+b'}+\frac{9(g_{23}-2g_{22})^2}{(18g_{44}+b')^2}\right),\\
\beta_{21} =& \frac{1}{32\pi^2}\left(\frac{g_{23}-2g_{21}-2g_{22}}{18g_{44}+b'}+\frac{(g_{23}-2g_{22})(36g_{43}-b')}{(18g_{44}+b')^2}\right),\\
\beta_{22} =& \frac{1}{32\pi^2}\left(-\frac{2g_{22}}{18g_{44}+b'}+\frac{54g_{46}(g_{23}-2g_{22})}{(18g_{44}+b')^2}\right),\\
\beta_{23} =& \frac{1}{32\pi^2}\left(-\frac{2g_{23}}{18g_{44}+b'}-\frac{54g_{45}(g_{23}-2g_{22})}{(18g_{44}+b')^2}\right),\\
\beta_{41} =& c_4+\frac{1}{32\pi^2}\left(\frac{29}{540}+\frac{36g_{43}-b'}{9(36g_{44}+2b')}+\frac{(36g_{43}-b')^2}{9(36g_{44}+2b')^2}\right),\\
\beta_{42} =& c_4'+\frac{1}{32\pi^2}\left(\frac{3g_{46}}{36g_{44}+2b'}+\frac{6g_{46}(36g_{43}-b')}{(36g_{44}+2b')^2}\right),\\
\beta_{43} =& c_4''+\frac{1}{32\pi^2}\left(\frac{3g_{45}}{36g_{44}+2b'}+\frac{6g_{45}(36g_{43}-b')-36g_{46}^2}{(36g_{44}+2b')^2}\right),\\
\beta_{44} =& c_4''+\frac{1}{32\pi^2}\frac{90g_{46}^2}{(18g_{44}+b')^2},\\
\beta_{45} =& c_4''+\frac{1}{32\pi^2}\frac{90g_{45}^2}{(18g_{44}+b')^2},\\
\beta_{46} =& c_4''+\frac{1}{32\pi^2}\frac{90g_{45}g_{46}}{(18g_{44}+b')^2},
\end{aligned} \tag{3.48}$$

where c_4 is defined in (3.29) and

$$c_4' \equiv \frac{n_S-n_M-n_D}{2304\pi^2}, \quad c_4'' \equiv \frac{n_S+2n_M-n_D}{2304\pi^2}. \tag{3.49}$$

We first note that the couplings g_{41} and g_{42} do not appear in these equations, since the corresponding operators contain less than two powers of σ. Next, we observe that the beta functions of g_0, g_{21} and g_{41} are exactly the same as (3.44) at one-loop (i.e., neglecting the terms with the β_{ij} on the r.h.s.). As discussed in the previous section, this was fully expected in the case of g_{41}. It is not generally true for the dimensionful couplings such as g_0 and g_{21}, but in the present case it is so, as all the terms in the beta functions derive from the heat kernel coefficient B_4. As we have seen in Section 2.3, the contributions from this coefficient are scheme independent. We also note that the second term in β_{41} is equal to the scheme–independent part of the Weyl invariant β_4, given in (3.34).

We can also explicitly see that the beta functions of the various g_{2i} and g_{4i} are generally not equal, and thus Weyl invariance is broken. Even if we started from an initial point where these couplings were the same, the flow would lead us away from that situation. It is remarkable, however, that if we neglect the

matter contributions and set $g_{22} = g_{23} \equiv \hat{g}_2$ and $g_{44} = g_{45} = g_{46} \equiv \hat{g}_4$, we find that $\beta_{22} = \beta_{23} \equiv \hat{\beta}_2$ and $\beta_{44} = \beta_{45} = \beta_{46} \equiv \hat{\beta}_4$.

In [68], the beta functions for conformally reduced gravity in the presence of the conformal anomaly were calculated via dimensional regularization techniques in flat space perturbation theory. If we did the FRGE calculation above only in flat space, we would not be able to compute the beta functions of the couplings which multiply operators containing $\hat{R}$, namely g_{21}, g_{41}, g_{42} and g_{43}, and the remaining beta functions would be exactly the $\hat{\beta}_i$ above, upon equating the couplings. The question then naturally arises, whether we can relate the beta functions we have derived here to those obtained by flat space perturbation theory techniques.

The beta functions in [68] read

$$\begin{aligned} k\partial_k\lambda &= \left(4 - 4\alpha + \frac{8\alpha^2}{Q^2}\right)\lambda - \frac{8\pi^2\alpha^2}{Q^4}\gamma^2\left(1 + \frac{4\alpha^2}{Q^2} + \frac{6\alpha^4}{Q^4}\right), \\ k\partial_k\gamma &= \left(2 - 2\alpha + \frac{2\alpha^2}{Q^2}\right)\gamma\,, \\ k\partial_k\zeta &= \frac{80\pi^2\alpha^2}{Q^4}\zeta^2\,. \end{aligned} \tag{3.50}$$

In those calculations, the field σ is assumed to scale as $\sigma \to \sigma - \alpha\omega$ under (3.3), and α is thus the anomalous scaling dimension of σ. The couplings λ, γ and ζ, Q^2 respectively multiply the (Lorentzian) operators of order zero, two and four in the conformally reduced effective action. Lastly, the first two beta functions are given for the case $\zeta = 0$. We could also assume this anomalous scaling in our calculations, in which case our beta functions would also come with an α–dependence, but we shall not pursue this here.

In order to compare these with our results, we make the identifications

$$g_0 = \lambda\ , \quad \hat{g}_2 = -\tfrac{1}{6}\gamma\ , \quad \hat{g}_4 = \tfrac{1}{36}\zeta\ , \quad Q^2 = (4\pi)^2(2b' + \zeta)\ . \tag{3.51}$$

The first three definitions are chosen to agree with the Euclidean version of [68], which involves a change of sign. Since the anomaly should be the same independently of the signature, we do not change the sign of the Riegert action under Euclidean continuation.

With these definitions, the equations for the couplings $g_0, \hat{g}_2, \hat{g}_4$ for the flat space case become

$$\begin{aligned} \beta_\lambda &= -\frac{8\lambda}{Q^2} + \frac{8\pi^2\gamma^2}{Q^4}\ , \\ \beta_\gamma &= -\frac{2\gamma(Q^2 + 24\pi^2\zeta)}{Q^4}\ , \\ \beta_\zeta &= \frac{80\pi^2\zeta^2}{Q^4}\ . \end{aligned} \tag{3.52}$$

The equation for ζ exactly agrees with (3.50) in the special case $\alpha = 1$, as does the equation for γ when we set $\zeta = 0$, modulo an overall sign. We find agreement also in the equation for λ up to scheme-dependent terms, again in the case $\alpha = 1$ and modulo an overall sign. As we can see, it is the beta functions in the Weyl-breaking procedure that reproduce the results of [68].

However, as it turns out, this procedure breaks not only Weyl invariance, but also global scale invariance. That is to say, in addition to the ratios between the coefficients of the operators in (3.8) being different, as we have seen from the full set of beta functions above, new terms not originally present in the action are also generated, and hence not even the form (3.40) is preserved. These new terms will contribute to the beta functions (3.48) and will themselves have non-zero beta functions. For example, expanding the trace in (3.43), the matter contributions proportional to c_0 and c_2 multiply the operators $\int dx\sqrt{\hat{g}}$ and $\int dx\sqrt{\hat{g}}\hat{R}$, and we will also have operators such as $\int dx\sqrt{\hat{g}}\, e^{2\bar{\sigma}}$, $\int dx\sqrt{\hat{g}}\, e^{4\bar{\sigma}}\hat{R}$, etc. The flow thus takes place in a much larger class of actions, where the dependence on $\hat{g}_{\mu\nu}$ and σ is not restricted by the demand of invariance under (3.3).

Nonetheless, we do not expect these new terms to contribute to the beta functions of the g_{4i} above, as the new terms will come with powers of $e^{\bar{\sigma}}$ which do not correspond to those of the operators multiplying the couplings $g_{41} \dots g_{46}$ in (3.40). For the same reason, we do not expect the couplings in (3.40) to be present in the new beta functions β_{4j} ($j > 6$), apart from g_{44} contributions in the denominator. Thus, we can already say something on the existence of fixed points by considering the β_{4i} that we have written.

From (3.52), we note that the beta function for ζ vanishes in the case $\zeta = 0$, in accordance with [68]. It is this fixed point of the coupling ζ that has been argued to constitute an IR stable fixed point of the theory, driving its low energy dynamics. In terms of the couplings g_{44}, g_{45} and g_{46} the vanishing of ζ is equivalent to the vanishing of those beta functions for $g_{45} = g_{46} = 0$, neglecting the local matter contribution. Remarkably, the beta functions for g_{42} and g_{43} also vanish in this situation. The remaining beta function for g_{41}, on the other hand, is non-vanishing for any real value of the couplings, and one might be tempted to conclude that there is then no fixed point solution. But g_{41} is not a coupling for conformally reduced gravity in this Weyl breaking setting, since the corresponding operator does not contain the dynamical field σ and, unlike in the Weyl invariant case, g_{41} is independent of the other fourth-order couplings. Therefore, there is no reason to require that its beta function vanish. If we do not impose the vanishing of β_{41}, we find agreement with the results of [68], at least within the restricted set of beta functions (3.52).

In order to draw more general conclusions, we would have to study the flow of the other couplings that have not been included in the action (3.40), but which will be generated by quantum effects. Lastly, we note that, within our restricted set of beta functions, once we take into account the local matter contribution, no fixed point solution for real value of the couplings is admissible.

3.3 Conclusions

We have here calculated the beta functions of gravity in a conformally reduced setting by means of the functional renormalization group equation. In this context, the dynamics of gravity has been essentially reduced to that of a scalar field. While it is not clear that this significant simplification can adequately capture the main features of the gravitational flow, we have seen that in the case of the Einstein-Hilbert truncation it yields a fixed point in the UV with properties that are quite close to those obtained in the presence of transverse gravitons, as was first shown in [67, 85]. From a theoretical point of view, it has the advantage of sidestepping several issues, such as gauge fixing, which do arise in the complete formulation of gravity, and it serves as a testing ground in which to explore various ideas.

In this chapter, we have have considered, in addition to local terms up to second order in curvature, truncations containing the non-local terms responsible for the conformal anomaly of massless matter fields. This non-local action depends only on the number of massless fields and is thus not itself subject to renormalization group flow. It does, however, affect the running of the other couplings.

Following the general discussion in [67, 103], we have seen that the IR cutoff can be implemented in two inequivalent ways, which either maintain or break the Weyl invariance (3.3) of the flow. In the case of the Weyl invariant procedure, we have extended the results of [67] by including the contributions of matter, and the curvature squared term. A physically acceptable fixed point is not present in this truncation in pure gravity, but it reappears in the presence of suitable matter fields. As an example, we have considered the case of one massless Maxwell field and no scalar or Dirac fields, and found a non-Gaussian fixed point with three UV-relevant associated directions. This is in qualitative agreement with results in the case of full gravity, as we will see in subsequent chapters. The fixed point may or may not reappear in pure conformally reduced gravity when higher-order terms are included. We should also mention that a fixed point with the correct properties does not appear if we restrict ourselves to conformal fluctuations *after* having expanded the action. This is somehow to be expected, since scalar fields tend to generate a fixed point with negative G.

We have shown that the Weyl breaking procedure leads to beta functions which are very different from the invariant ones, but which generally agree with those given in [68], at least as far as the case of a flat space background is concerned. The set of beta functions that we have derived following this procedure and in the case of flat space seem to admit the IR stable fixed point found in [68], provided we neglect the local matter contribution. This renormalization group flow, however, will break not only Weyl invariance, but also global scale invariance, and it will hence generate new couplings that are not present in the class of actions that we have considered. As these new couplings will have non-zero beta functions, a proper discussion of the fixed points in this theory would require an extension of

our current analysis. The physical relevance of such an extension to the study of the gravitational renormalization group, however, is not clear.

From a mathematical perspective, both of these are consistent procedures. As we have observed in Section 3.1.1, the Weyl transformations (3.3) should not be regarded as a gauge invariance in conformally reduced gravity, and therefore it is not mandatory to preserve them in the quantum theory. From a physical standpoint, however, one could interpret this choice as that between treating the cutoff scale k as internal to the theory (when $\bar{g}_{\mu\nu}$ is used to define the cutoff), or as an absolute external scale (when $\hat{g}_{\mu\nu}$ is used to define the cutoff), and we may therefore expect that the correct procedure for describing the renormalization group flow of quantum gravity is the first one.

A particular feature of gravity is that the metric itself defines the proper length and mass scale of all dimensionful physical quantities [67, 103]. When implementing our coarse graining in a quantum gravity context, the requirement of diffeomorphism invariance implies that our scale k should be set not by some rigid external metric, but rather result from the intrinsic dynamics of the theory. This is the procedure followed in the full gravity case. On the other hand, one could argue that at least at low energies there are various sets of phenomena that define dynamical mass scales which are to a large extent unaffected by gravity, such as electroweak physics determining the mass of the electron or strong interaction physics determining the mass of the nucleons. In principle one could use electroweak or strong mass units to define the fiducial metric $\hat{g}$ that is employed in the second type of cutoff. However, when one considers the very high energy regime of Planck-scale physics, neither atoms nor nuclei, nor even the vacuum expectation value of the Higgs field, are there to provide an absolute reference scale, and gravity is then so strong that its influence cannot be neglected. Inasmuch as we want to be able to freely evolve our effective theories of gravity between these energy regimes by following their renormalization group flow, it seems that only the former cutoff implementation procedure is meaningful.

The results in this chapter thus provide tentative support for the asymptotic safety scenario, as seen in the case of the Weyl–invariant cutoff procedure, and partially indicate that non-local operators might play a role in the renormalization group behavior of gravity in the IR, at least as seen in the case of the Weyl–breaking procedure for the flat space background. In order to verify both these suggested features, we would of course like to explore the gravitational renormalization group flow in its full setting. This is what we will proceed to do in the remainder of this work.

4

The RG flow of $f(R)$ gravity

Based on P. F. Machado and F. Saueressig, *On the renormalization group flow of f(R)-gravity*, Phys. Rev. D 77, 124045 (2008), arXiv:0712.0445 [hep-th].

In this chapter, we construct an improved functional renormalization group equation (FRGE) for gravity in d-dimensions and for a generic cutoff profile function. Using this FRGE, we derive a flow equation for truncation subspaces spanned by arbitrary functions $f(R)$ of the curvature scalar. This setup allows us to consider a very large class of truncations, of which the Einstein-Hilbert is an example. We first illustrate the use of this flow equation in the case of the Einstein-Hilbert truncation and discuss its main features. Then, specializing to $d = 4$ and for a particular choice of the cutoff function, we derive an autonomous partial differential equation governing the renormalization group flow of $f(R)$ gravity. From this differential equation, we independently recover the results of [69], which indicate the existence of a non-Gaussian fixed point with a three-dimensional UV critical surface in polynomial truncations of R of up to order six.

4.1 An improved FRGE for gravity

Although the FRGE formalism is a powerful tool for the non-perturbative analysis of the renormalization group behavior of field theories, in order to perform computations within this setting we must resort to approximation schemes, as previously discussed. The most commonly employed of these schemes is the truncation approximation, whereby the full renormalization group flow is projected into a subspace parametrized by only a subset of the infinitely many couplings present in the effective average action. Studying the behavior of the theory within

this subspace then implies calculating only a subset of its beta functions, associated with the couplings that have been retained in the truncation. Since the renormalization group flow will generally not close on the truncation subspace, couplings which are disregarded for lying outside the truncation will potentially influence the running of the couplings that have instead been retained. Assessing the reliability of results obtained within a given truncation, and hence ensuring that any features that have been observed are not truncation artifacts, is a central concern within the FRGE approach. The most relevant strategy for addressing this concern is that of progressively enlarging the truncation considered. If our results are largely unaffected under the extension of the subspace and the addition of new running couplings, we have further inductive evidence for their reliability.

Motivated by these considerations, we will here construct a flow equation for $f(R)$ gravity, thus allowing us to treat truncations consisting of arbitrary functions of the curvature scalar R. In this construction, we will perform a transverse-traceless decomposition [113] of the gravitational and ghost fields entering our effective average action, introduce auxiliary fields to treat the Jacobians resulting from this decomposition and implement a type I cutoff on each of these field components. In addition, we will make use of a distinguished, geometrically motivated gauge-fixing condition which will lead to considerable simplifications in our calculations. A flow equation employing the transverse-traceless decomposition and type I cutoffs for the field components was first derived in [37, 82], where it was used to study the Einstein-Hilbert truncation, and subsequently applied in the case of the Einstein-Hilbert+R^2 truncation in [40]. Our improvements on this flow equation are the exponentiation of the Jacobians and the use of the "geometrical" gauge-fixing condition, as first suggested in [69]. We will now comment on these improvements in detail.

4.1.1 The geometric gauge-fixing condition

Our starting point is a scale-dependent Euclidean functional integral $\mathbf{Z}_k$ for gravitational actions. As before, and following [35], diffeomorphism invariance is assured by means of the background field method, whereby the quantum metric $\gamma_{\mu\nu}$ is decomposed into an arbitrary but fixed background metric $\bar{g}_{\mu\nu}$ and a (not necessarily small) fluctuation field $h_{\mu\nu}$

$$\gamma_{\mu\nu} = \bar{g}_{\mu\nu} + h_{\mu\nu} \,. \tag{4.1}$$

The formal expression for the generating functional $\mathbf{Z}_k$ then includes integrations over the quantum fluctuations $h_{\mu\nu}$ and the Faddeev-Popov ghosts C^μ, $\bar{C}_\mu$,

$$\begin{aligned} \mathbf{Z}_k[\text{sources}] = \int \mathcal{D}h_{\mu\nu}\mathcal{D}C^\mu\mathcal{D}\bar{C}_\mu \, \exp\Big[& -S[h+\bar{g}] - S_{\text{gf}}[h;\bar{g}] \\ & - S_{\text{gh}}[h,C,\bar{C};\bar{g}] - \Delta_k S[h,C,\bar{C};\bar{g}] - S_{\text{source}}\Big] \,. \end{aligned} \tag{4.2}$$

Here, $S[\gamma] = S[h + \bar{g}]$ is a diffeomorphism invariant action functional which, for the time being, we assume to be positive definite. In addition, $S_{\rm gf}[h;\bar{g}]$ denotes the gauge-fixing term,

$$S_{\rm gf}[h;\bar{g}] = \frac{1}{2\alpha}\int d^dx\sqrt{\bar{g}}\,\bar{g}^{\mu\nu}\,F_\mu[h;\bar{g}]\,F_\nu[h;\bar{g}] \tag{4.3}$$

which depends on the gauge-fixing parameter α and implements the gauge-fixing condition $F_\mu[h,\bar{g}] = 0$. For the construction of the FRGE, it is particularly convenient to choose a $F_\mu[h;\bar{g}]$ which is linear in $h_{\mu\nu}$. Explicitly, we take

$$F_\mu[h;\bar{g}] = \sqrt{2}\,\kappa\left(\bar{\nabla}^\nu\,h_{\mu\nu} - \frac{1+\rho}{d}\,\bar{\nabla}_\mu\,h^\nu{}_\nu\right), \tag{4.4}$$

with $\kappa = (32\pi G)^{-1/2}$. Here and in the following, barred and unbarred quantities are constructed with respect to the background metric and the full quantum metric, respectively. In particular, $\bar{\nabla}_\mu$ denotes the covariant derivative based on $\bar{g}_{\mu\nu}$, while ∇_μ is covariant with respect to $\gamma_{\mu\nu}$. The constant ρ parameterizes the freedom of implementing different gauge choices, with the harmonic gauge, which was employed in [37,40,82], being obtained by setting $\rho = \frac{d}{2} - 1$. In the following, however, it will be more convenient to set $\rho = 0$, as this will result in significant simplifications. We shall call this gauge the "geometric gauge".

The ghost action arising from the gauge fixing (4.4) is constructed in the standard way, by varying the gauge condition under infinitesimal gauge transformations and exponentiating the resulting determinant, and reads

$$S_{\rm gh}[h,C,\bar{C};\bar{g}] = -\sqrt{2}\int d^dx\sqrt{\bar{g}}\,\bar{C}_\mu\,\mathcal{M}^\mu{}_\nu\,C^\nu\,, \tag{4.5}$$

with the Faddeev-Popov operator

$$\mathcal{M}^\mu{}_\nu = \bar{\nabla}^\rho\,\gamma^\mu{}_\nu\,\nabla_\rho + \bar{\nabla}^\rho\,\gamma_{\rho\nu}\nabla^\mu - 2\,\frac{1+\rho}{d}\,\bar{\nabla}_\mu\,\bar{g}^{\rho\sigma}\,\gamma_{\rho\nu}\nabla_\sigma\,. \tag{4.6}$$

The remaining terms in (4.2), $\Delta_k S[h,C,\bar{C};\bar{g}]$ and $S_{\rm Source}$, respectively contain the scale-dependent IR cutoff and the source terms for the metric fluctuations and ghosts, and will be discussed in Section 4.1.3. Note that, here and in the following, we omit the tensor indices in the arguments of our functionals for ease of notation, but it is understood these arguments do carry the appropriate indices, e.g., $S\,[h+\bar{g}] = S\,[h_{\mu\nu}+\bar{g}_{\mu\nu}]$.

4.1.2 The transverse-traceless decomposition

A common technical difficulty in practical applications of the FRGE for gauge theories and gravity is the construction of the IR cutoff $\Delta_k S[h,C,\bar{C};\bar{g}]$ and the inversion of $\Gamma_k^{(2)}+\mathcal{R}_k$, which requires the (partial) diagonalization of these operators. To facilitate this in our case, we perform a transverse-traceless decomposition

of the metric fluctuations and the ghost fields and impose the cutoff on each of the resulting component fields. Following [37, 41], we will call this cutoff a "type Ib cutoff". We then decompose the metric fluctuations $h_{\mu\nu}$ into a trace part $h^{\rm tr}_{\mu\nu} = \frac{1}{d}\bar{g}_{\mu\nu}h$, encoded in the scalar h, a longitudinal part, encoded by the transverse vector ξ_μ and the scalar σ, and a transverse traceless part $h^{\rm T}_{\mu\nu}$ according to

$$h_{\mu\nu} = h^{\rm T}_{\mu\nu} + \bar{\nabla}_\mu\xi_\nu + \bar{\nabla}_\nu\xi_\mu + \bar{\nabla}_\mu\bar{\nabla}_\nu\sigma - \frac{1}{d}\bar{g}_{\mu\nu}\bar{\nabla}^2\sigma + \frac{1}{d}\bar{g}_{\mu\nu}h\,, \tag{4.7}$$

with the component fields subject to the constraints

$$\bar{g}^{\mu\nu}h^{\rm T}_{\mu\nu} = 0\,, \quad \bar{\nabla}^\mu h^{\rm T}_{\mu\nu} = 0\,, \quad \bar{\nabla}^\mu\xi_\mu = 0\,, \quad h = \bar{g}_{\mu\nu}h^{\mu\nu}\,. \tag{4.8}$$

Similarly, the ghost fields $C^\mu, \bar{C}_\mu$ are decomposed into their transverse and longitudinal parts $C^{{\rm T}\mu}, \bar{C}^{\rm T}_\mu$ and $\eta, \bar{\eta}$ as

$$\bar{C}_\mu = \bar{C}^{\rm T}_\mu + \bar{\nabla}_\mu\bar{\eta}\,, \quad C_\mu = C^{\rm T}_\mu + \bar{\nabla}_\mu\eta\,, \qquad \bar{\nabla}^\mu\,\bar{C}^{\rm T}_\mu = 0\,, \quad \bar{\nabla}^\mu\,C^{\rm T}_\mu = 0\,. \tag{4.9}$$

From eqs. (4.7) and (4.9), it is clear that not all modes of the component fields contribute to the metric and ghost fields. In the metric decomposition, the constant mode of the σ-vectors, $\mathcal{C}_\mu = \bar{\nabla}_\mu\sigma$ satisfying the conformal Killing equation

$$\bar{\nabla}_\mu\mathcal{C}_\nu + \bar{\nabla}_\nu\mathcal{C}_\mu - \frac{2}{d}\bar{g}_{\mu\nu}\bar{\nabla}_\mu\mathcal{C}^\mu = 0\,, \tag{4.10}$$

and transversal vectors solving the Killing equation

$$\bar{\nabla}_\mu\xi_\nu + \bar{\nabla}_\nu\xi_\mu = 0 \tag{4.11}$$

do not contribute to $h_{\mu\nu}$. Analogously, the ghost fields $\bar{C}_\mu, C^\mu$ are independent of the constant modes of $\eta, \bar{\eta}$. These modes are unphysical and must be excluded from the spectrum. In fact, this is also a necessary requirement for the invertibility of the Jacobians arising from the coordinate transformations (4.7) and (4.9), as we will see below.

A virtue of the TT-decomposition is that the component fields (almost) provide an orthogonal basis for the quantum fluctuations. Evaluating the scalar product in the ghost sector gives

$$\langle\bar{C}, C\rangle \equiv \int d^dx\sqrt{\bar{g}}\,\bar{C}_\mu\,C^\mu = \int d^dx\sqrt{\bar{g}}\,\{\bar{C}^{\rm T}_\mu\,C^{\mu{\rm T}} - \bar{\eta}\,\bar{\nabla}^2\,\eta\}\,, \tag{4.12}$$

establishing that this decomposition is orthogonal. In the metric sector, on the other hand, the inner product becomes

$$\begin{aligned}\langle h^{(1)}, h^{(2)}\rangle &\equiv \int d^dx\sqrt{\bar{g}}\,h^{(1)}_{\mu\nu}\,\bar{g}^{\mu\rho}\,\bar{g}^{\nu\sigma}\,h^{(2)}_{\rho\sigma} \\ &= \int d^dx\sqrt{\bar{g}}\Big[h^{(1){\rm T}}_{\mu\nu}\,h^{(2){\rm T}\mu\nu} - 2\,\xi^{(1)}_\mu\,\big[\bar{g}^{\mu\nu}\bar{\nabla}^2 + \bar{R}^{\mu\nu}\big]\,\xi^{(2)}_\nu \\ &\quad - 2\xi^{(1)}_\mu\,\bar{R}^{\mu\nu}\bar{\nabla}_\nu\sigma^{(2)} - 2\xi^{(2)}_\mu\,\bar{R}^{\mu\nu}\bar{\nabla}_\nu\sigma^{(1)} \\ &\quad + \sigma^{(1)}\big[\frac{d-1}{d}(\bar{\nabla}^2)^2 + \bar{\nabla}_\mu\bar{R}^{\mu\nu}\bar{\nabla}_\nu\big]\sigma^{(2)} + \frac{1}{d}h^{(1)}h^{(2)}\Big]\,,\end{aligned} \tag{4.13}$$

which is orthogonal up to the ξ_μ-σ-mixed terms. We note that these crossterms vanish, however, for the Einstein backgrounds (satisfying $\bar{R}_{\mu\nu} = C\bar{g}_{\mu\nu}$) considered in the next section, i.e.,

$$\int d^dx\sqrt{\bar{g}}\,\xi_\mu \bar{R}^{\mu\nu}\bar{\nabla}_\nu\sigma = -C\int d^dx\sqrt{\bar{g}}\,\sigma\bar{\nabla}^\mu\xi_\mu = 0.$$

Thus, in that case, the component fields do provide an orthogonal basis for the quantum fluctuations.

The inner products (4.13) and (4.12) can be used to compute the Jacobians of the coordinate transformations (4.7) and (4.9). For this purpose, we follow [104] and consider the Gaussian integral over $h_{\mu\nu}$ and $\bar{C}_\mu, C^\mu$. In the metric sector, this yields

$$\begin{aligned}\int \mathcal{D}h_{\mu\nu}\,\exp\left[-\tfrac{1}{2}\langle h,h\rangle\right] = \;& J_{\rm grav}\int \mathcal{D}h^{\rm T}_{\mu\nu}\mathcal{D}\xi_\mu\mathcal{D}\sigma\mathcal{D}h \\ & \times\exp\Big[-\tfrac{1}{2}\int d^dx\sqrt{\bar{g}}\left\{h^{\rm T}_{\mu\nu}h^{{\rm T}\mu\nu} + \tfrac{1}{d}h^2 + [\xi_\mu,\sigma]\,M^{(\mu,\nu)}\,[\xi_\nu,\sigma]^{\rm T}\right\}\Big],\end{aligned} \tag{4.14}$$

where $M^{(\mu,\nu)}$ is a $(d{+}1)\times(d{+}1)$-matrix differential operator whose first d columns act on transverse spin-one fields ξ_μ and whose last column acts on the spin zero fields σ. The corresponding matrix can be read off from (4.13),

$$M^{(\mu,\nu)} = \begin{bmatrix} -2\left[\bar{g}^{\mu\nu}\bar{\nabla}^2 + \bar{R}^{\mu\nu}\right] & -2\bar{R}^{\mu\lambda}\bar{\nabla}_\lambda \\ 2\bar{\nabla}_\lambda\bar{R}^{\lambda\nu} & \frac{d-1}{d}(\bar{\nabla}^2)^2 + \bar{\nabla}_\mu\bar{R}^{\mu\nu}\bar{\nabla}_\nu \end{bmatrix}. \tag{4.15}$$

The Jacobian $J_{\rm grav}$ is found by performing the Gaussian integrals in (4.14) and, up to an infinite normalization constant which can be absorbed into the normalization of the measure, reads

$$J_{\rm grav} = \Big(\det{}'_{(1{\rm T},0)}\left[M^{(\mu,\nu)}\right]\Big)^{1/2}. \tag{4.16}$$

Here, the subscript $(1{\rm T},0)$ refers to the matrix structure explained above and the prime indicates that the unphysical modes are left out. The Jacobian introduced by the change of coordinates in the ghost sector (4.9) can be determined analogously. Setting

$$\begin{aligned}&\int \mathcal{D}C^\mu\,\mathcal{D}\bar{C}_\mu\exp[-\langle\bar{C},C\rangle] = \\ &\qquad J_{\rm gh}\int \mathcal{D}C^{{\rm T}\mu}\,\mathcal{D}\bar{C}^{\rm T}_\mu\,\mathcal{D}\eta\,\mathcal{D}\bar{\eta}\exp\left[-\int d^dx\sqrt{\bar{g}}\left\{\bar{C}^{\rm T}_\mu\,C^{\mu{\rm T}} - \bar{\eta}\,\bar{\nabla}^2\,\eta\right\}\right]\end{aligned} \tag{4.17}$$

and performing the Grassmann functional integrals results in

$$J_{\rm gh} = \left(\det{}'_0[-\bar{\nabla}^2]\right)^{-1}. \tag{4.18}$$

In order to include the contribution from the Jacobians in the partition function (4.2), we follow the Faddeev-Popov trick and introduce a set of auxiliary fields to exponentiate the determinants. This leads to an additional term $S_{\rm aux}[\text{aux. fields}; \bar{g}]$ in $\mathbf{Z}_k$. Let us first consider $J_{\rm grav}$, arising from the metric sector. Introducing the transverse ghost $\bar{c}^{\rm T}_\mu, c^{{\rm T}\mu}$, a "longitudinal" Grassmann scalar $\bar{b}, b$, a transverse vector field $\zeta^{\rm T}_\mu$ and a real auxiliary scalar ω, we can use standard results on Gaussian integration to write (4.16) as

$$J_{\rm grav} = \int \mathcal{D}c^{\rm T}_\mu \mathcal{D}\bar{c}^{{\rm T}\mu}\, \mathcal{D}b\, \mathcal{D}\bar{b}\, \mathcal{D}\zeta^{\rm T}_\mu\, \mathcal{D}\omega \exp\Bigg[- \int d^dx \sqrt{\bar{g}} \Big\{ [\zeta^{\rm T}_\mu, \omega] \big[M^{(\mu,\nu)}\big]' [\zeta^{\rm T}_\nu, \omega]^{\rm T} + [\bar{c}^{\rm T}_\mu, \bar{b}] \big[M^{(\mu,\nu)}\big]' [c^{\rm T}_\nu, b]^{\rm T} \Big\} \Bigg] . \tag{4.19}$$

Lastly, the Jacobian from the ghost sector (4.18) is exponentiated by introducing a new complex scalar field $s, \bar{s}$,

$$J_{\rm gh} = \int \mathcal{D}\bar{s}\, \mathcal{D}s\, \exp\left[- \int d^dx\, \sqrt{\bar{g}}\, \bar{s}\, [-\bar{\nabla}^2]' s \right] . \tag{4.20}$$

By combining the results (4.19) and (4.20), we then find

$$\begin{aligned} S_{\rm aux}[\zeta^{\rm T},\, \bar{s}, s, \omega, \bar{c}^{\rm T}, c^{\rm T}, \bar{b}, b; \bar{g}] = \int d^dx\, \sqrt{\bar{g}} \Big\{ & [\zeta^{\rm T}_\mu, \omega] \big[M^{(\mu,\nu)}\big]' [\zeta^{\rm T}_\nu, \omega]^{\rm T} \\ & + [\bar{c}^{\rm T}_\mu, \bar{b}] \big[M^{(\mu,\nu)}\big]' [c^{\rm T}_\nu, b]^{\rm T} + \bar{s}\, [-\bar{\nabla}^2]' s \Big\} . \end{aligned} \tag{4.21}$$

Here, the primes are placed as a reminder that the unphysical modes have been excluded from the auxiliary fields.

In [37, 82], instead of working with the fields ξ, σ, and $\bar{\eta}, \eta$, non-local field redefinitions were introduced,

$$\begin{aligned} & \xi^\mu \to \hat{\xi}^\mu = \sqrt{-\bar{\nabla}^2 - \overline{\rm Ric}}\, \xi^\mu , \quad \sigma \to \hat{\sigma} = \sqrt{(\bar{\nabla}^2)^2 + \tfrac{d}{d-1} \bar{\nabla}_\mu R^{\mu\nu} \bar{\nabla}_\nu}\, \sigma , \\ & \eta \to \hat{\eta} = \sqrt{-\bar{\nabla}^2}\, \eta , \quad \bar{\eta} \to \hat{\bar{\eta}} = \sqrt{-\bar{\nabla}^2}\, \bar{\eta} , \end{aligned} \tag{4.22}$$

where $\overline{Ric}(B)_\mu = R^\nu_\mu B_\nu$. The Jacobians arising from these transformations eliminate the Jacobians from the TT-decomposition in the case of the background Einstein spaces $\bar{\gamma}_{\mu\nu}$ employed in those calculations, and hence no auxiliary fields needed to be introduced. However, while these redefinitions are adequate for truncations including up to two powers of curvature, they pose a problem in higher-order truncations, causing poles to appear in the evaluation of the traces, due to the fact that the heat kernel expansion will involve derivatives of the trace arguments. Overcoming this limitation by exponentiating the TT Jacobians and sidestepping the field redefinition, we can treat truncations including arbitrarily high powers of curvature in our FRGE.

4.1.3 The FRGE in terms of component fields

After discussing the new ingredients for the improved FRGE with a type Ib cutoff, we are now in the position to construct the corresponding flow equation. To lighten our notation, let us first introduce the index sets

$$\begin{aligned} I_1 &= \{h^{\mathrm{T}}, \xi, \sigma, h\}\,, \quad I_2 = \{\bar{C}^{\mathrm{T}}, C, \bar{\eta}, \eta\}\,, \\ I_3 &= \{\zeta^{\mathrm{T}}, \omega, \bar{s}, s, \bar{c}^{\mathrm{T}}, c^{\mathrm{T}}, \bar{b}, b\}\,, \end{aligned} \tag{4.23}$$

and a shorthand notation for the quantum fields,

$$\chi = \left\{h^{\mathrm{T}}, \xi, \sigma, h, \zeta^{\mathrm{T}}, \omega, \bar{s}, s, C, \eta, c^{\mathrm{T}}, b, \bar{C}^{\mathrm{T}}, \bar{\eta}, \bar{c}^{\mathrm{T}}, \bar{b}\right\}. \tag{4.24}$$

The two remaining ingredients in the scale-dependent partition function (4.2) which have not yet been specified are the IR cutoff $\Delta_k S$ and the source terms. As previously discussed, the IR cutoff is constructed in such a way that, for all fields (including the auxiliaries), the integration over the $p^2 = -\bar{\nabla}^2$-eigenmodes with large eigenvalues $p^2 \gg k^2$ is unaffected while the contributions of the modes with small eigenvalues $p^2 \ll k^2$ are suppressed. To this end, $\Delta_k S$ provides a momentum-dependent mass term which is quadratic in the fields (4.24),

$$\begin{aligned} \Delta_k S = {} & \tfrac{1}{2} \sum_{\zeta_1, \zeta_2 \in I_1} \langle \zeta_1, (\mathcal{R}_k^{\mathrm{grav}})_{\zeta_1 \zeta_2} \zeta_2 \rangle + \tfrac{1}{2} \sum_{\psi_1, \psi_2 \in I_2} \langle \psi_1, (\mathcal{R}_k^{\mathrm{gh}})_{\psi_1 \psi_2} \psi_2 \rangle \\ & + \tfrac{1}{2} \sum_{\varsigma_1, \varsigma_2 \in I_3} \langle \varsigma_1, (\mathcal{R}_k^{\mathrm{aux}})_{\varsigma_1 \varsigma_2} \varsigma_2 \rangle\,. \end{aligned} \tag{4.25}$$

The operators $\mathcal{R}_k^{\mathrm{grav}}$, $\mathcal{R}_k^{\mathrm{gh}}$, and $\mathcal{R}_k^{\mathrm{aux}}$ depend on the background metric only. In order to implement the desired suppression behavior, they must vanish for $p^2/k^2 \to \infty$ (and in particular for $k^2 \to 0$) while, for $p^2/k^2 \to 0$, they must behave as $\mathcal{R}_k \to \mathcal{Z}_k k^2$, where $\mathcal{Z}_k$ is a possibly matrix-valued k-dependent function. In addition, hermiticity requires that $(\mathcal{R}_k)_{\zeta_2 \zeta_1} = (\mathcal{R}_k)^\dagger_{\zeta_1 \zeta_2}$ and $(\mathcal{R}_k)_{\psi_2 \psi_1} = -(\mathcal{R}_k)^\dagger_{\psi_1 \psi_2}$ for bosonic and Grassmann-valued fields, respectively. Furthermore, $(\mathcal{R}_k)_{\psi_1 \psi_2} = 0$ if both $\psi_1, \psi_2 \in \{C^{\mathrm{T}}, \eta, c^{\mathrm{T}}, b\}$ or $\{\bar{C}^{\mathrm{T}}, \bar{\eta}, \bar{c}^{\mathrm{T}}, \bar{b}\}$. In the sequel, we will denote the three terms in (4.25) by $\Delta_k S_{\mathrm{grav}}, \Delta_k S_{\mathrm{gh}}$ and $\Delta_k S_{\mathrm{aux}}$, respectively.

Finally, we specify S_{source}, which introduces source terms for all component fields, again including the auxiliaries. Denoting the sources for the bosonic field and ghost fields by J and K, we set

$$\begin{aligned} S_{\mathrm{source}} = {} & - \sum_{\zeta \in I_1} \langle J_\zeta, \zeta \rangle - \langle J_{\zeta^{\mathrm{T}}}, \zeta^{\mathrm{T}} \rangle - \langle J_\omega, \omega \rangle - \langle \bar{J}_{\bar{s}}, \bar{s} \rangle - \langle J_s, s \rangle \\ & - \sum_{\psi \in \{C^{\mathrm{T}}, \eta, c^{\mathrm{T}}, b\}} \langle \bar{K}_\psi, \psi \rangle - \sum_{\psi \in \{\bar{C}^{\mathrm{T}}, \bar{\eta}, \bar{c}^{\mathrm{T}}, \bar{b}\}} \langle K_\psi, \psi \rangle\,. \end{aligned} \tag{4.26}$$

In the following, we denote the sources collectively by $\mathcal{J}$, which allows us to write (4.26) schematically as

$$S_{\mathrm{source}}[\mathcal{J}; \bar{g}] = -\langle \mathcal{J}, \chi \rangle\,. \tag{4.27}$$

The relations between the component sources and the standard sources for the metric fluctuations $h_{\mu\nu}, \bar{C}_\mu, C^\mu$ have been worked out in detail in [37], where it was shown that the standard sources can be reconstructed from the $\mathcal{J}$.

With these results at hand, we can write the scale-dependent partition function (4.2) in terms of the component fields,

$$\mathbf{Z}_k[\mathcal{J};\bar{g}] = \int \mathcal{D}\chi \exp\left[-S[h+\bar{g}] - S_{\rm gf}[h;\bar{g}] - S_{\rm gh} - \Delta_k S - S_{\rm aux} - S_{\rm source}\right]. \tag{4.28}$$

Note that the k-dependence on the right-hand side of this equation arises solely through the IR cutoff $\Delta_k S$.

We now explicitly derive our improved FRGE from this partition function, in an analogous manner to [37]. From (4.28), the scale-dependent generating functional for the connected Green's functions is given by

$$W_k[\mathcal{J};\bar{g}] = \ln \mathbf{Z}_k[\mathcal{J};\bar{g}]\,, \tag{4.29}$$

and the classical component fields are obtained as

$$\varphi_i \equiv \langle \chi_i \rangle = \frac{1}{\sqrt{\bar{g}}} \frac{\delta W_k}{\delta \mathcal{J}^i}\,, \tag{4.30}$$

where we have collectively denoted the classical counterparts of the quantum fields (4.24) by

$$\varphi = \left\{ \bar{h}^{\rm T}, \bar{\xi}, \bar{\sigma}, \bar{h}, \bar{\zeta}^{\rm T}, \bar{\omega}, \bar{t}, t, v^{\rm T}, \varrho, u^{\rm T}, \tau, \bar{v}^{\rm T}, \bar{\varrho}, \bar{u}^{\rm T}, \bar{\tau} \right\}. \tag{4.31}$$

The classical counterparts of the fundamental fields $h_{\mu\nu}$, $\bar{C}^\mu$ and C_μ can be reconstructed by substituting the corresponding component fields into the formulas for the TT-decomposition. For later purposes, we also define the classical analogue of the quantum metric (4.1)

$$g_{\mu\nu} \equiv \langle \gamma_{\mu\nu} \rangle = \bar{g}_{\mu\nu} + \bar{h}_{\mu\nu}\,. \tag{4.32}$$

We then construct the scale-dependent effective action as the Legendre-transform on W_k with respect to the component sources $\mathcal{J}$, taking the latter as functions of the classical fields[1],

$$\tilde{\Gamma}_k\left[\varphi;\bar{g}\right] = \langle \mathcal{J}, \varphi \rangle - W_k\left[\mathcal{J};\bar{g}\right]\,. \tag{4.33}$$

The effective average action Γ_k is defined as the difference between $\tilde{\Gamma}_k$ and the cutoff action with the classical fields inserted,

$$\Gamma_k[\varphi;\bar{g}] \equiv \tilde{\Gamma}_k[\varphi;\bar{g}] - \Delta_k S[\varphi;\bar{g}]\,. \tag{4.34}$$

[1] As was shown in [37], taking the Legendre transform with respect to the sources for the (physical) component fields is equivalent to taking the Legendre transform with respect to the sources for the fundamental fields.

The derivation of the FRGE governing the k-dependence of $\Gamma_k[\varphi;\bar{g}]$ proceeds in several steps. First, we differentiate (4.29) with respect to $t=\ln(k)$,

$$\begin{aligned}-k\partial_k W_k = &\tfrac{1}{2}\mathrm{Tr}'\left[\sum_{\zeta_1,\zeta_2\in I_1}\langle\zeta_1\otimes\zeta_2\rangle k\partial_k(\mathcal{R}_k)_{\zeta_1\zeta_2}\right]\\ &+\tfrac{1}{2}\mathrm{Tr}'\left[\sum_{\psi_1,\psi_2\in I_2}\langle\psi_1\otimes\psi_2\rangle k\partial_k(\mathcal{R}_k)_{\psi_1\psi_2}\right]\\ &+\tfrac{1}{2}\mathrm{Tr}'\left[\sum_{\chi_1,\chi_2\in I_3}\langle\chi_1\otimes\chi_2\rangle k\partial_k(\mathcal{R}_k)_{\chi_1\chi_2}\right],\end{aligned} \tag{4.35}$$

where we have expressed the right-hand side in a matrix notation. We then introduce the Hessian of the effective action,

$$\left(\tilde{\Gamma}_k^{(2)}\right)^{ij}(x,y)\equiv(-1)^{[j]}\frac{1}{\sqrt{\bar{g}(x)\bar{g}(y)}}\frac{\delta^2\tilde{\Gamma}_k}{\delta\varphi_i(x)\delta\varphi_j(y)}, \tag{4.36}$$

with $[j]=0,1$ for commuting fields φ_j and Grassmann fields φ_j, respectively. This Hessian is the inverse of the connected two-point function

$$(G_k)_{ij}(x,y)\equiv\langle\chi_i\chi_j\rangle-\varphi_i(x)\varphi_j(y)=\frac{1}{\sqrt{\bar{g}(x)\bar{g}(y)}}\frac{\delta^2 W_k}{\delta\mathcal{J}^i(x)\delta\mathcal{J}^j(y)}, \tag{4.37}$$

in the sense that

$$\int d^dy\sqrt{\bar{g}(y)}\,(G_k)_{ij}(x,y)\left(\tilde{\Gamma}_k^{(2)}\right)^{jl}(y,z)=\delta_i^l\frac{\delta(x-z)}{\sqrt{\bar{g}(z)}}. \tag{4.38}$$

Using these relations, we can express the expectation values $\langle\chi_i(x)\chi_j(y)\rangle$ in eq. (4.35) through

$$\left(\tilde{\Gamma}_k^{(2)}\right)^{-1}_{ij}(y,z)+\phi_i(x)\phi_j(y).$$

Finally, performing the Legendre transform (4.33) and subtracting $\Delta_k S[\varphi;\bar{g}]$ yields the desired FRGE for $\Gamma_k[\varphi;\bar{g}]$

$$\begin{aligned}k\partial_k\Gamma_k[\varphi;\bar{g}]=&\tfrac{1}{2}\mathrm{Tr}'\Big[\sum_{\zeta_1,\zeta_2\in\bar{I}_1}\left(\Gamma_k^{(2)}+\mathcal{R}_k\right)^{-1}_{\zeta_1\zeta_2}k\partial_k(\mathcal{R}_k)_{\zeta_1\zeta_2}\Big]\\ &+\tfrac{1}{2}\mathrm{Tr}'\Big[\sum_{\psi_1,\psi_2\in\bar{I}_2}\left(\Gamma_k^{(2)}+\mathcal{R}_k\right)^{-1}_{\psi_1\psi_2}k\partial_k(\mathcal{R}_k)_{\psi_1\psi_2}\Big]\\ &+\tfrac{1}{2}\mathrm{Tr}'\Big[\sum_{\chi_1,\chi_2\in\bar{I}_3}\left(\Gamma_k^{(2)}+\mathcal{R}_k\right)^{-1}_{\chi_1\chi_2}k\partial_k(\mathcal{R}_k)_{\chi_1\chi_2}\Big].\end{aligned} \tag{4.39}$$

Here, we have again used a matrix notation on the right-hand side, and the barred index sets run over the classical fields,

$$\bar{I}_1 = \{\bar{h}^{\mathrm{T}}, \bar{\xi}, \bar{\sigma}, \bar{h}\}\,, \quad \bar{I}_2 = \{\bar{v}^{\mathrm{T}}, v^{\mathrm{T}}, \bar{\varrho}, \varrho\}\,, \quad \bar{I}_3 = \{\bar{\zeta}^{\mathrm{T}}, \bar{\omega}, \bar{t}, t, \bar{u}^{\mathrm{T}}, u^{\mathrm{T}}, \bar{\tau}, \tau\}\,. \tag{4.40}$$

The first, second and third term in (4.39) thus encode the contributions from the gravitational, ghost and auxiliary fields, respectively.

Eq. (4.39) is the desired exact FRGE for the effective average action employing the improved TT-cutoff. Compared to [37, 82], the new feature is the appearance of the third trace term, capturing the contribution of the auxiliary fields, which replaces the momentum dependent field redefinitions in the metric and ghost sector. As it will turn out in the next section, this form of the FRGE is very convenient when studying truncations involving a general function $f(R)$.

4.2 Constructing the flow equation of $f(R)$ gravity

After deriving the exact FRGE (4.39) in the last section, we now proceed by projecting the resulting renormalization group flow on truncation subspaces spanned by arbitrary functions of the curvature scalar. In view of recent applications of renormalization group methods to gravity theories including extra dimensions [77, 114], we do not fix the space-time dimension d. In addition, we keep the shape of the IR cutoff generic.

4.2.1 The truncation ansatz

Let us start by specifying our truncation ansatz for $\Gamma_k[\varphi; \bar{g}]$, which we take to be of the form

$$\Gamma_k[\varphi; \bar{g}] = \bar{\Gamma}_k[g] + S_{\mathrm{gf}}[g - \bar{g}; \bar{g}] + S_{\mathrm{gh}}[g - \bar{g}, \bar{C}^{\mathrm{T}}, C^{\mathrm{T}}, \bar{\eta}, \eta; \bar{g}] + S_{\mathrm{aux}}\,, \tag{4.41}$$

with

$$\bar{\Gamma}_k[g] = \frac{1}{16\pi G}\int d^d x \sqrt{g}\, f_k(R)\,. \tag{4.42}$$

This ansatz captures the renormalization group flow of $f(R)$ gravity by promoting the classical function $f(R)$ to be scale-dependent. Note that, modulo the presence of the auxiliary fields term S_{aux}, this truncation is exactly of the type (2.22), introduced in Section 2.2.2. The features and limitations of this truncation have been discussed in detail in that section. For convenience, we summarize that discussion here. In our truncation, the renormalization group effects in the gauge-fixing, ghost and auxiliary sector are neglected by treating $S_{\mathrm{gf}}, S_{\mathrm{gh}}$ and S_{aux} as classical and not containing any scale-dependent couplings. In effect, this implies neglecting a term $\hat{\Gamma}_k[g, \bar{g}]$ in our effective average action, which encodes the deviations from $\bar{\Gamma}_k[g]$ for $g \neq \bar{g}$. The main reason for this is technical simplicity,

as evaluating the functional traces otherwise becomes a formidable and sometimes impossible task. The motivation behind this simplification is twofold. First, it was argued in [35] that neglecting the renormalization group running in $S_{\rm gf}$ and $S_{\rm gh}$ is, to leading order, compatible with the modified Ward identities of the theory. Secondly, even when treating $S_{\rm gf}$ as classical, renormalization group effects in this sector can be included by taking $\alpha = 0$, which corresponds to a fixed point of the renormalization group flow [37, 81]. Recent studies which have gone beyond this ansatz suggest that implementing the running of the ghost sector [80] will not have a large effect on results otherwise obtained. Similarly, generally setting $\hat{\Gamma}_k[g, \bar{g}] \neq 0$ will lead to quantitative differences in the results but is not expected to alter the qualitative picture.

When substituting the truncation ansatz (4.41) into the FRGE (4.39) we find that the gravitational trace only receives contributions from

$$\Gamma_k^{\rm grav}[g; \bar{g}] \equiv \bar{\Gamma}_k[g] + S_{\rm gf}[g - \bar{g}; \bar{g}]\,, \tag{4.43}$$

while the ghost and auxiliary traces are evaluated based on the classical actions $S_{\rm gh}$ and $S_{\rm aux}$,

$$\begin{aligned} k\partial_k \Gamma_k[\varphi; \bar{g}] = {} & \tfrac{1}{2}{\rm Tr}'\Big[\sum_{\zeta_1,\zeta_2 \in \bar{I}_1} \Big(\Gamma_k^{\rm grav(2)} + \mathcal{R}_k\Big)^{-1}_{\zeta_1\zeta_2} k\partial_k(\mathcal{R}_k)_{\zeta_1\zeta_2}\Big] \\ & + \tfrac{1}{2}{\rm Tr}'\Big[\sum_{\psi_1,\psi_2 \in \bar{I}_2} \Big(S_{\rm gh}^{(2)} + \mathcal{R}_k\Big)^{-1}_{\psi_1\psi_2} k\partial_k(\mathcal{R}_k)_{\psi_1\psi_2}\Big] \\ & + \tfrac{1}{2}{\rm Tr}'\Big[\sum_{\chi_1,\chi_2 \in \bar{I}_3} \Big(S_{\rm aux}^{(2)} + \mathcal{R}_k\Big)^{-1}_{\chi_1\chi_2} k\partial_k(\mathcal{R}_k)_{\chi_1\chi_2}\Big]\,. \end{aligned} \tag{4.44}$$

The index sets here are given by (4.40).

Our main task now is to evaluate the traces appearing on the right-hand side of (4.44). This is done as follows. First, in Section 4.2.2, we first compute the Hessians of the various terms appearing in (4.41). This computation can be simplified by choosing the background metric $\bar{g}_{\mu\nu}$ as the one-parameter family of metrics on the d-sphere S^d (parameterized by the radius r or, equivalently, the curvature scalar of the sphere), as this suffices to distinguish different functions of the curvature scalar.

For these backgrounds, the unphysical modes discussed in Section 4.1.2 correspond to the lowest $-\bar{\nabla}^2$-eigenmode ($l = 1$) of the transverse vector ξ_μ and the two lowest eigenmodes ($l = 0, 1$) for σ in the gravitational sector. In the ghost sector, strictly speaking only the lowest mode ($l = 0$) of the scalar $\eta, \bar{\eta}$ must be excluded, as can be seen from (4.9). Using Table D.1 in Appendix D.1, one can explicitly check that these modes are annihilated by the operators appearing in the Jacobians (4.16) and (4.18) restricted to S^d. However, as in [41, 69], we here take the viewpoint that, since the ghost contribution is supposed to cancel out the contributions of the gauge degrees of freedom, and since our gauge choice $\rho = 0$

aligns the gauge orbits with the directions $\xi_\mu^{\mathrm{T}}, \sigma$ in the $\alpha \to 0$ limit, as we will see shortly, these cancellations should here occur mode by mode. For this reason, we also exclude the lowest mode ($l = 1$) of the transverse ghost field $C^{\mathrm{T}\mu}, \bar{C}_\mu^{\mathrm{T}}$ as well as the second lowest mode ($l = 1$) for the scalar ghost $\eta, \bar{\eta}$. This implies that all analogous modes in the auxiliary sector are also excluded.

In Section 4.2.3, we use these results to construct the IR cutoff operators ΔS_k explicitly. Lastly, we substitute those results back into (4.44), finding cancellations between several terms appearing on the right-hand side, so that the final result (4.61) takes a surprisingly simple form.

4.2.2 Computing the Hessian $\Gamma_k^{(2)}$

We start by deriving the term quadratic in the metric fluctuations $h_{\mu\nu}$ arising from $\bar{\Gamma}_k[g = \bar{g} + h; \bar{g}]$, viz. (4.42). For this purpose, we expand $\bar{\Gamma}_k[\bar{g} + h; \bar{g}]$ in a Taylor series in $h_{\mu\nu}$,

$$\bar{\Gamma}_k[\bar{g} + h; \bar{g}] = \bar{\Gamma}_k[\bar{g}; \bar{g}] + \mathcal{O}(h) + \bar{\Gamma}_k^{\mathrm{quad}}[\bar{g} + h; \bar{g}] + \mathcal{O}(h^3)\,. \tag{4.45}$$

Here, $\bar{\Gamma}_k^{\mathrm{quad}}[\bar{g} + h; \bar{g}]$ is found by taking the second variation of $\bar{\Gamma}_k[\bar{g} + h; \bar{g}]$ with respect to $h_{\mu\nu}$ and setting $g_{\mu\nu} = \bar{g}_{\mu\nu}$ afterwards. Applying the chain rule, we obtain

$$\begin{aligned}\delta^2\bar{\Gamma}_k = \frac{1}{16\pi G_k}\int d^dx \Big[& f_k(R)\delta^2\sqrt{g} + f_k'(R)\left(2(\delta\sqrt{g})(\delta R) + \sqrt{g}(\delta^2 R)\right) \\ & + \sqrt{g} f_k''(R)(\delta R)^2\Big],\end{aligned} \tag{4.46}$$

where, here and in the following, the prime denotes a derivative with respect to R, i.e., $f_k'(R) = \frac{\partial f_k(R)}{\partial R}$, etc. We then substitute in the above expression the variations of the metric and Ricci scalar, which we have collected in Table B.1 in Appendix B. Note that the result simplifies considerably once we set $g_{\mu\nu} = \bar{g}_{\mu\nu}$ with a spherically symmetric background metric. Performing the TT decomposition of $h_{\mu\nu}$ according to (4.7), a lengthy but straightforward computation yields

$$\bar{\Gamma}_k^{\mathrm{quad}}[h; \bar{g}] = \frac{1}{32\pi G}\int d^dx \sqrt{\bar{g}}\,\mathcal{L}_k\,, \tag{4.47}$$

with

$$\begin{aligned}\mathcal{L}_k = &\tfrac{1}{2}\,h^{\mathrm{T}}_{\mu\nu}\left[f_k'\,\bar\nabla^2 - f_k + \tfrac{2(d-2)}{d(d-1)}\,\bar R\,f_k'\right]h^{\mu\nu\mathrm{T}} + \tfrac{1}{d}\,\left(d\,f_k - 2\,\bar R\,f_k'\right)\,\xi_\mu\left[\bar\nabla^2 + \tfrac{1}{d}\,\bar R\right]\xi^\mu\\ &+ \tfrac{1}{4d^2}\,h\left[4(d-1)^2 f_k''\bar\nabla^4 - 2(d-1)\left((d-2)f_k' - 4\,\bar R\,f_k''\right)\bar\nabla^2\right.\\ &\qquad\left.+ (d-2)(d\,f_k - 4\,\bar R\,f_k') + 4\,\bar R^2\,f_k''\right]h\\ &+ \tfrac{1}{2d^2}\,\sigma\left[2(d-1)^2 f_k''\bar\nabla^8 - (d-1)((d-2)f_k' - 4\bar R f_k'')\bar\nabla^6\right.\\ &\qquad\left.- \left(d(d-1)f_k - \bar R(df_k' + 2\bar R f_k'')\right)\bar\nabla^4 - \bar R(df_k - 2\bar R f_k')\bar\nabla^2\right]\sigma\\ &- \tfrac{1}{d^2}\,h\Big[2(d-1)^2 f_k''\bar\nabla^6 - (d-1)((d-2)f_k' - 4\bar R f_k'')\bar\nabla^4\\ &\qquad - \bar R((d-2)f_k' - 2\bar R f_k'')\bar\nabla^2\Big]\sigma\,.\end{aligned} \tag{4.48}$$

Here, the barred quantities are constructed from the background metric $\bar g_{\mu\nu}$ and we have suppressed the argument of $f_k(\bar R)$.

Following the procedure outlined above, we also extract the quadratic terms arising from $S_{\mathrm{gf}}, S_{\mathrm{gh}}$ and S_{aux}. Applying the TT decomposition in the first two cases yields

$$\begin{aligned}S^{\mathrm{quad}}_{\mathrm{gf}} = \frac{\kappa^2}{\alpha}\int d^dx\sqrt{\bar g}\,\Big\{&\xi_\mu\left[\bar\nabla^2 + \tfrac{1}{d}\,\bar R\right]^{2\prime}\xi^\mu - \tfrac{1}{d^2}\,\sigma\left[\left((d-1)\bar\nabla^2 + \bar R\right)^2\,\bar\nabla^2\right]''\sigma\\ &- \tfrac{\rho^2}{d^2}\,h\,\bar\nabla^2\,h + \tfrac{\rho}{d^2}\,h\left[(d-1)\bar\nabla^4 + \bar R\,\bar\nabla^2\right]''\sigma\Big\}\end{aligned} \tag{4.49}$$

and

$$S^{\mathrm{quad}}_{\mathrm{gh}} = -\sqrt{2}\int d^dx\,\sqrt{\bar g}\,\Big\{\,\bar C^{\mathrm{T}}_\mu\left[\bar\nabla^2 + \tfrac{1}{d}\,\bar R\right]'C^{\mathrm{T}\mu} - \tfrac{2}{d}\,\bar\eta\left[(d-1-\rho)\,\bar\nabla^4 + \bar R\,\bar\nabla^2\right]''\eta\Big\}\,, \tag{4.50}$$

while substituting the spherical symmetric background metric simplifies S_{aux} to

$$\begin{aligned}S^{\mathrm{quad}}_{\mathrm{aux}} = \int d^dx\,\sqrt{\bar g}\,\Big\{&\zeta^{\mathrm{T}\mu}\left[-\bar\nabla^2 - \tfrac{1}{d}\bar R\right]'\zeta^{\mathrm{T}}_\mu + \bar c^{\mathrm{T}\mu}\left[-\bar\nabla^2 - \tfrac{1}{d}\bar R\right]'c^{\mathrm{T}}_\mu\\ &+ \bar s\,[-\bar\nabla^2]''\,s + \bar b\left[\bar\nabla^4 + \tfrac{1}{d-1}\bar R\bar\nabla^2\right]''b + \omega\left[\bar\nabla^4 + \tfrac{1}{d-1}\bar R\bar\nabla^2\right]''\omega\Big\}\,.\end{aligned} \tag{4.51}$$

Here, the primes on the operators indicate that the corresponding number of lowest eigenmodes are excluded from the physical fields. Note that, for the special case $d = 4$, eqs. (4.47), (4.49) and (4.50) are in precise agreement with earlier findings [115]. We also remark that, while in the harmonic gauge used in [37] performing the TT-decomposition in the ghost sector is optional, working in the gauge (4.4) requires this decomposition in order to diagonalize the quadratic fluctuations.

4.2.3 Adapting the cutoff operators

Our next task is to explicitly construct the IR cutoff operators (4.25). For this, it is useful to split $\mathcal{R}_k(p^2)$ into its matrix part and a scalar function R_k, encoding the momentum-dependent mass term,

$$\big[\mathcal{R}_k(p^2)\big]_{\varphi_1\varphi_2} = \big[\mathcal{Z}_k\big]_{\varphi_1\varphi_2} R_k(p^2) = \big[\mathcal{Z}_k\big]_{\varphi_1\varphi_2} k^2 R^{(0)}(-\bar{\nabla}^2/k^2)\,. \tag{4.52}$$

The dimensionless profile functions $R^{(0)}(-\bar{\nabla}^2/k^2)$ interpolate between $R^{(0)}(0) = 1$ and $R^{(0)}(\infty) = 0$ and otherwise allow one to adjust the "shape" of the momentum-dependent mass-squared term. The specific form of these profile functions are given in Appendix E for the more commonly employed choices. As per the usual cutoff implementation prescription (viz. Section 2.3), the aim of the IR cutoff is the regularization of Hessians

$$\big[\Gamma_k^{(2)}\big]_{\varphi_1\varphi_2} = \big[f(-\bar{\nabla}^2, k, \ldots)\big]_{\varphi_1\varphi_2} \tag{4.53}$$

in such a way that, in the type I scheme, all covariant Laplacians appear in the form

$$\bar{P}_k = -\bar{\nabla}^2 + R_k(p^2)\,. \tag{4.54}$$

Thus, as a result of the IR regularization,

$$\big[\Gamma_k^{(2)} + \mathcal{R}_k\big]_{\varphi_1\varphi_2} = \big[f(-\bar{\nabla}^2 + R_k, k, \ldots)\big]_{\varphi_1\varphi_2} \tag{4.55}$$

depends on the covariant Laplacian $-\bar{\nabla}^2$ through the combination (4.54) only.

With these prerequisites, we can now explicitly construct $\Delta_k S$ for the truncation (4.41). In order to simplify the resulting expressions, we use the gauge-freedom retained in (4.3) to set

$$\rho = 0, \quad \alpha \to 0\,. \tag{4.56}$$

As eq. (4.59) below will illustrate, this gauge choice leads to a factorization of the physical and gauge degrees of freedom contained in $h_{\mu\nu}$ in such a way that the physical degrees of freedom are parameterized by $h^{\mathrm{T}}_{\mu\nu}$ and h, while the gauge degrees of freedom are confined to ξ^{T}_μ and its longitudinal component, σ. Thus, from a geometrical point of view, (4.56) aligns the gauge orbits with the directions $\xi^{\mathrm{T}}_\mu, \sigma$, motivating the name "geometric gauge". This feature will later lead to a considerable simplification of the flow equation. In particular, we will find that the matrix structure of the operator $\Gamma_k^{(2)} + \mathcal{R}_k$ diagonalizes, so that the latter can be easily inverted.

Let us start by constructing the IR cutoff for the auxiliary fields. Considering (4.51), it is straightforward to establish that the prescription (4.55) is implemented by

$$\begin{aligned}\Delta_k S_{\mathrm{aux}} = \int d^d x \sqrt{g} \Big\{ & \zeta^{\mathrm{T}\mu} R_k \zeta^{\mathrm{T}}_\mu + \bar{c}^{\mathrm{T}\mu} R_k c^{\mathrm{T}}_\mu + \bar{s} R_k s \\ & + \bar{b}\left[\bar{P}_k^2 - \tfrac{1}{d-1}\bar{R}R_k - \bar{\nabla}^4\right] b + \omega\left[\bar{P}_k^2 - \tfrac{1}{d-1}\bar{R}R_k - \bar{\nabla}^4\right]\omega \Big\}\,.\end{aligned} \tag{4.57}$$

Analogously, starting from (4.50), we find the IR cutoff in the ghost sector,

$$\Delta_k S_{\rm gh} = \sqrt{2}\int d^dx\sqrt{\bar g}\left\{\bar C^{\rm T}_\mu R_k C^{{\rm T}\mu} + \tfrac{2(d-1)}{d}\bar\eta\left[P_k^2 - \tfrac{1}{d-1}\bar R R_k - (-\bar\nabla^2)^2\right]\eta\right\}. \tag{4.58}$$

The construction of $\Delta_k S_{\rm grav}$ is slightly more involved. Here, we first observe that, for $\rho = 0$, eq. (4.49) diagonalizes and contains the fields ξ_μ and σ only. Combining (4.47) and (4.49) gives

$$\begin{aligned}\Gamma_k^{\rm grav;quad} = \frac{1}{32\pi G}\int d^dx\sqrt{\bar g}\Big\{&\tfrac{1}{2}\,h^{\rm T}_{\mu\nu}\left[f_k'\,\bar\nabla^2 - f_k + \tfrac{2(d-2)}{d(d-1)}\,\bar R\,f_k'\right]h^{\mu\nu{\rm T}}\\ &+\tfrac{1}{4d^2}\,h\Big[4(d-1)^2 f_k''\bar\nabla^4 - 2(d-1)\left((d-2)f_k' - 4\,\bar R\,f_k''\right)\bar\nabla^2\\ &+(d-2)(d\,f_k - 4\,\bar R\,f_k') + 4\,\bar R^2\,f_k''\Big]\,h\Big\}\\ &+\frac{\kappa^2}{\alpha}\int d^dx\sqrt{\bar g}\Big\{\,\xi_\mu\left[\bar\nabla^2 + \frac{1}{d}\,\bar R\right]^2\xi^\mu\\ &-\frac{1}{d^2}\,\sigma\left[\left((d-1)\bar\nabla^2 + \bar R\right)^2\,\bar\nabla^2\right]\sigma + \mathcal{O}(\alpha)\Big\}.\end{aligned} \tag{4.59}$$

Compared to the terms appearing in $S_{\rm gf}$, the $\xi\xi, \sigma\sigma$ and $h\sigma$-contributions from $\bar\Gamma_k^{\rm quad}$ are suppressed by one power of α and are indicated by $\mathcal{O}(\alpha)$ in the formula above. In the limit $\alpha \to 0$, these terms do not contribute to the flow equation and will thus be neglected in the following discussion. Again following the rule (4.55), we find the IR cutoff in the metric sector,

$$\begin{aligned}\Delta_k S_{\rm grav} = \frac{1}{32\pi G}\int d^dx\sqrt{\bar g}\Big\{&\tfrac{1}{2}h^{\rm T}_{\mu\nu}\left[-f_k'\,R_k\right]h^{\mu\nu{\rm T}} + \tfrac{1}{4d^2}\,h\Big[4(d-1)^2 f_k''(\bar P_k^2 - \bar\nabla^4)\\ &+2(d-1)\left((d-2)f_k' - 4\bar R f_k''\right)R_k\Big]\,h\Big\}\\ &+\frac{\kappa^2}{\alpha}\int d^dx\sqrt{\bar g}\Big\{\,\xi_\mu\left[\bar P_k^2 - \bar\nabla^4 - \tfrac{2}{d}\bar R R_k\right]\xi^\mu + \tfrac{1}{d^2}\,\sigma\Big[\left((d-1)\bar P_k - \bar R\right)^2\bar P_k\\ &-\left((d-1)(-\bar\nabla)^2 - \bar R\right)^2\,(-\bar\nabla^2)\Big]\sigma + \mathcal{O}(\alpha)\Big\}.\end{aligned} \tag{4.60}$$

This result completes the adaptation of the IR cutoff to the truncation (4.41). From the results (4.57), (4.58) and (4.60), it is straightforward to read off the entries of the cutoff operator $\mathcal{R}_k$ and construct $\Gamma_k^{(2)} + \mathcal{R}_k$, which indeed assumes a diagonal form in field space. For convenience, these entries are summarized in Tables 4.1 and 4.2.

We can now explicitly write the traces in (4.44) for the truncation (4.41). Substituting the operators $\mathcal{R}_k$ and $(\Gamma_k^{(2)} + \mathcal{R}_k)^{-1}$ listed in Tables 4.1 and 4.2 and

Index	Cutoff operator $\mathcal{R}_k$
$h^{\mathrm{T}}h^{\mathrm{T}}$	$-\frac{1}{32\pi G}f'_k\,R_k$
hh	$\frac{1}{64\pi G d^2}\tilde{\mathcal{R}}_k^{hh}$
$\xi\xi$	$\frac{1}{16\pi\alpha}\left[\bar{P}_k^2-\bar{\nabla}^4-\frac{2}{d}\bar{R}R_k\right]$
$\sigma\sigma$	$\frac{(d-1)^2}{16\pi\alpha d^2}\left[\left(\bar{P}_k-\frac{1}{d-1}\bar{R}\right)^2\bar{P}_k+\left(\bar{\nabla}^2+\frac{1}{d-1}\bar{R}\right)^2\bar{\nabla}^2\right]$
$\bar{C}^{\mathrm{T}}C^{\mathrm{T}}$	$\sqrt{2}R_k$
$\bar{\eta}\eta$	$2\sqrt{2}\,\frac{d-1}{d}\left[\bar{P}_k^2-\bar{\nabla}^4-\frac{1}{d-1}\bar{R}R_k\right]$
$\zeta\zeta$	$2R_k$
$\bar{c}^{\mathrm{T}}c^{\mathrm{T}}$	R_k
$\bar{s}s$	R_k
$\bar{b}b$	$\left[\bar{P}_k^2-\bar{\nabla}^4-\frac{1}{d-1}\bar{R}R_k\right]$
$\omega\omega$	$2\left[\bar{P}_k^2-\bar{\nabla}^4-\frac{1}{d-1}\bar{R}R_k\right]$

Table 4.1: Matrix entries of the operator $\mathcal{R}_k$ to leading order in α. The first column indicates the indices of the matrix element in field space, while the second column contains the corresponding matrix element of $\mathcal{R}_k$. The elements are symmetric under the exchange of bosonic indices, while they acquire a minus sign when Grassmann-valued indices are swapped. $\tilde{\mathcal{R}}_k^{hh}$ is defined in eq. (4.62).

recalling that unphysical modes are to be excluded, we find

$$\begin{aligned}k\partial_k\bar{\Gamma}_k=&-\tfrac{1}{2}\mathrm{Tr}_0''\left[\frac{k\partial_k R_k}{\bar{P}_k-\frac{1}{d-1}\bar{R}}\right]-\tfrac{1}{2}\mathrm{Tr}_{1\mathrm{T}}'\left[\frac{k\partial_k R_k}{\bar{P}_k-\frac{1}{d}\bar{R}}\right]\\&+\tfrac{1}{2}\mathrm{Tr}_{2\mathrm{T}}\left[\frac{k\partial_k(Z_{Nk}f'_kR_k)}{Z_{Nk}\left(f'_k\,\bar{P}_k+f_k-\frac{2(d-2)}{d(d-1)}\,\bar{R}\,f'_k\right)}\right]+\tfrac{1}{2}\mathrm{Tr}_0\left[\frac{k\partial_k\left(Z_{Nk}\widetilde{\mathcal{R}}_k^{hh}\right)}{Z_{Nk}\widetilde{\Gamma}_k^{(2)hh}}\right],\end{aligned}\tag{4.61}$$

where $\bar{\Gamma}_k$ and $f_k(\bar{R})$ were introduced in eq. (4.42). Here, Z_{Nk} captures the scale-dependence of Newton's constant via $G\equiv Z_{Nk}^{-1}G_{\hat{k}}$, with $G_{\hat{k}}$ denoting its value at some reference scale $\hat{\kappa}$. The subscripts 0,1T,2T on the operator-traces indicate that their arguments act on fields with spin $s=0$, 1, 2, while the primes imply that the corresponding number of lowest $-\bar{\nabla}^2$-eigenvalues are excluded from the trace. In addition, we have introduced

$$\widetilde{\mathcal{R}}_k^{hh}=4\,(d-1)^2f_k''\left(\bar{P}_k^2-(-\bar{\nabla}^2)^2\right)+2\,(d-1)\left((d-2)\,f'_k-4\,\bar{R}\,f''_k\right)R_k\,,\tag{4.62}$$

Index	Matrix element of $\Gamma_k^{(2)} + \mathcal{R}_k$
$h^{\mathrm{T}}h^{\mathrm{T}}$	$\frac{1}{32\pi G}\Big[- f_k' \, \bar{P}_k - f_k + \frac{2(d-2)}{d(d-1)} \, \bar{R} \, f_k' \Big]$
hh	$\frac{1}{64\pi G d^2} \widetilde{\Gamma}_k^{(2)hh}$
$\xi\xi$	$\frac{1}{16\pi\alpha} \Big[\bar{P}_k - \frac{1}{d} \bar{R} \Big]^2$
$\sigma\sigma$	$\frac{(d-1)^2}{16\pi\alpha d^2} \Big[\big(\bar{P}_k - \frac{1}{d-1} \bar{R} \big)^2 \bar{P}_k \Big]$
$\bar{C}^{\mathrm{T}} C^{\mathrm{T}}$	$\sqrt{2} \Big[P_k - \frac{1}{d} \, \bar{R} \Big]$
$\bar{\eta}\eta$	$2\sqrt{2} \, \frac{d-1}{d} \, \Big[\bar{P}_k - \frac{1}{d-1} \bar{R} \Big] \, \bar{P}_k$
$\zeta\zeta$	$2 \Big[\bar{P}_k - \frac{1}{d} \bar{R} \Big]$
$\bar{c}^{\mathrm{T}} c^{\mathrm{T}}$	$\Big[\bar{P}_k - \frac{1}{d} \bar{R} \Big]$
$\bar{s}s$	$\bar{P}_k$
$\bar{b}b$	$\Big[\bar{P}_k - \frac{1}{d-1} \bar{R} \Big] \, \bar{P}_k$
$\omega\omega$	$2 \Big[\bar{P}_k - \frac{1}{d-1} \bar{R} \Big] \, \bar{P}_k$

Table 4.2: Matrix entries of the operator $\Gamma_k^{(2)} + \mathcal{R}_k$ to leading order in α. The first column indicates the indices of the matrix element in field space, while the second column contains the corresponding matrix element of $\Gamma_k^{(2)} + \mathcal{R}_k$. The elements are symmetric under the exchange of bosonic indices, while they acquire a minus sign when Grassmann-valued indices are swapped. $\widetilde{\Gamma}_k^{(2)hh}$ is defined in eq. (4.63).

and

$$\begin{aligned} \widetilde{\Gamma}_k^{(2)hh} = & \, 4\,(d-1)^2 f_k'' \, \Big(\bar{P}_k - \tfrac{1}{d-1} \bar{R} \Big)^2 + 2\,(d-1)(d-2)\, f_k' \, \Big(\bar{P}_k - \tfrac{2}{d-1} \bar{R} \Big) \\ & + d(d-2) f_k \,, \end{aligned} \tag{4.63}$$

in order to write the last scalar trace in compact form. After carrying out the variations $\Gamma_k^{(2)}[g, \ldots; \bar{g}]$, we can identify $g_{\mu\nu} = \bar{g}_{\mu\nu}$ in (4.61), and we drop the bar on the metric in the sequel. For later reference, we denote the four terms appearing on the right-hand side of (4.61) by $\mathcal{S}_k^i$, $i = 1, \ldots, 4$, respectively.

Note that the first two terms on the right-hand side of our flow equation (4.61) contain the contribution from all vector fields and all but the h scalar fields, respectively. If we had not imposed the same mode exclusion for those fields in their respective sectors, combining their contribution under a single primed (or, in the scalar sector, double primed) trace would have to be compensated by the presence of "single mode" terms on the right-hand side of our equation,

corresponding to those modes which are not present in the primed traces but which should not be excluded in our computation. For $d > 2$ and spherical backgrounds, these terms do not contribute to truncation subspaces which contain terms linear in R as the highest power of the curvature scalar. This is due to the fact that the trace terms are always proportional to the volume of the background sphere and, therefore, inherit extra inverse powers of the curvature scalar $V \propto R^{-d/2}$. Thus, contributions coming from discrete eigenvalues are effectively suppressed by a factor $R^{d/2}$ and hence, for $d > 2$, only start to affect the running of couplings multiplying $\int d^d x \sqrt{g} R^n, n > 1$. For the case of higher-order truncations, and particularly when recovering the fixed point results of [41, 69] in Section 4.4.2, we have also verified that the presence of those terms leads only to a very small change in the numerical results.

Let us close this subsection with the following observation. An interesting feature of the RG equation (4.61) is that it consists of a 'universal', $f_k(R)$-independent part, and a truncation-dependent part. The former encompasses the terms $\mathcal{S}_k^1$ and $\mathcal{S}_k^2$ in the first line and captures the contribution of the scalars $\eta, \sigma, s, b, \omega$ and the auxiliary vector fields ζ_μ, c_μ. The second part, which consists of the traces $\mathcal{S}_k^3$ and $\mathcal{S}_k^4$, stems from the gravitational degrees of freedom $h^{\mathrm{T}}_{\mu\nu}$ and h, and encodes all information about the particular form of $f_k(R)$. Retrospectively, the appearance of this structure is not surprising: it is a direct consequence of the geometrical gauge-choice (4.56), which ensures that the gravitational degrees of freedom are carried by $h^{\mathrm{T}}_{\mu\nu}$ and h only.

4.2.4 Heat-kernel techniques for trace evaluation

In order to construct non-perturbative beta functions from the flow equation (4.61), the final step is the evaluation of the operators traces in terms of curvature invariants of the background manifold. As we have discussed in Chapter 2 and explicitly seen in the case of conformally reduced gravity in Chapter 3, this can be done by standard heat-kernel techniques. In this section, we briefly illustrate this method for the traces in our flow equation (4.61).

In order to be able to apply heat-kernel methods in the current setting, we first have to complete the traces by adding and subtracting the missing modes according to

$$\mathrm{Tr}_s^{\prime\ldots\prime}[W(-\nabla^2)] = \mathrm{Tr}_s[W(-\nabla^2)] - \sum_{l\in\{l_1,\ldots l_m\}} D_l(d,s) W(\Lambda_l(d,s))\,. \tag{4.64}$$

Here, W is an arbitrary, smooth, operator-valued function and s denotes the spin of the fields on which the covariant Laplacian acts. The discrete sum in (4.64) can be evaluated using the multiplicities $D_l(d,s)$ and eigenvalues $\Lambda_l(d,s)$ for $-\nabla^2$ acting on a spin s field, given in Table D.1 of Appendix D . To evaluate the complete traces, we make use of the asymptotic heat kernel expansion for the

trace of the operator $-\nabla^2$ (cf. Chapter 2) to arrive at

$$\begin{aligned}\mathrm{Tr}\left[W(-\nabla^2)\right] = (4\pi)^{-d/2}\int d^dx\sqrt{g}\,\big\{&Q_{d/2}[W]\,\mathrm{tr}\,\mathbf{b}_0 + Q_{d/2-1}[W]\,\mathrm{tr}\,\mathbf{b}_2\\ &+Q_{d/2-2}[W]\,\mathrm{tr}\,\mathbf{b}_4 + \ldots\big\}\,,\end{aligned} \tag{4.65}$$

where the functionals $Q_n[W]$ have been defined in (2.34) and the $\mathrm{tr}\,\mathbf{b}_n$ are the heat kernel coefficients of the Laplacian operator, which we have collected in Appendix D.1.

It is convenient to reexpress the functionals $Q_n[W]$ for $n > 0$ in terms of dimensionless threshold functions Φ, $\tilde{\Phi}$, Υ, $\tilde{\Upsilon}$, encoding the dependence of our evaluated traces on the choice of the cutoff shape function. These functions are defined in Appendix E, where their relation to the functionals $Q_n[W]$ appearing in our traces is also given. In particular, the evaluated traces $\mathcal{S}^1_k, \mathcal{S}^2_k$ and $\mathcal{S}^3_k$ may be written in terms of the standard threshold functions (E.1) via (E.10), while the Q_n in the last trace in (4.61) is given by the generalized threshold functions (E.2) by means of (E.10).

Typically, the coupling constants g_i will enter the right-hand side of the flow equation also by means of their k-derivatives. In this respect, it is convenient to define their anomalous dimension $\eta_{g_i}(k) \equiv k\partial_k \ln(g_i)$. The anomalous dimension of Newton's constant is then given by

$$\eta_G(k) \equiv -k\partial_k \ln(Z_{Nk}) = k\partial_k \ln(G)\,. \tag{4.66}$$

With these tools, we have now all the ingredients to derive the beta functions for most choices of $f_k(R)$. To conclude this section, we illustrate the techniques just introduced by expanding the "universal terms" in the first line of (4.61) up to linear order in the curvature scalar. These results will be very useful when deriving the beta functions of the Einstein-Hilbert truncation in the next section and the $\ln(R)$ and R^{-n} truncations in Chapter 5. Following the steps just outlined and using the expressions for the heat kernel coefficients given in Appendix D.1, we find for the first two traces in our flow equation

$$\begin{aligned}\mathcal{S}^1_k &= -\frac{k^d}{(4\pi)^{d/2}}\left\{\Phi^1_{d/2}\int d^dx\sqrt{g} + k^{-2}\big(\tfrac{1}{d-1}\Phi^2_{d/2} + \tfrac{1}{6}\,\Phi^1_{d/2-1}\big)\int d^dx\sqrt{g}R\right\}\,,\\ \mathcal{S}^2_k &= -\frac{k^d}{(4\pi)^{d/2}}\left\{(d-1)\,\Phi^1_{d/2}\int d^dx\sqrt{g}\right.\\ &\qquad\left. + k^{-2}\left(\tfrac{d-1}{d}\Phi^2_{d/2} + \tfrac{(d+2)(d-3)}{6d}\,\Phi^1_{d/2-1}\right)\int d^dx\sqrt{g}R\right\},\end{aligned} \tag{4.67}$$

where we have defined

$$\begin{aligned}&\Phi^p_n \equiv \Phi^p_n(0)\,, \quad \tilde{\Phi}^p_n \equiv \tilde{\Phi}^p_n(0)\,,\\ &\Upsilon^p_{n;m} \equiv \Upsilon^p_{n;m}(1,0,0)\,, \quad \tilde{\Upsilon}^p_{n,m,l} \equiv \tilde{\Upsilon}^p_{n,m,l}(1,0,0)\,,\end{aligned} \tag{4.68}$$

in order to lighten our notation. Here and in the following, Φ^p_n, $\tilde{\Phi}^p_n$, $\Upsilon^p_{n;m}$ and $\tilde{\Upsilon}^p_{n,m,l}$ without argument will denote the cutoff-shape dependent threshold constants defined above, while, for the related threshold functions, the argument will always be given explicitly.

We close this subsection with the following remark. In order to evaluate the contributions of the traces to our truncation, we use the early time expansion of the heat-kernel,

$$\mathrm{Tr}\left[\mathrm{e}^{-s\nabla^2}\right] = \left(\frac{1}{4\pi}\right)^{d/2} \int d^dx\sqrt{g}\left[\mathrm{tr}\,\mathbf{b}_0\, s^{-\frac{d}{2}} + \mathrm{tr}\,\mathbf{b}_2 s^{-\frac{d}{2}+1} + \dots\right], \tag{4.69}$$

expanding for small values of s. Based on perturbation theory, one would at first sight expect that, while this is adequate for investigations of the gravitational renormalization group flow in the UV, in the IR this should be based on the late-time expansion of the heat-kernel [116,117], expanding the traces for large values s. Analyzing the Laplace-transformed functions $\widetilde{W}(s)$ arising from (4.61), one however finds that, thanks to the IR cutoff, $\lim_{s\to\infty}\widetilde{W}(s) = 0$ for $k > 0$. Thus, even for small values of k, the main contribution to the integral in (2.34) (or, more precisely, (2.31)) arises from small values s, so that the early time expansion of the heat kernel can also be used to investigate the gravitational renormalization group flow in the IR.

4.3 The Einstein-Hilbert truncation

As a first application of our flow equation, we consider the Einstein-Hilbert truncation, which consists in setting

$$f_k = -R + 2\Lambda, \tag{4.70}$$

where Λ is the running cosmological constant. The Einstein-Hilbert truncation has been extensively analyzed in a number of studies [35–39,69,82], and we therefore refrain from perfoming a detailed investigation of its properties here. Rather, we will calculate its beta functions in $d = 4$ and for the case of the optimized cutoff (E.12) so as to establish its most prominent feature, the existence of a UV-attractive non-trivial fixed point for $\tilde{G} > 0, \tilde{\Lambda} > 0$, where $\tilde{G} \equiv k^2 G$ and $\tilde{\Lambda} \equiv \Lambda k^{-2}$ are the dimensionless Newton's and cosmological constant respectively.

4.3.1 Deriving the beta functions

In order to derive the beta functions of the Einstein-Hilbert truncation, we must evaluate the 'non-universal' traces $\mathcal{S}^3_k$ and $\mathcal{S}^4_k$ in the right-hand side of the flow equation (4.61). Substituting the ansatz (4.70) into the traces, following the steps outlined in the previous section and using the heat kernel coefficient formulas in

Appendix D.1, we find

$$\begin{aligned} S_k^{\text{3EH}} =& \tfrac{1}{2}\text{Tr}_{\text{2T}}\left[\frac{k\partial_k\left(G^{-1}R_k\right)}{G^{-1}\left(P_k-2\Lambda+\frac{2}{3}R\right)}\right] \\ =& \tfrac{1}{2}\text{Tr}_{\text{2T}}\left[\frac{k\partial_k\left(G^{-1}R_k\right)}{G^{-1}\left(P_k-2\Lambda\right)}-\frac{2}{3}\frac{k\partial_k\left(G^{-1}R_k\right)}{G^{-1}\left(P_k-2\Lambda\right)^2}R+\mathcal{O}(R^2)\right] \\ =& \frac{k^4}{(4\pi)^2}\left\{5\left[\Phi_2^1(-2\tilde{\Lambda})-\tfrac{1}{2}\eta_G\tilde{\Phi}_2^1(-2\tilde{\Lambda})\right]\int d^4x\sqrt{g}\right. \\ & -k^{-2}\left[\frac{10}{3}\left(\Phi_2^2(-2\tilde{\Lambda})-\tfrac{1}{2}\eta_G\tilde{\Phi}_2^2(-2\tilde{\Lambda})\right)\right. \\ & \left.\left.+\ \frac{5}{6}\left(\Phi_1^1(-2\tilde{\Lambda})-\tfrac{1}{2}\eta_G\tilde{\Phi}_1^1(-2\tilde{\Lambda})\right)\right]\int d^4x\sqrt{g}R+\mathcal{O}(R^2)\right\}, \end{aligned} \tag{4.71}$$

and

$$\begin{aligned} S_k^{\text{3EH}} =& \tfrac{1}{2}\text{Tr}_{\text{2T}}\left[\frac{k\partial_k\left(G^{-1}R_k\right)}{G^{-1}\left(P_k-\frac{4}{3}\Lambda\right)}\right] \\ =& \frac{k^4}{(4\pi)^2}\left\{\left[\Phi_2^1(-\tfrac{4}{3}\tilde{\Lambda})-\tfrac{1}{2}\eta_G\tilde{\Phi}_2^1(-\tfrac{4}{3}\tilde{\Lambda})\right]\int d^4x\sqrt{g}\right. \\ & \left.+\ \frac{k^{-2}}{6}\left[\Phi_1^1(-\tfrac{4}{3}\tilde{\Lambda})-\tfrac{1}{2}\eta_G\tilde{\Phi}_1^1(-\tfrac{4}{3}\tilde{\Lambda})\right]\int d^4x\sqrt{g}R\right\}, \end{aligned} \tag{4.72}$$

while the left-hand side of the flow equation reads

$$k\partial_k\bar{\Gamma}=\frac{k^4}{16\pi\tilde{G}}\int d^4x\sqrt{g}\left[2\left(k\partial_k\tilde{\Lambda}-\frac{\tilde{\Lambda}k\partial_k\tilde{G}}{\tilde{G}}+\frac{4\tilde{\Lambda}}{\tilde{G}}\right)+\left(\frac{k\partial_k\tilde{G}}{\tilde{G}}-\frac{2}{\tilde{G}}\right)\frac{R}{k^2}\right] \tag{4.73}$$

expressed in terms of the dimensionless couplings. Setting $d=4$ in (4.67), adding all contributions $\mathcal{S}_k^i$ and comparing the coefficients on both sides of the flow equation for the case of the optimized cutoff, we arrive at the beta functions

$$\begin{aligned} \beta_{\tilde{\Lambda}} =& -2\tilde{\Lambda}+\frac{3(108-819\tilde{\Lambda}+1860\tilde{\Lambda}^2-2396\tilde{\Lambda}^3+2592\tilde{\Lambda}^4-1472\tilde{\Lambda}^5)\tilde{G}}{2(4\tilde{\Lambda}-3)[(42\tilde{\Lambda}^2-97\tilde{\Lambda}+48)\tilde{G}+36\pi(4\tilde{\Lambda}-3)(1-2\tilde{\Lambda})^2]} \\ & +\frac{(1557-6267\tilde{\Lambda}+8394\tilde{\Lambda}^2-3736\tilde{\Lambda}^3)\tilde{G}^2}{8\pi(4\tilde{\Lambda}-3)[(42\tilde{\Lambda}^2-97\tilde{\Lambda}+48)\tilde{G}+36\pi(4\tilde{\Lambda}-3)(1-2\tilde{\Lambda})^2]}, \\ \beta_{\tilde{G}} =& 2\tilde{G}-\frac{3(108-819\tilde{\Lambda}+1860\tilde{\Lambda}^2-2396\tilde{\Lambda}^3+2592\tilde{\Lambda}^4-1472\tilde{\Lambda}^5)\tilde{G}^2}{2[(42\tilde{\Lambda}^2-97\tilde{\Lambda}+48)\tilde{G}+36\pi(4\tilde{\Lambda}-3)(1-2\tilde{\Lambda})^2]}, \end{aligned} \tag{4.74}$$

from which we can read off the anomalous dimension of Newton's constant,

$$\eta_G=-\frac{3(108-819\tilde{\Lambda}+1860\tilde{\Lambda}^2-2396\tilde{\Lambda}^3+2592\tilde{\Lambda}^4-1472\tilde{\Lambda}^5)\tilde{G}}{2[(42\tilde{\Lambda}^2-97\tilde{\Lambda}+48)\tilde{G}+36\pi(4\tilde{\Lambda}-3)(1-2\tilde{\Lambda})^2]} \tag{4.75}$$

The vanishing of these beta functions implies the fixed point solutions

$$\text{GFP} : \left\{ \tilde{\Lambda} = 0 \,, \quad \tilde{G} = 0 \right\},$$

and

$$\text{NGFP} : \left\{ \tilde{\Lambda} = 0.129, , \quad \tilde{G} = 0.984 \right\}.$$

The stability coefficients associated with the NGFP are given by

$$\theta_{0,1} = 2.382 \pm 2.168 i \,. \tag{4.76}$$

Hence, the NGFP is UV-attractive in both directions of the $(\tilde{\Lambda}, \tilde{G})$-plane. This fixed point constitutes the first FRGE evidence for the asymptotic safety of gravity, and its stability with respect to the choice of gauge fixing, cutoff schemes and cutoff profile functions has been confirmed in a series of works [35–39, 69, 82]. The crucial question is then whether or not such a fixed point will persist under extensions of the truncation subspace. A non-Gaussian fixed point with similar characteristics to the ones above was first found to exist in the case of R^2 truncations [40, 118]. In Section 4.4.2, recovering the results of [69], we will see that this fixed point persists also when including higher-order $f(R)$ terms in the truncation, as was verified for polynomials in R up to order eight [41].

4.3.2 RG flow and singularity structure

The beta functions (4.74) may also be integrated numerically, yielding a renormalization group flow diagram for the Einstein-Hilbert truncation. This flow diagram is given in Figure 4.1. We note the presence of a unique trajectory connecting the NGFP to the GFP, called the "separatrix'. Particularly interesting are the trajectories with positive cosmological constant to the right of the separatrix. These have been shown in [88] to lead to an extended semiclassical regime in which Newton's constant and the cosmological constant essentially do not run, and have been argued to be the type of trajectory that is realized by nature. Note however, that these trajectories cannot be extended arbitrarily deep into the IR. This is due to the presence of singularities in the beta functions (4.74). For the case $\tilde{G} = 0$, this singularity occurs at $\tilde{\Lambda} = 1/2$. It is clear the renormalization group flow exists beyond these singularities, but the trajectories beyond them cannot be connected to those emanating from the NGFP. Such singularities are found for the Einstein-Hilbert truncation in all cutoff scheme implementations apart from the case of type III cutoffs [41], and is usually taken as an indication that the Einstein-Hilbert truncation is insufficient to adequately capture the renormalization group in the IR. In the next chapter, we shall see how this singularity can be avoided via non-local $f(R)$ truncations.

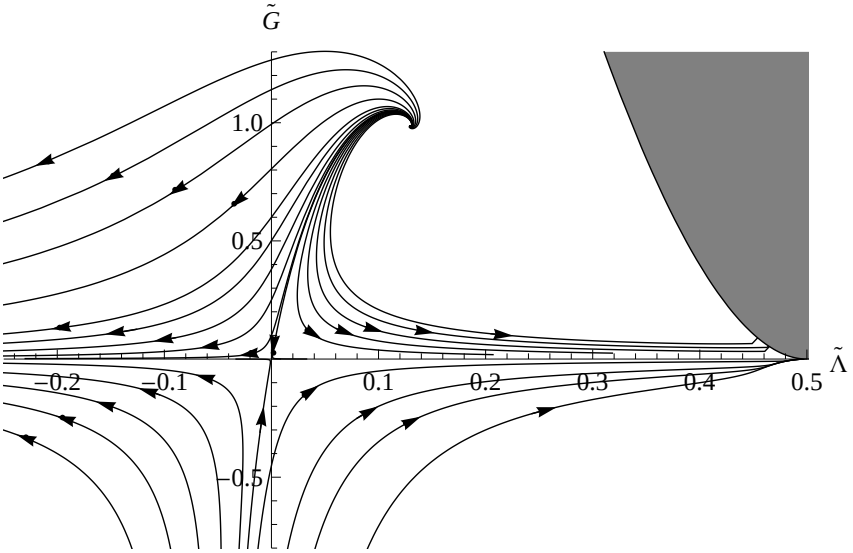

Figure 4.1: The renormalization group flow of 4-dimensional quantum gravity in the Einstein-Hilbert truncation. The arrows point in the direction of decreasing k and the border of the shaded area is given by the singularities of the beta functions, beyond which the flow cannot be numerically integrated.

4.4 A differential equation capturing the RG flow of $f_k(R)$

In this section, we specialize our generic flow equation to $d = 4$ and the case of the optimized cutoff (E.15). Using the heat-kernel results collected in Appendix D.1 then allows us to explicitly evaluate the traces in (4.61) for an arbitrary function $f_k(R)$, resulting in an autonomous partial differential equation governing the RG flow of $f(R)$ gravity.

4.4.1 Deriving the non-perturbative flow equation

We start with the following observation. When the operator traces appearing in (4.61) are evaluated via the heat-kernel expansion, their arguments $W(z)$ enter the series expansion via the functionals $Q_n[W]$. In $d = 4$, the coefficients multiplying the heat-kernel coefficients $\mathrm{tr}[a_{2l}]$ for $l \geq 2$ are thereby proportional to $Q_{2-l}[W]$, which are essentially the lth derivatives of $W(z)$ evaluated at $z = 0$ (2.34). The virtue of working with the optimized cutoff appears when (E.15) is substituted into $W(z)$ and the derivatives are computed explicitly, as one then finds that,

starting from a finite value $l_{\rm term}$, all derivatives vanish at $z = 0$.[2] Thus, working with the optimized cutoff has the significant advantage that the knowledge of only a finite number of heat-kernel coefficients suffices to evaluate the traces (4.61). We stress that we do not expect this feature to persist once a different cutoff profile is used, such as, e.g., the exponential cutoff (E.13).

For the purpose of this section, it is useful to redefine $f_k(R)$ by absorbing the wave function renormalization Z_{Nk}, working with $\tilde{f}_k(R) \equiv Z_{Nk} f_k(R)$ and dropping the tilde in the following. Furthermore, V here denotes the volume of S^4.

Let us now proceed with the explicit evaluation of the right-hand side of (4.61). In contrast to the procedure just employed in the Einstein-Hilbert truncation, we do not perform a series expansion of the trace arguments with respect to R here. Evaluating the terms in the first line of the flow equation gives

$$\begin{aligned}
\mathcal{S}_k^1 = &- \frac{V}{(4\pi)^2}\left[k^4\Phi_2^1(-\tfrac{R}{3k^2})\; b_0|_0 + k^2\Phi_1^1(-\tfrac{R}{3k^2})\; b_2|_0 + \frac{1}{1-\frac{R}{3k^2}}\; b_4|_0\right] \\
&+ \left[1+5\theta(1-\tfrac{R}{3k^2})\right]\left[1-\tfrac{R}{3k^2}\right]^{-1}, \\
\mathcal{S}_k^2 = &- \frac{V}{(4\pi)^2}\left[k^4\Phi_2^1(-\tfrac{R}{4k^2})\; b_0|_{1\rm T} + k^2\Phi_1^1(-\tfrac{R}{4k^2})\; b_2|_{1\rm T} + \frac{1}{1-\frac{R}{4k^2}}\; b_4|_{1\rm T}\right] \\
&+ \left[10\,\theta\left(1-\tfrac{R}{4k^2}\right) - \theta\left(1+\tfrac{R}{4k^2}\right)\right]\left[1-\tfrac{R}{4k^2}\right]^{-1}.
\end{aligned} \tag{4.77}$$

Here, the terms proportional to V arise from the evaluation of the complete traces, and the heat-kernel coefficients $b_{2k}|_s$ are given in (D.10) and (D.11). Furthermore, the $\Phi_n^p(w)$ denote the threshold functions for the optimized cutoff (E.17). The V-independent terms capture the contribution of the finite number of $-\nabla^2$-eigenmodes required to complete the traces (cf. Section 4.2.4).

The evaluation of the $f_k(R)$-dependent traces $\mathcal{S}_k^3$ and $\mathcal{S}_k^4$ is slightly more involved. For the 2T trace, we find

$$\begin{aligned}
S_k^3 = &\frac{V}{2(4\pi)^2}\,\eta_f\left[k^4\tilde{\Phi}_2^1(w_4)\,b_0|_{2\rm T} + k^2\tilde{\Phi}_1^1(w_4)\,b_2|_{2\rm T} + \frac{1}{1+w_4}\,b_4|_{2\rm T} - \frac{k^{-2}}{1+w_4}\,b_6|_{2\rm T}\right] \\
&+ \frac{V}{(4\pi)^2}\left[k^4\Phi_2^1(w_4)\,b_0|_{2\rm T} + k^2\Phi_1^1(w_4)\,b_2|_{2\rm T} + \frac{1}{1+w_4}\,b_4|_{2\rm T}\right] \\
&+ \frac{5}{2}\,\frac{\eta_f\,(1+\frac{R}{3k^2})+2}{1+w_4}\theta(1+\tfrac{R}{3k^2}) + 5\frac{\eta_f\,(1+\frac{R}{6k^2})+2}{1+w_4}\theta(1+\tfrac{R}{6k^2}),
\end{aligned} \tag{4.78}$$

where the heat kernel coefficients $b_{2k}|_{2\rm T}$ are listed in (D.11). The argument of the

[2] Strictly speaking, this "derivative expansion" truncates for the traces $\mathcal{S}_k^1$ and $\mathcal{S}_k^2$ only. The traces $\mathcal{S}_k^3$ and $\mathcal{S}_k^4$ give rise to an infinite series of terms which, starting at $l_{\rm term}$, are proportional to $\delta(k^2)$ and its derivatives. In the following we will neglect the contributions of such terms to the flow equation.

threshold functions is given by the dimensionless quantity

$$w_4 \equiv \frac{f_k}{k^2\, f_k'} - \frac{R}{3k^2}\,, \tag{4.79}$$

and, in analogy to (4.66), we have defined the "anomalous dimension" of $f_k'(R)$ as

$$\eta_f(k) \equiv k\partial_k \ln(f_k'(R))\,. \tag{4.80}$$

Finally, we evaluate the scalar trace $\mathcal{S}_k^4$. Setting $d = 4$ and comparing its argument $W_5(z)$ with the schematic notation used in (E.11) motivates the definition

$$u_k \equiv 36 f_k''\,, \quad v_k \equiv \frac{12}{k^2}\,(f_k' - 2Rf_k'')\,, \quad w_k \equiv \frac{4}{k^4}\left(2f_k - 2Rf_k' + R^2 f_k''\right)\,. \tag{4.81}$$

In terms of these, the derivatives of $W_5(z)|_{z=0}$ become

$$\begin{aligned}
W_5(0) &= 12\,\frac{3k\partial_k f_k'' + 12 f_k'' + k^{-2}\,(k\partial_k f_k' - 2Rk\partial_k f_k'' + 2f_k' - 4Rf_k'')}{u_k + v_k + w_k}\,,\\
W_5'(0) &= 12\,k^{-4}\,\frac{k\partial_k f_k' - 2Rk\partial_k f_k''}{u_k + v_k + w_k}\,,\\
W_5''(0) &= -\,72k^{-4}\frac{k\partial_k f_k''}{u_k + v_k + w_k}\,.
\end{aligned} \tag{4.82}$$

As mentioned above, the higher-order derivatives $W_5^{\prime\cdots\prime}(0)$ are proportional to $\delta(k^2)$ or derivatives thereof and will not be included in the following. Using the generalized threshold functions (E.2), we can explicitly evaluate $\mathcal{S}_k^5$,

$$\begin{aligned}
\mathcal{S}_k^4 = \frac{V}{2(4\pi)^2}\Big\{ & 36k^4\big[k\partial_k f_k''\tilde{\Upsilon}^1_{2,0,1}(a,b,c) + 4f_k''\Upsilon^1_{2,1}(a,b,c)\big]\\
& + 12k^2\big[(k\partial_k f_k' - 2Rk\partial_k f_k'')\tilde{\Upsilon}^1_{2,0,0}(a,b,c) + 2(f_k' - 2Rf_k'')\Upsilon^1_{2,0}(a,b,c)\big]\\
& + 36k^2\big[k\partial_k f_k''\,\tilde{\Upsilon}^1_{1,0,1}(a,b,c) + 4f_k''\Upsilon^1_{1,1}(a,b,c)\big]\,b_2|_0\\
& + 12\big[(k\partial_k f_k' - 2Rk\partial_k f_k'')\tilde{\Upsilon}^1_{1,0,0}(a,b,c) + 2(f_k' - 2Rf_k'')\Upsilon^1_{1,0}(a,b,c)\big]\,b_2|_0\\
& + W_5(0)\,b_4|_0 + W_5'(0)\,b_6|_0 + W_k''(0)\,b_8|_0\Big\}\,,
\end{aligned} \tag{4.83}$$

where the heat-kernel coefficients $b_{2k}|_0$ are given by (D.10).

We see that, thanks to the optimized cutoff, the right-hand side of eq. (4.61) can indeed be explicitly computed for general function $f_k(R)$. Substituting the $f_k(R)$-ansatz into the left-hand side, on the other hand, yields

$$k\partial_k\bar{\Gamma}_k[g] = 2\kappa^2 V\, k\partial_k f_k(R)\,. \tag{4.84}$$

The flow equation governing the scale-dependence of $f_k(R)$ is obtained by substituting (4.77), (4.78) and (4.83) into the right-hand side of (4.61) and equating

this to (4.84). Explicitly substituting the threshold functions from Appendix E leads to the following partial differential equation for $f_k(R)$,

$$
\begin{aligned}
2\kappa^2 V\, k\partial_k f_k(R) &= \Big[1+5\theta\big(1-\tfrac{R}{3k^2}\big)-\tfrac{Vk^4}{2(4\pi)^2}\big(1+\tfrac{1}{3}\tfrac{R}{k^2}+\tfrac{29}{1080}\tfrac{R^2}{k^4}\big)\Big]\Big[1-\tfrac{R}{3k^2}\Big]^{-1}\\
&+\Big[10\theta(1-\tfrac{R}{4k^2})-\theta(1+\tfrac{R}{4k^2})-\tfrac{Vk^4}{(4\pi)^2}\big(\tfrac{3}{2}+\tfrac{R}{4k^2}-\tfrac{67}{1440}\tfrac{R^2}{k^4}\big)\Big]\Big[1-\tfrac{R}{4k^2}\Big]^{-1}\\
&+\frac{Vk^4}{(4\pi)^2}\frac{\eta_f\,\big(\frac{5}{12}-\frac{5}{24}\frac{R}{k^2}-\frac{271}{864}\frac{R^2}{k^4}+\frac{7249}{108864}\frac{R^3}{k^6}\big)+\big(\frac{5}{2}-\frac{5}{6}\frac{R}{k^2}-\frac{271}{432}\frac{R^2}{k^4}\big)}{1+\frac{f_k}{k^2 f_k'}-\frac{R}{3k^2}}\\
&+5\frac{\big(\frac{1}{2}\eta_f\,(1+\frac{R}{3k^2})+1\big)\theta(1+\frac{R}{3k^2})+\big(\eta_f\,(1+\frac{R}{6k^2})+2\big)\theta(1+\frac{R}{6k^2})}{1+\frac{f_k}{k^2 f_k'}-\frac{R}{3k^2}}\\
&+\tfrac{1}{8}\tfrac{Vk^8}{(4\pi)^2}\Big[k\partial_k f_k''\big(9-\tfrac{91}{60}\tfrac{R^2}{k^4}-\tfrac{29}{90}\tfrac{R^3}{k^6}-\tfrac{181}{10080}\tfrac{R^4}{k^8}\big)+f_k''\big(72-\tfrac{91}{15}\tfrac{R^2}{k^4}-\tfrac{29}{45}\tfrac{R^3}{k^6}\big)\\
&\qquad+k^{-2}k\partial_k f_k'\big(2+\tfrac{R}{k^2}+\tfrac{29}{180}\tfrac{R^2}{k^4}+\tfrac{37}{4536}\tfrac{R^3}{k^6}\big)+k^{-2}f_k'\big(12+4\tfrac{R}{k^2}+\tfrac{29}{90}\tfrac{R^2}{k^4}\big)\Big]\\
&\qquad\times\Big[2f_k+3k^2f_k'(1-\tfrac{2R}{3k^2})+9k^4f_k''(1-\tfrac{R}{3k^2})^2\Big]^{-1}.
\end{aligned}
\tag{4.85}
$$

In order to discuss its properties, it is useful to rewrite eq. (4.85) in terms of dimensionless quantities. This is done by first noting that the volume and curvature scalar of the background 4-spheres are related by $V = 384\,\pi^2 R^{-2}$. Using this relation to eliminate V, eq. (4.85) becomes a partial differential equation in k and R. The dimensionful quantities R and $f_k(R)$ are then traded for their dimensionless counterparts,

$$
\tilde{R} \equiv k^{-2}\,R \quad \text{and} \quad \tilde{f}_k(\tilde{R}) \equiv \frac{1}{16\pi G_{\hat{k}}}\,k^{-4}\,f_k(R/k^2)\,. \tag{4.86}
$$

In terms of these,

$$
k\partial_k f_k = 16\pi G_{\hat{k}}\,k^4\,\Big(k\partial_k\tilde{f}_k+4\tilde{f}_k-2\tilde{R}\tilde{f}_k'\Big)\,, \tag{4.87}
$$

while the anomalous dimension (4.80) becomes

$$
\eta_f = \frac{1}{\tilde{f}_k'}\,\Big(k\partial_k\tilde{f}_k'+2\tilde{f}_k'-2\tilde{R}\tilde{f}_k''\Big)\,, \tag{4.88}
$$

and similar relations hold for the other derivatives of $f_k(R)$. Reexpressing the dimensionful quantities in (4.85) through the dimensionless ones leads to the following autonomous partial differential equation governing the renormalization

group flow of $\tilde{f}_k(\tilde{R})$,

$$
\begin{aligned}
384\pi^2 \left(k\partial_k \tilde{f}_k + 4\tilde{f}_k - 2\tilde{R}\tilde{f}_k'\right) &= \frac{5\tilde{R}^2\theta\left(1-\frac{\tilde{R}}{3}\right) - \left(12 + 4\,\tilde{R} - \frac{61}{90}\,\tilde{R}^2\right)}{1-\frac{\tilde{R}}{3}} \\
&+ \frac{10\,\tilde{R}^2\,\theta(1-\frac{\tilde{R}}{4}) - \tilde{R}^2\,\theta(1+\frac{\tilde{R}}{4}) - \left(36 + 6\,\tilde{R} - \frac{67}{60}\,\tilde{R}^2\right)}{1-\frac{\tilde{R}}{4}} \\
&+ \frac{\eta_f\,\left(10 - 5\tilde{R} - \frac{271}{36}\tilde{R}^2 + \frac{7249}{4536}\tilde{R}^3\right) + \left(60 - 20\tilde{R} - \frac{271}{18}\tilde{R}^2\right)}{1 + \frac{\tilde{f}_k}{\tilde{f}_k'} - \frac{\tilde{R}}{3}} \\
&+ \frac{5\tilde{R}^2}{2}\,\frac{\eta_f\,\left((1+\frac{\tilde{R}}{3})\theta(1+\frac{\tilde{R}}{3}) + (2+\frac{\tilde{R}}{3})\theta(1+\frac{\tilde{R}}{6})\right) + 2\theta(1+\frac{\tilde{R}}{3}) + 4\theta(1+\frac{\tilde{R}}{6})}{1 + \frac{\tilde{f}_k}{\tilde{f}_k'} - \frac{\tilde{R}}{3}} \\
&+ \Big[\tilde{f}_k'\,\eta_f\,\left(6 + 3\tilde{R} + \tfrac{29}{60}\tilde{R}^2 + \tfrac{37}{1512}\,\tilde{R}^3\right) + \tilde{f}_k''\left(216 - \tfrac{91}{5}\tilde{R}^2 - \tfrac{29}{15}\tilde{R}^3\right) \\
&+ \left(k\partial_k\tilde{f}_k'' - 2\tilde{R}\tilde{f}_k'''\right)\left(27 - \tfrac{91}{20}\tilde{R}^2 - \tfrac{29}{30}\,\tilde{R}^3 - \tfrac{181}{3360}\,\tilde{R}^4\right) + \tilde{f}_k'\left(36 + 12\tilde{R} + \tfrac{29}{30}\tilde{R}^2\right)\Big] \\
&\qquad \times \left[2\tilde{f}_k + 3\tilde{f}_k'(1-\tfrac{2}{3}\tilde{R}) + 9\tilde{f}_k''(1-\tfrac{\tilde{R}}{3})^2\right]^{-1}.
\end{aligned}
\tag{4.89}
$$

This equation constitutes the desired autonomous partial differential equation for the renormalization group flow of $f(R)$ gravity.

A peculiar feature of (4.89) is the appearance of discontinuities on its right-hand side, induced by the θ-function terms. The origin of these contributions can be traced back to the use of the optimized cutoff, for which the finite sums of the type (4.64) gives rise to step functions. The observed discontinuities probably reflect the price to be paid for being able to truncate the heat-kernel expansion at a finite order. Repeating the construction above using a different cutoff-scheme will eventually remove these stepfunctions but requires one to carry out the heat-kernel expansion to all orders in R. We also note that similar discontinuities have already been observed when constructing the β-functions of the R^2-truncation using the exponential cutoff-scheme [40]. In that case, the discontinuities were not in the parameter $\tilde{R}$ but in the space-time dimension d. Evaluating the finite sums for the exponential cutoff induced contributions to the flow equation which were proportional to $\delta_{2,d}$ and $\delta_{4,d}$, so that the flow equations could change discontinuously with the space-time dimension. While it is clearly desirable to get a better understanding of such discontinuities, we will nevertheless leave this topic for the time being, and rather elucidate some other properties of the flow equation (4.89) in the next subsection.

4.4.2 Fixed points of the RG equation

From the dimensionless flow equation (4.89), it is now straightforward to obtain an ordinary differential equation describing the fixed functionals $\tilde{f}_*(\tilde{R})$ of the renormalization group flow of $f(R)$ gravity. By definition, these satisfy $k\partial_k \tilde{f}_k(\tilde{R}) = 0$ and consequently are solutions of the non-linear ordinary differential equation

$$
\begin{aligned}
768\pi^2 \left(2\tilde{f}_* - \tilde{R}\tilde{f}_*'\right) &= \left[5\tilde{R}^2\theta\left(1-\tfrac{\tilde{R}}{3}\right) - 12 - 4\,\tilde{R} + \tfrac{61}{90}\,\tilde{R}^2\right]\left[1-\tfrac{\tilde{R}}{3}\right]^{-1} \\
&+ \left[10\tilde{R}^2\theta\left(1-\tfrac{\tilde{R}}{4}\right) - \tilde{R}^2\theta\left(1+\tfrac{\tilde{R}}{4}\right) - 36 - 6\,\tilde{R} + \tfrac{67}{60}\,\tilde{R}^2\right]\left[1-\tfrac{\tilde{R}}{4}\right]^{-1} \\
&+ \frac{\left(80 - 30\tilde{R} - \frac{271}{9}\tilde{R}^2 + \frac{7249}{2268}\tilde{R}^3\right) - 2\tilde{R}\frac{\tilde{f}_*''}{\tilde{f}_*'}\left(10 - 5\tilde{R} - \frac{271}{36}\tilde{R}^2 + \frac{7249}{4536}\tilde{R}^3\right)}{1 + \tilde{f}_*/\tilde{f}_*' - \tilde{R}/3} \\
&+ 5\tilde{R}^2\frac{\left(1-\tilde{R}\frac{\tilde{f}_*''}{\tilde{f}_*'}\right)\left((1+\frac{\tilde{R}}{3})\theta(1+\frac{\tilde{R}}{3}) + (2+\frac{\tilde{R}}{3})\theta(1+\frac{\tilde{R}}{6})\right) + \theta(1+\frac{\tilde{R}}{3}) + 2\theta(1+\frac{\tilde{R}}{6})}{1 + \tilde{f}_*/\tilde{f}_*' - \tilde{R}/3} \\
&- \Big[2\tilde{R}\tilde{f}_*'''\left(27 - \tfrac{91}{20}\tilde{R}^2 - \tfrac{29}{30}\,\tilde{R}^3 - \tfrac{181}{3360}\,\tilde{R}^4\right) - \tilde{f}_*'\left(48 + 18\,\tilde{R} + \tfrac{29}{15}\,\tilde{R}^2 + \tfrac{37}{756}\,\tilde{R}^3\right) \\
&\qquad - \tilde{f}_*''\left(216 - 12\tilde{R} - \tfrac{121}{5}\,\tilde{R}^2 - \tfrac{29}{10}\,\tilde{R}^3 - \tfrac{37}{756}\,\tilde{R}^4\right)\Big] \\
&\times \left[2\tilde{f}_* + 3\tilde{f}_*'(1-\tfrac{2}{3}\tilde{R}) + 9\tilde{f}_*''(1-\tfrac{\tilde{R}}{3})^2\right]^{-1}.
\end{aligned}
\tag{4.90}
$$

Due to its non-linearity, finding exact analytic solutions to this equation is rather involved, and a detailed analysis of the renormalization group flows following from the partial differential equations (4.89) and (4.90) is beyond the scope of the present work. Nonetheless, let us end our discussion by pointing out some of their properties.

We first investigate the possibility of a Gaussian fixed point arising from the flow equation (4.90). In this course, we reinstall the dimensionless Newton's constant by setting

$$
\tilde{f}_*(\tilde{R}) = \frac{1}{16\pi\tilde{G}^*}\tilde{\tilde{f}}_*(\tilde{R})\,, \tag{4.91}
$$

where $\tilde{G}^*$ indicates that $\tilde{G}$ is taken at the fixed point, $k\partial_k\tilde{G} = 0$. Substituting (4.91) into (4.90), we see that, due to its homogeneity properties, the right-hand side of the flow equation is independent of $\tilde{G}^*$. Schematically, (4.90) takes the form

$$
768\pi^2\left(2\tilde{\tilde{f}}_* - \tilde{R}\tilde{\tilde{f}}_*'\right) = 16\pi\tilde{G}^*\big[\,\ldots\big]\,, \tag{4.92}
$$

with the terms inside the bracket being independent of $\tilde{G}^*$. At the GFP, we have $\tilde{G}^* = 0$, so that the "quantum corrections" on the right-hand side decouple, and (4.92) reduces to

$$
2\tilde{\tilde{f}}_*^{\mathrm{GFP}} - \tilde{R}\tilde{\tilde{f}}_*'^{\mathrm{GFP}} = 0\,. \tag{4.93}
$$

n	$\tilde{g}_0^*$	$\tilde{g}_1^*$	$\tilde{g}_2^*$	$\tilde{g}_3^*$	$\tilde{g}_4^*$	$\tilde{g}_5^*$	$\tilde{g}_6^*$
1	0.00523	-0.0202					
2	0.00329	-0.0127	0.00151				
3	0.00518	-0.0196	0.00070	-0.0097			
4	0.00506	-0.0206	0.00024	-0.0110	-0.0091		
5	0.00507	-0.0206	0.00023	-0.0098	-0.0085	-0.00357	
6	0.00504	-0.0208	0.0001	-0.0104	-0.0102	-0.0038	0.00272

Table 4.3: Location of the NGFP obtained from the fixed functional equation (4.90) by expanding $\tilde{f}_k(\tilde{R})$ in a power series in $\tilde{R}$ up to order $\tilde{R}^n$, including k-dependent coupling constants $\tilde{g}_i(k)$, $i = 0, \ldots, n$.

This equation has the solution $\tilde{\tilde{f}}_*^{\rm GFP} = \tilde{\beta}_* \tilde{R}^2$, with $\tilde{\beta}_*$ an arbitrary integration constant. The corresponding fixed functional is given by

$$\bar{\Gamma}_*^{\rm GFP} = \frac{1}{16\pi \tilde{G}^*} \int d^4x \sqrt{g} \tilde{\beta}_* R^2 \,. \tag{4.94}$$

We note that, with respect to classical power counting, this is just the marginal operator of $f(R)$ gravity. Furthermore, for $\tilde{\beta}_*$ finite, the coupling $\beta_* = (16\pi \tilde{G}^*)^{-1} \tilde{\beta}_*$ gets shifted to infinity as $\tilde{G}^* \to 0$, which is in agreement with the vanishing of the GFP observed in [40].

The flow equation (4.89) and (4.90) can be used to investigate the UV properties of the renormalization group flow. Once we specify a $\tilde{f}_k$ representing a particular truncation subspace, we can straightforwardly use these equations to derive the resulting (optimized cutoff dependent) fixed point structure of the flow. In particular, it allows us to progressively probe the existence and stability properties of the candidate NGFP in truncation spaces incorporating successively higher powers of the scalar curvature, and hence help us assess whether the feature of asymptotic safety found in the Einstein-Hilbert and R^2 truncations are representative of the gravitational flow or artifacts of our approximation. In [69], the fixed point structure of polynomial truncations up to sixth order in the curvature scalar was investigated. This study revealed the existence of a NGFP with a three-dimensional UV critical surface in all truncations considered, constituting non-trivial evidence for the asymptotic safety scenario. We here use our flow equation to recover those results.

In this light, let us consider the UV limit of (4.89). For fixed background curvature, this corresponds to expanding (4.89) for $\tilde{R} = R/k^2 \ll 1$. Note that all θ-functions have positive arguments in this limit and contribute to the flow equation.

We now make a polynomial ansatz for $\tilde{f}_k(\tilde{R})$, setting

$$\tilde{f}_k(\tilde{R}) = \sum_{i=0}^{n} g_{2i}(k)\, \tilde{R}^i \,, \quad n \geq 1 \in \mathbb{N} \,. \tag{4.95}$$

n	θ'	θ''	θ_2	θ_3	θ_4	θ_5	θ_6
1	2.38	-2.17					
2	1.38	-2.32	26.9				
3	2.71	-2.27	2.07	-4.24			
4	2.87	-2.44	1.54	-3.86	-5.25		
5	2.56	-2.69	1.76	-4.37	-3.86 + 4.62i	-3.86 - 4.62i	
6	2.39	-2.38	1.51	-4.16	-4.67 + 6.08i	-4.67 - 6.08i	-8.67

Table 4.4: Stability coefficients for the NGFP with increasing dimension of the truncation space. The first two critical exponents are a complex pair $\theta = \theta' + i\theta''$.

Here, $\tilde{g}_2(k) = -(16\pi\tilde{G})^{-1}$, so that a negative $\tilde{g}_2(k)$ corresponds to a positive Newton's constant. Substituting this ansatz into (4.89), expanding its right-hand side in powers of $\tilde{R}$, and matching the coefficients up to $\tilde{R}^n$ yields the non-perturbative beta functions for the dimensionless couplings $\tilde{g}_2 i(t)$,

$$k\partial_k \tilde{g}_{2i} = \beta_{\tilde{g}_{2i}}(\tilde{g}_0, \ldots, \tilde{g}_{2n}), \quad i = 0, \ldots, n\,. \tag{4.96}$$

Numerically solving for the vanishing of the resulting equations, we find that these beta functions indeed give rise to a NGFP with $\tilde{G}_* > 0, \tilde{\Lambda}_* > 0$, whose n-dependent position is shown in Table 4.3. Linearizing the flow around the NGFP and computing the eigenvalues of the corresponding stability matrix, we obtain the stability coefficients associated with this fixed point. These are summarized in Table 4.4. We see that only three eigendirections are UV-attractive at the NGFP, implying that the corresponding UV critical surface is three-dimensional. Furthermore, note that the stability coefficients and fixed point values are considerably stable under extension of the truncation subspace. Our findings are in agreement with the analysis carried out in [69] and provide an independent confirmation of their results. In a subsequent study by the same authors [41], this analysis was extended to $f(R)$ polynomial truncations of up to order eight. Also there a non-trivial fixed point with three UV-relevant directions and similar numerical values was found. This provides encouraging prospects for the asymptotic safety of gravity.

4.5 Summary

We have constructed a functional renormalization group equation (FRGE) for d dimensional gravity in detail, by means of which we can study truncations of the $f(R)$ form. This equation will provide the basis for our analysis of non-local truncations in the subsequent chapter. Using this equation, we have rederived the main features of the Einstein-Hilbert truncation, where the non-perturbative renormalization group behavior of four-dimensional gravity was first investigated

and where evidence for a UV-attractive non-Gaussian fixed point of the gravitational flow was first established in the FRGE context.

For a particular choice of the cutoff function in $d = 4$ and the case of de Sitter background metrics, our FRGE was evaluated analytically to yield a partial differential equation capturing the renormalization group flow of $f(R)$ gravity. Specifying $f(R)$ to be a polynomial function, we have recovered the results of [69], which has indicated the existence and stability of a non-Gaussian fixed point with three UV-relevant directions under successive extensions of the truncation subspace to polynomials of up to order six. These results suggest that the non-Gaussian fixed point found in the Einstein-Hilbert case is not a truncation artifact and provide non-trivial evidence for the asymptotic safety scenario.

5

Non-local truncations in the $f(R)$ sector

Based on P. F. Machado and F. Saueressig, *On the renormalization group flow of f(R)-gravity*, Phys. Rev. D 77, 124045 (2008), arXiv:0712.0445 [hep-th].

In this chapter, we study the renormalization group behavior of non-local truncations of the $f(R)$ form. The non-local terms in these truncations serve as prototypes for interactions which become dominant for small values of the curvature scalar, and which have been suggested to drive the gravitational physics of the deep IR. Using the flow equation (4.61) derived in the previous chapter, we first discuss two general features of $f(R)$ truncations containing non-local terms, the decoupling of a large class of such non-local interactions from the renormalization group flow, and the resolution of the infrared singularities in the renormalization group trajectories with positive cosmological constant found in the Einstein-Hilbert truncation. The non-perturbative flow of particular non-local extensions of the Einstein-Hilbert truncation including including $\int d^dx\sqrt{g}\ln(R)$ and $\int d^dx\sqrt{g}R^{-n}$ interactions is then investigated in detail. Lastly, we discuss the impact of non-local $f(R)$ truncations on the asymptotic safety conjecture.

5.1 General RG properties of non-local $f(R)$-gravity

Theories of $f(R)$-gravity, in which the gravitational Lagrangian is based on an arbitrary function of the curvature scalar, have recently attracted considerable attention within the cosmology literature. One of the prime reasons for this originates from the observation [119] that non-local terms which become dominant as R decreases can provide a natural explanation for the observed late-time acceleration of our universe, without the need of introducing dark energy (see, e.g., [58]

for a review and more references). By combining these non-local interactions with higher-derivative curvature terms, $f(R)$-gravity can furthermore generate an inflationary phase in the early universe while at the same time satisfying the experimental bounds of gravity tests at solar system scales [120].

Since we may think of these non-local $f(R)$ theories as the effective low-energy limit of a quantum theory of gravity, their phenomenological successes make it interesting to investigate them also from a renormalization group perspective. With respect to the FRGE approach, the motivations for this are two-fold. First, this type of analysis is a step towards addressing the suggestions that the renormalization group running induced by non-local operators in the IR is responsible for cosmological effects, such as the observed small but non-zero value of the cosmological constant [55, 68, 96]. At the level of the gravitational renormalization group flow, this would most likely be reflected by the existence of an IR fixed point which attracts the renormalization group flow for $k \to 0$. In Chapter 3, we explored this suggestion for truncations of the type of the non-local Riegert action (3.14) in the case of conformally reduced gravity. While truncations of this form cannot be investigated in the case of full diffeomorphism-invariant gravity due to limitations in our current calculational techniques, the more tractable $f(R)$ truncations studied in this chapter give us a first qualitative understanding of the renormalization group flow in the presence of non-local interactions. Secondly, inasmuch as we are interested in the behavior of the effective average action for gravity at all energy scales k, if interactions of this type are present in some low energy regime, they must in principle also be included in our theory space for Γ_k. It is therefore important to understand if and how such non-local terms affect the renormalization group behavior of gravity.

Lastly, we note that non-local $f(R)$ monomials explicitly containing inverse powers of the derivatives of the metric, such as the $\int d^dx\sqrt{g}R\ln(-\nabla^2)R$ and $\int d^dx\sqrt{g}R(-\nabla^2)^{-1}R$ interactions proposed in [68] and [121], will not be considered here. Although these interactions are probably more physical than the ones which we will shortly treat, the evaluation of the resulting traces in the flow equation in the presence of the former is beyond current techniques. When discussing non-local truncations and their features in the following, we therefore do not refer to truncations of that type.

The starting point of our investigations is the flow equation (4.61). A remarkable property of this equation is the fact that it is valid for any space-time dimension d, cutoff profile function R_k, and arbitrary function $f_k(R)$. This makes it worthwhile to pause and highlight some general features of the resulting renormalization group flow before analyzing concrete models specifying some of these quantities. We begin by formulating a decoupling theorem for non-local interactions and then move to consider sufficient properties of $f_k(R)$ required for resolving IR singularities of renormalization group trajectories in truncated flow spaces, such as the $\tilde{\Lambda} = 1/2$ line observed in the Einstein-Hilbert truncation and reviewed in the previous chapter.

5.1.1 The perturbative decoupling of non-local interactions

We here discuss a general feature of the beta functions for interaction monomials which are built from non-local curvature terms. It is useful to distinguish two classes of monomials in this context, interactions which blow up as the curvature scalar becomes small, such as R^{-n}- or $\ln(R)$-terms, and non-local interactions which remain finite as $R \to 0$, such as $R\ln(R)$-terms. Based on the flow equation (4.61), one can argue that the beta functions for the scale-dependent couplings multiplying interactions of the first kind are always trivial, while, in the second case, they are always proportional to a coupling constant multiplying an interaction monomial containing (some power of) $\ln(R)$, so that both types of interactions can be consistently decoupled from the renormalization group flow.

Let us start by investigating the beta functions for non-local couplings of the first kind. For this purpose, we will consider $\bar{\Gamma}_k[g]$ as a Laurent series in R,

$$\bar{\Gamma}_k[g] = \int d^d x \sqrt{g} \sum_{n \geq -n_0} \mu_n R^n \,, \quad n_0 > 0 \,, \tag{5.1}$$

corresponding to $f_k(R) = 16\pi G \sum_{n\geq -n_0} \mu_n R^n$, where μ is a k-dependent coupling.[1] Substituting this ansatz into (4.61) and dividing by the volume V, we see that the left-hand side of the flow equation is a Laurent series whose highest order pole is given by R^{-n_0}. The coefficients in this expansion are proportional to the $\ln k$-derivatives of the non-local couplings.

In order to extract the beta functions for these couplings, we now have to perform a Laurent series expansion of the right-hand side of the flow equation. As in Section 4.2.4, this is done by first series expanding the arguments of the traces in R and then using the heat-kernel expansion (4.65) to evaluate the $-\nabla^2$-dependent traces. The first step reveals striking feature of the flow equation. Due to the homogeneity property of its right-hand side with respect to the function $f_k(R)$, expanding the arguments of the traces does not give rise to terms containing inverse powers of R. Thus, even though $f_k(R)$ contains poles as $R \to 0$, the expansion of the trace arguments only yields terms which are regular as $R \to 0$. Taking into account that the heat-kernel expansion (4.69) also contains positive powers of R only, we find that the right-hand side of the flow equation is regular at $R = 0$. Comparing the pole structure on both sides of the flow equation, we then conclude that the beta functions of the non-local couplings appearing in (5.1) are trivial,

$$k\partial_k \mu_n = 0 \,, \; -n_0 \leq n < 0 \,, \tag{5.2}$$

confirming our first claim. Eq. (5.2) implies that non-local couplings of the first kind are scale-independent constants along an arbitrary renormalization group trajectory. In particular, once we start with $\mu_n(\hat{k}) = 0$ at an initial scale $\hat{k}$, the

[1] As illustrated in the next section, this argument also applies to $\ln(R)$-terms, which are not explicitly included in the ansatz (5.1).

renormalization group flow does not dynamically generate non-local couplings of the form R^{-n}.

The situation becomes slightly more complicated for non-local couplings of the second kind. In this case, expanding the arguments of the traces and using the heat-kernel expansion, one finds that such interactions also appear on the right-hand side of the flow equation. Thus, the beta functions for this type of non-local couplings are non-trivial. However, since the heat-kernel expansion (4.69) does not contain $(\ln(R))^n$-terms, the only source for the logarithmic factors in the non-local interactions is the expansion of the traces. This implies that the corresponding non-local terms on the right-hand side of the flow equation are necessarily proportional to a non-local coupling constant multiplying $\ln(R)$-terms in $f_k(R)$. While it is difficult to construct the resulting beta functions explicitly, we can still conclude that the resulting flow equation permits us to consistently set the corresponding non-local couplings to zero. In other words, if there are no interaction terms containing (powers of) $\ln(R)$ present at the initial scale $\hat{k}$, they will not be generated by the renormalization group flow. Note that the same argument also applies to fractional powers of the curvature tensor, which do not arise from the heat-kernel expansion (4.69) either, so that it is also possible to consistently decouple such interaction monomials.

This situation is reminiscent of the observations made in [86, 122], where the renormalization group flow of non-local functions $f_k(V)$ of the space-time volume V were studied. There, the beta functions for the non-local couplings V^2 and $V\ln(V)$ were explicitly derived, and it was found that, even though the beta functions of the non-local couplings were non-trivial, they could be consistently decoupled from the renormalization group equations by setting these couplings to zero. Noting that such interaction monomials are also excluded in the heat-kernel expansion, it is tempting to speculate that all coupling constants whose interaction monomials do not appear in the heat-kernel expansion can be consistently set to zero in the flow equation.

5.1.2 Resolving the IR singularities of $\tilde{\Lambda}_0 > 0$ trajectories

In this subsection, we discuss a feature of the renormalization group trajectories found in the Einstein-Hilbert truncation (cf. Figure 4.1), namely, the termination of trajectories with positive values of the cosmological and extended semiclassical regime at $\tilde{\Lambda}_{k_{\text{term}}} = 1/2$ for a finite value $k_{\text{term}} > 0$. In principle, this class of trajectories would give rise to a positive cosmological constant in the IR, and it was argued in [88] that the renormalization group trajectory realized by nature is of this type. In this light, it is an important question whether or not the termination of these trajectories is due to using an insufficient truncation to describe this part of the gravitational renormalization group flow. In [41], it was shown that the use of a type III cutoff scheme could resolve those singularities. Here, we follow a different approach, and ask whether there are extensions of the Einstein-Hilbert truncation which allow the continuation of these trajectories down to $k = 0$. In

the remainder of this section, we will use the renormalization group equation for $f(R)$-gravity to show that such extensions indeed exist.

Let us begin by sketching the origin of the IR singularity in the Einstein-Hilbert truncation,

$$f_k(R) = -R + 2\Lambda\,. \tag{5.3}$$

From the renormalization group equation (4.61), we observe that its universal part is independent of Λ and therefore cannot be responsible for the singularity. Consequently, the singularity must arise from the $f_k(R)$-dependent part. For conciseness, we illustrate its origin in $\mathcal{S}_k^3$, noting that the analysis for $\mathcal{S}_k^4$ is completely analogous.

Substituting the ansatz (5.3) into S_k^4, we find

$$\begin{aligned} S_k^{4\mathrm{EH}} =& \tfrac{1}{2}\mathrm{Tr}_{2\mathrm{T}}\left[\frac{k\partial_k\left(Z_N R_k\right)}{Z_N\left(P_k - 2\Lambda + \frac{d^2-3d+4}{d(d-1)}R\right)}\right] = \tfrac{1}{2}\mathrm{Tr}_{2\mathrm{T}}\left[\frac{k\partial_k\left(Z_N R_k\right)}{Z_N\left(P_k - 2\Lambda\right)} + \mathcal{O}(R)\right] \\ =& \frac{(d-2)(d+1)}{2(4\pi)^{d/2}}\,k^d\left[\Phi^1_{d/2}(-2\tilde{\Lambda}) - \tfrac{1}{2}\eta_G\tilde{\Phi}^1_{d/2}(-2\tilde{\Lambda})\right]\int d^dx\sqrt{g} + \mathcal{O}(R)\,. \end{aligned} \tag{5.4}$$

Here, we have carried out a Taylor expansion of the argument with respect to R in the first step and then used the heat-kernel expansion (4.65), together with (E.10), to obtain the last line, where we have expressed the cosmological constant through its dimensionless counterpart $\tilde{\Lambda} = \Lambda/k^2$. Substituting the threshold functions for the optimized cutoff (E.16), this becomes[2]

$$S_k^{4\mathrm{EH}} = \tfrac{(d-2)(d+1)}{2(4\pi)^{d/2}}\left[\tfrac{1}{\Gamma(d/2+1)} - \tfrac{1}{2\Gamma(d/2+2)}\eta_G\right]\,k^d\,\frac{1}{1-2\tilde{\Lambda}}\int d^dx\sqrt{g} + \mathcal{O}(R)\,. \tag{5.5}$$

From this expression, we see that the right-hand side of the flow equation, and therefore also the beta functions for $\tilde{G}, \tilde{\Lambda}$, have a pole at $\tilde{\Lambda} = 1/2$. This leads to the termination of the Einstein-Hilbert truncation trajectories with positive cosmological constant at a finite value $k_{\mathrm{term}} > 0$, as can be seen in Figure 4.1. Our aim now is to characterize sufficient properties of $f_k(R)$ which can remove the poles at $\tilde{\Lambda} = 1/2$ from the right-hand side of the flow equation. Again, we will focus on $\mathcal{S}_k^3$, noting that the same mechanism applies to $\mathcal{S}_k^4$.

The main idea behind the resolution of the $\tilde{\Lambda} = 1/2$ singularity is to exploit the homogeneity of the trace-argument in f_k and its derivatives in such a way that the $\tilde{\Lambda}$-terms arising in the denominators are multiplied by some power of R. The $\tilde{\Lambda}$-terms are then dressed up as $\tilde{\Lambda}R^\epsilon$ and expanded in the Taylor series. In that case, the right-hand side of the flow equation has *no poles* of the form $(1-2\tilde{\Lambda})^{-p}, p > 0$, and the singularity is resolved. This can be achieved if $f_k'(R)$

[2]For explicitness, we use the optimized cutoff from Appendix E.2. Other cutoff profile functions like, e.g., the exponential cutoff lead to qualitatively similar results.

contains a term which diverges in the limit $R \to 0$,

$$\lim_{R\to 0} f_k'(R) = \mu\, R^{-\epsilon} + \dots\,, \quad \epsilon > 0\,, \tag{5.6}$$

where μ is a scale-dependent coupling constant. The relation (5.6) is easily integrated to yield the corresponding condition on $f_k(R)$,

$$\begin{aligned} &\lim_{R\to 0} f_k(R) = \frac{\mu}{1-\epsilon}\, R^{1-\epsilon} + \dots\,, && \epsilon > 0,\, \epsilon \neq 1 \\ &\lim_{R\to 0} f_k(R) = u\, \ln(R) + \dots\,, && \epsilon = 1\,. \end{aligned} \tag{5.7}$$

Let us illustrate the workings of this mechanism in detail by adding a term of the form (5.7) to the Einstein-Hilbert truncation,[3]

$$f_k(R) = -R + 2\Lambda + 16\pi G\, \mu\, R^{1-\epsilon}\,. \tag{5.8}$$

Here, μ has been rescaled for later convenience. Substituting this ansatz into $\mathcal{S}_k^4$, we find

$$\begin{aligned} \mathcal{S}_k^4 &= \frac{1}{2}\mathrm{Tr}_{2\mathrm{T}}\left[\frac{Z_N^{-1} k\partial_k\left(Z_N\,(\frac{16\pi G\,\mu}{1-\epsilon} - R^\epsilon)\,R_k\right)}{(\frac{16\pi G\mu}{1-\epsilon} - R^\epsilon)(P_k - \frac{2(d-2)}{d(d-1)}R) - R^{1+\epsilon} + 2\tilde{\Lambda}R^\epsilon + 16\pi G\,\mu\, R}\right] \\ &= \frac{1}{2}\mathrm{Tr}_{2\mathrm{T}}\left[\frac{k\partial_k\,(\mu\, R_k)}{\mu\, P_k} + \mathcal{O}(R^\epsilon, R)\right] \\ &= \frac{(d-2)(d+1)}{2(4\pi)^{d/2}} k^d\, \left[\Phi^1_{d/2}(0) + \tfrac{1}{2}\,\eta_\mu\, \tilde{\Phi}^1_{d/2}(0)\right] \int d^dx\sqrt{g} + \mathcal{O}(R^\epsilon, R)\,. \end{aligned} \tag{5.9}$$

Using the threshold functions for the optimized cutoff, we observe that the poles at $\tilde{\Lambda} = 1/2$ have been removed. Thus, the singularities at $\tilde{\Lambda} = 1/2$ vanish with the inclusion of interaction terms of the form (5.7). This will be further illustrated in the following section, where it will be shown explicitly that the truncations including $\int d^dx\sqrt{g}\ln(R)$ and $\int d^dx\sqrt{g}R^{-n}$ interactions contain renormalization group trajectories with positive cosmological constant in the IR extending to $k \to 0$.

One cautious remark is now in order. Once terms of the form (5.7) are included in the truncation subspace, one has to be very careful about taking the limit in which their corresponding couplings are sent to zero. The reason is that taking this limit does not commute with the Taylor expansion of the trace arguments. This can be easily seen from the following simplified example. Setting $g(x) = g_1x^{-1} + g_2, h(x) = h_1x^{-1} + h_2$, with g_1, g_2, h_1, h_2 constant, and considering the expansion of the quotient

$$\frac{g(x)}{h(x)} = \frac{g_1x^{-1} + g_2}{h_1x^{-1} + h_2} = \frac{g_1 + g_2x}{h_1 + h_2x} = \frac{g_1}{h_1} + \left(\frac{g_2}{h_1} - \frac{g_1h_2}{h_1^2}\right)x + \mathcal{O}(x^2)\,, \tag{5.10}$$

[3]For $\epsilon = 1$, one should replace $R^{1-\epsilon}$ by $\ln(R)$, which is easily done in the formulas below.

we see that taking the "non-local couplings" g_1, h_1 to zero after the expansion leads to a quite different result than doing so before the Taylor series is constructed. From this example, it is clear that considering the renormalization group equation on a truncation subspace which involves couplings of the form (5.7) and setting the new coupling to zero does not automatically yield the beta functions obtained in the Einstein-Hilbert case. This suggests that, in order to correctly decouple this type of non-local interactions from the flow, we should set the non-local couplings to zero already at the level of our ansatz for Γ_k. We will return to this at the end of this chapter.

5.2 The $ln(R)$ and R^{-n} truncations

We will now use the flow equation (4.61) to study the renormalization group flow of the specific non-local extensions of the Einstein-Hilbert action

$$\bar{\Gamma}_k[g] = \frac{1}{16\pi G}\int d^dx\sqrt{g}\{-R + 2\Lambda + 16\pi G\,\nu\,\ln(R)\}\,, \tag{5.11}$$

and

$$\bar{\Gamma}_k[g] = \frac{1}{16\pi G}\int d^dx\sqrt{g}\{-R + 2\Lambda + 16\pi G\,\mu\,R^{-n}\}\,, \qquad n \geq 1 \in \mathbb{Z}\,. \tag{5.12}$$

The non-local terms included in these truncations serve as prototypes for interactions which become dominant for small values of the curvature scalar, and constitute simple models which allow us to investigate how the flow is affected by the class of non-local interactions we are considering here. In this respect, the primary goal of this analysis is the qualitative understanding of the renormalization group flow for the non-local couplings ν, μ.

In [86, 122], the renormalization group flow of truncations including non-local functions of the spacetime volume V was analyzed. The study of the non-local functions of R considered here can be seen as a natural next step in the program of investigating the renormalization group features of non-local interactions, laying the qualitative groundwork for considering truncations including more physically motivated terms, such as those coming from the conformal anomaly.

5.2.1 The $ln(R)$ truncation

Let us start by analyzing the non-perturbative beta functions arising from the $\ln(R)$-truncation (5.11), for which

$$f_k(R) = -R + 2\Lambda + 16\pi G\,\nu\,\ln(R)\,. \tag{5.13}$$

We begin by deriving the beta functions governing the scale-dependence of the couplings G, Λ and ν, and subsequently investigate their properties analytically and numerically.

The beta functions of the $\ln(R)$-truncation

Our first task in the construction of the beta functions of the $\ln(R)$-truncation is the evaluation of the truncation-dependent traces $\mathcal{S}_k^3$ and $\mathcal{S}_k^4$ in (4.61) up to linear order in R. Substituting the ansatz (5.13) and using the heat-kernel techniques reviewed in Section 4.2.4, this yields

$$\begin{aligned}
\mathcal{S}_k^3 &= \frac{k^d}{(4\pi)^{d/2}}\, C_0^{2\mathrm{T}}\, \Big\{\Phi^1_{d/2} + \tfrac{1}{2}\eta_\nu\, \tilde{\Phi}^1_{d/2}\Big\} \int d^dx\sqrt{g} \\
&\quad + \frac{k^{d-2}}{(4\pi)^{d/2}} \Big\{ C_0^{2\mathrm{T}} \Big[\big(\tfrac{d-2}{d(d-1)} - \tfrac{\Lambda}{16\pi G\nu}\big)\big(\eta_\nu\, \tilde{\Phi}^2_{d/2} + 2\,\Phi^2_{d/2}\big) + \frac{k^2\,(\eta_\nu+\eta_G)}{32\pi G\,\nu}\, \tilde{\Phi}^1_{d/2}\Big] \\
&\qquad + C_2^{2\mathrm{T}}\, \Big[\Phi^1_{d/2-1} + \tfrac{1}{2}\,\eta_\nu\, \tilde{\Phi}^1_{d/2-1}\Big]\Big\} \int d^dx\sqrt{g}R\,, \\
\mathcal{S}_k^4 &= \frac{k^d}{(4\pi)^{d/2}} \Big\{2\Upsilon^1_{d/2,1} + \tfrac{1}{2}\eta_\nu \tilde{\Upsilon}^1_{d/2,0,1}\Big\} \int d^dx\sqrt{g} \\
&\quad + \frac{k^{d-2}}{(4\pi)^{d/2}} \Big\{ \frac{d+2}{2(d-1)} \Big(2\Upsilon^2_{d/2,2} - \Upsilon^1_{d/2,0,0} + \tfrac{1}{2}\eta_\nu\big(\tilde{\Upsilon}^2_{d/2,1,1} - \tilde{\Upsilon}^1_{d/2,0,0}\big)\Big) \\
&\qquad + C_2^{\mathrm{S}} \Big(2\Upsilon^1_{d/2-1,1} + \tfrac{1}{2}\eta_\nu \tilde{\Upsilon}^1_{d/2-1,0,1}\Big)\Big\} \int d^dx\sqrt{g}R\,,
\end{aligned} \tag{5.14}$$

for the 2T and scalar trace, respectively. Here, $\eta_G(k)$ and $\eta_\nu(k)$ are the anomalous dimensions of Newton's constant and of the non-local coupling, viz. (4.66) and the C^s_{2k} are defined in (D.12). Inserting the truncation ansatz into the left-hand side of the flow equation (4.61) in turn gives

$$k\partial_k\bar{\Gamma}_k[g] = \frac{1}{16\pi G_{\hat{k}}} \int d^dx\sqrt{g}\Big[- R\,k\partial_k Z_N + 2\,k\partial_k(Z_N\Lambda)\Big] + \int d^dx\sqrt{g}\ln(R)\,k\partial_k\nu\,, \tag{5.15}$$

where, here and in the following, $g_{\hat{k}}$ denotes the value of the coupling $g(k)$ at a particular scale $\hat{k}$. Taking into account the contributions from the universal traces (4.67) and equating the coefficients of the invariants $\int d^dx\sqrt{g}$, $\int d^dx\sqrt{g}R$ and $\int d^dx\sqrt{g}\ln(R)$ spanning our truncation space leads to the following system of coupled differential equations

$$\begin{aligned}
k\partial_k\nu &= 0\,, \\
k\partial_k Z_N &= \frac{16\pi G_{\hat{k}} k^{d-2}}{(4\pi)^{d/2} - \frac{1}{2}\,k^d\,\nu^{-1}\,\tilde{\Phi}^1_{d/2}\,C_0^{2\mathrm{T}}} \Big[\big(\tfrac{(d-2)(d+1)}{16\pi G}\tfrac{\Lambda}{\nu} - \tfrac{d^3-4d^2+d-3}{d(d-1)}\big)\,\Phi^2_{d/2} \\
&\qquad + \big(\tfrac{d^2-6}{6d} - C_2^{2\mathrm{T}}\big)\Phi^1_{d/2-1} - \tfrac{d+2}{d-1}\big(\Upsilon^2_{d/2,2} - \tfrac{1}{2}\Upsilon^1_{d/2,1}\big) - \tfrac{1}{3}\Upsilon^1_{d/2-1,1}\Big]\,, \\
k\partial_k(Z_N\Lambda) &= \frac{G_{\hat{k}}k^d}{(4\pi)^{d/2-1}}\big[(d^2-3d-2)\,\Phi^1_{d/2} + 4\Upsilon^1_{d/2,1}\big]\,.
\end{aligned} \tag{5.16}$$

The beta functions resulting from these equations are most conveniently expressed in terms of the dimensionless couplings

$$\tilde{G} = k^{d-2}\, Z_N^{-1}\, G_{\hat{k}} = k^{d-2}\, G\,, \quad \tilde{\Lambda} = k^{-2}\Lambda\,, \quad \tilde{\nu}_k = k^{-d}\nu\,. \tag{5.17}$$

In terms of these, the eqs. (5.16) imply the following set of autonomous first order differential equations

$$k\partial_k G = \beta_{\tilde{G}}(\tilde{G},\tilde{\Lambda},\tilde{\nu})\,, \quad k\partial_k\tilde{\Lambda} = \beta_{\tilde{\Lambda}}(\tilde{G},\tilde{\Lambda},\tilde{\nu})\,, \quad k\partial_k\tilde{\nu}_k = \beta_{\tilde{\nu}}(\tilde{G},\tilde{\Lambda},\tilde{\nu})\,, \tag{5.18}$$

where

$$\begin{aligned}
\beta_{\tilde{G}}(\tilde{G},\tilde{\Lambda},\tilde{\nu}) &= (d-2+\eta_G)\;\tilde{G}\,,\\
\beta_{\tilde{\Lambda}}(\tilde{G},\tilde{\Lambda},\tilde{\nu}) &= -\,(2-\eta_G)\,\tilde{\Lambda} + (4\pi)^{1-d/2}\,\tilde{G}\left((d^2-3d-2)\,\Phi^1_{d/2} + 4\,\Upsilon^1_{d/2,1}\right)\,,\\
\beta_{\tilde{\nu}}(\tilde{G},\tilde{\Lambda},\tilde{\nu}) &= -\,d\,\tilde{\nu}_k\,.
\end{aligned} \tag{5.19}$$

Here, the anomalous dimension of Newton's constant is given by

$$\begin{aligned}
\eta_G = -\,\frac{32\pi\tilde{G}}{2\,(4\pi)^{d/2} - \tilde{\nu}_k^{-1}\tilde{\Phi}^1_{d/2}\,C_0^{2\mathrm{T}}}\Big[&\big(\tfrac{(d-2)(d+1)}{16\pi\tilde{G}}\,\tfrac{\tilde{\Lambda}}{\tilde{\nu}_k} - \tfrac{d^3-4d^2+d-3}{d(d-1)}\big)\,\Phi^2_{d/2}\\
&+\big(\tfrac{d^2-6}{6d} - C_2^{2\mathrm{T}}\big)\Phi^1_{d/2-1} - \tfrac{d+2}{d-1}\big(\Upsilon^2_{d/2,2} - \tfrac{1}{2}\Upsilon^1_{d/2,1}\big) - \tfrac{1}{3}\Upsilon^1_{d/2-1,1}\Big]\,.
\end{aligned} \tag{5.20}$$

Note that, unlike the case of the Einstein-Hilbert truncation, in which η_G contained contributions from all orders in $\tilde{G}$ (cf. (4.75)), the anomalous dimension of Newton's constant obtained here is linear in $\tilde{G}$. This indicates that the $\ln(R)$ truncation does not capture non-perturbative contributions from an infinite number of graviton loops and therefore may not appropriately describe quantum gravity in the UV.

This completes the derivation of the beta functions for the $\ln(R)$-truncation. These beta functions are consistent in the sense that they incorporate all contributions proportional to the interaction monomials spanning the truncation subspace. As expected from the general discussion in Section 5.1.1, the beta function for the dimensionful non-local coupling ν is indeed trivial, $k\partial_k\nu = 0$. Furthermore, the only poles of (5.19) occur at the line

$$\tilde{\nu}_{\mathrm{sing}} = \tfrac{1}{2}\,(4\pi)^{-d/2}\,C_0^{2\mathrm{T}}\,\tilde{\Phi}^1_{d/2}, \tag{5.21}$$

showing explicitly that the singularity at $\tilde{\Lambda} = 1/2$ has been resolved, in full agreement with the arguments given in Section 5.1.

A second property which can be directly deduced from the beta functions (5.19) is the decomposition of the coupling constant space into various sectors

whose trajectories do not mix under the renormalization group flow. Since $\beta_{\tilde{G}}(\tilde{G}=0,\tilde{\Lambda},\tilde{\nu})=0$ and $\beta_{\tilde{\nu}}(\tilde{G},\tilde{\Lambda},\tilde{\nu}=0)=0$, the $\tilde{G}=0$- and $\tilde{\nu}=0$-planes cannot be crossed by the trajectories. In other words, a renormalization group trajectory starting with positive $\tilde{G}_{\hat{k}}$ (or $\tilde{\nu}_{\hat{k}}$) will never evolve to $\tilde{G}<0$ (or $\tilde{\nu}_k<0$), and vice versa.

The fixed points of the renormalization group flow

In order to gain some first insights into the dynamics arising from (5.18), we analyze the fixed point structure of the beta functions. At the fixed points, all beta functions vanish simultaneously,

$$\beta_{\tilde{G}}(\tilde{G}^*,\tilde{\Lambda}^*,\tilde{\nu}^*)=0\,,\quad \beta_{\tilde{\Lambda}}(\tilde{G}^*,\tilde{\Lambda}^*,\tilde{\nu}^*)=0\,,\quad \beta_{\tilde{\nu}}(\tilde{G}^*,\tilde{\Lambda}^*,\tilde{\nu}^*)=0\,, \tag{5.22}$$

and many properties of the renormalization group flow can be captured by linearizing the renormalization group equation at such points and studying the flow in their vicinity. Introducing the generalized couplings $\vec{g}=[\tilde{G},\tilde{\Lambda},\tilde{\nu}_k]$ and the Jacobi matrix

$$\mathbf{B}=(B_{ij})\,,\qquad B_{ij}=\left.\frac{\partial\beta_{g_i}}{\partial\tilde{g}_j}\right|_{\mathrm{FP}}\,, \tag{5.23}$$

the linearized flow equation reads

$$k\partial_k\tilde{g}_i\approx\sum_j B_{ij}(\tilde{g}_j-\tilde{g}_j^*)\,. \tag{5.24}$$

Using the stability coefficients $\theta^i=-\lambda^i$, with λ^i the eigenvalue of $\mathbf{B}$ associated with the right eigenvectors V^i, B_{ij} can be diagonalized, so that eq. (5.24) is easily solved. These analytic solutions provide a good picture of which renormalization group trajectories are dragged into the fixed point or repelled along an unstable direction.

Applying this construction to the beta functions (5.19), we first observe that $\beta_{\tilde{\nu}}=0$ forces all fixed points onto the $\tilde{v}=0$ plane. Substituting this condition into the remaining beta functions, $\beta_{\tilde{G}}$ and $\beta_{\tilde{\Lambda}}$ simplify considerably and their roots are easily found analytically,

$$\begin{aligned}
\text{GFP}:&\quad \left\{\tilde{G}^*=0\,,\,\tilde{\Lambda}^*=0\,,\,\tilde{\nu}^*=0\right\},\\
\text{IRFP}:&\quad \left\{\tilde{G}^*=0\,,\,\tilde{\Lambda}^*=\frac{\tilde{\Phi}^1_{d/2}}{2\Phi^2_{d/2}}\,,\,\tilde{\nu}^*=0\right\},\\
\text{NGFP}:&\quad \left\{\tilde{G}^*=-\frac{(4\pi)^{d/2-1}\,d(d-2)\,\tilde{\Phi}^1_{d/2}}{4\Phi^2_{d/2}\left((d^2-3d-2)\Phi^1_{d/2}+4\Upsilon^1_{d/2,1}\right)}\,,\,\tilde{\Lambda}^*=-\frac{(d-2)\,\tilde{\Phi}^1_{d/2}}{4\phi^2_{d/2}}\,,\,\tilde{\nu}^*=0\right\}.
\end{aligned} \tag{5.25}$$

Here, GFP denotes the Gaussian Fixed Point, while the other fixed points have been labeled Infrared Fixed Point (IRFP), and Non-Gaussian Fixed Point (NGFP). Let us discuss the stability properties of these fixed points in turn.

At the GFP, the stability matrix $\mathbf{B}$ becomes

$$\mathbf{B}_{\rm GFP} = \begin{bmatrix} d-2 & 0 & 0 \\ (4\pi)^{1-d/2}\big((d^2-3d-2)\Phi^1_{d/2}+4\Upsilon^1_{d/2,1}\big) & -2 & 0 \\ 0 & 0 & -d \end{bmatrix}, \tag{5.26}$$

with stability coefficients and associated right eigenvectors

$$\begin{aligned} &\theta_1 = 2-d\,, \quad V^1 = \Big[\,1\,,\tfrac{1}{d}(4\pi)^{1-d/2}\big((d^2-3d-2)\Phi^1_{d/2}+4\Upsilon^1_{d/2,1}\big)\,,\,0\,\Big]^{\rm T}\,, \\ &\theta_2 = 2\,, \qquad V^2 = [\,0\,,\,1\,,0\,]^{\rm T}\,, \\ &\theta_3 = d\,, \qquad V^3 = [\,0\,,\,0\,,\,1\,]^{\rm T}\,. \end{aligned} \tag{5.27}$$

This information can be used to solve the renormalization group equation in the vicinity of the GFP, giving

$$\begin{aligned} \tilde{G} =& \alpha_1 \frac{k^{d-2}}{M^{d-2}}\,, \\ \tilde{\Lambda} =& \alpha_2 \frac{k^{-2}}{M^{-2}} + \alpha_1 \frac{(4\pi)^{1-d/2}}{d}\big((d^2-3d-2)\Phi^1_{d/2}+4\Upsilon^1_{d/2,1}\big)\frac{k^{d-2}}{M^{d-2}}\,, \\ \tilde{\nu} =& \alpha_3 \frac{k^{-d}}{M^{-d}}\,. \end{aligned} \tag{5.28}$$

Here, $\{\alpha_i\}$ denotes the set of integration constants and M is an arbitrary fixed mass scale. It is natural to define the dimensionful integration constants

$$G_0 = m_{\rm Pl}^{2-d}\,, \quad \Lambda_0 = \alpha_2\, m_{\rm Pl}^2\,, \quad \nu_0 = \alpha_3\, m_{\rm Pl}^d\,, \tag{5.29}$$

where we have identified M with the Planck mass $m_{\rm Pl}$ by setting $\alpha_1 = 1$. By using the relations (5.17), we then obtain the scale-dependence of the dimensionful coupling constants in the vicinity of the GFP,

$$\begin{aligned} G =& G_0\,, \\ \Lambda =& \Lambda_0 + \frac{(4\pi)^{1-d/2}}{d}\, G_0\,\big((d^2-3d-2)\Phi^1_{d/2}+4\Upsilon^1_{d/2,1}\big)\,k^d\,, \\ \nu =& \nu_0\,. \end{aligned} \tag{5.30}$$

These equations show that G, Λ and ν run towards constant, non-zero values as $k \to 0$. In particular, Λ does not vanish in the IR unless we make the special choice $\alpha_2 = 0$. Thus, the GFP does not determine the behavior of the cosmological constant Λ_0 in the infrared.

Let us now turn to the IRFP (5.25). Here, the matrix $\mathbf{B}$ becomes

$$\mathbf{B}_{\rm IRFP} = \begin{bmatrix} d & 0 & 0 \\ (4\pi)^{1-d/2}\big((d^2-3d-2)\Phi^1_{d/2}+4\Upsilon^1_{d/2,1}\big) & 2 & \frac{4(4\pi)^{d/2}}{(d+1)(d-2)\Phi^2_{d/2}} \\ 0 & 0 & -d \end{bmatrix}, \tag{5.31}$$

and the eigensystem of $\mathbf{B}_{\mathrm{IRFP}}$ is

$$\begin{aligned}
\theta_1 &= -d\,, \quad V^1 = \Big[\,1\,,\tfrac{1}{d-2}(4\pi)^{1-d/2}\big((d^2-3d-2)\Phi^1_{d/2}+4\Upsilon^1_{d/2,1}\big)\,,\,0\,\Big]^{\mathrm{T}}\,,\\
\theta_2 &= -2\,, \quad V^2 = \big[\,0\,,\,1\,,0\,\big]^{\mathrm{T}}\,,\\
\theta_3 &= d\,, \qquad V^3 = \left[\,0\,,-\tfrac{4(4\pi)^{d/2}}{(d^3+d^2-4d-4)\Phi^2_{d/2}}\,,\,1\,\right]^{\mathrm{T}}\,.
\end{aligned} \tag{5.32}$$

Note that the stability coefficient θ_2 has now changed sign compared to the eigensystem of the GFP (5.27), making the eigendirection V^2 IR-attractive (hence the name IRFP). Solving the linearized flow equation results in

$$\begin{aligned}
\tilde{G} =& \alpha_1 \frac{k^d}{M^d}\,,\\
\tilde{\Lambda} =& \alpha_2 \frac{k^2}{M^2} + \alpha_1 \frac{(4\pi)^{1-d/2}}{d-2}\left((d^2-3d-2)\Phi^1_{d/2}+4\Upsilon^1_{d/2,1}\right)\frac{k^d}{M^d}\\
&- \alpha_3 \frac{4(4\pi)^{d/2}}{(d^3+d^2-4d-4)\,\Phi^2_{d/2}}\frac{k^{-d}}{M^{-d}} + \frac{\tilde{\Phi}^1_{d/2}}{2\Phi^2_{d/2}}\,,\\
\tilde{\nu}_k =& \alpha_3 \frac{k^{-d}}{M^{-d}}\,,
\end{aligned} \tag{5.33}$$

where we have again denoted the integration constants by α_i. Using the relations (5.17), we obtain the scale-dependence of the dimensionful coupling constants,

$$\begin{aligned}
G =& G_0\,\frac{k^2}{m^2_{\mathrm{Pl}}},\\
\Lambda =& \Lambda_0 \frac{k^4}{m^4_{\mathrm{Pl}}} + \frac{(4\pi)^{1-d/2}}{d-2}\left((d^2-3d-2)\Phi^1_{d/2}+4\Upsilon^1_{d/2,1}\right)G_0\frac{k^{d+2}}{m^2_{\mathrm{Pl}}}\\
&- \nu_0 \frac{4(4\pi)^{d/2}}{(d^3+d^2-4d-4)\,\Phi^2_{d/2}}\,k^{2-d} + \frac{\tilde{\Phi}^1_{d/2}}{2\Phi^2_{d/2}}k^2\,,\\
\nu =& \nu_0\,.
\end{aligned} \tag{5.34}$$

Thus, for $d > 2$, the IRFP has an unstable direction in ν, driving the renormalization group trajectories with $\nu_0 \neq 0$ away from the fixed point. For trajectories in the plane $\nu_0 = 0$, however, the IRFP is an infrared attractor for both Newton's constant and the cosmological constant. In this case both G and Λ are dynamically driven to zero as $k \to 0$, independently of their values at the initial scale $\hat{k}$.

Finally, determining the stability coefficients of the NGFP, we find that it is UV-attractive for all three couplings $\tilde{G}, \tilde{\Lambda}$ and $\tilde{\nu}_k$. However, not only does it lie in the unphysical region $\tilde{G} < 0$, but also, due to the fact that the renormalization group flow in this truncation subspace decomposes into a $\tilde{G} > 0$ and a $\tilde{G} < 0$ sector, no trajectories with positive $\tilde{G}$ will ever reach this fixed point.

Numerical solutions of the flow equations

After discussing their fixed point structure, we now proceed by integrating the flow equations (5.18) numerically. This requires fixing the space-time dimension and the cutoff-scheme explicitly, so we will restrict ourselves to $d = 4$ and to the optimized cutoff (E.15) in the following. Given the decomposition of the coupling constant space, we will furthermore limit our focus on trajectories with $G > 0$, as these are the physically relevant ones. For $d = 4$ and the optimized cutoff, the fixed points (5.25) are located at

$$\begin{aligned} \text{GFP}: &\quad \left\{\tilde{G}^* = 0\,,\, \tilde{\Lambda}^* = 0\,,\, \tilde{\nu}^* = 0\right\}, \\ \text{IRFP}: &\quad \left\{\tilde{G}^* = 0\,,\, \tilde{\Lambda}^* = \tfrac{1}{6}\,,\, \tilde{\nu}^* = 0\right\}, \\ \text{NGFP}: &\quad \left\{\tilde{G}^* = -\tfrac{8\pi}{9}\,,\, \tilde{\Lambda}^* = -\tfrac{1}{6}\,,\, \tilde{\nu}^* = 0\right\}. \end{aligned} \tag{5.35}$$

We note that the NGFP is indeed situated in the region $\tilde{G} < 0$ and hence will not play a role in the subsequent discussion. Moreover, the singular line (5.21) is located at

$$\tilde{\nu}_{\text{sing}} = 0.00263\,. \tag{5.36}$$

Due to the existence of the IRFP, the most interesting region of the parameter space is the one comprising the renormalization group flow of $\tilde{G}, \tilde{\Lambda}$ on the fixed plane $\tilde{\nu} = 0$, which is shown in Figure 5.1. This diagram clearly illustrates the separation between trajectories with positive and negative values $\tilde{G}$. The renormalization group flow in the upper half plane is thereby dominated by the GFP and the IRFP. The renormalization group trajectories in this region fall into three distinct classes, which, in analogy to the classification of the Einstein-Hilbert truncation trajectories performed in [38], are labelled Type Iã, IIã, and IIIã, respectively. The class IIã consists of the single trajectory ("separatrix") hitting the GFP as $k \to 0$. The trajectories of Type Iã run to the left of the separatrix and lead to a negative cosmological constant $\tilde{\Lambda}_0$ in the infrared. The trajectories of Type IIIã, to the right of the separatrix, are captured by the IRFP as $k \to 0$, which implies that the corresponding dimensionful couplings G, Λ go to zero as $k \to 0$.

The IR behavior of these classes can also be understood at the level of the linearized solutions (5.30) and (5.34), as follows. The classes Iã and IIã correspond to linearized solutions $\alpha_2 < 0$ and $\alpha_2 = 0$, respectively. The solutions with $\alpha_2 > 0$ are driven away from the GFP regime and captured by the IRFP (5.34), giving $G_0 = 0, \Lambda_0 = 0$ independently of any integration constants. The latter feature is also illustrated in Figure 5.2 (a). Note that, due to the absence of an UV fixed point in the $\ln(R)$-truncation, we do not expect that the classes of renormalization group trajectories discussed here give rise to a well-defined behavior as $k \to \infty$. This is possibly owed to the fact that our truncation subspace is insufficient for a proper description of quantum gravity in the UV, as we will shortly discuss. Going away from the $\tilde{\nu} = 0$ plane, we have to distinguish the two cases $\nu < 0$ and

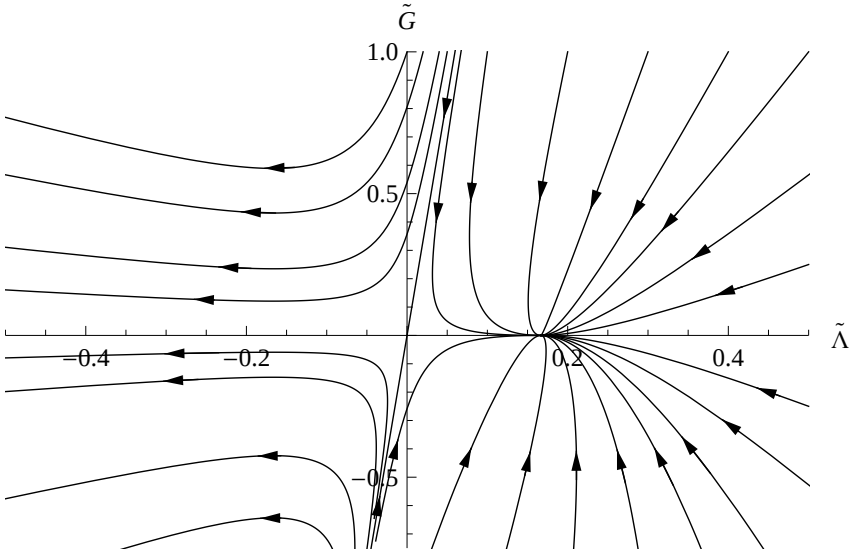

Figure 5.1: Renormalization group flow of the $\ln(R)$-truncation in the fixed plane $\tilde{\nu} = 0$. The flow is dominated by the GFP at $\tilde{G}^* = 0, \tilde{\Lambda}^* = 0$ and the IRFP at $\tilde{G}^* = 0, \tilde{\Lambda}^* = 1/6$. All renormalization group trajectories running to the left of the "separatrix" are captured by the IRFP as $k \to 0$.

$\nu > 0$. To illustrate the behavior in these regions, some examples for trajectories starting with $\Lambda(k = 1) > 0$ are shown in Figures 5.2 and 5.3. For the trajectories with $\nu < 0$ we find that both G, Λ decrease with decreasing values k. Comparing the series of diagrams (a), (b), (c), in which the modulus of the non-local coupling is continuously increased, we observe that this "quenching" works more efficiently for small non-local coupling $|\nu|$, the case of $\nu = 0$, corresponding to the IRFP, being the most efficient.

Finally, for the trajectories with $\nu > 0$, we distinguish two different behaviors. Trajectories starting with $\tilde{\nu}_{\hat{k}} < \tilde{\nu}_{\text{sing}}$ run into the singularity and terminate at finite $k_{\text{term}} = (\tilde{\nu}_{\hat{k}}/\tilde{\nu}_{\text{sing}})^{1/4}\hat{k}$, whereas trajectories in the region $\tilde{\nu}_{\hat{k}} > \tilde{\nu}_{\text{sing}}$ are non-singular and can lead to increasing values of G, Λ as k decreases. An example of the latter behavior is shown in Figure 5.3 (d).

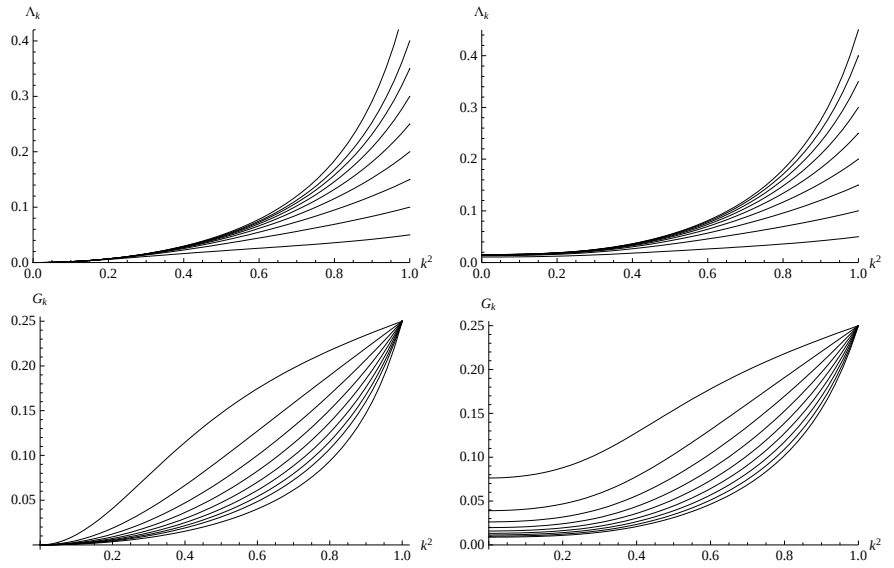

Figure 5.2: Numerical solutions to the $\ln(R)$-truncation flow equations in terms of the dimensionful couplings, for (a) $\nu_{\hat{k}} = 0$ and (b) $\nu_{\hat{k}} = -5 \times 10^{-5}$ imposed at $\hat{k} = 1$. Here, we have taken $G_{\hat{k}} = 0.25$, while $\Lambda_{\hat{k}}$ assumes various values. We see that, for $\nu_{\hat{k}} \lesssim 0$, the cosmological constant is quenched in the IR limit, going to zero (a), or small but non-zero (b) values.

5.2.2 The R^{-n} truncation

We now turn towards our second class of non-local truncations, the R^{-n} truncations (5.12), for which

$$f_k(R) = -R + 2\Lambda + 16\pi G\,\mu\,R^{-n}\,. \tag{5.37}$$

Deriving the renormalization group equations

Following the calculation of the previous section, we first compute the contribution from the truncation-dependent traces $\mathcal{S}_k^3$ and $\mathcal{S}_k^4$. Substituting the ansatz (5.37) into (4.61) and evaluating the resulting expressions up to linear order in R, we

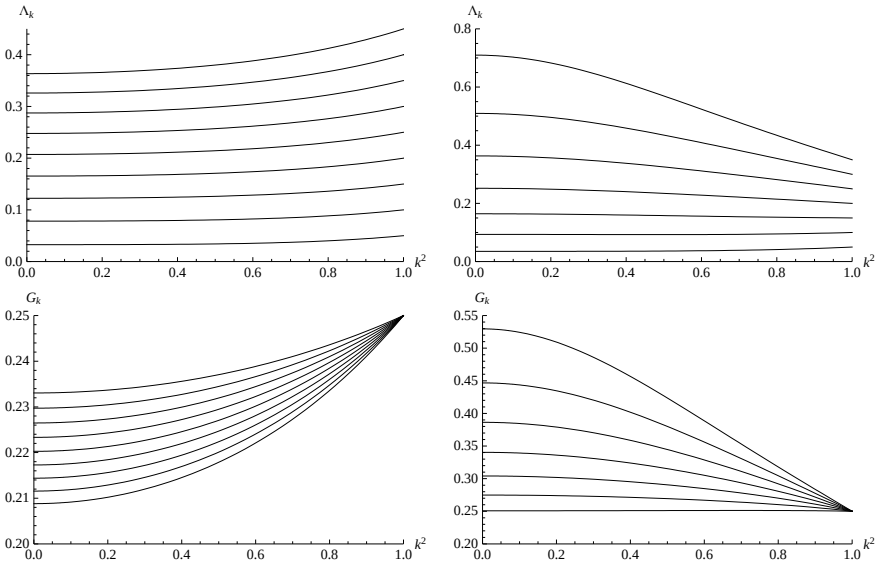

(c) (d)

Figure 5.3: Numerical solutions to the $\ln(R)$-truncation flow equations in terms of the dimensionful couplings, for (a) $\nu_{\hat{k}} = 0$, (b) $\nu_{\hat{k}} = -5 \times 10^{-5}$, (c) $\nu_{\hat{k}} = -5 \times 10^{-2}$ and (d) $\nu_{\hat{k}} = 0.01$ imposed at $\hat{k} = 1$. Here, we have taken $G_{\hat{k}} = 0.25$, while $\Lambda_{\hat{k}}$ assumes various values. We see that, for $\nu_{\hat{k}} \lesssim 0$, the cosmological constant is quenched in the IR limit, going to zero (a), or small but non-zero (b) values.

find

$$
\begin{aligned}
\mathcal{S}_k^3 = & \frac{k^d}{(4\pi)^{d/2}} C_0^{2\mathrm{T}} \left\{ \Phi^1_{d/2} + \tfrac{1}{2}\eta_\mu \, \tilde{\Phi}^1_{d/2} \right\} \int d^d x \sqrt{g} \\
& + \frac{k^{d-2}}{(4\pi)^{d/2}} \left\{ C_0^{2\mathrm{T}} \left[\frac{d\,((2n-1)+d) - 4n}{n\,d(d-1)} \left(\Phi^2_{d/2} + \tfrac{1}{2}\,\eta_\mu \, \tilde{\Phi}^2_{d/2} \right) \right] \right. \\
& \left. + C_2^{2\mathrm{T}} \left[\Phi^1_{d/2-1} + \tfrac{1}{2}\,\eta_\mu \, \tilde{\Phi}^1_{d/2-1} \right] \right\} \int d^d x \sqrt{g} R \,, \\
\mathcal{S}_k^4 = & \frac{k^d}{(4\pi)^{d/2}} \left\{ 2\Upsilon^1_{d/2,1} + \tfrac{1}{2}\eta_\mu \tilde{\Upsilon}^1_{d/2,0,1} \right\} \int d^d x \sqrt{g} \\
& + \frac{k^{d-2}}{(4\pi)^{d/2}} \left\{ \tfrac{4n+2+d}{2(n+1)(d-1)} \left[2\Upsilon^2_{d/2,2} - \Upsilon^1_{d/2,0} + \tfrac{1}{2}\eta_\mu (\tilde{\Upsilon}^2_{d/2,1,1} - \tilde{\Upsilon}^1_{d/2,0,0}) \right] \right. \\
& \left. + C_2^{\mathrm{S}} \left[2\Upsilon^1_{d/2-1,1} + \tfrac{1}{2}\eta_\mu \tilde{\Upsilon}^1_{d/2-1,0,1} \right] \right\} \int d^d x \sqrt{g} R \,.
\end{aligned}
\tag{5.38}
$$

Here, $\eta_\mu(k)$ is the anomalous dimension (4.66), and all threshold functions are evaluated at zero argument (viz. (4.68)). The left-hand side of (4.61) now reads

$$k\partial_k\bar{\Gamma}_k[g] = \frac{1}{16\pi G_{\hat{k}}}\int d^dx\sqrt{g}\Big[-R\,k\partial_k Z_N + 2\,k\partial_k(Z_N\tilde{\Lambda})\Big] + \int d^dx\sqrt{g}\frac{1}{R^n}\,k\partial_k\mu\,. \tag{5.39}$$

Comparing the coefficients multiplying the interaction monomials in the truncation ansatz again leads to three coupled differential equations encoding the scale-dependence of Z_N, Λ and μ. Rewriting these equations in terms of the dimensionless coupling constants

$$\tilde{G} = k^{d-2}\,G\,, \quad \Lambda = k^{-2}\tilde{\Lambda}\,, \quad \tilde{\mu} = k^{-(d+2n)}\mu\,, \tag{5.40}$$

we arrive at the renormalization group equations of the R^{-n} truncation,

$$k\partial_k\tilde{G} = \beta_{\tilde{G}}(\tilde{G},\tilde{\Lambda},\tilde{\mu})\,, \quad k\partial_k\tilde{\Lambda} = \beta_{\tilde{\Lambda}}(\tilde{G},\tilde{\Lambda},\tilde{\mu})\,, \quad k\partial_k\tilde{\mu} = \beta_{\tilde{\mu}}(\tilde{G},\tilde{\Lambda},\tilde{\mu})\,, \tag{5.41}$$

with

$$\begin{aligned}
\beta_{\tilde{G}}(\tilde{G},\tilde{\Lambda},\tilde{\mu}) &= (d-2+\eta_G)\;\tilde{G}\,,\\
\beta_{\tilde{\Lambda}}(\tilde{G},\tilde{\Lambda},\tilde{\mu}) &= -\,(2-\eta_G)\,\tilde{\Lambda} + (4\pi)^{1-d/2}\,\tilde{G}\left((d^2-3d-2)\,\Phi^1_{d/2} + 4\,\Upsilon^1_{d/2,1}\right)\,,\\
\beta_{\mu}(\tilde{G},\tilde{\Lambda},\tilde{\mu}) &= -\,(d+2n)\;\tilde{\mu}\,.
\end{aligned} \tag{5.42}$$

The anomalous dimension of Newton's constant is given by

$$\eta_G = -\,\mathrm{H}_{n,d}\,\tilde{G}\,, \tag{5.43}$$

where

$$\begin{aligned}
\mathrm{H}_{n,d} \equiv \frac{2}{(4\pi)^{d/2-1}}\Big\{&\tfrac{2+d+4n}{(n+1)(d-1)}\left[2\Upsilon^2_{d/2,2} - \Upsilon^1_{d/2,0}\right] + 4\,C_2^{\mathrm{S}}\,\Upsilon^1_{d/2-1,1}\\
&- \tfrac{d^2-6-6d\,C_2^{2\mathrm{T}}}{3d}\,\Phi^1_{d/2-1} + 2\left[\tfrac{1}{n}\,C_0^{2\mathrm{T}} + \tfrac{2(d-2)}{d(d-1)}\,C_0^{2\mathrm{T}} - \tfrac{d^2-d+1}{d(d-1)}\right]\,\Phi^2_{d/2}\Big\}\,,
\end{aligned} \tag{5.44}$$

and the d-dependent constants C^s_{2k} are given in (D.12). Observe that $\mathrm{H}_{n,d}$ is a (truncation-dependent) constant, independent of any coupling constants, so that η_G is again linear in $\tilde{G}$, as was found in the $\ln(R)$ truncation.

Furthermore, again confirming the results of Section 5.1, we note that the beta function for the non-local coupling μ is trivial, so that μ is a k-independent constant along a renormalization group trajectory. Not only that, but the non-local coupling $\tilde{\mu}$ also decouples from the flow of $\tilde{G},\tilde{\Lambda}$, in the sense that $\beta_{\tilde{G}}(\tilde{G},\tilde{\Lambda},\tilde{\mu}), \beta_{\tilde{G}}(\tilde{G},\tilde{\Lambda},\tilde{\mu})$ are independent of $\tilde{\mu}$. Thus, the renormalization group flow for $\tilde{G},\tilde{\Lambda}$ is not altered by the value of the constant μ and can be studied independently from the flow of $\tilde{\mu}$.

Finally, we observe that the beta functions have no poles in the coupling space, being well-defined for any value $\tilde{G}, \tilde{\Lambda}, \tilde{\mu}$. In a similar manner to the case of the $\ln(R)$-truncation, the coupling constant space decomposes into various regions whose renormalization group trajectories do not mix under the renormalization group flow. These regions are separated by the fixed planes $\tilde{G} = 0$ and $\tilde{\mu} = 0$, as well as the fixed plane at $\tilde{G}^* = (d-2)/\mathrm{H}_{n,d}$. The latter is due to the linearity of η_G, which implies that $\beta_{\tilde{G}}(\tilde{G}^*, \tilde{\Lambda}, \tilde{\mu}) = 0$ for any value $\tilde{\Lambda}, \tilde{\mu}$, so that the $\tilde{G}^*$-plane cannot be crossed by the renormalization group flow either.

Fixed points of the renormalization group flow

In order to better understand the renormalization group flow encoded by (5.42), we follow the strategy of Section 5.2.1 and analyze the fixed points of the beta functions. The conditions $\beta_\mu(\tilde{G}^*, \tilde{\Lambda}^*, \tilde{\mu}^*) = 0$ implies that all fixed points must be located on the $\mu = 0$-plane. Solving $\beta_{\tilde{G}}(\tilde{G}^*, \tilde{\Lambda}^*, \tilde{\mu}^*) = 0, \beta_{\tilde{\Lambda}}(\tilde{G}^*, \tilde{\Lambda}^*, \tilde{\mu}^*) = 0$ analytically, we find that there are two roots, yielding a GFP and a NGFP,

$$\begin{aligned} \text{GFP}: \quad & \{\tilde{G}^* = 0\,,\, \tilde{\Lambda}^* = 0\,,\, \tilde{\mu}^* = 0\}\,, \\ \text{NGFP}: \quad & \{\tilde{G}^* = -\tfrac{d-2}{\mathrm{H}_{n,d}}\,,\, \tilde{\Lambda}^* = -\tfrac{d-2}{\mathrm{H}_{n,d}}\,\frac{(4\pi)^{1-d/2}\big[(d^2-3d-2)\,\Phi^1_{d/2}+4\,\Upsilon^1_{d/2,1}\big]}{d}\,, \\ & \qquad \tilde{\mu}^* = 0\}\,. \end{aligned} \tag{5.45}$$

Focusing on the NGFP for the moment, we see that its position crucially depends on the sign of $\mathrm{H}_{n,d}$ which, for fixed d, in turn depends on the exponent n of the R^{-n}-term in our ansatz. Noting that $\tilde{G}^* < 0$ ($\tilde{G}^* > 0$) for $\mathrm{H}_{n,d} > 0$, ($\mathrm{H}_{n,d} < 0$), respectively, we define n_{crit} as the (possibly non-integer) positive real root of the quadratic equation $\mathrm{H}_{n,d} = 0$, assuming it exists. The existence and actual value of the transition point n_{crit} are thereby cutoff-scheme dependent and hence non-universal features of our flow equations.

Let us proceed by discussing the stability properties of the GFP and NGFP in turn. Linearizing the renormalization group flow at the GFP, the stability matrix (5.23) becomes

$$\mathbf{B}_{\text{GFP}} = \begin{bmatrix} d-2 & 0 & 0 \\ (4\pi)^{1-d/2}\big((d^2-3d-2)\Phi^1_{d/2}+4\Upsilon^1_{d/2,1}\big) & -2 & 0 \\ 0 & 0 & -d-2n \end{bmatrix}, \tag{5.46}$$

with corresponding stability coefficients and respective right eigenvectors

$$\begin{aligned} &\theta_1 = 2-d\,, && \tilde{V}^1 = \Big[1\,,\, \tfrac{1}{d}(4\pi)^{1-d/2}\big((d^2-3d-2)\Phi^1_{d/2}+4\Upsilon^1_{d/2,1}\big)\,,\, 0\Big]^{\mathrm{T}}\,, \\ &\theta_2 = 2\,, && \tilde{V}^2 = [\,0\,,\,1\,,0\,]^{\mathrm{T}}\,, \\ &\theta_3 = 2n+d\,, && \tilde{V}^3 = [\,0\,,\,0\,,\,1\,]^{\mathrm{T}}\,. \end{aligned} \tag{5.47}$$

With this information at hand, it is then straightforward to solve the linearized flow equations close to the GFP. The result is here very similar to our findings in the $\ln(R)$-truncation, indicating that G, Λ and μ approach α_i-dependent constants as $k \to 0$. In particular, the IR value of Λ vanishes only if the corresponding integration constant $\alpha_2 = 0$.

Turning to the NGFP, we find that the stability matrix becomes

$$\mathbf{B}_{\mathrm{NGFP}} = \begin{bmatrix} 2-d & 0 & 0 \\ (4\pi)^{1-d/2}\big((d^2-3d-2)\Phi^1_{d/2} + 4\Upsilon^1_{d/2,1}\big) & -d & 0 \\ 0 & 0 & -d-2n \end{bmatrix}, \quad (5.48)$$

with eigensystem

$$\begin{aligned} &\theta_1 = d-2\,, && \tilde{V}^1 = \Big[1\,, \tfrac{1}{d}(4\pi)^{1-d/2}\big((d^2-3d-2)\Phi^1_{d/2} + 4\Upsilon^1_{d/2,1}\big)\,, 0\Big]^{\mathrm{T}}\,, \\ &\theta_2 = d\,, && \tilde{V}^2 = \big[0\,,1\,,0\big]^{\mathrm{T}}\,, \\ &\theta_3 = 2n+d\,, && \tilde{V}^3 = \big[0\,,0\,,1\big]^{\mathrm{T}}\,. \end{aligned} \quad (5.49)$$

Looking at the stability coefficients θ_i, we note that, for $d > 2$, the NGFP is UV attractive along all eigendirections V^i. Solving the linearized flow equation, we then find

$$\begin{aligned} \tilde{G} =& \alpha_1 \frac{k^{2-d}}{M^{2-d}} - \frac{d-2}{H_{n,d}}\,, \\ \tilde{\Lambda} =& \alpha_2 \frac{k^{-d}}{M^{-d}} + \frac{(4\pi)^{1-d/2}}{d^2}\big((d^2-3d-2)\Phi^1_{d/2} + 4\Upsilon^1_{d/2,1}\big)\left(\alpha_1 \frac{k^{2-d}}{M^{2-d}} - \frac{d(d-2)}{H_{n,d}}\right), \\ \tilde{\mu} =& \alpha_4 \frac{k^{-d-2n}}{M^{-d-2n}}\,, \end{aligned} \quad (5.50)$$

where M again denotes a fixed mass scale. This result indicates that the NGFP is indeed a UV attractor for the renormalization group flow, i.e., for $k \to \infty$, all the dimensionless coupling constants $\tilde{G}, \tilde{\Lambda}, \tilde{\mu}$ approach their fixed point values (5.45) independently of the integration constants α_i. One might be tempted to suggest that, for the case of $\mathrm{H}_{n,d} < 0$, for which $\tilde{G}^* > 0, \tilde{\Lambda}^* > 0$ this fixed point is the generalization of the NGFP found in the Einstein-Hilbert truncation. We shall argue to the contrary shortly.

Numerical solutions of the flow equations

After discussing the general fixed point structure of the beta functions (5.42), we now restrict ourselves to $d = 4$ and the optimized cutoff (E.15) and proceed with the numerical investigation of the renormalization group flow. In this case, the

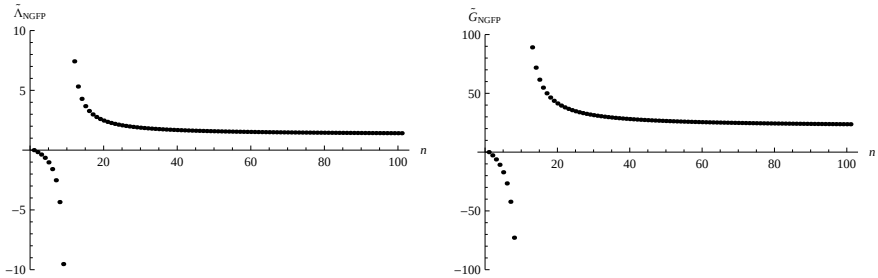

(a) (b)

Figure 5.4: Coordinates of the NGFP on the $\tilde{\mu} = 0$-plane for different values of n, using $d = 4$ and the optimized cutoff. The transition from $\tilde{G}^*_{\rm NGFP} < 0$ to $\tilde{G}^*_{\rm NGFP} > 0$ occurs for $n_{\rm crit} \simeq 9.09$.

fixed points (5.45) are located at

$$\begin{aligned} \text{GFP}: &\quad \{\tilde{G}^* = 0\,,\, \tilde{\Lambda}^* = 0\,,\, \mu^* = 0\}\,, \\ \text{NGFP}: &\quad \{\tilde{G}^* = \tfrac{2}{\mathrm{H}_{n,4}}\,,\, \tilde{\Lambda}^* = \tfrac{3}{8\pi \mathrm{H}_{n,4}}\,,\, \mu^* = 0\}\,, \end{aligned} \tag{5.51}$$

with the function (5.44), which determines the position of the NGFP, given by

$$\mathrm{H}_{n,4} = \frac{-7n^2 + 57n + 60}{24\pi n(n+1)}\,. \tag{5.52}$$

We observe that $\mathrm{H}_{n,4}$ has a zero at positive values $n_{\rm crit} \simeq 9.09$. At this value the NGFP passes from $\tilde{G}_* < 0, \tilde{\Lambda}_* < 0$ at $n < n_{\rm crit}$ to $\tilde{G}_* > 0, \tilde{\Lambda}_* > 0$ for $n > n_{\rm crit}$. This n-dependence of the NGFP is illustrated in Figure 5.4. We will now discuss the renormalization group flow for truncations with $n < n_{\rm crit}$ and $n > n_{\rm crit}$ in turn.

Let us first consider the case $n < n_{\rm crit}$. Choosing $n = 1$, the typical renormalization group flow in the $\mu = 0$-plane is exemplified in Figure 5.5. This diagram nicely illustrates the separation between trajectories with negative and positive $\tilde{G}$. The renormalization group flow on the upper half plane, $\tilde{G} > 0$, is completely dominated by the GFP. In analogy with the previous section, we can again classify the renormalization group trajectories in this region as type Iã or IIIã, according to whether they lie to the left or to the right of the "separatrix", i.e., the renormalization group trajectory of type IIã hitting the GFP as $k \to 0$. We note that the trajectories of all three classes can be continued to the IR, $k \to 0$, where they give rise to a negative, positive or vanishing value of $\tilde{\Lambda}$, respectively. Due to the absence of a UV fixed point, it is unclear, however, whether these trajectories give rise to a well-defined theory in the UV as $k \to \infty$.

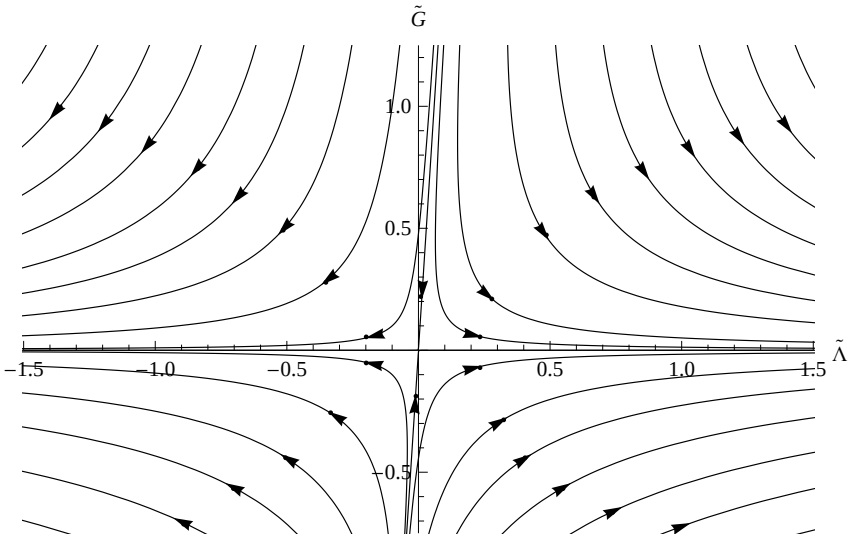

Figure 5.5: Typical renormalization group flow of the R^{-n} truncations for $n < n_{\rm crit}$ on the fixed plane $\tilde{\mu} = 0$, choosing $n = 1$ as an example.

For $n > n_{\rm crit}$ the renormalization group flow in the upper half plane is governed by the interplay of the NGFP and the GFP. Using the example $n = 100$, this is illustrated in Figure 5.6. Here, we see that *all* renormalization group trajectories with $\tilde{G} > 0$ emanate from the NGFP in the UV. We can classify them into type-A and type-B trajectories, depending on whether they run below or above the $\tilde{G}^*_{\rm NGFP}$-plane. According to their behavior in the IR, these trajectories can be further divided into type Ia, IIa and IIIa, depending on whether they give rise to a negative, zero ("separatrix") or positive cosmological constant $\tilde{\Lambda}_0$. A remarkable feature of this phase diagram is that all trajectories with $G > 0$ have a well defined IR limit $k = 0$. Taking into account the μ-independence of the flow, all renormalization group trajectories on the upper half plane are complete, in the sense that they give rise to a well-defined $\bar{\Gamma}_k[g]$ on the entire interval $0 \leq k \leq \infty$.

The typical renormalization group flow of the dimensionful couplings G, Λ along trajectories of type IIIã ($n < n_{\rm crit}$) and type A-IIIa ($n > n_{\rm crit}$) is shown in the diagrams (a) and (b) of Figure 5.7, respectively. In both cases, we find no significant decrease of the cosmological constant as $k \to 0$. Moreover, due to the sign difference in its beta function, we find that G increases towards the IR for $n < n_{\rm crit}$, while it decreases in the converse case. The renormalization group flow of type B trajectories is qualitatively very similar to the one found in the A-region and therefore not shown explicitly.

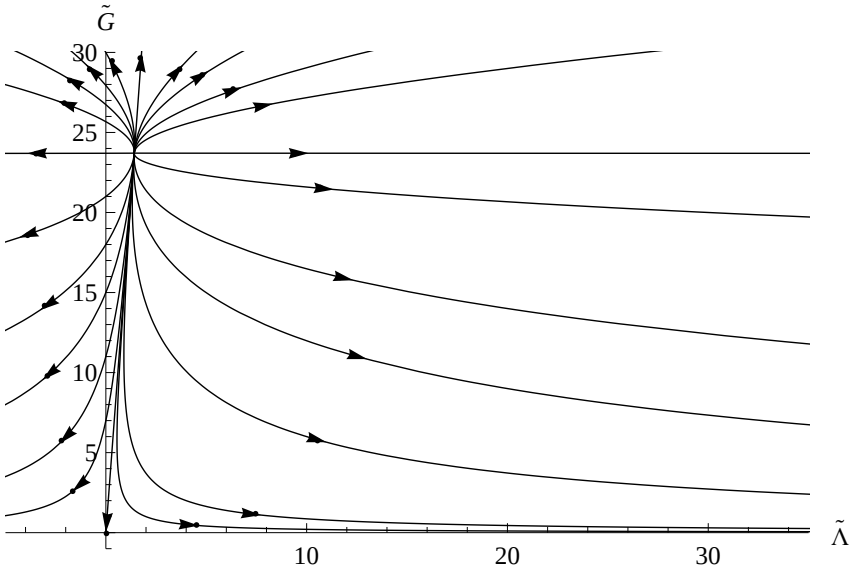

Figure 5.6: Typical renormalization group flow of the R^{-n} truncations with $n > n_{\rm crit}$, illustrated by the choice $n = 100$, in the fixed plane $\tilde{\mu} = 0$. The flow is dominated by the interplay between the NGFP at $\tilde{G}^* > 0, \tilde{\Lambda}^* > 0$ and the GFP at the origin. All renormalization group trajectories are well-defined at all scales $0 \leq k \leq \infty$.

5.3 Constraining the asymptotically safe theory space

In light of our general discussion of the decoupling of non-local $f(R)$ interactions in Section 5.1 and our analysis of the $\ln(R)$ and R^{-n} truncations, which we may take as representative of the class of interactions we have considered, we must now comment on the relation between our results and the asymptotic safety conjecture. Notably, all our truncations give rise to a fixed point which is UV attractive for both Newton's constant and the cosmological constant. However, for some truncations this fixed point is located at negative values of $\tilde{G}$, and we have furthermore seen how the renormalization group flow in all specific cases considered decomposes into two regions, comprising trajectories with $\tilde{G} > 0$ and $\tilde{G} < 0$, respectively. These particular fixed points are thus unphysical and cannot provide a sensible UV limit to trajectories starting with positive values of Newton's constant in the IR.

One might be tempted to suggest that this shift in the NGFP to an unphysical region is an artifact of our truncation, in the sense that more refined truncations could lead to a fixed point at $\tilde{G}^* > 0$. As an example, we have seen that in the R^{-n} truncations a NGFP with positive $\tilde{G}$ does exist for $n > n_{\rm crit}$. This suggestion

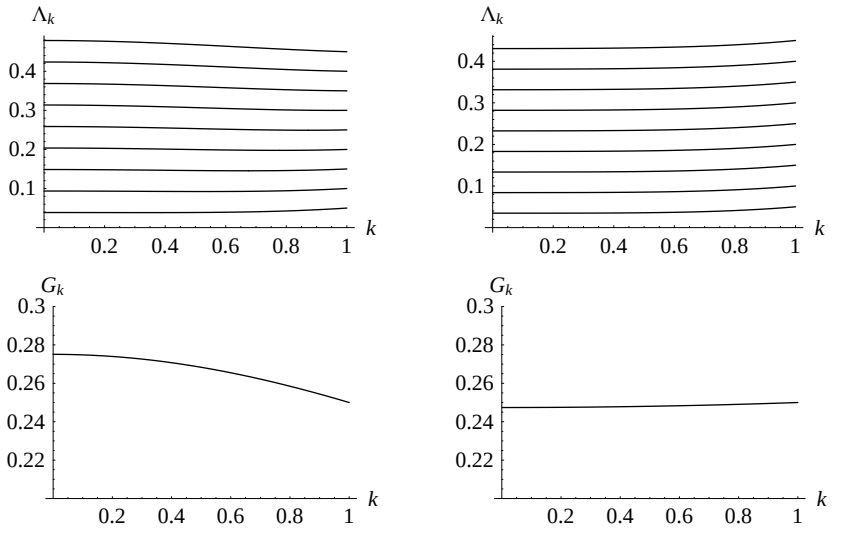

Figure 5.7: Numerical solutions to the flow equations of the R^{-n} truncations for (a) $n < n_{\rm crit}$ and (b) A-type trajectories with $n > n_{\rm crit}$, in terms of the dimensionful couplings. Imposing the initial conditions at $\hat{k} = 1$ we have set $G_{\hat{k}} = 0.25$ with $\Lambda_{\hat{k}}$ taking various values. Due to its decoupling these results are valid for any value $\mu_{\hat{k}}$.

is not tenable for two reasons. First, it is not clear how our truncation could be refined to generate a reasonable candidate NGFP. One can explicitly verify that adding higher-derivative terms such as R^n will not shift the fixed point solutions for $\tilde{G}, \tilde{\Lambda}$. The reason for this is that the coefficients multiplying the operators $\int d^dx\sqrt{g}$ and $\int d^dx\sqrt{g}R$ in the right-hand side of the flow equation, which yield the beta functions of G and Λ, are determined by the contributions of the non-local operators in the series expansion in R. Adding more non-local terms of the type considered here, on the other hand, would not improve the situation either, since this would still only result in unphysical or most likely spurious fixed points.

Secondly, truncations of this type cannot adequately capture the renormalization group of gravity in the UV. This can be seen by comparing the anomalous dimensions of Newton's constant η_G obtained in the $\ln(R)$ and R^{-n} truncation with the one obtained in the Einstein-Hilbert truncation (viz. (5.20) and (5.43) vs. (4.75), respectively). While η_G in the Einstein-Hilbert case receives contributions from arbitrary powers of $\tilde{G}$, the η_G arising in our non-local truncations are ony linear in $\tilde{G}$. Since no refinement of these truncations is likely to improve the situation, for the same reasons as those presented in the previous paragraph, our findings indicate that effective average actions containing non-zero values of

such non-local couplings cannot describe gravitational physics in the high energy regime.

As a consequence, we can constrain the theory space of asymptotically safe effective average actions to a theory space which does not contain such interaction monomials. Since the latter can be consistently decoupled from the renormalization group flow, as we have seen from the triviality or linearity of their corresponding beta functions, this constraint is warranted and well-defined. And indeed, decoupling such contributions, we can explicitly verify the existence of a candidate NGFP in support of the asymptotic safety scenario in higher-derivative $f(R)$, as we have done in the previous chapter.

5.4 Conclusions

In this chapter, we used the functional renormalization group equation for $f(R)$-gravity (4.61) derived in Chapter 4 to study truncations including interaction monomials which are built from non-local curvature terms, such as $\ln(R)$ and R^{-n}. Based on the feature that the operator traces in this flow equation are homogeneous with respect to the function $f_k(R)$, we have deduced on general grounds that such non-local interaction terms can be consistently decoupled from the gravitational renormalization group flow. This implies that, if the couplings multiplying these terms are set to zero at a particular scale, the flow will not generate non-zero values for these couplings dynamically.

Combined with the results of [86, 122] in which non-local $f(V)$ truncations were studied, where V is the spacetime volume, these observations suggest that all gravitational interactions which do not occur in the heat-kernel expansion can be consistently decoupled from the gravitational renormalization group flow. This does not imply, however, that the effective average action Γ_k is local at all scales k. In fact, more complicated non-local interactions built from the curvature scalar and the (inverse) Laplace operator ∇^2, of the type $\int d^dx\sqrt{g}R(\nabla^2)^{-1}R$ or, possibly, $\int d^dx\sqrt{g}R\ln(-\nabla^2)R$, which for instance appear in the late-time expansion of the heat kernel [116, 117], are likely to be dynamically generated. Including such interactions in a truncation ansatz for Γ_k is, however, beyond the scope of the formalism employed in this work. Nevertheless, it would be very interesting to extend the present formalism in such a way as to allow for the inclusion of such terms in the truncation ansatz, both from a phenomenological perspective (see, e.g., [123]), and from a more fundamental point of view, with respect to curing the conformal factor instability [121, 124] or finding a dynamical solution to the cosmological constant problem.

We have investigated in detail the non-perturbative renormalization group flows arising from non-local extensions of the Einstein-Hilbert truncation containing $\int d^dx\sqrt{g}\ln(R)$ ($\ln(R)$ truncation) or $\int d^dx\sqrt{g}R^{-n}$ (R^{-n} truncation) terms in the ansatz for Γ_k. These investigations were motivated by recent attempts to explain the origin of dark matter from a modified theory of gravity which in-

cludes interactions that become dominant as the curvature scalar becomes small. In addition, the flow behavior of these specific examples may be seen as qualitatively representative of the class of non-local truncations considered in this chapter. Including such non-local interactions in the truncation ansatz significantly changes the structure of the non-perturbative beta functions obtained in the Einstein-Hilbert and higher-derivative truncations.

On the one hand, we find that IR singularities of renormalization group trajectories with positive cosmological constant found in the Einstein-Hilbert truncation (and including the "RG-trajectory realized by nature" [88]) are resolved. In addition, in the case of the $\ln(R)$ truncation, we find an infrared fixed point (IRFP) which, for renormalization group trajectories sitting on the plane of vanishing non-local coupling, dynamically drives both Newton's constant and a positive cosmological constant to zero as $k \to 0$, abolishing the need of fine-tuning these couplings at the initial scale. This constitutes a first explicit, non-perturbative example illustrating suggestions that Λ could be dynamically driven to zero through strong quantum gravity renormalization group effects in the infrared.

On the other hand, neither truncation can adequately describe gravitational physics in the UV. This may be seen already at the level of the anomalous dimension η_G of Newton's constant found here, which, unlike in the case of the Einstein-Hilbert or polynomial $f(R)$ truncations, are only linear in $\tilde{G}$, and thus are not expected to encode the contribution of an infinite number of graviton loops. Refining these truncations to include other interaction monomials does not alter this situation. From a renormalization group perspective, truncations of this type thus do not seem to lead to a class of viable UV gravity theories.

Our results therefore pose another warning to modified models of IR gravity, in addition to the other issues that have been raised in the literature in that respect (see, e.g., [125] for a review). Inasmuch as our IR theory of gravity is the low-energy limit of a quantum theory, one should be careful about modifying it. Even if the suggested modifications might satisfy experimental constraints and lead to stable dynamics at the classical level, it will not necessarily lead to a feasible quantum theory in the UV, even at the effective level.

With regard to the asymptotic safety scenario, our findings allow us to constrain the space of asymptotically safe theories to a subspace that does not contain the non-local interaction monomials here considered. Together with the results of the higher-derivative studies [41,69], which have established the existence of a UV non-trivial fixed point of the gravitational flow in polynomial $f(R)$ truncations of up to order eight, the prospects for the asymptotic safety of gravity in the $f(R)$ sector are thus encouraging.

In light of this, there are two natural next steps for exploring asymptotic safety within our non-perturbative framework. The first would be to extend the mapping of the renormalization group behavior of gravity in this sector by considering truncations built from functions of the curvature scalar and the Laplace operator ∇^2, such as the non-local interactions mentioned above. Unfortunately, this class of truncations cannot yet be studied within the FRGE formalism. The second

would be to go beyond the $f(R)$ sector, studying truncations which include invariants built from the other curvature quantities, such as the Riemann tensor. This is what we will proceed to do in the following chapter.

6

The RG flow of higher-derivative gravity

Based on D. Benedetti, P. F. Machado and F. Saueressig, *Taming perturbative divergences in asymptotically safe gravity*, Nucl. Phys. B 824, 168-191 (2010), arXiv:0902.4630 [hep-th]

and

D. Benedetti, P. F. Machado and F. Saueressig, *Asymptotic safety in higher-derivative gravity*, Mod. Phys. Lett. A 24, 2233-2241 (2009), arXiv:0901.2984 [hep-th].

In this chapter, we extend previous FRGE computations by including a Weyl-squared term in the ansatz for the effective action, thus taking us beyond truncations in the $f(R)$ sector. We start by considering the pure gravity beta function in this higher-derivative setting, computing the corresponding beta functions and deriving the fixed point structure, and comment on the relation of our results to perturbative computations in the literature. We then add a minimally coupled scalar field to our truncation, noting that this setup provides the prototype of a gravitational theory which is perturbatively non-renormalizable at one-loop level, and study the resulting renormalization group flow. We will work with $d = 4$.

6.1 Four-derivative truncations in pure gravity

As we have seen in the course of this thesis, the non-perturbative renormalization group behavior of gravity has been intensively investigated by use of the functional renormalization group equation formalism within the truncation approximation [35]. These studies have gathered substantial evidence for the asymptotic safety scenario [35–41, 107]. A non-Gaussian fixed point with strikingly stable characteristic features and in agreement with this scenario has been found in the pure gravity case from the original Einstein-Hilbert truncation [35] to truncations including terms with up to the eighth power of the Ricci scalar [41]. Furthermore,

this fixed point has also been found to persist in Einstein-Hilbert truncation studies of matter-coupled gravity [41, 82, 83, 108, 126].

The main caveat of these $f(R)$-type truncations, however, is that they neglect the contribution of interaction terms built from the other curvature operators and omit the four-derivative propagator for the helicity-two states, which could, in principle, have a major impact on the asymptotic safety scenario. An a priori argument suggesting the importance of these terms is that they feature as non-renormalizable counterterms in the perturbative quantization of General Relativity [15–20,127]. In this chapter, we move towards closing this gap by explicitly including such four-derivative terms in our truncation subspace.

6.1.1 The truncation ansatz

We begin by specifying the class of truncated effective average actions to be studied. In keeping with our discussion in Section 2.2.2, our starting point is the ansatz

$$\Gamma_k[g,\bar{g}] = \bar{\Gamma}_k[g] + S^{\rm gf}[g,\bar{g}] + S^{\rm gh}[g,\bar{g},\text{ghosts}] + S^{\rm aux}, \tag{6.1}$$

which restricts the ghost $S^{\rm gh}[g,\bar{g},\text{ghosts}]$ and gauge $S^{\rm gf}$ actions to the classical ones, and where $S^{\rm aux}$ collects the contribution of auxiliary fields introduced to exponentiate the Jacobi determinants arising from eventual field decompositions. For the gravitational part of the effective average action, $\bar{\Gamma}_k$, we will now include all interaction terms up to fourth order in the derivative expansion,

$$\bar{\Gamma}_k[g] = \Gamma_k^{\rm grav}[g] \equiv \int d^4x\sqrt{g}\left[\frac{1}{16\pi G}(-R+2\Lambda) - \frac{\omega}{3\sigma}R^2 + \frac{1}{2\sigma}C^2 + \frac{\theta}{\sigma}E\right], \tag{6.2}$$

where $C^2 \equiv C_{\mu\nu\rho\sigma}C^{\mu\nu\rho\sigma}$ is the square of the Weyl tensor, $E = R_{\mu\nu\rho\sigma}R^{\mu\nu\rho\sigma} - 4R_{\mu\nu}R^{\mu\nu} + R^2$ is the integrand of the Gauss-Bonnet topological invariant, and where we have neglected a surface term.

Capturing the C^2 interaction

Before discussing the other terms in (6.1), we will first comment on the key implementation that will allow us to study the renormalization group flow of gravity in our higher-derivative truncation. When extracting the beta functions of the gravitational couplings by means of the FRGE, the main step is the evaluation of the functional traces appearing in the right-hand side of that equation. The main limitation to extracting the beta functions in any given truncation is precisely our ability to evaluate these traces. In this respect, we may employ to our advantage the freedom ensured by the background field formalism and choose a class of background metrics that simplifies this evaluation when we set $g = \bar{g}$ by, e.g., making the resulting operator expressions amenable to current heat-kernel techniques. This class should be general enough to distinguish the interaction monomials contained in $\Gamma_k^{\rm grav}$ and, most importantly, simple enough to allow for

the evaluation of the traces. In the $f(R)$ truncations previously studied, the backgrounds chosen were the maximally symmetric spaces S^4, which are insufficient in the former respect for the evaluation of (6.1). Instead, we will consider here the class of generic compact Einstein backgrounds $\mathcal{E}$ satisfying

$$\bar{R}_{\mu\nu} = \tfrac{\bar{R}}{4}\,\bar{g}_{\mu\nu}\,. \tag{6.3}$$

Utilizing these backgrounds, all differential operators within our particular traces organize themselves into Lichnerowicz form

$$\begin{aligned}
&\Delta_{2L}\phi_{\mu\nu} \equiv -\nabla^2\phi_{\mu\nu} - 2R_{\mu\ \nu}^{\ \alpha\ \beta}\phi_{\alpha\beta}\,,\\
&\Delta_{1L}\phi_{\mu} \equiv \left[-\nabla^2 - \tfrac{1}{4}R\right]\,\phi_{\mu}\,,\\
&\Delta_{0L}\phi \equiv -\nabla^2\phi\,,
\end{aligned} \tag{6.4}$$

i.e., minimal second-order differential operators $\Delta_{sL} = -\nabla^2 + \mathbf{Q}_s$, with spin-dependent matrix potentials $\mathbf{Q}_s$ acting on transverse-traceless matrices ($s = 2$), transverse vectors ($s = 1$) and scalars ($s = 0$). Following a type II cutoff scheme procedure (viz. Section 2.3), we can choose to impose the cutoff $\mathcal{R}_k$ on the spectra of these operators. This feature is crucial for the non-perturbative evaluation of the traces, as it makes them amenable to standard heat kernel techniques without having to resort to non-minimal (or k-dependent) differential operators. The generalization of the background metrics from maximally symmetric to Einstein thus provides the crucial ingredient for investigating the non-perturbative features of the gravitational RG flow including higher-derivative tensorial operators. We should note, however, that these backgrounds allow us to distinguish only two of the three higher-derivative couplings, and hence determine the non-perturbative β-functions only of the linear combinations

$$g_{4a} \equiv -\frac{\omega_k}{3\sigma_k} + \frac{\theta_k}{6\sigma_k}\,, \quad g_{4b} \equiv \frac{1}{2\sigma_k} + \frac{\theta_k}{\sigma_k}\,. \tag{6.5}$$

Distinguishing also the third four-derivative coupling would require abandoning the Einstein condition in our background metrics, which remains beyond current trace evaluation techniques. In any case, finding a non-Gaussian fixed point for the linear combinations (6.5) implies that, barring miraculous cancellations, none of the couplings ω, θ go to infinity, and λ and either ω or θ must be non-zero.

Gauge-fixing and ghost terms

Let us now return to the other terms in (6.1). The gauge-fixing term is of the form

$$S_{\rm gf} = \tfrac{1}{2}\int d^4x\sqrt{\bar{g}}F_\mu Y^{\mu\nu}F_\nu\,, \tag{6.6}$$

with

$$F_\mu = \bar{\nabla}^\nu h_{\mu\nu} - \frac{1+\rho}{4}\bar{\nabla}_\mu h\,, \quad Y^{\mu\nu} = \left[\alpha + \beta\bar{\nabla}^2\right]\bar{g}^{\mu\nu}\,. \tag{6.7}$$

Setting $\beta = 0$ in this equation, we recover the gauge-fixing term that was used in Chapters 4 and 5. The de Donder gauge corresponds to setting $\rho = 1$, while the geometric gauge corresponds to $\rho = 0$. In the presence of four-derivative operators, however, it is natural to consider a gauge-fixing term which also contains four derivatives. Thus, in the present case, we take $\alpha = 0$ and keep the term proportional to β in (6.7). We will also set $\rho = 0$, analogous to the $f(R)$ case.

As we have previously discussed, in principle also the gauge fixing parameter β should be treated as running, i.e., $\beta = \beta(k)$. However, it may be generally argued [37, 128] that β has an RG fixed point at $1/\beta^* = 0$, which implies that, if we set $1/\beta(\hat{k}) = 0$ for some scale $\hat{k}$, this condition will remain so for all scales $\hat{k} \leq k$. Thus, we will here set $\beta \to \infty$ and implement the gauge-fixing as a delta function, rather than a Gaussian. Not only does this allow us to sidestep the running of the gauge-fixing term, it will also lead to considerable simplifications in our subsequent calculations.

In the sequel, we will employ a transverse-traceless (TT) decomposition of the metric fluctuations and ghosts, via

$$h_{\mu\nu} = h^{\mathrm{T}}_{\mu\nu} + \bar{\nabla}_\mu \xi_\nu + \bar{\nabla}_\nu \xi_\mu + \bar{\nabla}_\mu \bar{\nabla}_\nu \sigma - \frac{1}{d} \bar{g}_{\mu\nu} \bar{\nabla}^2 \sigma + \frac{1}{d} \bar{g}_{\mu\nu} h \,, \tag{6.8}$$

and

$$A_\mu = A^{\mathrm{T}}_\mu + \bar{\nabla}_\mu \alpha \,, \tag{6.9}$$

where A_μ stands for the ghost fields.

With our choice for ρ, the TT-decomposition of S^{gf} yields

$$S^{\mathrm{gf}} = -\frac{\beta}{2} \int d^4x \sqrt{\bar{g}} \left\{ \xi_\mu \big[(\Delta_{1L} + \tfrac{\bar{R}}{4}) \Delta_{1L}^2 \big] \xi^\mu + \sigma \big[(\tfrac{3}{4}\Delta_{0L} - \tfrac{\bar{R}}{4})^2 (\Delta_{0L} - \tfrac{\bar{R}}{4}) \Delta_{0L} \big] \sigma \right\} \tag{6.10}$$

The ghost sector now contains, in addition to the usual (complex) $\bar{C}, C$-ghost fields, a third ghost [129] due to the two-derivative contribution $(\det \beta \nabla^2)^{1/2}$. Introducing the complex-valued Grassmann fields $\bar{B}_\mu$, B^μ and the real field b_μ for the latter term, and TT-decomposing the ghost sector of the resulting action leads to

$$\begin{aligned} S^{\mathrm{quad}}_{\mathrm{C-ghost}} &= -\int d^4x \sqrt{\bar{g}} \Big\{ \bar{C}^{\mathrm{T}}_\mu \Delta_{1L} C^{\mathrm{T}\mu} + \tfrac{1}{2} \bar{\eta} \big[3\Delta_{0L} - \bar{R} \big] \Delta_{0L} \eta \Big\} \,, \\ S^{\mathrm{quad}}_{\mathrm{B-ghost}} &= -\int d^4x \sqrt{\bar{g}} \Big\{ \bar{B}^{\mathrm{T}}_\mu \big[\Delta_{1L} + \tfrac{\bar{R}}{4} \big] B^{\mathrm{T}\mu} + \bar{B} \left[\Delta_{0L} - \tfrac{\bar{R}}{4} \right] \Delta_{0L} \, B \\ &\qquad + \tfrac{1}{2} b^{\mathrm{T}}_\mu \big[\Delta_{1L} + \tfrac{\bar{R}}{4} \big] b^{\mathrm{T}\mu} + \tfrac{1}{2} b \left[\Delta_{0L} - \tfrac{\bar{R}}{4} \right] \Delta_{0L} \, b \Big\} \,. \end{aligned} \tag{6.11}$$

Note that, in the literature on higher-derivative gravity, the contribution of the $\bar{B}, B$-ghost field is usually absorbed into the usual $\bar{C}, C$-ghost, hence the need of only a third (real) ghost. We prefer here to introduce a fourth ghost to clearly separate the higher-derivative contribution from the usual second-order term. The two choices are of course equivalent.

The auxiliary fields

Finally, there are additional contributions to the flow equation arising from the Jacobi determinants introduced via the TT-decomposition,

$$\begin{aligned} J_{\text{grav}} &= \Big(\det{}'_{(1\text{T},0)} \Big[M^{(\mu,\nu)} \Big] \Big)^{1/2} , \\ J_{\text{C}-\text{gh}} &= J_{\text{B}-\text{gh}} = \big(\det{}'[\Delta_{0L}] \big)^{-1} , \\ J_{\text{b}-\text{gh}} &= \big(\det{}'[\Delta_{0L}] \big)^{1/2} . \end{aligned}$$

Here, the primes indicate that the unphysical modes are left out from the determinants. We will return to those shortly. $M^{(\mu,\nu)}$ is a $(d+1) \times (d+1)$-matrix differential operator whose first d columns act on the transverse spin one fields ξ_μ and whose last column acts on the spin zero fields σ and which reads

$$M^{(\mu,\nu)} = \begin{bmatrix} 2\, g^{\mu\nu} \Delta_{1L} & -\frac{R}{2} D^\mu \\ \frac{R}{2} D^\nu & \frac{3}{4} \Delta_{0L}^2 - \frac{R}{4} \Delta_{0L} \end{bmatrix} . \tag{6.12}$$

In order to account for these contributions, we follow [41,69] and introduce appropriate auxiliary fields so as to exponentiate these determinants via the Faddeev-Popov trick. The resulting "auxiliary action" then becomes

$$\begin{aligned} S^{\text{aux}} = \int d^4x \, \sqrt{g} \, \Big\{ & [\zeta_\mu^{\text{T}}, \omega] \big[M^{(\mu,\nu)} \big]' [\zeta_\nu^{\text{T}}, \omega]^{\text{T}} + [\bar{c}_\mu^{\text{T}}, \bar{c}] \big[M^{(\mu,\nu)} \big]' [c_\nu^{\text{T}}, c]^{\text{T}} \\ & + \bar{s} \, \Delta'_{0L} \, s + \bar{t} \, \Delta'_{0L} \, t + \bar{\chi} \, \Delta'_{0L} \, \chi + \tfrac{1}{2} \phi \, \Delta'_{0L} \, \phi \Big\} . \end{aligned} \tag{6.13}$$

Here, the gravitational sector contains the transverse ghost $\bar{c}_\mu^{\text{T}}, c^{\text{T}\mu}$, a "longitudinal" Grassmann scalar $\bar{c}, c$, a transverse vector ζ_μ^{T} and a real scalar ω, while the ghost determinants are captured by the contribution of the complex scalar fields s, $\bar{s}$, t, $\bar{t}$, the complex Grassmann fields $\bar{\chi}$, χ, and the real scalar field ϕ.

Now, under the TT-decomposition of the metric and ghost fields, we must ensure that the unphysical modes are excluded from the spectrum of the component fields. In the following, we impose a "mode by mode" cancellation between the gauge-degrees of freedom in the metric and the ghost sector [69], as was done in Chapter 4, which results in a precise cancellation of all the unphysical mode contributions from the traces in the flow equation. For a generic Einstein space these modes are the lowest Δ_{1L}-eigenmode of the transverse vector ξ_μ, corresponding to the n_{KV} Killing vectors, and the lowest Δ_{0L} mode of the scalar σ. Accordingly, the lowest mode of the transverse ghost fields $\bar{C}_\mu^{\text{T}}$, C_μ^{T} and of the scalar ghosts $\{\bar{\eta}, \eta, \bar{B}, B, b\}$ are also excluded. Lastly, from the auxiliary fields we must remove the contributions from the lowest mode of the vectors $\{\bar{c}_\mu^{\text{T}}, c^{\text{T}\mu}, \zeta_\mu^{\text{T}}\}$ and the scalars $\{\bar{c}, c, \omega, \bar{t}, t, \bar{s}, s, \bar{\chi}, \chi, \phi\}$.

In the particular case of an S^4 background, we must additionally exclude the second-lowest eigenmodes of the $\{\sigma, \bar{\eta}, \eta, \bar{c}, c, \omega\}$ fields, corresponding to the

$n_{\mathrm{CKV}} = 5$ conformal Killing vectors. In the sequel, however, we will for convenience take our Einstein space to have $n_{\mathrm{KV}} = n_{\mathrm{CKV}} = 0$. We have verified that adding the contribution from these single modes does not alter our numerical results at any relevant level.

6.1.2 Constructing the flow equation

Taking into account all the field contributions above, the flow equation schematically reads

$$
\begin{aligned}
\partial_t\Gamma_k =& \tfrac{1}{2}\mathrm{Tr}_{2T}\frac{\partial_t\mathcal{R}_{h^Th^T}}{\Gamma^{(2)}_{h^Th^T}+\mathcal{R}_{h^Th^T}} + \tfrac{1}{2}\mathrm{Tr}_{1T}\frac{\partial_t\mathcal{R}_{\xi\xi}}{\Gamma^{(2)}_{\xi\xi}+\mathcal{R}_{\xi\xi}} \\
&+ \tfrac{1}{2}\mathrm{Tr}_0\begin{pmatrix}\Gamma^{(2)}_{hh}+\mathcal{R}_{hh} & \Gamma^{(2)}_{h\sigma}+\mathcal{R}_{h\sigma}\\ \Gamma^{(2)}_{\sigma h}+\mathcal{R}_{\sigma h} & \Gamma^{(2)}_{\sigma\sigma}+\mathcal{R}_{\sigma\sigma}\end{pmatrix}^{-1}\begin{pmatrix}\partial_t\mathcal{R}_{hh} & \partial_t\mathcal{R}_{h\sigma}\\ \partial_t\mathcal{R}_{\sigma h} & \partial_t\mathcal{R}_{\sigma\sigma}\end{pmatrix} \\
&+ \tfrac{1}{2}\sum_{j=0,1}\frac{\partial_t\mathcal{R}_{hh}(\lambda_j)}{\Gamma^{(2)}_{hh}(\lambda_j)+\mathcal{R}_{hh}(\lambda_j)} \\
&- \mathrm{Tr}_{1T}\frac{\partial_t\mathcal{R}_{\bar{C}^TC^T}}{\Gamma^{(2)}_{\bar{C}^TC^T}+\mathcal{R}_{\bar{C}^TC^T}} - \mathrm{Tr}_0\frac{\partial_t\mathcal{R}_{\bar{\eta}\eta}}{\Gamma^{(2)}_{\bar{\eta}\eta}+\mathcal{R}_{\bar{\eta}\eta}} \\
&- \mathrm{Tr}_{1T}\frac{\partial_t\mathcal{R}_{\bar{B}^TB^T}}{\Gamma^{(2)}_{\bar{B}^TB^T}+\mathcal{R}_{\bar{B}^TB^T}} - \mathrm{Tr}_0\frac{\partial_t\mathcal{R}_{\bar{B}B}}{\Gamma^{(2)}_{\bar{B}B}+\mathcal{R}_{\bar{B}B}} \\
&+ \tfrac{1}{2}\mathrm{Tr}_{1T}\frac{\partial_t\mathcal{R}_{b^Tb^T}}{\Gamma^{(2)}_{b^Tb^T}+\mathcal{R}_{b^Tb^T}} + \tfrac{1}{2}\mathrm{Tr}_0\frac{\partial_t\mathcal{R}_{bb}}{\Gamma^{(2)}_{bb}+\mathcal{R}_{bb}} \\
&+ \tfrac{1}{2}\mathrm{Tr}_{1T}\frac{\partial_t\mathcal{R}_{\zeta^T\zeta^T}}{\Gamma^{(2)}_{\zeta^T\zeta^T}+\mathcal{R}_{\zeta^T\zeta^T}} + \tfrac{1}{2}\mathrm{Tr}_0\frac{\partial_t\mathcal{R}_{\omega\omega}}{\Gamma^{(2)}_{\omega\omega}+\mathcal{R}_{\omega\omega}} \\
&- \mathrm{Tr}_{1T}\frac{\partial_t\mathcal{R}_{\bar{c}^Tc^T}}{\Gamma^{(2)}_{\bar{c}^Tc^T}+\mathcal{R}_{\bar{c}^Tc^T}} - \mathrm{Tr}_0\frac{\partial_t\mathcal{R}_{\bar{c}c}}{\Gamma^{(2)}_{\bar{c}c}+\mathcal{R}_{\bar{c}c}} \\
&+ \mathrm{Tr}_0\frac{\partial_t\mathcal{R}_{\bar{s}s}}{\Gamma^{(2)}_{\bar{s}s}+\mathcal{R}_{\bar{s}s}} + \mathrm{Tr}_0\frac{\partial_t\mathcal{R}_{\bar{t}t}}{\Gamma^{(2)}_{\bar{t}t}+\mathcal{R}_{\bar{t}t}} \\
&- \mathrm{Tr}_0\frac{\partial_t\mathcal{R}_{\bar{\chi}\chi}}{\Gamma^{(2)}_{\bar{\chi}\chi}+\mathcal{R}_{\bar{\chi}\chi}} + \tfrac{1}{2}\mathrm{Tr}_0\frac{\partial_t\mathcal{R}_{\phi\phi}}{\Gamma^{(2)}_{\phi\phi}+\mathcal{R}_{\phi\phi}}\,,
\end{aligned}
\tag{6.14}
$$

where the subscripts "2T", "1T" and "0" respectively indicate traces taken on the space of symmetric transverse-traceless matrices, transverse vectors and scalars and where $t \equiv \ln(k)$. The next steps in the derivation of this equation are the computation of the Hessians $\Gamma^{(2)}_{\mathbf{\Phi\Phi}}$ and the construction of the cutoff operators $\mathcal{R}_{\mathbf{\Phi\Phi}}$. To this effect, it is useful to note that, in the limit $\beta \to \infty$, the contributions to the second variation of $\xi\xi$ and $\sigma\sigma$ are dominated by the gauge fixing term and the σ-h cross term vanishes. Thus, the combined contribution from σ and h splits

into the sum of the hh-trace and the contribution of the $\sigma\sigma$-part, and we need only take into account the second variations coming from $S_{\rm gf}$ for the ξ and σ terms.

Computing the Hessians

We now compute the Hessians arising from our ansatz (6.1) with (6.2). Since the gauge fixing, ghost and auxiliary fields are already quadratic in the fields, we can just read off their contributions from the expressions above. For the gravitational sector, we first organize $\Gamma_k^{\rm grav}$ into the five interaction monomials

$$\begin{aligned} I_0 &= \int \mathrm{d}^4x\sqrt{g}\,, \qquad I_1 = \int \mathrm{d}^4x\sqrt{g}R\,, \\ I_2 &= \int \mathrm{d}^4x\sqrt{g}R^2\,, \quad I_3 = \int \mathrm{d}^4x\sqrt{g}R_{\mu\nu}R^{\mu\nu}\,, \quad I_4 = \int d^4x\sqrt{g}E, \end{aligned} \tag{6.15}$$

noting that we can reexpress $R_{\mu\nu\rho\sigma}R^{\mu\nu\rho\sigma}$ in terms of $R_{\mu\nu}R^{\mu\nu}$, R^2 and E by means of the four-dimensional topological invariant $\int d^4x\sqrt{g}E = 32\pi^2\chi$, where χ is the Euler character. Computing the second variation of these invariants and referring to Appendix B for the intermediate formulas, we arrive at

$$\begin{aligned} \delta^2 I_0 &= \int_{\mathcal{E}} d^4x\sqrt{\bar g}\,\{\tfrac{1}{8}h^2 - \tfrac{1}{2}h^{\mathrm{T}\mu\nu}h^{\mathrm{T}}_{\mu\nu} - \xi^\mu\Delta_{1L}\xi_\mu - \tfrac{1}{8}\sigma\left[3\Delta_{0L} - \bar R\right]\Delta_{0L}\sigma\} \\ \delta^2 I_1 &= \int_{\mathcal{E}} d^4x\sqrt{\bar g}\Big\{\tfrac{3}{16}h\Delta_{0L}h - \tfrac{1}{2}h^{\mathrm{T}\,\mu\nu}\Big[\Delta_{2L} + \tfrac{1}{2}\bar R\Big]h^{\mathrm{T}}_{\mu\nu} - \tfrac{1}{2}\bar R\,\xi^\nu\Delta_{1L}\,\xi_\nu \\ &\qquad + \tfrac{1}{8}h\big[3\Delta_{0L} - \bar R\big]\Delta_{0L}\sigma + \tfrac{1}{16}\sigma\big[\Delta_{0L} - \bar R\big]\big[3\Delta_{0L} - \bar R\big]\Delta_{0L}\sigma\Big\}, \end{aligned} \tag{6.16}$$

while the variations of the four-derivative terms yield

$$\begin{aligned} \delta^2 I_2 = \int_{\mathcal{E}} d^4x\sqrt{\bar g}\Big\{ &\tfrac{3}{8}\,h\left[3\Delta_{0L} - \bar R\right]\Delta_{0L}\,h - \bar R\,h^{\alpha\beta\mathrm{T}}\,\Delta_{2L}\,h^{\mathrm{T}}_{\alpha\beta} \\ &+ \tfrac{3}{8}\sigma\,\left[3\Delta_{0L} - \bar R\right]\Delta^3_{0L}\,\sigma + \tfrac{3}{4}h\left[3\Delta_{0L} - \bar R\right]\Delta^2_{0L}\,\sigma\Big\}, \end{aligned} \tag{6.17}$$

and

$$\begin{aligned} \delta^2 I_3 = \int_{\mathcal{E}} d^4x\sqrt{\bar g}\Big\{ &\tfrac{1}{2}\,h^{\mathrm{T}\alpha\beta}\left[\Delta_{2L} - \tfrac{1}{2}\bar R\right]\Delta_{2L}\,h^{\mathrm{T}}_{\alpha\beta} + \tfrac{1}{8}h\left[3\Delta_{0L} - \bar R\right]\Delta_{0L}h \\ &+ \tfrac{1}{8}\sigma\left[3\Delta_{0L} - \bar R\right]\Delta^3_{0L}\sigma + \tfrac{1}{4}h\left[3\Delta_{0L} - \bar R\right]\Delta^2_{0L}\sigma\Big\}. \end{aligned} \tag{6.18}$$

Reinstating the corresponding coupling constants and combining these contributions with those coming from the gauge-fixing sector, we arrive at the final expressions for the Hessians of the metric fluctuation components. These are collected in Table 6.1, together with the expressions for the ghost and auxiliary field sectors. Here and in the sequel, we have defined for convenience

$$g_0 \equiv \frac{\Lambda_k}{8\pi G_k}, \quad g_2 \equiv -\frac{1}{16\pi G_k}, \tag{6.19}$$

while the four-derivative couplings g_{4a}, g_{4b} are given by (6.5).

Index	Hessian $\Gamma_k^{(2)}$
$h^{\mathrm{T}}h^{\mathrm{T}}$	$2g_{4b}\Delta_{2L}^2 - [2g_{4a}R - \frac{1}{3}g_{4b}R + g_2]\Delta_{2L} - \frac{1}{2}g_2R - g_0$
$\xi_\mu\xi^\mu$	$-\beta[\Delta_{1L} + \frac{R}{4}]\Delta_{1L}^2 - [g_2R + 2g_0]\Delta_{1L}$
hh	$\frac{1}{8}\big[18g_{4a}\Delta_{0L}^2 + 3(g_2 - 2g_{4a}R)\Delta_{0L} + 2g_0\big]$
$\sigma\sigma$	$-\frac{\beta}{16}\big[3\Delta_{0L} - R\big]^2\big[\Delta_{0L} - \frac{R}{4}\big]\Delta_{0L}$ $+\frac{1}{8}\big[6g_{4a}\Delta_{0L}^2 + g_2\Delta_{0L} - g_2R - 2g_0\big]\big[3\Delta_{0L} - R\big]\Delta_{0L}$
$h\sigma$	$\frac{1}{8}\big[g_2 + 6\,g_{4a}\,\Delta_{0L}\big]\big[3\Delta_{0L} - R\big]\Delta_{0L}$
$C_\mu^{\mathrm{T}}C^{\mathrm{T}\mu}$	Δ_{1L}
$\bar\eta\eta$	$\frac{1}{8}[3\Delta_{0L} - R]\Delta_{0L}$
$\bar B_\mu^T B^{T\mu}$	$-[\Delta_{1L} + \frac{R}{4}]$
$\bar B B$	$-[\Delta_{0L} - \frac{R}{4}]\Delta_{0L}$
$b_\mu^T b^{T\mu}$	$-[\Delta_{1L} + \frac{R}{4}]$
bb	$-[\Delta_{0L} - \frac{R}{4}]\Delta_{0L}$
$\zeta_\mu^T\zeta^{T\mu}$	$4\Delta_{1L}$
$\omega\omega$	$\frac{1}{2}[3\Delta_{0L} - R]\Delta_{0L}$
$\bar c_\mu^{\mathrm{T}}c^{\mathrm{T}\mu}$	$2\Delta_{1L}$
$\bar c c$	$\frac{1}{4}[3\Delta_{0L} - R]\Delta_{0L}$
$\bar s s$	Δ_{0L}
$\phi\phi$	Δ_{0L}

Table 6.1: Matrix entries of the operator $\Gamma_k^{(2)}$ in the gravitational, ghost and auxiliary sector (separated by the horizontal lines), respectively. The elements are symmetric under the change of bosonic indices, while they acquire a minus sign when Grassmann-valued indices are swapped.

Adapting the cutoff operators

We now construct the cutoff operators, using the general prescription

$$\Delta_{nL} \to P_{n,k} = \Delta_{nL} + R_k(\Delta_{nL})\,. \tag{6.20}$$

As a result, the Lichnerowicz Laplacian operators in the Hessian are replaced by

$$[\Gamma_k^{(2)}(P_{n,k})]_{\phi_1\phi_2} = [\Gamma_k^{(2)}(\Delta_{nL}) + \mathcal{R}_k(\Delta_{nL})]_{\phi_1\phi_2} \tag{6.21}$$

where $[\mathcal{R}_k]_{\phi_1\phi_2}$ is a function of Δ_{nL} and R_k. Following this prescription for each of the fields in (6.14), we arrive at the expressions for $\mathcal{R}_{\mathbf{\Phi\Phi}}$, which are collected in Table 6.2.

Index	Adapted cutoff operator $\mathcal{R}_k$
$h^{\mathrm{T}}h^{\mathrm{T}}$	$\left[(4\Delta_{2L}+2R_k)g_{4b}-(2g_{4a}-\frac{g_{4b}}{3})R-g_2\right]R_k$
$\xi_\mu\xi^\mu$	$\left[-\beta(3\Delta_{1L}^2+(3R_k+\frac{1}{2}R)\Delta_{1L}+R_k^2+\frac{1}{4}RR_k)-Rg_2-2g_0\right]R_k$
hh	$\frac{3}{8}\left[(12\Delta_{0L}+6R_k-2R)g_{4a}+g_2\right]R_k$
$\sigma\sigma$	$\frac{\beta}{16}\left[(3\Delta_{0L}-R)^2(\Delta_{0L}-\frac{1}{4}R)\Delta_{0L}\right.$ $\left.-(3\Delta_{0L}+3R_k-R)^2(\Delta_{0L}+R_k)(\Delta_{0L}+R_k-\frac{1}{4}R)\right]$
$\bar{C}_\mu^{\mathrm{T}}C^{\mathrm{T}\mu}$	R_k
$\bar{\eta}\eta$	$\frac{1}{8}[6\Delta_{0L}+3R_k-R]R_k$
$\bar{B}_\mu^T B^{T\mu}$	$-R_k$
$\bar{B}B$	$-\frac{1}{4}[8\Delta_{0L}+4R_k-R]R_k$
$b_\mu^T b^{T\mu}$	$-R_k$
bb	$-\frac{1}{4}[8\Delta_{0L}+4R_k-R]R_k$
$\zeta_\mu^T\zeta^{T\mu}$	$4R_k$
$\omega\omega$	$\frac{1}{2}[6\Delta_{0L}+3R_k-R]R_k$
$\bar{c}_\mu^{\mathrm{T}}c^{\mathrm{T}\mu}$	$2R_k$
$\bar{c}c$	$\frac{1}{4}[6\Delta_{0L}+3R_k-R]R_k$
$\bar{s}s$	R_k
$\phi\phi$	R_k

Table 6.2: Matrix entries of the operator $\mathcal{R}_k^{(2)}$in the gravitational, ghost, and auxiliary sector, respectively. Here, only the leading-order contributions in the limit $\beta\to\infty$ are considered. As in Table 6.1, the elements are symmetric under the change of bosonic indices, while they acquire a minus sign when Grassmann-valued indices are swapped.

6.1.3 Evaluating the traces

Using the results in Tables 6.1 and 6.2, we can combine the operator traces appearing in the right-hand side of (6.14) to yield

$$k\partial_k\Gamma_k[g,\bar{g}]=\mathcal{S}_{2\mathrm{T}}+\mathcal{S}_{\mathrm{hh}}+\mathcal{S}_{1\mathrm{T}}+\mathcal{S}_0. \tag{6.22}$$

The first two terms in this expression represent the contributions from the $h^{\mathrm{T}}h^{\mathrm{T}}$ and hh sectors respectively, and read

$$\mathcal{S}_{2\mathrm{T}}=\frac{1}{2}\mathrm{Tr}_{2\mathrm{T}}\left[\frac{\partial_t\left\{2g_{4b}(P_{2,k}^2-\Delta_{2L}^2)-(g_2+g_{\flat}R)R_{2,k}\right\}}{2g_{4b}P_{2,k}^2-(g_2+g_{\flat}R)P_{2,k}-\frac{1}{2}g_2R-g_0}\right],$$

$$\mathcal{S}_{hh} = \frac{1}{2}\mathrm{Tr}_0\left[\frac{\partial_t\left\{6g_{4a}(P_{0,k}^2-\Delta_{0L}^2)+(g_2-2g_{4a}R)R_{0,k}\right\}}{6g_{4a}P_{0,k}^2+(g_2-2g_{4a}R)P_{0,k}+\frac{2}{3}g_0}\right], \tag{6.23}$$

where we have defined $g_\flat \equiv 2g_{4a} - \frac{1}{3}g_{4b}$.

The last two terms represent the combined contributions of the transverse vectors and of all the other scalar fields, respectively, giving rise to

$$\mathcal{S}_{1\mathrm{T}} = -\frac{1}{2}\mathrm{Tr}_{1\mathrm{T}}\left[\frac{\partial_t R_{1,k}}{P_{1,k}}\right], \tag{6.24}$$

and

$$\mathcal{S}_0 = -\frac{3}{2}\mathrm{Tr}_0\left[\frac{\partial_t R_{0,k}}{3P_{0,k}-R}\right]. \tag{6.25}$$

Note that, owing to the special gauge choice (6.10) with $\rho = 0$ and to the $\beta \to \infty$ limit, $\mathcal{S}_{1\mathrm{T}}$ and $\mathcal{S}_0$ are again independent of Γ_k^{grav} and take a particularly simple form.

We can now proceed with the evaluation of the right-hand side of the flow equation (6.56). To this effect, it is convenient to introduce the dimensionless counterparts of the couplings g_{2i},

$$\tilde{g}_0 = g_0 k^{-4}\,, \quad \tilde{g}_2 = g_2 k^{-2}\,, \quad \tilde{g}_{4a} = g_{4a}\,, \quad \tilde{g}_{4b} = g_{4b}\,, \tag{6.26}$$

while we recall that the dimensionless Newton's and cosmological constants are given by $\tilde{G} = G\,k^2$ and $\tilde{\Lambda} = \Lambda\,k^{-2}$.

The key observation for the evaluation of the traces appearing in (6.56) is that their arguments contain only minimal second-order differential operators which commute with all other elements (such as the curvature scalars) inside the trace. In order to evaluate the traces, we can essentially follow the same steps as in the truncations previously studied, by first expanding the trace arguments in a Taylor series in R around $R = 0$, keeping only terms up to R^2, and computing the operator traces appearing as "expansion coefficients" via heat-kernel techniques. These techniques have been introduced in Sections 2.3 and 4.2.4, and we have collected all relevant expressions in the appendices. The main formula here is

$$\mathrm{Tr}[W(\Delta_{iL})] = \frac{1}{(4\pi)^2}\int d^4x\sqrt{g}\,\{Q_2[W]\mathrm{tr}_i\,\mathbf{b}_0 + Q_1[W]\mathrm{tr}_i\,\mathbf{b}_2 + Q_0[W]\mathrm{tr}_i\,\mathbf{b}_4 + \ldots\}\,, \tag{6.27}$$

where $W(z)$ is a smooth function representing the operator trace we are interested in evaluating, and where the $\mathbf{b}_{2i}$ are the heat kernel coefficients of the Lichnerowicz Laplacian, which are given in (D.25) to four-derivative order. The functionals $Q_n[W]$ are defined in (2.34). As in the $f(R)$ case, it is useful to express these functionals in terms of the dimensionless threshold functions $\Phi_n^p(w)$, $\tilde{\Phi}_n^p(w)$ and $\Upsilon_{n,m}^p(u,v,w)$, $\tilde{\Upsilon}_{n,m,l}^p(u,v,w)$ defined in Appendix E.1, which encode the dependence of our quantities on the choice of cutoff profile function. In particular, the

traces arising from $\mathcal{S}_{1\mathrm{T}}$ and $\mathcal{S}_0$ are of the form (E.10), whereas the $\mathcal{S}_{2\mathrm{T}}$ and $\mathcal{S}_{\mathrm{hh}}$ traces can be reexpressed via (E.11).

Following the strategy just outlined, the expansion of the 1T and 0 traces results in

$$\begin{aligned}\mathcal{S}_{1\mathrm{T}} &= -\tfrac{1}{(4\pi)^2}\int \mathrm{d}^4x\sqrt{g}\left[3k^4\Phi_2^1+\Phi_1^1k^2R+\tfrac{29}{480}\varphi R^2-\tfrac{\varphi}{30}R_{\mu\nu\rho\sigma}R^{\mu\nu\rho\sigma}\right],\\ \mathcal{S}_0 &= -\tfrac{1}{(4\pi)^2}\int \mathrm{d}^4x\sqrt{g}\left[k^4\Phi_2^1+\tfrac{1}{6}(\Phi_1^1+2\Phi_2^2)k^2R\right.\\ &\qquad\left.+(\tfrac{\varphi}{160}+\tfrac{1}{18}\Phi_1^2+\tfrac{1}{9}\Phi_2^3)R^2+\tfrac{\varphi}{360}R_{\mu\nu\rho\sigma}R^{\mu\nu\rho\sigma}\right].\end{aligned} \tag{6.28}$$

Here, all the Φ_n^p are evaluated at zero argument, and $\varphi \equiv k\partial_k \ln(R_k)|_{z=0}$ is a cutoff profile independent constant which, for our choice $R^{(0)}(0)=1$, evaluates to $\varphi = 2$.

The evaluation of the truncation-dependent traces $\mathcal{S}_{\mathrm{hh}}$ and $\mathcal{S}_{2\mathrm{T}}$, on the other hand, is slightly more involved. Applying (E.11), the expansion of $\mathcal{S}_{hh}$ on the truncation subspace takes the form

$$\mathcal{S}_{hh} = \frac{1}{2(4\pi)^2}\int d^4x\sqrt{g}\left\{k^4\,C_1 + C_2k^2R + \frac{1}{180}C_3R_{\alpha\beta\mu\nu}\,R^{\alpha\beta\mu\nu} + C_4R^2\right\}, \tag{6.29}$$

where the dimensionless coefficients C_i can be written in terms of the generalized threshold functions (E.2) with arguments

$$\Upsilon^p_{n,m} = \Upsilon^p_{n,m}(6\tilde{g}_{4a},\tilde{g}_2,2/3\tilde{g}_0), \quad \tilde{\Upsilon}^p_{n,m,l} = \tilde{\Upsilon}^p_{n,m,l}(6\tilde{g}_{4a},\tilde{g}_2,2/3\tilde{g}_0)$$

and read

$$C_1 = 24\,\tilde{g}_{4a}\Upsilon^1_{2,1} + 2\tilde{g}_2\Upsilon^1_{2,0} + 6\partial_t\tilde{g}_{4a}\tilde{\Upsilon}^1_{2,0,1} + (2\tilde{g}_2+\partial_t\tilde{g}_2)\tilde{\Upsilon}^1_{2,0,0},$$

$$\begin{aligned}C_2 =\,& 4\tilde{g}_{4a}\left(12\tilde{g}_{4a}\Upsilon^2_{2,2} - \Upsilon^1_{2,0} + \Upsilon^1_{1,1} + \tilde{g}_2\Upsilon^2_{2,1}\right) + \tfrac{1}{3}\tilde{g}_2\Upsilon^1_{1,0}\\ &- \partial_t\tilde{g}_{4a}\big(2\tilde{\Upsilon}^1_{2,0,0} - 12\tilde{g}_{4a}\tilde{\Upsilon}^2_{2,1,1} - \tilde{\Upsilon}^1_{1,0,1}\big) + (2\tilde{g}_2+\partial_t\tilde{g}_2)(2\tilde{g}_{4a}\tilde{\Upsilon}^2_{2,1,0} + \tfrac{1}{6}\tilde{\Upsilon}^1_{1,0,0}),\end{aligned}$$

$$C_3 = \frac{(12\tilde{g}_{4a}+\tilde{g}_2)\varphi + 6\partial_t\tilde{g}_{4a} + 2\tilde{g}_2 + \partial_t\tilde{g}_2}{6\tilde{g}_{4a} + \tilde{g}_2 + \frac{2}{3}\tilde{g}_0},$$

$$\begin{aligned}C_4 =\,& \tilde{g}_{4a}\big\{96\tilde{g}^2_{4a}\Upsilon^3_{2,3} - 8\tilde{g}_{4a}(\Upsilon^2_{2,1} - \Upsilon^2_{1,2} - \tilde{g}_2\Upsilon^3_{2,2}) + \tfrac{2}{3}(\tilde{g}_2\Upsilon^2_{1,1} - \Upsilon^1_{1,0})\big\}\\ &+ \partial_t\tilde{g}_{4a}\big\{24\tilde{g}^2_{4a}\tilde{\Upsilon}^3_{2,2,1} - 2\tilde{g}_{4a}(2\tilde{\Upsilon}^2_{2,1,0} - \tilde{\Upsilon}^2_{1,1,1}) - \tfrac{1}{3}\tilde{\Upsilon}^1_{1,0,0}\big\}\\ &+ \tilde{g}_{4a}\,(2\tilde{g}_2+\partial_t\tilde{g}_2)\,(4\tilde{g}_{4a}\tilde{\Upsilon}^3_{2,2,0} + \tfrac{1}{3}\tilde{\Upsilon}^2_{1,1,0}) + \tfrac{1}{80}C_3.\end{aligned} \tag{6.30}$$

Here, we have applied $R^{(0)}(0)=1$ to simplify C_3 and expressed the resulting coefficients in terms of the dimensionless coupling constants (6.26).

The projection of $\mathcal{S}_{2\mathrm{T}}$ proceeds in a similar fashion. In this case, all threshold functions appear with arguments

$$\Upsilon^p_{n,m} = \Upsilon^p_{n,m}(2\tilde{g}_{4b}, -\tilde{g}_2, -\tilde{g}_0), \quad \tilde{\Upsilon}^p_{n,m,l} = \tilde{\Upsilon}^p_{n,m,l}(2\tilde{g}_{4b}, -\tilde{g}_2, -\tilde{g}_0)\,.$$

Letting

$$\mathcal{S}_{2\mathrm{T}} = \frac{1}{2(4\pi)^2}\int d^4x\sqrt{g}\left\{k^4\widetilde{C}_1 + \widetilde{C}_2 k^2 R + \frac{10}{9}\widetilde{C}_3 R_{\alpha\beta\mu\nu}R^{\alpha\beta\mu\nu} + \widetilde{C}_4 R^2\right\}, \tag{6.31}$$

the coefficients $\widetilde{C}_i$ appearing in the trace expansion are

$$\begin{aligned}
\widetilde{C}_1 =& 40\tilde{g}_{4b}\Upsilon^1_{2,1} - 10\tilde{g}_2\Upsilon^1_{2,0} + 10\partial_t\tilde{g}_{4b}\tilde{\Upsilon}^1_{2,0,1} - 5(2\tilde{g}_2 + \partial_t\tilde{g}_2)\tilde{\Upsilon}^1_{2,0,0}\,,\\[2ex]
\widetilde{C}_2 =& 10g_{\flat}\big(4\tilde{g}_{4b}\Upsilon^2_{2,2} - \Upsilon^1_{2,0} - \tilde{g}_2\Upsilon^2_{2,1}\big) + 5\tilde{g}_2\big(4\tilde{g}_{4b}\Upsilon^2_{2,1} + \tfrac{2}{3}\Upsilon^1_{1,0} - \tilde{g}_2\Upsilon^2_{2,0}\big)\\
&- \tfrac{40}{3}\tilde{g}_{4b}\Upsilon^1_{1,1} + 5\partial_t\tilde{g}_{4b}\big(2g_{\flat}\tilde{\Upsilon}^2_{2,1,1} + \tilde{g}_2\tilde{\Upsilon}^2_{2,0,1} - \tfrac{2}{3}\tilde{\Upsilon}^1_{1,0,1}\big)\\
&- 5(2\tilde{g}_2 + \partial_t\tilde{g}_2)(g_{\flat}\tilde{\Upsilon}^2_{2,1,0} - \tfrac{1}{3}\tilde{\Upsilon}^1_{1,0,0} + \tfrac{1}{2}\tilde{g}_2\tilde{\Upsilon}^2_{2,0,0}) - 5\partial_t g_{\flat}\tilde{\Upsilon}^1_{2,0,0}\,,\\[2ex]
\widetilde{C}_3 =& \frac{(4\tilde{g}_{4b} - \tilde{g}_2)\varphi + 2\partial_t\tilde{g}_{4b} - (2\tilde{g}_2 + \partial_t\tilde{g}_2)}{2\tilde{g}_{4b} - \tilde{g}_2 - \tilde{g}_0}\,,\\[2ex]
\widetilde{C}_4 =& 5g_{\flat}\tilde{g}_2\left\{8\tilde{g}_{4b}\Upsilon^3_{2,2} - \Upsilon^2_{2,0} - 2\tilde{g}_2\Upsilon^3_{2,1} + \tfrac{2}{3}\Upsilon^2_{1,1}\right\} + \frac{10}{3}g_{\flat}\left\{\Upsilon^1_{1,0} - 4\tilde{g}_{4b}\Upsilon^2_{1,2}\right\}\\
&- \tfrac{20}{3}\tilde{g}_2\tilde{g}_{4b}\Upsilon^2_{1,1} + 5g_{\flat}^2\left\{8\tilde{g}_{4b}\Upsilon^3_{2,3} - 2\Upsilon^2_{2,1} - 2\tilde{g}_2\Upsilon^3_{2,2}\right\}\\
&+ 5\tilde{g}_2^2\left\{2\tilde{g}_{4b}\Upsilon^3_{2,1} + \tfrac{1}{3}\Upsilon^2_{1,0} - \tfrac{1}{2}\tilde{g}_2\Upsilon^3_{2,0}\right\} + 5\,(2\tilde{g}_2 + \partial_t\tilde{g}_2)\\
&\qquad\times\left\{g_{\flat}\,(\tfrac{1}{3}\tilde{\Upsilon}^2_{1,1,0} - \tilde{g}_2\tilde{\Upsilon}^3_{2,1,0} - g_{\flat}\tilde{\Upsilon}^3_{2,2,0}) + \tfrac{1}{6}\tilde{g}_2\tilde{\Upsilon}^2_{1,0,0} - \tfrac{1}{4}\tilde{g}_2^2\tilde{\Upsilon}^3_{2,0,0}\right\}\\
&+ 5\partial_t\tilde{g}_{4b}\left\{g_{\flat}(2g_{\flat}\tilde{\Upsilon}^3_{2,2,1} + 2\tilde{g}_2\tilde{\Upsilon}^3_{2,1,1} - \tfrac{2}{3}\tilde{\Upsilon}^2_{1,1,1}) - \tfrac{1}{3}\tilde{g}_2\tilde{\Upsilon}^2_{1,0,1} + \tfrac{1}{2}\tilde{g}_2^2\tilde{\Upsilon}^3_{2,0,1}\right\}\\
&- 5\partial_t g_{\flat}\left\{g_{\flat}\tilde{\Upsilon}^2_{2,1,0} + \tfrac{1}{2}\tilde{g}_2\tilde{\Upsilon}^2_{2,0,0} - \tfrac{1}{3}\tilde{\Upsilon}^1_{1,0,0}\right\} - \tfrac{29}{48}\widetilde{C}_3\,.
\end{aligned} \tag{6.32}$$

Note that the generalized threshold functions entering into C_i and $\widetilde{C}_i$ depend on *different arguments*.

6.1.4 The beta functions

Parametrizing the truncation (6.2) in terms of the g_{2i} couplings and specifying the background to be an Einstein space, the left-hand side of the flow equation

(6.56) reads

$$\partial_t \bar{\Gamma}_k^{\rm gr} = \int d^4x \sqrt{g} \big[\partial_t g_0 + \partial_t g_2 R + \big(\partial_t g_{4a} - \tfrac{1}{6} \partial_t g_{4b} \big) R^2 + \partial_t g_{4b} R_{\mu\nu\rho\sigma} R^{\mu\nu\rho\sigma} \big] \,. \tag{6.33}$$

Combining the $\mathcal{S}_i$ contributions on the right-hand side, expressing all couplings constants in terms of their dimensionless counterparts and equating the coefficients of the curvature polynomials on both sides of (6.56) then yields

$$\begin{aligned} k\partial_k \tilde{g}_0 &= -4\,\tilde{g}_0 + \frac{1}{2(4\pi)^2} \Big\{ C_1 + \widetilde{C}_1 - 8\Phi_2^1 \Big\} \,, \\ k\partial_k \tilde{g}_2 &= -2\,\tilde{g}_2 + \frac{1}{2(4\pi)^2} \Big\{ C_2 + \widetilde{C}_2 - \tfrac{7}{3}\Phi_1^1 - \tfrac{2}{3}\Phi_2^2 \Big\} \,, \\ k\partial_k \tilde{g}_{4ab} &= \frac{1}{(4\pi)^2} \Big\{ \tfrac{1}{360} C_3 + \tfrac{5}{9} \widetilde{C}_3 + \tfrac{11}{360} \varphi \Big\} \,, \\ k\partial_k \tilde{g}_{4a} - \tfrac{1}{6} k\partial_k \tilde{g}_{4b} &= \frac{1}{(4\pi)^2} \Big\{ \tfrac{1}{2} C_4 + \tfrac{1}{2} \widetilde{C}_4 - \tfrac{1}{18}\Phi_1^2 - \tfrac{1}{9}\Phi_2^3 - \tfrac{1}{15}\varphi \Big\} \,. \end{aligned} \tag{6.34}$$

Note that these beta functions are given in a rather implicit form, as the derivatives of $k\partial_k \tilde{g}_i$ appear on both the left- and right-hand side of the equation. By solving these equations for $k\partial_k \tilde{g}_i$, we obtain the beta functions

$$k\partial_k \tilde{g}_i = \beta_i(\tilde{g}_i) \tag{6.35}$$

This can be straightforwardly done using algebraic manipulation software. However, the resulting expressions are very lengthy and not very illuminating, so that we give here the implicit form of the beta functions only.

Fixed point solutions

Owing to their intricate structure, the beta functions (6.34) can only be analyzed numerically. Furthermore, their explicit evaluation requires specifying the particular profile of the IR cutoff function. In the following, all results are given for the optimized cutoff (E.12) with shape parameter $b = 1$, but we have also verified that using the exponential cutoff (E.13) or varying the shape parameter b confirms the picture reported below.

The fixed point structure of our beta functions exhibits, first, the two Gaussian fixed points (GFP) familiar from perturbation theory[1],

$$\tilde{G}^* = 0 \,, \qquad \tilde{\Lambda}^* = 0 \,, \qquad \sigma^* = 0 \,, \qquad \omega_{1,2}^* = -\tfrac{1}{60} \Big(45 \pm \sqrt{3927} \Big) \,, \tag{6.36}$$

[1] In a slight abuse of notation, we neglect the topological term here, setting $\theta = 0, \partial_t \theta = 0$. Also note that the existence of this GFP is actually compatible with the analysis [40], which did not consider the case of the inverse coupling $1/\sigma \to \infty$.

with stability properties given by the following eigensystem

$$\begin{aligned} &\theta_1 = 2\,, \quad V_1 = \{1,0,0,0\}^{\mathrm{T}}\,, && \theta_2 = -2\,, \quad V_2 = \{\tfrac{1}{8\pi},1,0,0\}^{\mathrm{T}}\,, \\ &\theta_3 = 0\,, \quad V_3 = \{0,0,1,0\}^{\mathrm{T}}\,, && \theta_4 = 0\,, \quad V_4 = \{0,0,0,0\}^{\mathrm{T}}\,. \end{aligned} \tag{6.37}$$

These GFPs correspond to the free theory, and their stability coefficients are given by the canonical mass dimension of the corresponding (dimensionful) couplings. In particular, the eigendirection associated with Newton's constant is UV repulsive, while the directions associated with the new couplings σ, ω are marginal. Going beyond the linear approximation, the marginal directions are found to be UV-attractive, in accordance with the one-loop calculations [130].

More interestingly, the beta functions (6.34) also admit a non-trivial fixed point solution with positive Newton's and cosmological constant. Its position is given by

$$\tilde{g}_0^* = 0.00442\,, \qquad \tilde{g}_2^* = -0.0101\,, \qquad \tilde{g}_{4a}^* = 0.008\,, \qquad \tilde{g}_{4b}^* = -0.0050\,, \tag{6.38}$$

which corresponds to $\tilde{G} = 1.96$, $\tilde{\Lambda} = 0.218$. The dimensionless, gauge-independent [131] combination $G\Lambda$ then takes the fixed point value

$$(G\Lambda)^* = 0.427\,,$$

which, together with the value of $\tilde{g}_{4a}^*$, is in good agreement with previous computations. Note also that the finite values for $\tilde{g}_{4a}^*$ and $\tilde{g}_{4b}^*$ imply a finite value of σ^*, to be compared with the one-loop result $\sigma^* = 0$. Thus, the non-perturbative corrections captured by the FRGE shift the fixed point underlying the asymptotic freedom obtained within perturbation theory to the non-Gaussian fixed point (6.38) featuring in the asymptotic safety program.

Linearizing the flow around this NGFP, we find the stability coefficients

$$\theta_0 = 2.51\,, \qquad \theta_1 = 1.69\,, \qquad \theta_2 = 8.40\,, \qquad \theta_3 = -2.11\,, \tag{6.39}$$

and associated normalized eigenvectors

$$\begin{aligned} V_0 &= \{\,0.12\,,\,0.10\,,\,-0.06\,,\,0.99\}^{\mathrm{T}}\,, && V_1 = \{\,-0.20\,,\,0.74\,,\,-0.10\,,\,0.63\}^{\mathrm{T}}\,, \\ V_2 &= \{\,0.74\,,\,-0.46\,,\,0.48\,,\,-0.11\,\}^{\mathrm{T}}\,, && V_3 = \{\,0.07\,,\,-0.21\,,\,0.97\,,\,-0.09\,\}^{\mathrm{T}}\,. \end{aligned} \tag{6.40}$$

We observe that the NGFP stability coefficients reported here are real. This is in contrast with the complex stability coefficients and the corresponding spiraling approach of the renormalization group flow characteristic for $f(R)$-type truncations, and reflects rather the behavior found within the perturbative one-loop computation [130]. One might be tempted to speculate that this difference originates from the contribution of the C^2 term. Performing a stability analysis of these numerical results by varying the cutoff profile and associated shape parameter, however, suggests that this is not the case. Indeed, particular choices of the shape

parameter can again lead to complex stability coefficients both when employing the exponential (E.13) and the optimized (E.12) cutoffs. In order to minimize the scheme dependence of our numerical results and obtain more stable critical exponents, an optimization analysis in the spirit of [75,114] should be perfomed. While we will not undertake such an analysis in the present work, it should constitute an important component in future studies within higher-derivative truncations. In any case, we stress again that, for all cutoff profiles and the range of shape parameters we have considered, a NGFP with three UV-relevant directions and similar values of $(G\Lambda)^*$ was found.

Note that the transition from asymptotic freedom to asymptotic safety lifts the degeneracy of the marginal couplings. Crucially, increasing the dimension of the truncation subspace with respect to the Einstein-Hilbert case adds one UV-attractive and one UV-repulsive eigendirection to the stability matrix, so that the UV critical hypersurface in the truncation subspace is now three-dimensional. We should note that the same number of UV-attractive eigendirections has been found within the $f(R)$ studies of [41] and reproduced in Chapter 4, which, however, did not include the power-counting marginal coupling $\tilde{g}_{4b}$. The condition that a trajectory be asymptotically safe, i.e., that it approach the fixed point as $k \to \infty$ implies a relation between the couplings $\tilde{g}_{2i}$ which, in the neighborhood of the NGFP, defines the UV critical surface via

$$\tilde{g}_{4b} = -0.116 + 0.745\tilde{g}_0 - 2.441\tilde{g}_2 + 11.06\tilde{g}_{4a}\,. \tag{6.41}$$

We then have a three-dimensional subspace of renormalization group trajectories which are attracted to the NGFP in the UV and are therefore "asymptotically safe".

6.2 Perturbation theory and asymptotic freedom

Gravity theories in which the action takes the form of our ansatz (6.2) have been the focus of various perturbative studies in the literature (see [132] for a review). The initial motivation behind many of these studies was the observation [133] that the presence of higher-derivative propagators softens the divergences encountered in the perturbative quantization, rendering the higher-derivative theory perturbatively renormalizable and asymptotically free at the one-loop level [131,134–137]. On the other hand, when seen as a fundamental theory, the extra terms responsible for the improved UV behavior also induce massive negative-norm states [138], the so-called "poltergeists", which are believed to spoil the unitarity of the theory and thus pose a significant obstacle to its feasibility as a candidate theory of quantum gravity. While some arguments have suggested that this shortcoming can be cured by quantum effects [134, 139], no such claims have yet been successfully verified.

Over and above the status of higher-derivative gravity as a fundamental theory, however, it is instructive to consider the relation between our FRGE calculations

and the perturbative results within that setting. We should stress again that we treat our four-derivative ansatz at the level of a truncated effective (average) action only, and hence bare action considerations are not relevant to our discussion here.

We start by showing that the known one-loop beta functions for the marginal couplings σ, ω [131, 137] can be recovered from our non-perturbative renormalization group equations (6.34). In contrast to their $\tilde{G}, \tilde{\Lambda}$ counterparts, the former are universal, i.e., they are independent of the choice of gauge-fixing or regularization scheme employed. Since their usual derivation employs a very special choice of gauge-fixing, dimensional regularization, and heat-kernel methods for minimal fourth-order differential operators, which is manifestly different from the route taken in this paper, this comparison provides a consistency check for the validity of our approach.

The one-loop counter-term for higher-derivative gravity obtained via dimensional regularisation is [131, 137]

$$\Delta S = \frac{\mu^{d-4}}{(4\pi)^2(d-4)} \int \mathrm{d}^d x \sqrt{g} \left[\frac{133}{20} C^2 - \frac{196}{45} E + \left(\frac{10}{9}\omega^2 + \frac{5}{3}\omega + \frac{5}{36} \right) R^2 \right] . \tag{6.42}$$

Here, μ is a dimensional parameter and we have neglected lower-derivative and surface terms, which do not play a role in the following. Denoting the coupling constant in front of E by θ/σ, the one-loop beta functions for the dimensionless couplings become [130, 131, 137]

$$\begin{aligned} \beta_\sigma &= -\frac{1}{(4\pi)^2} \frac{133}{10} \sigma^2 , \\ \beta_\omega &= -\frac{1}{(4\pi)^2} \frac{25 + 1098\omega + 200\omega^2}{60} \sigma , \\ \beta_\theta &= \frac{1}{(4\pi)^2} \frac{7(56 - 171\theta)}{90} \sigma . \end{aligned} \tag{6.43}$$

Due to our use of the Einstein backgrounds, we cannot disentangle the running of θ from σ, ω in our projected equations. In this case, the E term in (6.42) shifts the coefficients of the C^2, and R^2 terms. Using (A.7), the Einstein-space limit of (6.42) relevant for our computation is readily obtained as

$$\Delta S = \frac{\mu^{d-4}}{(4\pi)^2(d-4)} \int \mathrm{d}^d x \sqrt{g} \left[\frac{413}{180} C^2 + \left(\frac{10}{9}\omega^2 + \frac{5}{3}\omega - \frac{317}{540} \right) R^2 \right] . \tag{6.44}$$

The resulting projected beta functions are then given by

$$\beta_\sigma = -\frac{1}{(4\pi)^2} \frac{413}{90} \sigma^2 , \qquad \beta_\omega = \frac{1}{(4\pi)^2} \frac{317 - 1726\omega - 600\omega^2}{180} \sigma . \tag{6.45}$$

We now establish that these β-functions indeed arise as the one-loop limit of (6.34). In this limit, we first "switch off" the renormalization group improvement

of (6.34), by setting all the $\ln(k)$-derivatives appearing on its right-hand side to zero. At the level of the flow equation, (6.14) this corresponds to neglecting the running of the couplings in its right-hand side. We then expand $C_3, \widetilde{C}_3$ and $C_4, \widetilde{C}_4$ to leading order in σ. The resulting expressions can be expressed completely in terms of $\Phi_n^p(0)$ and φ (viz. eqs. (E.8) and (E.9)),

$$\begin{aligned} C_3 &= 2\varphi\,, \quad C_4 = \tfrac{1}{9}(2\Phi_2^3 + \Phi_1^2) + \tfrac{1}{80}C_3\,, \\ \widetilde{C}_3 &= 2\varphi\,, \quad \widetilde{C}_4 = \tfrac{5}{9}(4\omega+1)\Phi_1^2 + \tfrac{5}{18}(4\omega+1)^2\Phi_2^3 - \tfrac{29}{48}\widetilde{C}_3\,. \end{aligned} \tag{6.46}$$

Since the quantities $\Phi_n^{n+1}(0)$ and φ are independent of the choice of profile function $R_k^{(0)}$, we find that our one-loop beta functions are independent of the regularization scheme, as expected. Lastly, recasting the resulting equations in terms of σ and ω, we precisely reproduce the projected beta functions (6.45). This provides a non-trivial cross-check between the FRGE techniques employed here and results obtained previously using, e.g., a dimensional regularization scheme.

In the one-loop approximation, our results recover the asymptotic freedom of the higher-derivative couplings found in previous calculations within the perturbative setting [130, 131, 134–137, 140]. Taking into account contributions from all loop orders to arrive at our non-perturbative beta functions (6.34), this asymptotic freedom is shifted to "asymptotic safety". With respect to the lower-derivative couplings $\tilde{G}$ and $\tilde{\Lambda}$, on the other hand, non-trivial fixed point solutions are present already at the level of perturbation theory. This was first established in [130] in a one-loop FRGE computation, and more recently also found by means of covariant operator regularization in perturbation theory [140]. The origin of the discrepancy between these and the earlier works can be traced to the fact that all of the latter computed the beta functions of higher-derivative gravity by means of dimensional regularization, which is sensitive to logarithmic divergences only. Once the contribution of power-like divergences in the one-loop effective action are also taken into account, the non-trivial fixed points appear.

6.3 Taming perturbative divergences in gravity

The renormalization group analysis of $R^2 + C^2$ truncation in the first half of this chapter lends further support to the asymptotic safety scenario and indicates the persistence of the NGFP under inclusion of the C^2 direction in the truncation subspace. Indeed, all truncations studied so far, from the Einstein-Hilbert, to the R^2 and general (local) $f(R)$, up to the tensorial truncation we have just considered, give rise to a coherent picture pointing to the existence of a NGFP dominating the UV behavior of gravity. A possible criticism of these results, however, is that they are based on truncations which only contain interactions that are also unproblematic for the on-shell perturbative renormalizability of gravity. It is therefore a fundamental test for asymptotic safety to include potentially

dangerous terms in the truncation ansatz and study their effect on the fixed point structure of the theory.

In pure gravity, the first non-trivial counterterm would be the Riemann-cube term of [19,20]. Including this term in the truncation ansatz is, however, technically very involved and beyond current FRGE techniques.

A technically less demanding but equally illuminating alternative is to study truncations for matter-coupled gravity. In this case, the non-renormalizable counterterms already appear at one-loop and the occurrence of divergences proportional to R^2 and $C_{\mu\nu\rho\sigma}C^{\mu\nu\rho\sigma}$, which do not vanish on-shell, signal the break down of perturbative renormalizability. To date, investigations of matter-coupled truncations, while also corroborating the asymptotic safety scenario, have remained restricted to the Einstein-Hilbert case [41, 82, 83, 108, 126]. In this section we go beyond this restriction, and study the non-perturbative renormalization group flow of gravitational higher-derivative terms in the presence of a free, massless, minimally coupled scalar field.

6.3.1 Perturbative non-renormalizability and counterterms

Let us begin by reviewing the perturbative quantization of the Einstein-Hilbert action minimally coupled to a free scalar field. This provides the prototypical example of a gravitational theory which is perturbatively non-renormalizable at one-loop order [15], as may be seen by computing its one-loop counterterms $\Delta\Gamma^{\rm div}$. In general, the one-loop effective action for a gauge theory takes the form

$$\Gamma^{1-\rm loop}[\Phi] = S[\Phi] + \frac{1}{2}\,\mathrm{STr}\ln\left[\frac{\delta^2 S^{\rm tot}}{\delta\Phi^A\delta\Phi^B}\right], \tag{6.47}$$

where Φ^A is the full set of fields (including auxiliary fields and ghosts), $S^{\rm tot}[\Phi] = S[\Phi] + S^{\rm gf}[\Phi] + S^{\rm gh}[\Phi]$ is the total action of the theory, including the gauge-fixing and ghost terms $S^{\rm gf}$ and $S^{\rm gh}$, and STr is a generalized functional trace carrying a minus sign for fermionic fields and a factor 2 for complex fields. Typically, this trace contains divergences which require regularization.

In the case of gravity, our starting point is the action

$$S[g,\phi] = \int d^4x\sqrt{g}\,\left[\kappa^{-2}(-R+2\Lambda) + \frac{1}{2}\,g^{\mu\nu}\,\partial_\mu\phi\partial_\nu\phi\right], \tag{6.48}$$

supplemented by the gauge-fixing term

$$S^{\rm gf} = \frac{1}{2\kappa^2}\int d^4x\sqrt{\bar g}\,\bar g^{\mu\nu}F_\mu F_\nu\,, \qquad F_\mu = \bar\nabla^\alpha h_{\mu\alpha} - \tfrac{1}{2}\bar\nabla_\mu h\,, \tag{6.49}$$

and the corresponding ghost action. Here, $\kappa^2 = 16\pi G$, G and Λ are the dimensionful Newton's and cosmological constant, respectively, $g_{\mu\nu}$ denotes the Euclidean space-time metric, and ϕ is a real scalar field. The gauge-fixing is carried out via

the background field method, splitting the metric and scalar fluctuations into a background part, $\bar{g}_{\mu\nu}, \bar{\phi}$, and fluctuations around this background, $h_{\mu\nu}, f$, according to $g_{\mu\nu} = \bar{g}_{\mu\nu} + h_{\mu\nu}$ and $\phi = \bar{\phi} + f$. Adapting the results [141, 142] obtained via the Schwinger-DeWitt technique, the one-loop divergences arising from (6.48) are readily found to be[2]

$$\Delta\Gamma^{\rm div} = \frac{1}{(4\pi)^2\epsilon}\int d^4x\sqrt{g}\left[\tfrac{43}{60}R_{\mu\nu}R^{\mu\nu} + \tfrac{1}{40}R^2 + \tfrac{213}{180}E + \tfrac{5}{4}\kappa^4(\partial_\mu\phi\partial^\mu\phi)^2 \right. \\ \left. - \kappa^2(\tfrac{1}{3}R - 2\Lambda)(\partial_\mu\phi\partial^\mu\phi) - \tfrac{26}{3}\Lambda R + 20\Lambda^2\right], \tag{6.50}$$

where $\epsilon = (d-4)$ and $E = C_{\mu\nu\rho\sigma}C^{\mu\nu\rho\sigma} - 2R_{\mu\nu}R^{\mu\nu} + \frac{2}{3}R^2$ is the integrand of the Gauss-Bonnet term in four dimensions, with $C_{\mu\nu\rho\sigma}$ being the Weyl tensor.

In order to get information on the renormalizability, the divergences (6.50) have to be considered on-shell. The equations of motion resulting from (6.48) are

$$\nabla_\mu\nabla^\mu\phi = 0\,, \quad R = 4\Lambda + \tfrac{1}{2}\,\kappa^2\,(\partial_\mu\phi)^2\,, \quad R_{\mu\nu} = \Lambda g_{\mu\nu} + \tfrac{1}{2}\,\kappa^2\,\left[\partial_\mu\phi\,\partial_\nu\phi\right]\,. \tag{6.51}$$

Substituting these, eq. (6.50) can be suggestively written as[3]

$$\Delta\Gamma^{\rm div} = \frac{1}{8\pi^2\epsilon}\int d^4x\sqrt{g}\left[\frac{213}{360}E + \frac{203}{80}R^2 - \frac{463}{20}R\Lambda + \frac{463}{10}\Lambda^2\right]\,. \tag{6.52}$$

As the R^2 and E-terms are not of the form of the terms contained in the initial action, they cannot be absorbed by a renormalization of the coupling constants, indicating that the action (6.48) is indeed perturbatively non-renormalizable. The non-renormalizable on-shell counterterms are thus of fourth order in the gravitational sector and can be rewritten as

$$\Delta\Gamma^{\rm NR} = \frac{1}{(4\pi)^2\epsilon}\int d^4x\sqrt{g}\left[\frac{31}{18}\,R^2 + \frac{213}{180}\,C_{\mu\nu\rho\sigma}C^{\mu\nu\rho\sigma}\right]\,. \tag{6.53}$$

There is a common prejudice that these interactions have a devastating effect also on the possible non-perturbative renormalizability (i.e., asymptotic safety) of the theory. Extending the calculations presented in the first half of this chapter to include the contribution of a minimally coupled, massless scalar field, we will now show that this is not the case.

6.3.2 Matter coupling and beta functions

We now take the term $\bar{\Gamma}_k$ in our ansatz (6.1) to be of the form

$$\bar{\Gamma}_k[\Phi] = \Gamma_k^{\rm grav}[g] + \Gamma^{\rm matter}[g,\phi]\,, \tag{6.54}$$

[2]There is a typo in the coefficient of the squared potential in [142], the correct formula is given in [141].

[3]Note that this expression agrees both with the one-loop counterterm found by 't Hooft and Veltman [15] for $\Lambda = E = 0$, and with the one of Christensen and Duff [143] once the contribution of the scalar field is subtracted.

where $\Gamma_k^{\rm grav}$ is the four-derivative gravitational truncation (6.2) and $\Gamma_k^{\rm matter}$ is the (k-independent) action for a minimally coupled massless scalar field,

$$\Gamma^{\rm matter}[g,\phi] = \tfrac{1}{2}\int d^4x\sqrt{g}\; g^{\mu\nu}\,\partial_\mu\phi\,\partial_\nu\phi\,. \tag{6.55}$$

Note that this truncation is exactly of the form of a matter-coupled Einstein-Hilbert action plus perturbative counterterms. Applying the background field method also for the matter part of our ansatz (setting $\bar\phi = 0$, for convenience) and computing the second variation, we find that the matter traces decouple from the gravitational traces in the right-hand side of the flow equation, as we have already seen in Chapter 2 also for the case of minimally-coupled Dirac and Maxwell fields. In addition, since $\Gamma^{\rm matter}$ contains no running couplings, it will not contribute to the left-hand side of the FRGE. Our flow equation is thus given by

$$k\partial_k\Gamma_k[\Phi] = \partial_t\Gamma_k[g]^{\rm grav} = \mathcal{S}_{\rm 2T} + \mathcal{S}_{\rm hh} + \mathcal{S}_{\rm 1T} + \mathcal{S}_0 + \mathcal{S}_{\rm mat}, \tag{6.56}$$

where

$$\mathcal{S}_{\rm matter} = \frac{1}{2}{\rm Tr}_0\left[\frac{\partial_t R_{0,k}}{P_{0,k}}\right]. \tag{6.57}$$

is the scalar field contribution to the traces and the gravitational traces are given by (6.23)-(6.25). The latter have been evaluated in Section 6.1.3, while following the same evaluation procedure for the matter trace straightforwardly yields

$$\mathcal{S}_{\rm matter} = \frac{1}{(4\pi)^2}\int d^4x\sqrt{g}\left[k^4\Phi_2^1 + \frac{1}{6}k^2\Phi_1^1 R + \frac{\varphi}{2}(\frac{1}{180}R_{\mu\nu\rho\sigma}R^{\mu\nu\rho\sigma} + \frac{1}{80}R^2)\right]. \tag{6.58}$$

At the level of the beta functions, the matter coupling results in a shift by a constant with respect to the pure gravity expressions (6.34), leading to

$$\begin{aligned}
k\partial_k\tilde g_0 &= -4\,\tilde g_0 + \frac{1}{2(4\pi)^2}\left\{C_1 + \widetilde{C}_1 + (2n_s-8)\Phi_2^1\right\},\\
k\partial_k\tilde g_2 &= -2\,\tilde g_2 + \frac{1}{2(4\pi)^2}\left\{C_2 + \widetilde{C}_2 + \tfrac{n_s-7}{3}\Phi_1^1 - \tfrac{2}{3}\Phi_2^2\right\},\\
k\partial_k\tilde g_{4b} &= \frac{1}{(4\pi)^2}\left\{\tfrac{1}{360}C_3 + \tfrac{5}{9}\widetilde{C}_3 + \tfrac{11+n_s}{360}\varphi\right\},\\
k\partial_k\tilde g_{4a} - \tfrac{1}{6}\partial_t\tilde g_{4b} &= \frac{1}{(4\pi)^2}\left\{\tfrac{1}{2}C_4 + \tfrac{1}{2}\widetilde{C}_4 - \tfrac{1}{18}\Phi_1^2 - \tfrac{1}{9}\Phi_2^3 + (\tfrac{n_s}{160} - \tfrac{1}{15})\varphi\right\},
\end{aligned} \tag{6.59}$$

where we have explicitly indicated the matter contribution by the $n_S = 1$.

6.3.3 Fixed points of matter-coupled gravity

Solving (6.59), we arrive at the fixed points of our truncation. Remarkably, the fixed point structure originating from the matter-coupled case is very similar to

the pure gravity results of the previous section. First, we recover the matter-coupled analogues of the pure gravity GFPs

$$g^* = 0\,, \qquad \lambda^* = 0\,, \qquad \sigma^* = 0\,, \qquad \omega^*_{1,2} = -\tfrac{1}{120}\left(90 \pm \sqrt{15708 - 101 n_s}\right)\,, \tag{6.60}$$

existing for $0 \leq n_s \leq 155$ and with stability properties given by the following eigensystem

$$\begin{array}{llll} \theta_1 = 2\,, & V_1 = \{1,0,0,0\}^{\mathrm{T}}\,, & \theta_2 = -2\,, & V_2 = \{\tfrac{2+n_s}{16\pi},1,0,0\}^{\mathrm{T}}\,, \\ \theta_3 = 0\,, & V_3 = \{0,0,1,0\}^{\mathrm{T}}\,, & \theta_4 = 0\,, & V_4 = \{0,0,0,0\}^{\mathrm{T}}\,. \end{array} \tag{6.61}$$

Most importantly, we also find a generalization of the NGFP in the matter-coupled higher-derivative truncation. Its position and stability coefficients are given by

$$\tilde{g}^*_0 = 0.00438\,, \tilde{g}^*_1 = -0.0087\,, \tilde{g}^*_{4a} = 0.010\,, \tilde{g}^*_{4b} = -0.0043\,, \tag{6.62}$$

and

$$\theta_0 = 2.67\,, \quad \theta_1 = 1.39\,, \quad \theta_2 = 7.86\,, \quad \theta_3 = -1.50\,, \tag{6.63}$$

corresponding to

$$\tilde{G}^* = 2.279\,, \quad \tilde{\Lambda}^* = 0.251\,, \quad (G\Lambda)^* = 0.571\,. \tag{6.64}$$

We have collected this data, together with that from the pure gravity case, in Tables 6.3 and 6.4, where we have also included the results from previous FRGE four-derivative computations for comparison.

As we can see from the stability coefficients (6.63), our truncated flow is still characterized by three UV-attractive and one UV-repulsive eigendirections. We still have a three-dimensional subspace of renormalization group trajectories which are attracted to the NGFP in the UV and which are hence "asymptotically safe". Therefore, non-perturbative renormalizability persists also in the presence of the one-loop perturbative counterterms in the truncation ansatz.

6.4 Conclusions

In this chapter, we have studied the non-perturbative renormalization group flow of gravity in a higher-derivative truncation, moving beyond $f(R)$ truncations to include tensorial interactions in the truncated flow space. Using a new projection procedure for the truncated flow equation, we were able to distinguish two linear combinations of the three higher-derivative couplings and account for the presence of the helicity-two states propagator in our truncation ansatz. The resulting beta functions give rise, in addition to a trivial fixed point linked to the perturbative quantization, to a non-Gaussian fixed point with positive values of Newton's

Truncation	$\tilde{G}^*$	$\tilde{\Lambda}^*$	$\tilde{g}^*_{4a}$	$\tilde{g}^*_{4b}$	$(G\Lambda)^*$
R^2+C^2	1.960	0.218	0.008	-0.0050	0.427
LR II	0.292	0.330	0.005	–	0.096
CP	1.389	0.221	$*$	$*$	0.307
$R^2+C^2+\phi$	2.279	0.251	0.010	-0.0043	0.571

Table 6.3: Position of the NGFP obtained from the non-perturbative beta functions of the R^2+C^2-truncation, eq. (6.34). For comparison, we also give the data of the R^2-truncation [40] (LR II), and the perturbative one-loop result [130] (CP). In the latter line, the $*$ indicates that $\omega^* = -0.0228, \theta^* = 0.327$ approach finite values in the UV, while σ runs logarithmically to zero, realizing the asymptotic freedom of the one-loop result. The last line gives the position of the NGFP upon including a minimally coupled scalar field. Note that CP employed a type III cutoff scheme with the optimized cutoff, whereas LR II employed a type I scheme with the exponential cutoff.

Truncation	θ_1	θ_2	θ_3	θ_4
R^2+C^2	2.51	1.69	8.40	-2.11
LR II	$2.15+3.79$i	$2.15-3.79$i	28.8	–
CP	4	2	$*$	$*$
$R^2+C^2+\phi$	2.67	1.39	7.86	-1.50

Table 6.4: Stability coefficients of the NGFP obtained from the non-perturbative beta functions of the R^2+C^2-truncation, eq. (6.34). For comparison, we also give the data of the R^2-truncation [40] (LR II), and the perturbative one-loop result [130] (CP). In the latter line, the $*$ indicates the logarithmic running of the marginal coupling constants towards asymptotic freedom. The last line gives the stability coefficients of the NGFP upon including a minimally coupled scalar field.

constant and the cosmological constant and with similar properties to the ones observed within previous $f(R)$ type truncations. Despite the four-dimensional truncation space, the number of relevant interactions within the "R^2+C^2" truncation is found to be three. These results provide further evidence for the asymptotic safety scenario.

We then supplemented our higher-derivative truncation with a minimally coupled free scalar field. From the viewpoint of perturbative quantization, this setup provides a prototypical example of a quantum theory of gravity which is perturbatively non-renormalizable at the one-loop level [15]. There, higher-derivative interactions arise as perturbative counterterms, signaling the presence of divergences which cannot be absorbed by a renormalization of the coupling constants. However, despite the breakdown of the perturbative quantization scheme, there is the possibility that this gravity-scalar theory constitutes a well-defined and predictive quantum theory within the realm of asymptotic safety.

We have shown that the non-Gaussian fixed point found in the pure gravity

case and supporting the asymptotic safety conjecture persists under the addition of the scalar field to our truncation. This result explicitly shows that, contrary to a common concern, the inclusion of perturbative counterterms in the truncation subspace of a gravity-matter theory has *no qualitative effect* on its fixed point structure. In particular, we find *no indication* that these interactions are fatal to the non-perturbative renormalizability of the theory.

An interesting point surfaces when comparing the fixed point structure obtained for pure gravity ($n_s = 0$) and gravity coupled to one free scalar ($n_s = 1$) given in the top and bottom lines of Tables 6.3 and 6.4, respectively. Including the scalar field shifts the fixed point values obtained for pure gravity only very mildly, so that the resulting fixed point patterns are very similar. In a sense, this indicates that (at least for the present truncations) the UV behavior of the gravity-matter theory is still dominated by its gravitational sector, so that it still behaves "essentially gravitational" at high energies. Following [83, 144], it would be very interesting to determine which matter sectors lead to asymptotically safe gravity-matter theories, taking the higher-derivative terms into account.

Completing the four-derivative truncation so as to be able to decouple the running of all three higher-derivative couplings would be a natural continuation of our exploration of the truncated renormalization group flow of gravity. In addition, while our results on the interplay between the perturbative counterterms and asymptotic safety in the gravity-matter case are already trend-setting, it would also be desirable to carry out an analogous computation for pure gravity, where non-renormalizable divergences set in at two-loop level [19, 20]. Both of these studies, however, are still beyond the current technical scope of the functional renormalization group techniques employed in the case of gravity. Developing new computational methods in this setting thus seems to be a necessary next step.

7 Conclusions

Understanding gravity as a fundamental theory poses a challenge. While general relativity is an extremely successful theory at the classical level, attempts to reconcile it with quantum mechanics by means of perturbative quantization indicate a breakdown of the quantized theory when one reaches energy regimes of the order of the Planck scale (10^{19} GeV).

The predominant response to this problem, as exemplified by the string theory approach [26], has been to consider quantized general relativity simply as an effective low-energy limit of a (more) fundamental theory of gravity, which involves enlarged or modified field contents and symmetries when compared with those present at the classical level. This effective theory is appropriate for describing physics so long as we are considering phenomena below the cutoff set by the Planck scale. Once we reach the cutoff scale, however, we should abandon this theory altogether.

An alternative response, however, is based on the idea that these issues can be solved when approached from a non-perturbative perspective (see, e.g, [23] for reviews). From this viewpoint, the ultimate source of the problem above does not lie in the structure of general relativity, but in the use of perturbation theory in this setting. One possible non-perturbative resolution of this kind is Weinberg's asymptotic safety scenario [33]. This scenario posits the existence of a non-Gaussian fixed point of the renormalization group flow of gravity, with a finite number of ultraviolet-attractive directions, which controls the behavior of the theory in the ultraviolet (UV) and provides it with a predictive and well-defined high-energy limit. In this sense, understanding the non-perturbative renormalization group properties of quantized gravity could thus be central to establishing its validity in the Planck regime.

While the greatest challenge to the quantum gravity program is capturing the quantum behavior of gravity in the UV, its behavior in the deep infrared (IR) also

poses interesting questions. It has been suggested that quantum gravity gives rise to strong renormalization group effects in the IR which could be at the origin of observed cosmological phenomena [55]. One conjectured origin for such effects is the presence of non-local operators in the effective low-energy theory, such as the ones responsible for the conformal anomaly of the stress-energy tensor [57].

Although these two issues pertain to very different energy regimes and may be to a large extent decoupled from each other, they may also be treated under the same framework, from the point of view of the evolution of the effective dynamics of quantum gravity from IR to UV energy scales. The concept that can tie these effective descriptions together is precisely the renormalization group.

Motivated by these considerations, in this thesis we have investigated the non-perturbative renormalization group flow of gravity. The central tool in our investigation was a continuous Wilsonian renormalization group technique, the functional renormalization group equation (FRGE) [35, 65]. It encodes the scale-dependence of a coarse-grained effective action, taken to describe physics at a particular scale k, and allows us to construct the non-perturbative beta functions of the theory. Computations within this approach rely on a truncation approximation, whereby the full renormalization group flow is projected onto a subspace parametrized only by a subset of the renormalized couplings of the theory. The reliability of the results obtained in a given truncation is assessed by verifying their stability under the gradual extension of the truncation subspace.

The simplest, non-trivial gravity truncation one may consider is the Einstein-Hilbert truncation, parametrized by Newton's constant and the cosmological constant, and in which evidence for a non-trivial fixed point of gravity was first found [35]. The crucial questions in light of the asymptotic safety scenario are whether or not this fixed point persists under the enlargement of the truncation subspaces, and what are its resulting attractivity properties.

In this respect, there are three strategies we can aim to implement in order to answer these questions. The first is to apply further simplifications to the flow when extending the truncation, so as to include interactions which are otherwise intractable from the technical level and thus obtain a rough picture of what the effect of those terms might be. The second is to construct renormalization group equations that allow us to consider general classes of truncations subspaces, which might then allow us to make statements about large sectors of the full renormalization group flow space. The third is to include terms in the truncation which are known to be particularly problematic at the perturbative level, such as the perturbative counterterms, and check whether they also spoil any possible renormalizability results at the non-perturbative level. These are the strategies we have followed in this thesis.

In Chapter 3, we started our investigation within a conformally reduced simplification, and considered non-local truncations of the form of the effective action induced by the conformal anomaly. When implementing our coarse-graining operator in a Weyl–invariant way, which is related to preserving background-independence in the full theory, we found tentative evidence for a non-Gaussian

fixed point, in accordance with asymptotic safety. When implementing the coarse-graining in a Weyl–breaking way, on the other hand, we recovered the perturbative beta functions derived in [68], which admit a non-trivial IR fixed point solution that was in that work argued to drive the low-energy dynamics of the theory. Both implementations are consistent from a mathematical perspective, but from a physical perspective the former implementation is more justified. Indeed, this has been the procedure followed in previous conformally reduced FRGE studies [67], where a non-Gaussian fixed point was also found. It would of course be ideal to study a truncation of this form in the case of the full theory, where such coarse graining ambiguities do not arise. Considering such a truncation, however, is currently beyond the technical scope of the FRGE framework in gravity.

In Chapter 4, we returned to the case of full gravity, and constructed a functional renormalization group equation that allowed us to study general truncations of the $f(R)$ form, where $f(R)$ are arbitrary functions of the curvature scalar. By first taking $f(R)$ to be a polynomial of up to order six, we reproduced the results of [69], which established the existence of a non-Gaussian fixed point with three UV-attractive directions and remarkably stable numerical properties in all these truncation subspaces. Then, in Chapter 5 we considered non-local truncations built from non-polynomial functions of R. We established on general grounds that terms of this type can be consistently decoupled from the rest of the renormalization group flow. By explicitly studying two non-local extensions of this form to the Einstein-Hilbert truncation, the $ln(R)$ and R^{-n} truncations, we showed that, although these truncations lead to non-trivial modifications of the IR properties of the flow – in particular, the beta functions in the $ln(R)$ case admit a non-trivial fixed point which dynamically drives the cosmological constant to zero in the IR – they are unable to describe physics in the UV. The latter feature is characteristic of the class of non-local operators considered in that chapter and persists under the inclusion of other terms in the truncation. Using our decoupling result, we can therefore consistently remove all such terms from the gravitational flow to arrive at the region of the renormalization group space compatible with UV physics. The polynomial $f(R)$ results of [69] recovered in Chapter 4 then suggest that this region is dominated by a non-Gaussian fixed point in the UV. The prospects for asymptotic safety are thus encouraging, at least as far as the $f(R)$-sector is concerned.

On the other hand, a caveat of these truncations is that by considering only powers of the curvature scalar they omit tensorial terms which could have a major impact on the asymptotic safety scenario. It is precisely terms of the latter form which feature as non-renormalizable counterterms in the perturbative quantization of general relativity. In Chapter 6, we therefore moved beyond the $f(R)$-case by explicitly including such terms at four-derivative order in our truncation. Remarkably, we found that a non-Gaussian fixed point with a three-dimensional UV critical surface still persists in this setting. We then added a minimally coupled, massless scalar field to our truncation, noting that this setup provides the prototype of a gravitational theory which is perturbatively non-renormalizable at

one-loop level. The resulting fixed point structure was strikingly similar to the pure gravity case. Thus, contrary to a commonly raised objection with respect to the $f(R)$ results, we found that the inclusion of perturbative counterterms of this type in our truncation subspace has no qualitative effect on the non-perturbative renormalizability of the theory.

The coherent picture that arises from these studies, together with the other results in the literature cited throughout this thesis, provides significant evidence in favor of the asymptotic safety scenario, and suggests that non-perturbative effects might indeed provide a solution to the Planck-scale troubles of quantum gravity. While the evidence we have gathered here is inductive and cannot guarantee that a non-trivial fixed point will exist in the full flow space, it is nevertheless remarkable that such a fixed point persists in all truncations studied so far.

From the perspective of the FRGE approach to gravity, the limitations we have encountered in further extending the truncation subspaces that can be treated make a compelling argument for the development of new tools for the evaluation of the flow equation. These would enable one to tackle the notorious two-loop counterterm of perturbative gravity, so as to lend further evidence to the asymptotic safety scenario, or the conformal anomaly effective action in the full theory, so as to gain a better understanding of the renormalization group behavior of gravity in the IR, or to go beyond some of the restrictions of the truncation ansatz we have considered here.

From a more general perspective, there are of course several issues related to the quantum behavior of gravity that we have not touched upon in the present work. Particularly relevant examples concern the properties of our UV theory of gravity from the perspective of spacetime geometry, or how to construct quantum observables within a gravitational setting [25, 145]. While such issues have begun to be treated within the FRGE framework [43, 88, 146], they are also the primary focus of research within other non-perturbative approaches to gravity (e.g., [147, 148]). It would therefore be interesting to explore the connection between the FRGE and these frameworks. This may be pursued both at the level of reconstructing quantities such as the bare action and regularized path integrals from FRGE renormalization group trajectories, following [71], and of relating resulting theoretical predictions between such different approaches. In the latter context, a possible point of contact is the phenomenon of spontaneous dimensional reduction that has been reported across these works and which also features as an immediate consequence of asymptotic safety, though whether or not this is more than a coincidence remains to be established. While exploring this connection is no straightforward task, non-perturbative approaches to quantum gravity are few and far between, and understanding to which extent these approaches might be related can provide crucial insights into gravitational physics in the UV.

Ultimately, however, we would like to arrive at testable quantum gravity predictions. In the context of asymptotic safety, this requires understanding what are the observable consequences of our putative asymptotically safe theory of grav-

ity. Over and above the theoretical evidence we may gather for the asymptotic safety conjecture, or the merits and flaws of the different approaches we have here mentioned, the question of the ultimate nature of quantum gravity is something that must be determined by experimental data. It is perhaps overtly optimistic to expect any direct experimental or observable tests of quantum gravity in the near future, but one can aim to establish indirect tests for such theories in light of, e.g., astrophysical and cosmological observations [149]. Mapping the renormalization group flow of gravity could be an important step in that direction.

A

Notations and curvature conventions

In this section, we collect the notations and conventions used in this thesis. Throughout the work, (anti-)symmetrization is with unit strength,

$$A_{(\mu}B_{\nu)} = \tfrac{1}{2}(A_\mu B_\nu + A_\nu B_\mu), \qquad A_{[\mu}B_{\nu]} = \tfrac{1}{2}(A_\mu B_\nu - A_\nu B_\mu).$$

Our Euclidean space-time metric is positive definite, $\mathrm{sig}(g_{\mu\nu}) = \{+,+,+,+\}$. Covariant expressions constructed from the classical metric $g_{\mu\nu}$ are denoted as usual, while tensors covariant with respect to the background metric $\bar{g}_{\mu\nu}$ are distinguished by a bar. Our definition of the curvature invariants follows [150],

$$R^\rho{}_{\lambda\mu\nu} = \partial_\mu \Gamma^\rho{}_{\nu\lambda} + \dots\,, \quad R_{\mu\nu} = R^\lambda{}_{\mu\lambda\nu}\,, \quad R = g^{\mu\nu}R_{\mu\nu}\,, \tag{A.1}$$

and ∇_μ denotes the covariant derivative with respect to $g_{\mu\nu}$. The latter satisfies $2\nabla_{[\mu}\nabla_{\nu]}A_\lambda = R_{\mu\nu\lambda}{}^\sigma A_\sigma$. The contraction of the Bianchi-identity furthermore implies

$$\nabla_\lambda R^\lambda{}_{\sigma\mu\nu} = \nabla_\mu R_{\nu\sigma} - \nabla_\nu R_{\mu\sigma}\,. \tag{A.2}$$

The Weyl tensor is the traceless part of the Riemann tensor,

$$C_{\mu\nu\rho\sigma} = R_{\mu\nu\rho\sigma} - \frac{2}{d-2}\left(g_{\mu[\rho}R_{\sigma]\nu} - g_{\nu[\rho}R_{\sigma]\mu}\right) + \frac{2}{(d-1)(d-2)}R\, g_{\mu[\rho}g_{\sigma]\nu}\,, \tag{A.3}$$

and the square of the Weyl tensor is related to the other curvature invariants by

$$C_{\mu\nu\rho\sigma}C^{\mu\nu\rho\sigma} = R_{\mu\nu\rho\sigma}R^{\mu\nu\rho\sigma} - \frac{4}{d-2}R_{\mu\nu}R^{\mu\nu} + \frac{2}{(d-1)(d-2)}R^2\,. \tag{A.4}$$

For four-dimensional space-times, it is useful to introduce the Euler density

$$E := R^2 - 4R_{\mu\nu}R^{\mu\nu} + R_{\mu\nu\rho\sigma}\,R^{\mu\nu\rho\sigma}\,. \tag{A.5}$$

The integral $\int d^4x\sqrt{g}E = 32\pi^2\chi$ is a topological invariant and proportional to the Euler character χ of the space-time. In particular, it is independent of $g_{\mu\nu}$. Thus, its variation with respect to the space-time metric vanishes identically.

Throughout this thesis, we work with background metrics $\bar{g}_{\mu\nu}$ which are four-dimensional Einstein metrics unless otherwise noted. They satisfy the condition

$$\bar{R}_{\mu\nu} = \frac{\bar{R}}{4}\bar{g}_{\mu\nu}\,. \tag{A.6}$$

These spaces have the advantage that the transverse traceless decomposition of the metric, ghost and auxiliary fields is orthogonal. Furthermore, the relations (A.5) and (A.4) then simplify to

$$\bar{E} = \bar{R}_{\mu\nu\rho\sigma}\,\bar{R}^{\mu\nu\rho\sigma}\,, \quad \bar{C}_{\mu\nu\rho\sigma}\bar{C}^{\mu\nu\rho\sigma} = \bar{R}_{\mu\nu\rho\sigma}\bar{R}^{\mu\nu\rho\sigma} - \frac{1}{6}\bar{R}^2\,, \tag{A.7}$$

while the contracted Bianchi-identity (A.2) implies that the Riemann-tensor is covariantly constant

$$\bar{\nabla}^\lambda \bar{R}_{\lambda\sigma\mu\nu} = 0\,. \tag{A.8}$$

The maximally symmetric background metrics S^d used in the first five chapters of this thesis are a subset of the Einstein spaces defined above.

B

Second variations

B.1 Basic variations of curvature invariants

We here collect the second variations of the curvature invariants, which we have used to construct the flow equation in Chapter (4). These expressions are found in Table B.1

B.2 The Hessian $\Gamma_k^{(2)}$ for higher-derivative gravity

In this section, we present some of the intermediate steps in the derivation of the Hessians in Chapter 6. In four dimensions, the derivative expansion of $\Gamma_k^{\rm grav}[g]$ up to fourth order can be organized into the five interaction monomials,

$$\begin{aligned} I_0 &= \int \mathrm{d}^4x\sqrt{g}\,, \qquad I_1 = \int \mathrm{d}^4x\sqrt{g}R\,, \\ I_2 &= \int \mathrm{d}^4x\sqrt{g}R^2\,, \quad I_3 = \int \mathrm{d}^4x\sqrt{g}R_{\mu\nu}R^{\mu\nu}\,, \quad I_4 = \int d^4x\sqrt{g}E \end{aligned} \tag{B.1}$$

where $E = R^2 - 4R_{\mu\nu}R^{\mu\nu} + R_{\mu\nu\rho\sigma}\,R^{\mu\nu\rho\sigma}$ is the integrand of the Euler topological invariant, $\int d^4x\sqrt{g}E = 32\pi^2\chi$. Constructing the argument of the traces entering into the FRGE requires the second variation of these invariants. In this context, we first note that I_4 is a topological quantity, so that its variation with respect to the metric vanishes. To obtain the hessians of the other invariants, we split $g_{\mu\nu} = \bar{g}_{\mu\nu} + h_{\mu\nu}$, where $\bar{g}_{\mu\nu}$ denotes a fixed background metric and $h_{\mu\nu}$ is an arbitrary fluctuation. The general expressions for these variations, valid for an arbitrary background $\bar{g}_{\mu\nu}$, can be found in [129] (see also [49, 134, 137, 151]). For our purposes, however, it suffices to consider these variations on backgrounds $\bar{g}_{\mu\nu} = \bar{g}^{\mathcal{E}}_{\mu\nu}$, where the index $\mathcal{E}$ indicates that the background metric is a generic

Basic variations of curvature invariants

$\delta g_{\mu\nu}$	$\equiv$	$h_{\mu\nu}$
$\delta g^{\mu\nu}$	$=$	$-h^{\mu\nu}$
$\delta\Gamma^{\lambda}{}_{\mu\nu}$	$=$	$\frac{1}{2}g^{\lambda\sigma}\left(\nabla_\mu h_{\nu\sigma}+\nabla_\nu h_{\mu\sigma}-\nabla_\sigma h_{\mu\nu}\right)$
$\delta\sqrt{g}$	$=$	$\frac{1}{2}\sqrt{g}\,h$
$\delta R^{\lambda}{}_{\sigma\mu\nu}$	$=$	$\nabla_{[\mu}\nabla_\sigma h_{\nu]}{}^{\lambda}+\nabla_{[\mu}\nabla_{\nu]}h_\sigma{}^{\lambda}-\nabla_{[\mu}\nabla^{\lambda}h_{\nu]\sigma}$
$\delta R^{\alpha\beta}{}_{\mu\nu}$	$=$	$h_\lambda{}^{[\alpha}R^{\beta]\lambda}{}_{\mu\nu}-2\nabla_{[\mu}\nabla^{[\alpha}h^{\beta]}{}_{\nu]}$
$\delta R_{\mu\nu}$	$=$	$\frac{1}{2}\big(2R_{\sigma(\mu}h_{\nu)}{}^{\sigma}+2R_{\sigma\mu\nu\lambda}h^{\sigma\lambda}+2\nabla_{(\mu}\nabla^{\sigma}h_{\nu)\sigma}-\nabla_\mu\nabla_\nu h$
		$-\nabla_\sigma\nabla^\sigma h_{\mu\nu}\big)$
δR	$=$	$-R^{\mu\nu}h_{\mu\nu}+\nabla_\alpha\nabla_\beta h^{\alpha\beta}-\nabla_\alpha\nabla^\alpha h$
$\delta^2\sqrt{g}$	$=$	$\frac{1}{2}\sqrt{g}\left(\frac{1}{2}h^2-h_{\mu\nu}h^{\mu\nu}\right)$
$\delta^2\Gamma^{\lambda}{}_{\mu\nu}$	$=$	$-h^{\lambda\sigma}\left(\nabla_\mu h_{\nu\sigma}+\nabla_\nu h_{\mu\sigma}-\nabla_\sigma h_{\mu\nu}\right)$
$\delta^2 R^{\alpha\beta}{}_{\mu\nu}$	$=$	$-2\,h_{\lambda\sigma}\,h^{\lambda[\alpha}\,R^{\beta]\sigma}{}_{\mu\nu}-4h_\lambda{}^{[\alpha}\left(\nabla_{[\mu}\nabla^{\beta]}h_{\nu]}{}^{\lambda}-\nabla_{[\mu}\nabla^{\lambda}h^{\beta]}{}_{\nu]}\right)$
		$-\left(\nabla_{[\mu}h^{\alpha\sigma}+\nabla^\alpha h^\sigma{}_{[\mu}-\nabla^\sigma h^\alpha{}_{[\mu}\right)$
		$\left(\nabla^\beta h_{\nu]\sigma}+\nabla_{\nu]}h_\sigma{}^{\beta}-\nabla_\sigma h_{\nu]}{}^{\beta}\right)$
$\delta^2 R_{\mu\nu}$	$=$	$h^{\alpha\beta}\left(\nabla_{(\mu}\nabla_{\nu)}h_{\alpha\beta}+\nabla_\alpha\nabla_\beta h_{\mu\nu}-2\nabla_\alpha\nabla_{(\mu}h_{\nu)\beta}\right)$
		$+\left(\frac{1}{2}\nabla^\beta h-\nabla_\alpha h^{\alpha\beta}\right)\left(2\nabla_{(\mu}h_{\nu)\beta}-\nabla_\beta h_{\mu\nu}\right)$
		$+\frac{1}{2}\left(\nabla_\mu h_{\alpha\beta}\right)\left(\nabla_\nu h^{\alpha\beta}\right)+\left(\nabla_\alpha h_{\mu\beta}\right)\left(\nabla^\alpha h^\beta{}_\nu-\nabla^\beta h^\alpha{}_\nu\right)$
$\delta^2 R$	$=$	$R_{\alpha\beta}\,h^{\beta\gamma}\,h_\gamma{}^{\alpha}-R_{\alpha\beta\mu\nu}\,h^{\alpha\nu}\,h^{\beta\mu}-3h^{\alpha\beta}\nabla_\beta\nabla_\lambda h^\lambda{}_\alpha$
		$+2h^{\alpha\beta}\nabla_\alpha\nabla_\beta h+2h^{\alpha\beta}\nabla^2 h_{\alpha\beta}-h^{\alpha\beta}\nabla_\lambda\nabla_\beta h_\alpha{}^{\lambda}$
		$-\left(\nabla_\alpha h^{\beta\lambda}\right)\left(\nabla_\beta h^\alpha{}_\lambda\right)+\frac{3}{2}\left(\nabla_\lambda h_{\alpha\beta}\right)\left(\nabla^\lambda h^{\alpha\beta}\right)$
		$-2\left(\nabla_\alpha h^\alpha{}_\beta\right)\left(\nabla_\lambda h^{\lambda\beta}\right)+2\left(\nabla_\alpha h^{\alpha\beta}\right)\left(\nabla_\beta h\right)$
		$-\frac{1}{2}\left(\nabla_\alpha h\right)\left(\nabla^\alpha h\right)$

Table B.1: First and second variations of the curvature quantities used in the main text.

Einstein metric. At the two-derivative level, we then obtain

$$\begin{aligned}\delta^2 I_0 &= \int_{\mathcal{E}} d^4x\sqrt{\bar{g}}\left[\tfrac{1}{4}h^2-\tfrac{1}{2}h_{\mu\nu}h^{\mu\nu}\right]\,,\\ \delta^2 I_1 &= \int_{\mathcal{E}} d^4x\sqrt{\bar{g}}\Big[\tfrac{1}{2}h^{\alpha\beta}\left[\bar{\nabla}^2-\tfrac{1}{2}\bar{R}\right]h_{\alpha\beta}+\bar{R}_{\alpha\mu\beta\nu}h^{\alpha\beta}h^{\mu\nu}\\ &\qquad -\tfrac{1}{2}h\bar{\nabla}^2 h+h(\bar{\nabla}^\alpha\bar{\nabla}^\beta h_{\alpha\beta})+(\bar{\nabla}^\mu h_{\mu\alpha})(\bar{\nabla}_\nu h^{\nu\alpha})\Big]\,,\end{aligned}\tag{B.2}$$

while the variations of the four-derivative terms yield

$$\delta^2 I_2 = \int_{\mathcal{E}} d^4x\sqrt{\bar{g}}\Big\{ 2h\left[\bar{\nabla}^4 - \tfrac{1}{16}\bar{R}^2\right] h + \bar{R}h^{\alpha\beta}\bar{\nabla}^2 h_{\alpha\beta} + 2\bar{R}\,\bar{R}_{\alpha\mu\beta\nu}h^{\alpha\beta}h^{\mu\nu} \\ + 2(\bar{\nabla}_\alpha\bar{\nabla}_\beta h^{\alpha\beta})^2 + (\bar{\nabla}_\alpha\bar{\nabla}_\beta h^{\alpha\beta})\left[-4\bar{\nabla}^2 + \bar{R}\right] h + 2\bar{R}(\bar{\nabla}_\alpha h^{\alpha\beta})(\bar{\nabla}^\mu h_{\mu\beta})\Big\}, \tag{B.3}$$

and

$$\delta^2 I_3 = \int_{\mathcal{E}} d^4x\,\sqrt{\bar{g}}\Big\{ \tfrac{1}{2}h^{\alpha\beta}\left[\bar{\nabla}^4 + \tfrac{1}{2}\bar{R}\bar{\nabla}^2\right] h_{\alpha\beta} + \tfrac{1}{2}h\left[\bar{\nabla}^4 - \tfrac{1}{4}\bar{R}\bar{\nabla}^2 - \tfrac{1}{8}\bar{R}^2\right] h \\ - (\bar{\nabla}_\alpha\bar{\nabla}_\beta h^{\alpha\beta})\left[\bar{\nabla}^2 - \tfrac{\bar{R}}{2}\right] h + (\bar{\nabla}_\alpha h^{\alpha\beta})\left[\bar{\nabla}^2 + \tfrac{3\bar{R}}{4}\right](\bar{\nabla}^\mu h_{\mu\beta}) \\ + (\bar{\nabla}_\alpha\bar{\nabla}_\beta h^{\alpha\beta})^2 - 2h_{\alpha\beta}\bar{R}^{\alpha\mu\nu\beta}\left[\bar{\nabla}^2 + \tfrac{1}{4}\bar{R}\right] h_{\mu\nu} + 2h_{\alpha\beta}\bar{R}^{\alpha\lambda\beta\sigma}\bar{R}_{\lambda\mu\sigma\nu}h^{\mu\nu}\Big\}, \tag{B.4}$$

respectively. We have defined here $h = \bar{g}^{\mu\nu}h_{\mu\nu}$.

A remarkable feature of these variations is that they can naturally be written in terms of second order minimal operators of Lichnerowicz form (6.4). In particular, the four-derivative operators appearing in (B.4) and (B.3) factorize into squares of these (modified) Laplacians.

C

Trace evaluation for type III cutoffs

In this Appendix, we collect some of the formulas necessary for the evaluation of the traces of the fourth-order operators appearing in Chapter 3. As we have seen, the traces of the functions $W(\Delta)$ appearing on the right-hand side of the FRGE may be evaluated via the asymptotic keat kernel expansion

$$TrW(\Delta) = \frac{1}{(4\pi)^2}\Big[Q_{\frac{4}{p}}(W)\mathrm{B}_0(\Delta) + Q_{\frac{2}{p}}(W)\mathrm{B}_2(\Delta) + Q_0(W)\mathrm{B}_d(\Delta) + \dots\Big]\,, \quad \text{(C.1)}$$

where Δ is an elliptic operator of order p and the functionals $Q_n[W]$ are given by (2.34). For the specific cases of the operators $\hat{\mathcal{O}}_i$ appearing in (3.47), the heat kernel coefficients may be computed using the formulas in, e.g., [109–112], and read

$$\begin{aligned}
\mathrm{B}_4^{\mathrm{mat}} = \int d^4x\,\sqrt{\hat{g}}\Big\{ & 32\pi^2 c_4 \hat{R}^2 + \frac{n_S + 2n_M - n_D}{2}(\hat{\Box}\bar{\sigma})^2 \\
& + \frac{n_S + 2n_M - n_D}{2}((\hat{\nabla}\bar{\sigma})^2)^2 - \frac{n_S - n_M - n_D}{6}\hat{R}\hat{\Box}\bar{\sigma} \\
& - \frac{n_S + 2n_M - n_D}{6}\hat{R}(\hat{\nabla}\bar{\sigma})^2 + (n_S + 2n_M - n_D)\Box\bar{\sigma}(\hat{\nabla}\bar{\sigma})^2\Big\}\,, \\
\mathrm{B}_2^{\mathrm{mat}} = \int d^4x\,\sqrt{\hat{g}}\Big\{ & 32\pi^2 c_2 \hat{R} + (n_S + 8n_M - 10n_D)\hat{\Box}\bar{\sigma} \\
& - (n_S - 4n_M + 2n_D)(\hat{\nabla}\bar{\sigma})^2\Big\}\,, \\
\mathrm{B}_0^{\mathrm{mat}} = \int d^4x\,\sqrt{\hat{g}} 32\pi^2 c_0\,,
\end{aligned}$$

for the local matter contributions and

$$
\begin{aligned}
\mathrm{B}_0(\hat{\mathcal{O}}) =& \int dx\,\sqrt{\hat{g}}\,,\\
\mathrm{B}_2(\hat{\mathcal{O}}) =& \sqrt{\pi}\int dx\,\sqrt{\hat{g}}\Big\{\left[\frac{1}{12}+\frac{36g_{43}-b'}{12\tilde{Q}}\right]\hat{R}+\frac{3(g_{23}-2g_{22})}{2\tilde{Q}}e^{2\bar{\sigma}}\\
&-\frac{27g_{45}}{\tilde{Q}}(\hat{\nabla}\bar{\sigma})^2-\frac{27g_{46}}{\tilde{Q}}\hat{\Box}\bar{\sigma}\Big\}\,,\\
\mathrm{B}_4(\hat{\mathcal{O}}) =& \int dx\,\sqrt{\hat{g}}\Big\{\left[-\frac{4g_0}{\tilde{Q}}+\frac{9(g_{23}-2g_{22})^2}{\tilde{Q}^2}\right]e^{4\bar{\sigma}}\\
&+\left[\frac{g_{23}-2g_{22}-2g_{21}}{2\tilde{Q}}+\frac{(g_{23}-2g_{22})(36g_{43}-b')}{\tilde{Q}^2}\right]e^{2\bar{\sigma}}\hat{R}\\
&+\left[\frac{29}{2160}+\frac{36g_{43}-b'}{36\tilde{Q}}+\frac{(36g_{43}-b')^2}{36\tilde{Q}^2}\right]\hat{R}^2\\
&+\left[\frac{6g_{22}}{\tilde{Q}}-\frac{324g_{46}(g_{23}-2g_{22})}{\tilde{Q}^2}\right]e^{2\bar{\sigma}}\hat{\Box}\bar{\sigma}\\
&+\left[\frac{6g_{23}}{\tilde{Q}}-\frac{324g_{45}(g_{23}-2g_{22})}{\tilde{Q}^2}\right]e^{2\bar{\sigma}}(\hat{\nabla}\bar{\sigma})^2\\
&-\left[\frac{9g_{46}}{\tilde{Q}}+\frac{18g_{46}(36g_{43}-b')}{\tilde{Q}^2}\right]\hat{R}\hat{\Box}\bar{\sigma}\\
&-\left[\frac{9g_{45}}{\tilde{Q}}+\frac{18g_{45}(36g_{43}-b')+108g_{46}^2}{\tilde{Q}^2}\right]\hat{R}(\hat{\nabla}\bar{\sigma})^2\\
&+\frac{6480g_{45}g_{46}}{\tilde{Q}^2}(\hat{\nabla}\bar{\sigma})^2\hat{\Box}\bar{\sigma}+\frac{3240g_{45}^2}{\tilde{Q}^2}((\hat{\nabla}\bar{\sigma})^2)^2+\frac{3240g_{46}^2}{\tilde{Q}^2}(\hat{\Box}\bar{\sigma})^2\Big\}\,,
\end{aligned}
$$

where we have defined $\tilde{Q}\equiv(36g_{44}+2b')$. The case of the Weyl-invariant operators appearing in (3.32) in Section 4 may be readily obtained from the above by letting $\hat{g}_{\mu\nu}\mapsto\bar{g}_{\mu\nu}$ and $\bar{\sigma}\mapsto 0$.

Using the generalized optimized cutoff $R_k(z)=(k^p-z)\Theta(k^p-z)$ for the pth-order operators, the functions $Q_i\left(\frac{\partial_t R_k}{P_k}\right)$ may also be straightforwardly evaluated. Imposing the cutoff on the $\hat{\mathcal{O}}_i$ from Sections 4 and 5, we find

$$
Q_0=p\,,\qquad Q_{\frac{1}{2}}=\frac{2p}{\sqrt{\pi}}k^{p/2}\,,\qquad Q_1=pk^p\,,\qquad Q_2=\frac{p}{2}k^{2p}\,. \tag{C.2}
$$

D

Heat Kernel coefficients

This appendix collects the relevant formulas for the heat kernel expansion of the operator traces appearing in our flow equations.

D.1 Heat-kernel expansion on the d-spheres

D.1.1 Heat-kernel coefficients for unconstrained fields

The key formula for evaluating operator traces built from the covariant Laplacian $-\nabla^2$ is the early-time expansion of the heat-kernel

$$\mathrm{Tr}\left[\mathrm{e}^{-t(-\nabla^2+Q)}\right] = \left(\frac{1}{4\pi t}\right)^{d/2} \int d^d x \sqrt{g} \left\{ \mathrm{tr}\, \mathbf{b}_0 + t\,\mathrm{tr}\, \mathbf{b}_2(x;Q) + t^2\, \mathrm{tr}\, \mathbf{b}_4(x;Q) + \ldots \right\} . \tag{D.1}$$

Here, Q denotes a matrix potential, which we take to be proportional to the unit matrix in field space, and the $\mathbf{b}_{2k}$ are the heat-kernel or Seeley coefficients. Furthermore, "tr" denotes a matrix trace in field space running over the tensor indices of the fields on which $-\nabla^2$ acts. The derivation of the partial differential equation governing the renormalization group flow of $f(R)$ gravity in Chapter 4 requires the knowledge of (some of) the $\mathbf{b}_{2k}$ up to $k = 4$.

The first two coefficients in the expansion (D.1) are universal, in the sense that they do not depend on whether $-\nabla^2$ acts on unconstrained scalar, vector, or symmetric tensor fields:

$$\mathbf{b}_0 = \mathbf{1} , \qquad \mathbf{b}_2(x;Q) = P , \qquad P := Q + \frac{1}{6} R\, \mathbf{1} . \tag{D.2}$$

Here, $\mathbf{1}$ denotes the unit matrix in the corresponding field space, i.e., $\mathbf{1}_{(0)} := 1$, $[\mathbf{1}_{(1)}]_{\mu\nu} := g_{\mu\nu}$, and $[\mathbf{1}_{(2)}]_{\mu\nu\rho\sigma} := g_{\mu\rho} g_{\nu\sigma}$. Starting from $\mathbf{b}_4(x;Q)$, the heat-kernel

coefficients include the commutator of two covariant derivatives on field space,

$$\mathcal{R}_{\mu\nu} := [\nabla_\mu\,,\,\nabla_\nu] = \nabla_\mu\nabla_\nu - \nabla_\nu\nabla_\mu\,. \tag{D.3}$$

The corresponding terms then give different contributions to the $\mathbf{b}_{2k}$, depending on whether $-\nabla^2$ acts on scalars, vectors, or tensor fields. For $\mathbf{b}_4(Q)$ we have

$$\begin{aligned}
\mathbf{b}_4(Q) &= \left[\tfrac{5d^2-7d+6}{360d(d-1)}R^2 + \tfrac{1}{6}QR + \tfrac{1}{2}Q^2\right]\mathbf{1}_{(0)}\,,\\
[\mathbf{b}_4(Q)]_{\mu\nu} &= \left[\tfrac{5d^3-7d^2+6d-60}{360d^2(d-1)}R^2 + \tfrac{1}{6}QR + \tfrac{1}{2}Q^2\right]\left[\mathbf{1}_{(1)}\right]_{\mu\nu}\,,\\
[\mathbf{b}_4(Q)]_{\mu\nu\rho\sigma} &= \left[\tfrac{5d^3-7d^2+6d-120}{360d^2(d-1)}R^2 + \tfrac{1}{6}QR + \tfrac{1}{2}Q^2\right]\left[\mathbf{1}_{(2)}\right]_{\mu\nu\rho\sigma}\\
&\quad + \tfrac{R^2}{3d^2(d-1)^2}\Big[g_{\mu\nu}g_{\rho\sigma} - g_{\mu\sigma}g_{\nu\rho}\Big]\,,
\end{aligned} \tag{D.4}$$

for spin 0,1, and 2, respectively. In order to find the contributions from $\mathbf{b}_6(x;Q)$, we start from the general formulas in [152] and restrict to spherically symmetric backgrounds[1] . Taking into account the different normalizations, this yields

$$\begin{aligned}
\mathbf{b}_6(Q) =& \tfrac{1}{3!}\left[P^3 - \tfrac{d-3}{30\,d(d-1)}\,P\,R^2 - \tfrac{2(d+2)(d-3)}{945\,d^2(d-1)^2}R^3\right]\,,\\
[\mathbf{b}_6(Q)]_{\mu\nu} =& \tfrac{1}{3!}\left[P^3 - \tfrac{d^2-3d+30}{30\,d^2(d-1)}PR^2 - \tfrac{2d^3-2d^2+177d-126}{945\,d^3(d-1)^2}R^3\right]\left[\mathbf{1}_{(1)}\right]_{\mu\nu}\,,\\
[\mathbf{b}_6(Q)]_{\mu\nu\rho\sigma} =& \tfrac{1}{3!}\left[P^3 - \tfrac{d-3}{30\,d(d-1)}\,P\,R^2 - \tfrac{2(d+2)(d-3)}{945\,d^2(d-1)^2}R^3\right]\left[\mathbf{1}_{(2)}\right]_{\mu\nu\rho\sigma}\\
&+ \tfrac{1}{3d^2(d-1)^2}\,PR^2\Big[g_{\mu\nu}g_{\rho\sigma} - g_{\mu\rho}g_{\nu\sigma}\Big]\\
&+ \tfrac{1}{45d^3(d-1)^3}\,R^3\Big[(3d-2)g_{\mu\nu}g_{\rho\sigma} - 4(d-1)g_{\mu\rho}g_{\nu\sigma}\Big]\,.
\end{aligned} \tag{D.5}$$

For $k = 4$ we need the scalar coefficient $\mathbf{b}_8(Q)$ only. Using the general formulas in [152] this becomes

$$\begin{aligned}
\mathbf{b}_8(Q) =& \frac{1}{4!}\Big[P^4 - \tfrac{d-3}{15d(d-1)}R^2P^2 - \tfrac{8\,(d-3)(d+2)}{945\,d^2\,(d-1)^2}R^3P\\
&+ \tfrac{(d-3)(7d^3-32d^2-59d-60)}{18900\,d^3\,(d-1)^3}R^4\Big]\,.
\end{aligned} \tag{D.6}$$

Consulting the expansion of the traces (4.77), (4.78), and (4.83), we then see that the knowledge of these heat-kernel coefficients suffices to evaluate the right-hand side of (4.61) in Chapter 4.

D.1.2 Heat-kernel coefficients for fields with differential constraints

The fields $h^{\mathrm{T}}_{\mu\nu}$ and ξ^μ are subject to the constraints given by the TT decomposition and thus, to compute their heat kernel coefficients, we must modify the

[1] Note that the Heat-Kernel coefficients defined in [152] differ from the ones in (D.1) by a factor $(k/2)!$.

T_s	s	$\Lambda_l(d,s)$	$\nabla_l(d,s)$	
$T^{lm}_{\mu\nu}(x)$	2	$\frac{l(l+d-1)-2}{d(d-1)}R$	$\frac{(d+1)(d-2)(l+d)(l-1)(2l+d-1)(l+d-3)!}{2(d-1)!(l+1)!}$	$l\geq 2$
$T^{lm}_{\mu}(x)$	1	$\frac{l(l+d-1)-1}{d(d-1)}R$	$\frac{l(l+d-1)(2l+d-1)(l+d-3)!}{(d-2)!(l+1)!}$	$l\geq 1$
$T^{lm}(x)$	0	$\frac{l(l+d-1)}{d(d-1)}R$	$\frac{(2l+d-1)(l+d-2)}{l!(d-1)!}$	$l\geq 0$

Table D.1: Eigenvalues and degeneracies of $-\nabla^2$ on the d-sphere. Here $T^{lm}(x)$, $T^{lm}_{\mu}(x)$ and $T^{lm}_{\mu\nu}$ form a complete orthonormal basis for the $-\nabla^2$-eigenfunctions for scalars, transverse vectors and transverse traceless symmetric tensors. Their eigenvalues in d dimensions are given by $Lambda_l(d,s)$ with degeneracy $\nabla_l(d,s)$. We refer to [37] for more details.

formulas for spin 1 and 2 fields accordingly. To do so, we first note that the TT decompositions (4.7) and (4.9) imply the following relations between the heat-kernel traces over the constrained and unconstrained fields

$$\begin{aligned}
\mathrm{Tr}_{(1)}\left[\mathrm{e}^{t(\nabla^2+qR)}\right] &= \mathrm{Tr}_{1\mathrm{T}}\left[\mathrm{e}^{t(\nabla^2+qR)}\right] + \mathrm{Tr}_0\left[\mathrm{e}^{t(\nabla^2+\frac{dq+1}{d}R)}\right] - \mathrm{e}^{t\,\frac{dq+1}{d}R}\,,\\
\mathrm{Tr}_{(2)}\left[\mathrm{e}^{t(\nabla^2+qR)}\right] &= \mathrm{Tr}_{2\mathrm{T}}\left[\mathrm{e}^{t(\nabla^2+qR)}\right] + \mathrm{Tr}_{1\mathrm{T}}\left[\mathrm{e}^{t(\nabla^2+\left(\frac{d+1}{d(d-1)}+q\right)R)}\right]\\
&\quad + \mathrm{Tr}_0\left[\mathrm{e}^{t(\nabla^2+\left(\frac{2}{d-1}+q\right)R)}\right] + \mathrm{Tr}_0\left[\mathrm{e}^{t(\nabla^2+qR)}\right]\\
&\quad - \mathrm{e}^{t\left(\frac{2}{d-1}+q\right)R} - (d+1)\,\mathrm{e}^{t\left(\frac{1}{d-1}+q\right)R}\\
&\quad - \tfrac{d(d+1)}{2}\,\mathrm{e}^{t\left(\frac{2}{d(d-1)}+q\right)R}\,.
\end{aligned} \tag{D.7}$$

Here we set $Q = qR\mathbf{1}$. There are two types of terms appearing on the right-hand side of these equations, complete traces with respect to the constrained fields and contributions from a discrete set of eigenvalues, which are required to complete the traces. The relations (D.7) then allow us to compute the heat-kernel coefficients for the constrained fields from their unconstrained counterparts given in the last subsection. Defining $b_{2k}|_s := \mathrm{tr}\,[\,\mathbf{b}_{2k}|_s\,]$ with $s = 0, 1\mathrm{T}, 2\mathrm{T}$ denoting the spin of the constrained field and performing the trace over vector indices explicitly we find

$$\begin{aligned}
b_0|_{1\mathrm{T}} &= d-1\,,\\
b_2|_{1\mathrm{T}} &= \frac{1}{6d}\,(d+2)(d-3)\,R\,,\\
b_4|_{1\mathrm{T}} &= \frac{5d^4-12d^3-47d^2-186d+180}{360\,d^2\,(d-1)}\,R^2\,,
\end{aligned} \tag{D.8}$$

and

$$
\begin{aligned}
b_0|_{2\mathrm{T}} &= \frac{1}{2}(d-2)(d+1)\,,\\
b_2|_{2\mathrm{T}} &= \frac{(d-5)(d+1)(d+2)}{12\,(d-1)}\,R\,,\\
b_4|_{2\mathrm{T}} &= \frac{(d+1)(5d^4-22d^3-83d^2-392d-228)}{720\,d\,(d-1)^2}\,R^2\,,\\
b_6|_{2\mathrm{T}} &= \frac{(d+1)(d+2)(35d^5-287d^4-93d^3-7765d^2+1966d-14016)}{90720\,d^2\,(d-1)^3}\,R^3\,,
\end{aligned}
\tag{D.9}
$$

for the heat-kernel coefficients of $\mathrm{Tr}_{1\mathrm{T}}[\mathrm{e}^{\mathrm{i}t\nabla^2}]$ and $\mathrm{Tr}_{2\mathrm{T}}[\mathrm{e}^{\mathrm{i}t\nabla^2}]$, respectively. Since the traces (D.7) are evaluated under a Fourier integral (cfg. eq. (2.31)) it is also straightforward to deal with the discrete mode terms. Carrying out their (inverse) Fourier transform, these become proportional to δ-functions, which allow for an easy evaluation of the subsequent s-integral.

For the computations in Chapters 4 and 5 it is also convenient to give the numerical value of the heat-kernel coefficients for the special case $d = 4$. In the scalar sector, setting $Q = 0$, we have

$$
\begin{aligned}
&b_0|_0 = 1\,, \quad b_2|_0 = \frac{1}{6}\,R\,, \quad b_4|_0 = \frac{29}{2160}\,R^2\,,\\
&b_6|_0 = \frac{37}{54332}\,R^3\,, \quad b_8|_0 = \frac{149}{6531840}\,R^4\,,
\end{aligned}
\tag{D.10}
$$

while (D.8) and (D.9) yield

$$
\begin{aligned}
&\mathrm{tr}\,[b_0|_{1\mathrm{T}}] = 3\,, \quad \mathrm{tr}\,[b_2|_{1\mathrm{T}}] = \frac{1}{4}\,R\,, \quad \mathrm{tr}\,[b_4|_{1\mathrm{T}}] = -\frac{67}{1440}\,R^2\,,\\
&\mathrm{tr}\,[b_0|_{2\mathrm{T}}] = 5\,, \quad \mathrm{tr}\,[b_2|_{2\mathrm{T}}] = -\frac{5}{6}\,R\,, \quad \mathrm{tr}\,[b_4|_{2\mathrm{T}}] = -\frac{271}{432}\,R^2\,,\\
&\mathrm{tr}\,[b_6|_{2\mathrm{T}}] = -\frac{7249}{54432}\,R^3\,.
\end{aligned}
\tag{D.11}
$$

Lastly, when writing down the flow equations in Chapters 4 and 5, we used the following shorthand notation for the d-dependent factors of the heat-kernel coefficients, obtained by setting $R = 1$ in the formulas above

$$
\begin{aligned}
&C^{\mathrm{S}}_{2k}(d) := b_{2k}|_0(R=1)\,, \quad C^{1\mathrm{T}}_{2k}(d) := b_{2k}|_{1\mathrm{T}}(R=1)\,,\\
&C^{2\mathrm{T}}_{2k}(d) := b_{2k}|_{2\mathrm{T}}(R=1)\,.
\end{aligned}
\tag{D.12}
$$

D.2 Heat-kernel coefficients for Lichnerowicz Laplacians

When evaluating the operator traces appearing in Chapter 6, we require the heat-kernel expansion for the Lichnerowicz operators (6.4), evaluated at a generic Einstein manifold, up to fourth order in the derivative expansion. In this appendix, we derive the corresponding coefficients starting from the early time heat-kernel expansion of a generic two-derivative differential operator [152] (see also [41] for a nice exposition in the context of the FRG).

D.2.1 Heat-kernel coefficients for unconstrained fields

As we have seen when discussing the case of Laplacian operators the previous section, the early time heat-kernel expansion of a generic second order differential operator $\Delta = -\nabla^2 + \mathbf{Q}$ takes the form (D.1) with

$$\begin{aligned}\mathbf{b}_0 &= \mathbf{1}\,, \qquad \mathbf{b}_2 = P\,,\\ \mathbf{b}_4 &= \frac{1}{180}\left(R_{\mu\nu\alpha\beta}R^{\mu\nu\alpha\beta} - R_{\mu\nu}R^{\mu\nu} + \nabla^2 R\right)\mathbf{1} + \frac{1}{2}P^2 + \frac{1}{12}\mathcal{R}_{\mu\nu}\mathcal{R}^{\mu\nu} + \frac{1}{6}\nabla^2 P\,,\end{aligned} \tag{D.13}$$

and where the other quantities are defined in the section above. For our computations, we have to evaluate $\mathrm{tr}_s\,\mathbf{b}_{2k}$ for scalars ($s = 0$), vectors ($s = 1$), and symmetric tensors ($s = 2$). In the latter two cases, the tr_s are defined as

$$\mathrm{tr}_1\mathbf{b}_{2k} = g^{\mu\nu}[\mathbf{b}_{2k}]_{(\mu\nu)}\,, \qquad \mathrm{tr}_2\mathbf{b}_{2k} = g^{\mu\rho}g^{\nu\sigma}[\mathbf{b}_{2k}]_{(\mu\nu)(\rho\sigma)}\,, \tag{D.14}$$

respectively. The matrices $\mathcal{R}_{\mu\nu}\mathcal{R}^{\mu\nu}$ are trivial for the scalar case, whereas for vectors and tensors they respectively read

$$\begin{aligned}\left[\mathcal{R}_{\alpha\beta}\mathcal{R}^{\alpha\beta}\right]_{\mu\nu} &= -R_{\alpha\beta\gamma\mu}R^{\alpha\beta\gamma}{}_{\nu}\,,\\ \left[\mathcal{R}_{\alpha\beta}\mathcal{R}^{\alpha\beta}\right]_{\mu\nu\rho\sigma} &= -R_{\alpha\beta\gamma\mu}R^{\alpha\beta\gamma}{}_{\rho}\,g_{\nu\sigma} - R_{\alpha\beta\gamma\nu}R^{\alpha\beta\gamma}{}_{\sigma}\,g_{\mu\rho} + 2R_{\alpha\beta\mu\rho}R^{\alpha\beta}{}_{\nu\sigma}\,.\end{aligned} \tag{D.15}$$

The differential operators appearing in the traces of our higher derivative truncation are the Lichnerowicz operators (6.4), i.e., second order differential operators with matrix-potentials

$$\mathbf{Q}_0 = 0\,, \qquad [\mathbf{Q}_1]_{\mu\nu} = \frac{1}{4}g_{\mu\nu}R\,, \qquad [\mathbf{Q}_2]_{\mu\nu\alpha\beta} = 2R_{\mu\alpha\nu\beta}\,. \tag{D.16}$$

Their heat-kernel coefficients on a generic four-dimensional Einstein manifold without boundary can be obtained by substituting these potentials into the expressions for the generic heat-kernel expansion. Evaluating the spin-traces, we

obtain

$$\begin{aligned}
&\mathrm{tr}_0\mathbf{b}_0 = 1\,, \quad \mathrm{tr}_0\mathbf{b}_2 = \tfrac{1}{6}R\,, \quad \mathrm{tr}_0\mathbf{b}_4 = \tfrac{1}{180}R_{\mu\nu\alpha\beta}R^{\mu\nu\alpha\beta} + \tfrac{1}{80}R^2\,,\\
&\mathrm{tr}_1\mathbf{b}_0 = 4\,, \quad \mathrm{tr}_1\mathbf{b}_2 = \tfrac{5}{3}R\,, \quad \mathrm{tr}_1\mathbf{b}_4 = -\tfrac{11}{180}R_{\mu\nu\alpha\beta}R^{\mu\nu\alpha\beta} + \tfrac{41}{120}R^2\,,\\
&\mathrm{tr}_2\mathbf{b}_0 = 10\,, \quad \mathrm{tr}_2\mathbf{b}_2 = \tfrac{2}{3}R\,, \quad \mathrm{tr}_2\mathbf{b}_4 = \tfrac{19}{18}R_{\mu\nu\alpha\beta}R^{\mu\nu\alpha\beta} - \tfrac{1}{24}R^2\,.
\end{aligned} \tag{D.17}$$

This result completes the heat-kernel expansion for unconstrained fields.

D.2.2 Heat-kernel coefficients for fields with differential constraints

In order to apply the early-time heat-kernel expansion to our operator traces, the heat-kernel coefficients for the unconstrained fields given in the last subsection must be converted into the expansion coefficients for the transverse vectors (1T) and transverse-traceless symmetric matrices (2T) entering into the TT-decomposition.

In the decomposition of a vector field into its transverse and longitudinal parts,

$$A_\mu = A^{\mathrm{T}}_\mu + \nabla_\mu\Phi\,, \qquad \nabla^\mu A^{\mathrm{T}}_\mu = 0\,, \tag{D.18}$$

the spectra of $\nabla_\mu\Phi$ and Φ are related by

$$\Delta_{1L}\nabla_\mu\Phi = \nabla_\mu(\Delta_{0L} - \tfrac{1}{2}R)\Phi\,, \tag{D.19}$$

and the constant mode in Φ does not contribute to A_μ. Thus, the decomposition of the $s = 1$-trace takes the form

$$\mathrm{Tr}_{1\mathrm{T}}\left[\mathrm{e}^{\mathrm{i}t\Delta_{1L}}\right] = \mathrm{Tr}_1\left[\mathrm{e}^{\mathrm{i}t\Delta_{1L}}\right] - \mathrm{Tr}_0\left[\mathrm{e}^{\mathrm{i}t(\Delta_{0L}-R/2)}\right] + \mathrm{e}^{-\mathrm{i}tR/2}\,. \tag{D.20}$$

where the last term removes the constant Φ-mode from the $s = 0$-trace. A similar argument applies to the TT-decomposition of the symmetric tensor,

$$h_{\mu\nu} = h^{\mathrm{T}}_{\mu\nu} + 2\nabla_{(\mu}\xi_{\nu)} + \nabla_\mu\nabla_\nu\sigma + \frac{1}{4}g_{\mu\nu}\Delta_{0L}\sigma + \frac{1}{4}g_{\mu\nu}h\,, \tag{D.21}$$

where the components appearing on the RHS of this decomposition are subject to the constraints

$$g^{\mu\nu}\,h^{\mathrm{T}}_{\mu\nu} = 0\,, \quad \nabla^\mu h^{\mathrm{T}}_{\mu\nu} = 0\,, \quad \nabla^\mu\xi_\mu = 0\,, \quad h = g_{\mu\nu}h^{\mu\nu}\,. \tag{D.22}$$

In this case, one can use

$$\begin{aligned}
&\Delta_{2L}\nabla_\mu\xi_\nu = \nabla_\mu\Delta_{1L}\xi_\nu\,,\\
&\Delta_{2L}\left[\nabla_\mu\nabla_\nu + \tfrac{1}{4}g_{\mu\nu}\Delta_{0L}\right]\sigma = \left[\nabla_\mu\nabla_\nu + \tfrac{1}{4}g_{\mu\nu}\Delta_{0L}\right]\left[\Delta_{0L} - \tfrac{R}{2}\right]\sigma\,,\\
&\Delta_{2L}g_{\mu\nu}h = g_{\mu\nu}\left[\Delta_{0L} - \tfrac{R}{2}\right]h\,,
\end{aligned} \tag{D.23}$$

to relate the spectrum of Δ_{2L} to the ones of the vector and scalar fields. Furthermore, (D.21) indicates that the constant mode in σ, scalars subject to $\left[\nabla_\mu\nabla_\nu + \frac{1}{4}g_{\mu\nu}\Delta_{0L}\right]\sigma = 0$, and transverse vectors satisfying $\nabla_{(\mu}\xi_{\nu)} = 0$ do not contribute to $h_{\mu\nu}$, so that the corresponding modes have to be removed from the decomposed spectrum. By contracting the last two equations with ∇^ν, one can show that these are eigenmodes of Δ_{0L} and Δ_{1L} with eigenvalues $\Lambda_{0L} = 0$, $\Lambda_{0L} = \frac{R}{3}$, and $\Lambda_{1L} = 0$, respectively.[2] The multiplicity of the latter two is given by the number of Killing vectors n_{KV} and conformal Killing vectors n_{CKV} of the background. Taking into account (D.20), the operator trace for transverse-traceless tensors field can then be expressed in terms of traces over unconstrained fields

$$\begin{aligned}\mathrm{Tr}_{2\mathrm{T}}\left[\mathrm{e}^{\mathrm{i}t\Delta_{2L}}\right] = \mathrm{Tr}_2\left[\mathrm{e}^{\mathrm{i}t\Delta_{2L}}\right] - \mathrm{Tr}_1\left[\mathrm{e}^{\mathrm{i}t\Delta_{1L}}\right] - \mathrm{Tr}_0\left[\mathrm{e}^{\mathrm{i}t(\Delta_{0L}-R/2)}\right] \\ + n_{\mathrm{KV}} + n_{\mathrm{CKV}}\mathrm{e}^{-\mathrm{i}tR/6}\,.\end{aligned} \tag{D.24}$$

In Chapter 6, we have assumed that our background is generic, in the sense that its metric does not admit Killing or conformal Killing vectors.

From eqs. (D.20) and (D.24) it is then straightforward to compute the heat-kernel coefficients for Lichnerowicz Laplacians acting on transverse vectors and transverse traceless symmetric matrices. For a generic Einstein background, these read

$$\begin{aligned}&\mathrm{tr}_0\mathbf{b}_0 = 1\,, \quad \mathrm{tr}_0\mathbf{b}_2 = \tfrac{1}{6}R\,, \quad \mathrm{tr}_0\mathbf{b}_4 = \tfrac{1}{180}\,R_{\mu\nu\alpha\beta}R^{\mu\nu\alpha\beta} + \tfrac{1}{80}\,R^2\,,\\ &\mathrm{tr}_{1\mathrm{T}}\mathbf{b}_0 = 3\,, \quad \mathrm{tr}_{1\mathrm{T}}\mathbf{b}_2 = R\,, \quad \mathrm{tr}_{1\mathrm{T}}\mathbf{b}_4 = -\tfrac{1}{15}\,R_{\mu\nu\alpha\beta}R^{\mu\nu\alpha\beta} + \tfrac{29}{240}\,R^2\,,\\ &\mathrm{tr}_{2\mathrm{T}}\mathbf{b}_0 = 5\,, \quad \mathrm{tr}_{2\mathrm{T}}\mathbf{b}_2 = -\tfrac{5}{3}R\,, \quad \mathrm{tr}_{2\mathrm{T}}\mathbf{b}_4 = \tfrac{10}{9}\,R_{\mu\nu\alpha\beta}R^{\mu\nu\alpha\beta} - \tfrac{29}{48}\,R^2\,.\end{aligned} \tag{D.25}$$

These coefficients are the key ingredient for evaluating the operator traces in the higher derivative truncation.

[2] For a spherical background, these coincide with the two lowest eigenmodes of $-\nabla^2$ acting on scalars and the lowest eigenmode of $-\nabla^2$ acting on vector fields [40, 41].

E

Threshold functions and cutoff profiles

This appendix collects the details about the standardized dimensionless threshold functions $\Phi^p_n(w), \tilde{\Phi}^p_n(w)$ and $\Upsilon^p_{n;m}(u,v,w), \tilde{\Upsilon}^p_{n,m,l}(u,v,w)$, which were used to encapsulate the cutoff-scheme dependence of our flow equations in the main part of this paper. We start by giving their general definitions and some of their properties in Appendix E.1, before specializing to particular profile functions in Appendix E.2.

E.1 General definitions

In order to construct the β-functions for the dimensionless couplings, it is useful to convert the $Q_n[W]$ into standardized dimensionless threshold functions,

$$\begin{aligned}\Phi^p_n(w) &:= \frac{1}{\Gamma(n)} \int_0^\infty \mathrm{d}z\, z^{n-1}\, \frac{R^{(0)}(z) - zR^{(0)\prime}(z)}{(z + R^{(0)}(z) + w)^p}\,, \\ \tilde{\Phi}^p_n(w) &:= \frac{1}{\Gamma(n)} \int_0^\infty \mathrm{d}z\, z^{n-1}\, \frac{R^{(0)}(z)}{(z + R^{(0)}(z) + w)^p}\,,\end{aligned} \tag{E.1}$$

and their generalizations,

$$\Upsilon^p_{n,m}(u,v,w) := \frac{1}{\Gamma(n)} \int_0^\infty \mathrm{d}z\, z^{n-1}\, \frac{\left(z + R^{(0)}(z)\right)^m \left(R^{(0)}(z) - zR^{(0)\prime}(z)\right)}{\left(u\left(z + R^{(0)}(z)\right)^2 + v\left(z + R^{(0)}(z)\right) + w\right)^p}\,,$$

$$\tilde{\Upsilon}^p_{n,m,l}(u,v,w) := \frac{1}{\Gamma(n)} \int_0^\infty \mathrm{d}z\, z^{n-1}\, \frac{\left(z + R^{(0)}(z)\right)^m \left(2z + R^{(0)}(z)\right)^l R^{(0)}(z)}{\left(u\left(z + R^{(0)}(z)\right)^2 + v\left(z + R^{(0)}(z)\right) + w\right)^p}\,, \tag{E.2}$$

defined for $n > 0$. Here, $R^{(0)}(z)$ is a dimensionless profile function determining the shape of the IR cutoff, while the prime denotes the derivative with respect to the argument. The profile function satisfies

$$\lim_{z\to 0} R^{(0)}(z) = \text{const}\,, \qquad \lim_{z\to\infty} R^{(0)}(z) = 0\,, \tag{E.3}$$

For convenience, we choose $R^{(0)}(0) = 1$.

We note that both $\Phi^p_n(w)$ and $\tilde{\Phi}^p_n(w)$ satisfy a recursion relation when taking derivatives with respect to their argument,

$$\partial_w \Phi^p_n(w) = -p\,\Phi^{p+1}_n(w)\,, \qquad \partial_w \tilde{\Phi}^p_n(w) = -p\,\tilde{\Phi}^{p+1}_n(w)\,. \tag{E.4}$$

The standard threshold functions (E.1) are contained in (E.2) as a special case,

$$\Upsilon^p_{n;0}(0,1,w) = \Phi^p_n(w)\,, \quad \tilde{\Upsilon}^p_{n,0;0}(0,1,w) = \tilde{\Phi}^p_n(w)\,. \tag{E.5}$$

Obviously, the generalized threshold functions are homogeneous of degree $-p$ under a common rescaling of their arguments

$$\begin{aligned} \Upsilon^p_{n,m}(\lambda u, \lambda v, \lambda w) &= \lambda^{-p}\,\Upsilon^p_{n,m}(u,v,w)\,, \\ \tilde{\Upsilon}^p_{n,m,l}(\lambda u, \lambda v, \lambda w) &= \lambda^{-p}\,\tilde{\Upsilon}^p_{n,m,l}(u,v,w)\,. \end{aligned} \tag{E.6}$$

Furthermore, they satisfy recursion relations similar to (E.4),

$$\begin{aligned} \partial_u\,\Upsilon^p_{n,m}(u,v,w) &= -p\,\Upsilon^{p+1}_{n,m+2}(u,v,w)\,, \\ \partial_v\,\Upsilon^p_{n,m}(u,v,w) &= -p\,\Upsilon^{p+1}_{n,m+1}(u,v,w)\,, \\ \partial_w\,\Upsilon^p_{n,m}(u,v,w) &= -p\,\Upsilon^{p+1}_{n,m}(u,v,w)\,, \\ \partial_u\,\tilde{\Upsilon}^p_{n,m,l}(u,v,w) &= -p\,\tilde{\Upsilon}^{p+1}_{n,m+2,l}(u,v,w)\,, \\ \partial_v\,\tilde{\Upsilon}^p_{n,m,l}(u,v,w) &= -p\,\tilde{\Upsilon}^{p+1}_{n,m+1,l}(u,v,w)\,, \\ \partial_w\,\tilde{\Upsilon}^p_{n,m,l}(u,v,w) &= -p\,\tilde{\Upsilon}^{p+1}_{n,m,l}(u,v,w)\,. \end{aligned} \tag{E.7}$$

The recursion relations (E.4) and (E.7) are particularly useful when performing the series expansions of R-dependent arguments.

Lastly, note that the $\Phi^{n+1}_n(0)$ are "universal", i.e, independent of the choice of the profile function $R^{(0)}_k(z)$ and can be computed using only the generic properties (E.3) [41]

$$\Phi^{n+1}_n(0) = \frac{1}{\Gamma(n+1)} \int_0^\infty \mathrm{d}z\, \frac{\mathrm{d}}{\mathrm{d}z} \left[\frac{z^n}{z + R^{(0)}(z)}\right] = \frac{1}{\Gamma(n+1)}\,. \tag{E.8}$$

When evaluating the four-derivative truncations it is furthermore convenient to introduce

$$\varphi := \partial_t \ln(R_k)|_{z=0}\,, \tag{E.9}$$

which is also universal by virtue of (E.3).

The functionals $Q_n[W]$ appearing in the trace expansion of the FRGE may be expressed in terms of the threshold functions above. For the particular functions W occurring in this paper, these relations are

$$Q_n\left[\tfrac{\partial_t(g_kR_k)}{(2g_k)(P_k+c_k)^p}\right] = k^{2(n-p+1)}\left(\Phi^p_n(c_k/k^2)+\tfrac{1}{2}\partial_t\ln(g_k)\,\tilde\Phi^p_n(c_k/k^2)\right), \quad n>0, \tag{E.10}$$

and

$$\begin{aligned} &Q_n\left[\frac{\partial_t\left(g_k(P_k^2-\mathcal{O}^2)+\tilde g_kR_k\right)}{(u_kP_k^2+v_kP_k+w_k)^p}\right] \\ &\quad= k^{2(n-2p+2)}\left\{\partial_t g_k\,\tilde\Upsilon^p_{n,0,1}(u_k,v_k/k^2,w_k/k^4)+4g_k\Upsilon^p_{n,1}(u_k,v_k/k^2,w_k/k^4)\right\} \\ &\qquad+k^{2(n-2p+1)}\left\{\partial_t\tilde g_k\,\tilde\Upsilon^p_{n,0,0}(u_k,v_k/k^2,w_k/k^4)+2\tilde g_k\Upsilon^p_{n,0}(u_k,v_k/k^2,w_k/k^4)\right\}. \end{aligned} \tag{E.11}$$

In the case of the $f(R)$ truncations, $\mathcal{O}=-\nabla^2$, while for the higher derivate truncations, $\mathcal{O}=-\Delta^2_{sL}$.

E.2 Profile functions

All numerical evaluations require a particular choice of the dimensionless cutoff profile function $R^{(0)}(z)$. In this work, we have employed two one-parameter families of shape functions, the generalized optimized cutoff [72] [72],

$$R^{(0)}_{\rm opt}(z)=(1-bz)\,\theta(1-bz), \tag{E.12}$$

and the (smooth) exponential cutoff,

$$R^{(0)}_{\rm exp}(z)=\frac{bz}{\mathrm{e}^{bz}-1}. \tag{E.13}$$

Here b is a free shape parameter, essentially encoding how fast the fluctuation spectrum is cut off. At $z=0$, both cutoffs give

$$R^{(0)}|_{z=0}=1, \qquad \partial_tR^{(0)}|_{z=0}=0, \qquad \varphi=2. \tag{E.14}$$

In most of our calculations, we have restricted ourselves to the use of the optimized cutoff with shape parameter $b=1$. Unless otherwise noted, we have referred to this cutoff profile as 'the' optimized cutoff,

$$R^{(0)}_{\rm opt}(z)=(1-z)\,\theta(1-z). \tag{E.15}$$

The main virtue of this choice of cutoff is that all the integrals appearing in the (generalized) threshold functions can be carried out analytically. In particular,

$$\Phi_n^p(w) = \frac{1}{\Gamma(n+1)} \frac{1}{(1+w)^p}\,, \quad \tilde{\Phi}_n^p(w) = \frac{1}{\Gamma(n+2)} \frac{1}{(1+w)^p}\,. \tag{E.16}$$

Similarly, the generalized threshold functions (E.2) become

$$\begin{aligned} \Upsilon_{n,m}^p(u,v,w) &= \frac{1}{\Gamma(n+1)} \frac{1}{(u+v+w)^p}\,, \\ \tilde{\Upsilon}_{n,m;l}^p(u,v,w) &= \frac{(-1)^n}{\Gamma(n)} \frac{\beta(-1,n,l+1)+\beta(-1,n+1,l+1)}{(u+v+w)^p}\,. \end{aligned} \tag{E.17}$$

Here, $\beta(-1,n,l)$ denotes the incomplete beta function. For fixed values n,l, these become constants. This property leads to considerable simplifications in the analysis of the corresponding beta functions.

Bibliography

[1] M. Gell-Mann and F. E. Low, Phys. Rev. **95**, 1300 (1954).

[2] E. C. G. Stueckelberg and A. Petermann, Helv. Phys. Acta **26**, 499 (1953).

[3] N. N. Bogoliubov and D. V. Shirkov, *Introduction to the theory of quantized fields* (Wiley-Interscience, New York, 1959).

[4] K. G. Wilson, Phys. Rev. **B4**, 3174 (1971).

[5] K. G. Wilson, Phys. Rev. **B4**, 3184 (1971).

[6] K. G. Wilson, Phys. Rev. Lett. **28**, 548 (1972).

[7] K. G. Wilson and J. B. Kogut, Phys. Rept. **12**, 75 (1974).

[8] J. L. Cardy, *Scaling and renormalization in statistical physics* (Cambridge, UK: Univ. Pr., 1996).

[9] J. Zinn-Justin, *Quantum field theory and critical phenomena* (Oxford, UK: Clarendon, 2002).

[10] M. E. Fisher, Rev. Mod. Phys. **70**, 653 (1998).

[11] J. Polchinski, Nucl. Phys. **B231**, 269 (1984).

[12] J. J. Binney, N. J. Dowrick, A. J. Fisher, and M. E. J. Newman, *The Theory of critical phenomena: An Introduction to the renormalization group* (Oxford, UK: Clarendon, 1992).

[13] H. D. Politzer, Phys. Rept. **14**, 129 (1974).

[14] S. Deser, Annalen Phys. **9**, 299 (2000), gr-qc/9911073.

[15] G. 't Hooft and M. J. G. Veltman, Annales Poincare Phys. Theor. **A20**, 69 (1974).

[16] S. Deser and P. van Nieuwenhuizen, Phys. Rev. **D10**, 401 (1974).

[17] S. Deser and P. van Nieuwenhuizen, Phys. Rev. **D10**, 411 (1974).

[18] S. Deser, H.-S. Tsao, and P. van Nieuwenhuizen, Phys. Rev. **D10**, 3337 (1974).

[19] M. H. Goroff and A. Sagnotti, Phys. Lett. **B160**, 81 (1985).

[20] A. E. M. van de Ven, Nucl. Phys. **B378**, 309 (1992).

[21] C. P. Burgess, Living Rev. Rel. **7**, 5 (2004), gr-qc/0311082.

[22] N. E. J. Bjerrum-Bohr, J. F. Donoghue, and B. R. Holstein, Phys. Rev. **D67**, 084033 (2003), hep-th/0211072.

[23] D. Oriti, *Approaches to quantum gravity: Toward a new understanding of space, time and matter* (Cambridge, UK: Cambridge Univ. Pr., 2009).

[24] S. Carlip, Rept. Prog. Phys. **64**, 885 (2001), gr-qc/0108040.

[25] C. Rovelli, Class. Quant. Grav. **8**, 297 (1991).

[26] O. Aharony, S. S. Gubser, J. M. Maldacena, H. Ooguri, and Y. Oz, Phys. Rept. **323**, 183 (2000), hep-th/9905111.

[27] B. de Wit and H. Nicolai, Nucl. Phys. **B208**, 323 (1982).

[28] Z. Bern, J. J. Carrasco, L. J. Dixon, H. Johansson, and R. Roiban, Phys. Rev. Lett. **103**, 081301 (2009), 0905.2326.

[29] P. Horava, Phys. Rev. **D79**, 084008 (2009), 0901.3775.

[30] J. Ambjorn, J. Jurkiewicz, and R. Loll, Phys. Rev. **D72**, 064014 (2005), hep-th/0505154.

[31] J. Henson, (2006), gr-qc/0601121.

[32] C. Rovelli, Living Rev. Rel. **11**, 5 (2008).

[33] S. Weinberg, (1979), in 'General Relativity' ed. S.W. Hawking, W. Israel, Cambridge Univ. Pr.

[34] S. Weinberg, (2009), 0908.1964.

[35] M. Reuter, Phys. Rev. **D57**, 971 (1998), hep-th/9605030.

[36] W. Souma, Prog. Theor. Phys. **102**, 181 (1999), hep-th/9907027.

[37] O. Lauscher and M. Reuter, Phys. Rev. **D65**, 025013 (2002), hep-th/0108040.

[38] M. Reuter and F. Saueressig, Phys. Rev. **D65**, 065016 (2002), hep-th/0110054.

[39] D. F. Litim, Phys. Rev. Lett. **92**, 201301 (2004), hep-th/0312114.

[40] O. Lauscher and M. Reuter, Phys. Rev. **D66**, 025026 (2002), hep-th/0205062.

[41] A. Codello, R. Percacci, and C. Rahmede, Annals Phys. **324**, 414 (2009), 0805.2909.

[42] K. Gawedzki and A. Kupiainen, Phys. Rev. Lett. **55**, 363 (1985).

[43] O. Lauscher and M. Reuter, (2005), hep-th/0511260.

[44] M. Niedermaier, Class. Quant. Grav. **24**, R171 (2007), gr-qc/0610018.

[45] D. F. Litim, AIP Conf. Proc. **841**, 322 (2006), hep-th/0606044.

[46] J. Ambjorn, J. Jurkiewicz, and R. Loll, Phys. Rev. Lett. **95**, 171301 (2005), hep-th/0505113.

[47] S. Carlip, (2009), 0909.3329.

[48] R. Gastmans, R. Kallosh, and C. Truffin, Nucl. Phys. **B133**, 417 (1978).

[49] S. M. Christensen and M. J. Duff, Phys. Lett. **B79**, 213 (1978).

[50] L. Smolin, Nucl. Phys. **B208**, 439 (1982).

[51] P. Forgacs and M. Niedermaier, (2002), hep-th/0207028.

[52] M. Niedermaier, Nucl. Phys. **B673**, 131 (2003), hep-th/0304117.

[53] J. Ambjorn, A. Gorlich, J. Jurkiewicz, and R. Loll, Phys. Rev. **D78**, 063544 (2008), 0807.4481.

[54] C. Wetterich, Phys. Lett. **B301**, 90 (1993).

[55] N. C. Tsamis and R. P. Woodard, Ann. Phys. **238**, 1 (1995).

[56] I. L. Shapiro, Class. Quant. Grav. **25**, 103001 (2008), 0801.0216.

[57] I. Antoniadis, P. O. Mazur, and E. Mottola, New J. Phys. **9**, 11 (2007), gr-qc/0612068.

[58] S. Nojiri and S. D. Odintsov, ECONF **C0602061**, 06 (2006), hep-th/0601213.

[59] R. P. Woodard, Lect. Notes Phys. **720**, 403 (2007), astro-ph/0601672.

[60] S. Capozziello, M. De Laurentis, and V. Faraoni, (2009), 0909.4672.

[61] T. R. Morris, Prog. Theor. Phys. Suppl. **131**, 395 (1998), hep-th/9802039.

[62] C. Bagnuls and C. Bervillier, Phys. Rept. **348**, 91 (2001), hep-th/0002034.

[63] D. F. Litim, JHEP **07**, 005 (2005), hep-th/0503096.

[64] T. R. Morris, JHEP **07**, 027 (2005), hep-th/0503161.

[65] J. Berges, N. Tetradis, and C. Wetterich, Phys. Rept. **363**, 223 (2002), hep-ph/0005122.

[66] H. Gies, (2006), hep-ph/0611146.

[67] M. Reuter and H. Weyer, (2008), 0801.3287.

[68] I. Antoniadis and E. Mottola, Phys. Rev. **D45**, 2013 (1992).

[69] A. Codello, R. Percacci, and C. Rahmede, Int. J. Mod. Phys. **A23**, 143 (2008), arXiv:0705.1769.

[70] J. M. Pawlowski, Annals Phys. **322**, 2831 (2007), hep-th/0512261.

[71] E. Manrique and M. Reuter, Phys. Rev. **D79**, 025008 (2009), 0811.3888.

[72] D. F. Litim, Phys. Rev. **D64**, 105007 (2001), hep-th/0103195.

[73] D. F. Litim and J. M. Pawlowski, Phys. Rev. **D65**, 081701 (2002), hep-th/0111191.

[74] D. F. Litim and J. M. Pawlowski, Phys. Rev. **D66**, 025030 (2002), hep-th/0202188.

[75] D. F. Litim, Nucl. Phys. **B631**, 128 (2002), hep-th/0203006.

[76] D. F. Litim, Phys. Lett. **B486**, 92 (2000), hep-th/0005245.

[77] P. Fischer and D. F. Litim, AIP Conf. Proc. **861**, 336 (2006), hep-th/0606135.

[78] F. Freire and D. F. Litim, Phys. Rev. **D64**, 045014 (2001), hep-ph/0002153.

[79] E. Manrique and M. Reuter, (2009), 0907.2617.

[80] A. Eichhorn, H. Gies, and M. M. Scherer, (2009), 0907.1828.

[81] D. F. Litim and J. M. Pawlowski, (1998), hep-th/9901063.

[82] D. Dou and R. Percacci, Class. Quant. Grav. **15**, 3449 (1998), hep-th/9707239.

[83] R. Percacci and D. Perini, Phys. Rev. **D67**, 081503 (2003), hep-th/0207033.

[84] R. Percacci, Phys. Rev. **D73**, 041501 (2006), hep-th/0511177.

[85] M. Reuter and H. Weyer, Phys. Rev. **D80**, 025001 (2009), 0804.1475.

[86] M. Reuter and F. Saueressig, Fortsch. Phys. **52**, 650 (2004), hep-th/0311056.

[87] M. Reuter and H. Weyer, Phys. Rev. **D70**, 124028 (2004), hep-th/0410117.

[88] M. Reuter and H. Weyer, JCAP **0412**, 001 (2004), hep-th/0410119.

[89] M. Reuter and H. Weyer, Int. J. Mod. Phys. **D15**, 2011 (2006), hep-th/0702051.

[90] M. Reuter and F. Saueressig, JCAP **0509**, 012 (2005), hep-th/0507167.

[91] A. Bonanno and M. Reuter, JCAP **0708**, 024 (2007), 0706.0174.

[92] I. Antoniadis, P. O. Mazur, and E. Mottola, Nucl. Phys. **B388**, 627 (1992), hep-th/9205015.

[93] I. Antoniadis, P. O. Mazur, and E. Mottola, Phys. Lett. **B323**, 284 (1994), hep-th/9301002.

[94] I. Antoniadis, P. O. Mazur, and E. Mottola, Phys. Rev. **D55**, 4756 (1997), hep-th/9509168.

[95] I. Antoniadis, P. O. Mazur, and E. Mottola, Phys. Rev. **D55**, 4770 (1997), hep-th/9509169.

[96] I. Antoniadis, P. O. Mazur, and E. Mottola, Phys. Lett. **B394**, 49 (1997), hep-th/9611145.

[97] R. J. Riegert, Phys. Lett. **B134**, 56 (1984).

[98] P. O. Mazur and E. Mottola, Phys. Rev. **D64**, 104022 (2001), hep-th/0106151.

[99] I. Antoniadis, P. O. Mazur, and E. Mottola, Phys. Rev. Lett. **79**, 14 (1997), astro-ph/9611208.

[100] I. Antoniadis, P. O. Mazur, and E. Mottola, Phys. Lett. **B444**, 284 (1998), hep-th/9808070.

[101] E. Mottola and R. Vaulin, Phys. Rev. **D74**, 064004 (2006), gr-qc/0604051.

[102] M. J. Duff, Nucl. Phys. **B125**, 334 (1977).

[103] R. Floreanini and R. Percacci, Nucl. Phys. **B436**, 141 (1995), hep-th/9305172.

[104] E. Mottola, J. Math. Phys. **36**, 2470 (1995), hep-th/9502109.

[105] Z. Bern, E. Mottola, and S. K. Blau, Phys. Rev. **D43**, 1212 (1991).

[106] M. Reuter and C. Wetterich, Nucl. Phys. **B506**, 483 (1997), hep-th/9605039.

[107] P. F. Machado and F. Saueressig, Phys. Rev. **D77**, 124045 (2008), 0712.0445.

[108] R. Percacci and D. Perini, Phys. Rev. **D68**, 044018 (2003), hep-th/0304222.

[109] N. H. Barth, J. Phys. **A20**, 857 (1987).

[110] N. H. Barth, J. Phys. **A20**, 875 (1987).

[111] V. P. Gusynin, Phys. Lett. **B225**, 233 (1989).

[112] H. W. Lee, P. Y. Pac, and H. K. Shin, Phys. Rev. **D35**, 2440 (1987).

[113] J. W. York, Jr., J. Math. Phys. **14**, 456 (1973).

[114] P. Fischer and D. F. Litim, Phys. Lett. **B638**, 497 (2006), hep-th/0602203.

[115] G. Cognola, E. Elizalde, S. Nojiri, S. D. Odintsov, and S. Zerbini, JCAP **0502**, 010 (2005), hep-th/0501096.

[116] A. O. Barvinsky, Y. V. Gusev, G. A. Vilkovisky, and V. V. Zhytnikov, J. Math. Phys. **35**, 3543 (1994), gr-qc/9404063.

[117] A. O. Barvinsky and D. V. Nesterov, (2004), hep-th/0402043.

[118] O. Lauscher and M. Reuter, Class. Quant. Grav. **19**, 483 (2002), hep-th/0110021.

[119] S. M. Carroll, V. Duvvuri, M. Trodden, and M. S. Turner, Phys. Rev. **D70**, 043528 (2004), astro-ph/0306438.

[120] S. Nojiri and S. D. Odintsov, Phys. Rev. **D68**, 123512 (2003), hep-th/0307288.

[121] C. Wetterich, Gen. Rel. Grav. **30**, 159 (1998), gr-qc/9704052.

[122] M. Reuter and F. Saueressig, Phys. Rev. **D66**, 125001 (2002), hep-th/0206145.

[123] S. Deser and R. P. Woodard, Phys. Rev. Lett. **99**, 111301 (2007), 0706.2151.

[124] P. O. Mazur and E. Mottola, Nucl. Phys. **B341**, 187 (1990).

[125] T. P. Sotiriou and V. Faraoni, (2008), 0805.1726.

[126] L. N. Granda and S. D. Odintsov, Phys. Lett. **B409**, 206 (1997), hep-th/9706062.

[127] S. Deser and P. van Nieuwenhuizen, Phys. Rev. Lett. **32**, 245 (1974).

[128] D. F. Litim and J. M. Pawlowski, Phys. Lett. **B435**, 181 (1998), hep-th/9802064.

[129] N. H. Barth and S. M. Christensen, Phys. Rev. **D28**, 1876 (1983).

[130] A. Codello and R. Percacci, Phys. Rev. Lett. **97**, 221301 (2006), hep-th/0607128.

[131] G. de Berredo-Peixoto and I. L. Shapiro, Phys. Rev. **D71**, 064005 (2005), hep-th/0412249.

[132] I. L. Buchbinder, S. D. Odintsov, and I. L. Shapiro, *Effective action in quantum gravity* (Bristol, UK: IOP, 1992).

[133] K. S. Stelle, Phys. Rev. **D16**, 953 (1977).

[134] J. Julve and M. Tonin, Nuovo Cim. **B46**, 137 (1978).

[135] E. S. Fradkin and A. A. Tseytlin, Phys. Lett. **B104**, 377 (1981).

[136] E. S. Fradkin and A. A. Tseytlin, Nucl. Phys. **B201**, 469 (1982).

[137] I. G. Avramidi and A. O. Barvinsky, Phys. Lett. **B159**, 269 (1985).

[138] K. S. Stelle, Gen. Rel. Grav. **9**, 353 (1978).

[139] A. Salam and J. A. Strathdee, Phys. Rev. **D18**, 4480 (1978).

[140] M. R. Niedermaier, Phys. Rev. Lett. **103**, 101303 (2009).

[141] Y. V. Gryzov, A. Y. Kamenshchik, and I. P. Karmazin, Russ. Phys. J. 35 (1992) 201-205. (Izv. VUZ, Fiz. (1992) No. 2 121-126).

[142] A. O. Barvinsky, A. Y. Kamenshchik, and I. P. Karmazin, Phys. Rev. **D48**, 3677 (1993), gr-qc/9302007.

[143] S. M. Christensen and M. J. Duff, Nucl. Phys. **B170**, 480 (1980).

[144] H. Gies and M. M. Scherer, (2009), 0901.2459.

[145] S. B. Giddings, D. Marolf, and J. B. Hartle, Phys. Rev. **D74**, 064018 (2006), hep-th/0512200.

[146] M. Reuter and J.-M. Schwindt, JHEP **01**, 049 (2007), hep-th/0611294.

[147] J. Ambjorn, J. Jurkiewicz, and R. Loll, (2009), 0906.3947.

[148] B. Dittrich, Class. Quant. Grav. **23**, 6155 (2006), gr-qc/0507106.

[149] G. Amelino-Camelia, (2008), 0806.0339.

[150] S. M. Carroll, *Spacetime and geometry: An introduction to general relativity* (San Francisco, USA: Addison-Wesley, 2004).

[151] G. de Berredo-Peixoto and I. L. Shapiro, Phys. Rev. **D70**, 044024 (2004), hep-th/0307030.

[152] I. G. Avramidi, Lect. Notes Phys. **M64**, 1 (2000).

Publications

D. Benedetti, P. F. Machado and F. Saueressig, *Four-derivative interactions in asymptotically safe gravity* , to appear in the Proceedings of the XXV Max Born Symposium "The Planck Scale", Wroclaw, 29 June - 3 July, 2009, arXiv:0909.3265 [hep-th].

D. Benedetti, P. F. Machado and F. Saueressig, *Taming perturbative divergences in asymptotically safe gravity*, Nucl. Phys. B 824, 168-191 (2010), arXiv:0902.4630 [hep-th].

D. Benedetti, P. F. Machado and F. Saueressig, *Asymptotic safety in higher-derivative gravity*, Mod. Phys. Lett. A 24, 2233-2241 (2009), arXiv:0901.2984 [hep-th].

P. F. Machado and R. Percacci, *Conformally reduced quantum gravity revisited* , Phys. Rev. D 80, 024020 (2009), arXiv:0904.2510 [hep-th].

P. F. Machado and F. Saueressig, *On the renormalization group flow of f(R)-gravity*, Phys. Rev. D 77, 124045 (2008), arXiv:0712.0445 [hep-th].

Samenvatting

Het begrijpen van het kwantumgedrag van de zwaartekracht is een openstaand probleem in ons begrip van de fundamentele natuurkrachten. Op afstanden variërend van de kosmologische schalen (10^{28} cm) tot fracties van een millimeter (10^{-2} cm) kunnen we grotendeels de kwantum effecten op zwaartekrachtsinteracties verwaarlozen. In dit regime wordt zwaartekracht zeer goed beschreven door de klassieke algemene relativiteitstheorie. Op de schaal van subatomaire interacties (10^{-15} cm) kunnen we zwaartekracht geheel verwaarlozen omdat de andere krachten vele malen sterker zijn. Echter, wanneer we steeds kleinere schalen beginnen te onderzoeken worden de kwantumcorrecties steeds groter en de zwaartekracht steeds sterker, totdat we aankomen bij de Planck schaal (10^{-33} cm), waar de kwantumzwaartekrachteffecten domineren. Het begrijpen van het kwantumgedrag van de zwaartekracht houdt derhalve in dat we haar gedrag begrijpen onder verandering van de lengteschaal, van extreem grote tot extreem kleine schaal.

Een van de krachtigste theoretische raamwerken voor het onderzoeken van gedrag onder schaling is de renormalisatiegroep, die ons in staat stelt de schaalafhankelijkheid van een fysisch systeem op te slaan in zijn microscopische parameters en daarmee de evolutie van de theorie over verschillende lengteschalen te onderzoeken via de evolutie van zijn parameters. Deze laatste noemen we de renormalisatiegroepstroming van de theorie. In dit proefschrift hebben we de renormalisatiegroepstroming van de zwaartekracht onderzocht.

Ons onderzoek concentreerde zich voornamelijk op het gedrag van de zwaartekracht op de Planck schaal. Precies op deze schaal stort de perturbatieve kwantumzwaartekracht in, de theorie die men krijgt als men algemene relativiteitstheorie kwantiseert met behulp van storingstheorie, een methode die zeer succesvol is gebleken in het geval van de andere fundamentele krachten. Deze

ineenstorting manifesteert zich in het ontstaan van oneindigheden die alleen opgevangen kunnen worden met de introductie van oneindig veel nieuwe parameters. Als gevolg raakt al het voorspellend vermogen van de theorie verloren. De meest gehoorde reactie op dit probleem is dat op de Planck schaal gekwantiseerde zwaartekracht vervangen moet worden door een fundamentelere theorie, die nieuwe concepten introduceert zoals extra dimensies, nieuwe vrijheidsgraden of tot op heden onontdekte symmetrieën. Een alternatief is dat zwaartekracht asymptotisch veilig is.

Het asymptotischeveiligheidsscenario postuleert het bestaan van een niettriviaal vast punt van de renormalisatiegroepstroming van de zwaartekracht, die het schalingsgedrag van de theorie op de kleinste schalen dicteert. Op dit vaste punt zijn alle behalve een eindig aantal essentiële parameters van de theorie ongelijk nul en hebben bovendien een eindige waarde. Als resultaat hiervan blijft de theorie vrij van desastreuze oneindigheden en behoudt zij haar voorspellend vermogen tot op willekeurig kleine lengte schalen. Of zwaartekracht al dan niet asymptotisch veilig is was de eerste en voornaamste vraag die ten grondslag lag aan dit proefschrift.

Hoewel de grootste uitdaging binnen het kwantumzwaartekrachtprogramma het gedrag van zwaartekracht op de kleinste schaal betreft, wordt er ook gesuggereerd dat kwantumzwaartekracht aanleiding geeft tot sterke renormalisatiegroepeffecten op de grootst mogelijke schalen, die verantwoordelijk kunnen zijn voor waargenomen kosmologische fenomenen. Het vermoeden bestaat dat zulke effecten veroorzaakt worden door niet-lokale kwantuminteracties die voortkomen uit de renormalisatiegroepevolutie van de effectieve dynamica van de kwantumzwaartekracht. Het op waarde schatten van deze beweringen was een tweede drijfveer voor het huidige werk.

Het voornaamste gereedschap in ons onderzoek was een continu renormalisatiegroepalgoritme van Wilson, de zogenaamde functionele renormalisatiegroepvergelijking (FRGE), die we besproken hebben in hoofdstuk 2. Deze legt de schaalafhankelijkheid vast van een grofmazige effectieve actie, die de natuurkunde op een bepaalde schaal beschrijft, en ons dus in staat stelt de renormalisatiegroepstroming van de theorie te construeren. Berekeningen binnen deze methode berusten op een afkappingsbenadering, waarbij de volledige renormalisatiegroepstroming geprojecteerd wordt op een deelruimte die slechts een aantal van de parameters en bijbehorende operatoren van de theorie omvat. De betrouwbaarheid van de resultaten met een bepaalde afkapping kan beoordeeld worden door hun stabiliteit te onderzoeken onder geleidelijke uitbreiding van de deelruimte. Voorgaande FRGE studies in de literatuur hebben het bestaan van een niettriviaal vast punt van de renormalisatiegroepstroming aangetoond in afkappingen opgespannen door polynomen in de scalaire kromming tot op orde zes, hetgeen gezien kan worden als onderbouwing voor het asymptotischeveiligheidsvermoeden. De cruciale vraag is dan of het vaste punt behouden blijft onder verdere uitbreiding van de afkapping. In dit proefschrift hebben we dit vraagstuk aangepakt door drie verschillende elkaar aanvullende strategieën te volgen.

Als eerste hebben we, in hoofdstuk 3, de renormalisatiegroepstroming van de zwaartekracht onderzocht beperkt tot de hoekgetrouwe sector. Deze simplificatie maakte het mogelijk om afkappingen te beschouwen die termen bevatten die anders om technische redenen onhandelbaar zouden zijn. Hiermee verkrijgen we een ruw beeld van de effecten van dergelijke termen op het gedrag van de volledige theorie. In het bijzonder hebben we afkappingen beschouwd met niet-lokale termen waarvan beweerd wordt dat ze de theorie voorzien van niet-triviale dynamica op grote afstand. We hebben ontdekt dat de resulterende renormalisatiegroepstroming op twee niet-equivalente manieren geïmplementeerd kan worden, die de symmetrie van de theorie onder lokale schaalveranderingen breekt ofwel behoudt. In het eerste geval kwamen onze bevindingen overeen met resultaten in de literatuur die wijzen op niet-triviale dynamica op grote afstand gestuurd door renormalisatiegroepeffecten. In het laatste geval hebben we staving gevonden voor het bestaan van een niet-triviaal vast punt in overeenstemming met asymptotische veiligheid. Hoewel beide implementaties wiskundig consistent zijn, hebben we beargumenteerd dat de laatste meer gerechtvaardigd is vanuit een fysisch oogpunt en representatiever beschouwd moet worden voor de volledige stroming.

De tweede strategie die we gevolgd hebben in hoofdstukken 4 en 5, waarbij we zijn teruggekeerd naar de volledige zwaartekracht, was om een FRGE te construeren die ons in staat zou stellen om algemene afkappingen opgespannen door willekeurige functies $f(R)$ van de scalaire kromming R te bestuderen, en daarmee grote delen van de volledige renormalisatiegroepstromingsruimte. Gebruikmakend van deze vergelijking hebben we eerst de resultaten van eerder genoemde FRGE studies gereproduceerd, die het bestaan van een niet-triviaal vast punt met opvallend goede numerieke eigenschappen aantonen met afkappingssubruimtes opgespannen door polynomen $f(R)$ tot op orde zes. Vervolgens beschouwden we niet-lokale afkappingen opgespannen door niet-polynomiale functies van R. We stelden vast dat in het algemeen de termen van dit type op consistente wijze losgekoppeld kunnen worden van de rest van de stroming en we hebben, op basis van twee expliciete realisaties van deze afkappingen, laten zien dat, hoewel zulke niet-lokale afkappingen zeker tot grote renormalisatiegroepeffecten leiden op de grootste schalen, ze niet in staat zijn de natuurkunde op kleine schaal te beschrijven. Aangezien de polynomiale $f(R)$-resultaten erop duiden dat dit gebied gedomineerd wordt door een niet-triviaal vast punt die de korteafstandsdynamica beheerst, zijn de vooruitzichten voor asymptotische veiligheid goed, tenminste voor zover het de $f(R)$-sector betreft.

Als laatste hebben we in hoofdstuk 6 in onze afkapping termen meegenomen waarvan bekend is dat ze bij uitstek problematisch zijn uit het oogpunt van perturbatieve kwantisatie. Allereerst gingen we een stap verder dan het $f(R)$-geval door expliciet tensoroperatoren met vier afgeleiden op te nemen in onze afkapping. Het zijn precies termen bestaande uit tensoren die verantwoordelijk zijn voor onabsorbeerbare divergenties in perturbatief gekwantiseerde algemene relativiteitstheorie, en hun aanwezigheid zou dus een grote impact kunnen hebben op het asymptotischeveiligheidsscenario. Opvallend genoeg hebben we ontdekt

dat het niet-triviale vaste punt in overeenstemming met asymptotische veiligheid nog steeds standhield in deze setting. Vervolgens voegden we een minimaal gekoppeld, massaloos scalair veld toe aan onze afkapping, hetgeen leidt tot een systeem dat het prototype is van een perturbatief gekwantiseerde zwaartekrachtstheorie die al divergeert in eerste orde in de kwantumfluctuaties. Het resulterende vaste punt leek opvallend veel op dat in het geval van pure zwaartekracht. Dus, in tegenstelling tot een vaak geopperd bezwaar met betrekking tot de $f(R)$-resultaten, hebben we gevonden dat het meenemen van tensortermen in onze afkapping geen kwalitatieve effecten heeft op het schalingsgedrag van de theorie op de Planck schaal.

Het samenhangende beeld dat ontstaat uit dit onderzoek levert significant bewijs ter ondersteuning van het asymptotischeveiligheidsscenario. Daarmee suggereert het dat gekwantiseerde zwaartekracht zijn voorspellend vermogen behoudt tot op willekeurig kleine afstandsschaal en de zwaartekrachtsprocessen adequaat beschrijft zonder de fundamentele eigenschappen van de theorie te hoeven aanpassen. Hoewel het gevonden bewijs hier inductief van aard is en daarom niet kan garanderen dat een niet-triviaal vast punt bestaat in de volledige stromingsruimte, is het toch opvallend dat een dergelijk vast punt zich manifesteert in alle afkappingen tot dusver onderzocht. Onze resultaten suggereren dat renormalisatiegroepeffecten een antwoord bieden op de Planckschaalproblemen van de kwantumzwaartekracht. Ook al is het in kaart brengen van de renormalisatiegroepstroming van de zwaartekracht zeer zeker nog niet voltooid, dit proefschrift is een stap in die richting.

Acknowledgements

Um galo sozinho não tece uma manhã
- João Cabral de Melo Neto
(Brazilian poet, 1920-1999).[1]

To my supervisor, Renate Loll, for the guidance on all areas of academic life, the feedback on my research and on this thesis, and for giving me the freedom to pursue different avenues of research (so long as the physics was - mostly - right!).

To Jan Ambjørn, for the hospitality during my stay at Niels Bohr Institutet, where I first explored the work that would eventually lead to this thesis.

To Roberto Percacci, for the fruitful exchanges and the scientific collaboration.

To the members of the reading committee, Jan, Roberto, Daniel Litim, Gerard 't Hooft and Bernard de Wit, for accepting this job, for their comments and for their efforts.

I also acknowledge useful discussions with Alessandro Codello, Elisa Manrique, Martin Reuter and Daniel Litim.

To the people at the Institute for Theoretical Physics, past and present, for the stimulating scientific environment.

To Frank Saueressig, for bouncing the $f(R)$ project off me, for the collaboration in which that resulted and for the helpful comments on my thesis manuscript.

To Dario Benedetti, for being the 'B' in BMS, for the discussions, the Perimeter Institute visits and for the friendship.

To those colleagues whose friendship made life in The Netherlands all the more enjoyable, Joe, Pietro and Daniel, and going to the institute all the more fun, Lih King, Daniele and Fernando.

To the other friends I have met while here, Camilo, David, Christian, Julian, Gerardo, Alessandro, Melvin and Pien.

To the good people from all the Christmas dinners.

To Stan and Verônica, for holding the door to quantitative biology open.

[1] "A rooster alone does not weave a morning"

Four years in The Netherlands should've given me mastery over the Dutch language. It didn't. Thanks to Timothy and Melvin for the Dutch translations in the thesis. Thanks also to Arnaud for providing the template for the thesis layout.

To Paolo di Marco and Harvey Brown, for their contribution to my development as a scientist.

To my best men, Estrela and Felipe, for the mustaches.

To my friends in Brazil, who always make an ocean and eight years distances so easy to bridge.

To my sisters, Marina and Paloma, for maintaining the balance.

To my parents, Fernando and Verônica, for their love and support.

And, of course, to my wife, Alina.

Curriculum Vitae

Pedro Farias Machado was born on the 3rd of August 1982 in Belo Horizonte, in the state of Minas Gerais, Brazil. He completed his secondary education at the Liceo Scientifico Fundação Torino in Belo Horizonte in 2001. In the same year, he started his undergraduate studies in Physics and Philosophy at the University of Oxford, from which he graduated in 2005 with an MPhys thesis on particle physics phenomenology under the supervision of Dr. Roman Walczak. During the Fall of 2005, he was a junior guest researcher at the Niels Bohr Institute, under the guidance of Prof. dr. Jan Ambjørn. In January 2006, he joined the group of Prof. dr. Renate Loll at the Institute for Theoretical Physics and Spinoza Institute, Utrecht University, and started his doctoral research in theoretical high energy physics on the topic of quantum gravity. The results of that research are presented in this thesis.